



<https://theses.gla.ac.uk/>

Theses Digitisation:

<https://www.gla.ac.uk/myglasgow/research/enlighten/theses/digitisation/>

This is a digitised version of the original print thesis.

Copyright and moral rights for this work are retained by the author

A copy can be downloaded for personal non-commercial research or study, without prior permission or charge

This work cannot be reproduced or quoted extensively from without first obtaining permission in writing from the author

The content must not be changed in any way or sold commercially in any format or medium without the formal permission of the author

When referring to this work, full bibliographic details including the author, title, awarding institution and date of the thesis must be given

Enlighten: Theses

<https://theses.gla.ac.uk/>
research-enlighten@glasgow.ac.uk

Thesis submitted for the degree of Doctor of Philosophy,
University of Glasgow.

**STRUCTURAL GEOLOGY OF THE LEWISIAN COMPLEX
NORTH OF LOCH MAREE, NW SCOTLAND**

by

LUIS ALBERTO D'AVILA FERNANDES

**DEPARTMENT OF GEOLOGY
UNIVERSITY OF GLASGOW
NOVEMBER 1987**

ProQuest Number: 10997352

All rights reserved

INFORMATION TO ALL USERS

The quality of this reproduction is dependent upon the quality of the copy submitted.

In the unlikely event that the author did not send a complete manuscript and there are missing pages, these will be noted. Also, if material had to be removed, a note will indicate the deletion.



ProQuest 10997352

Published by ProQuest LLC (2018). Copyright of the Dissertation is held by the Author.

All rights reserved.

This work is protected against unauthorized copying under Title 17, United States Code
Microform Edition © ProQuest LLC.

ProQuest LLC.
789 East Eisenhower Parkway
P.O. Box 1346
Ann Arbor, MI 48106 – 1346

DEDICATION

I dedicate this thesis to all those who have suffered and contributed to its completion, especially my parents, Reimi, Themis and also the several million of my people whose work supported my education.

PREFACE

*And so these men of Indostan
Disputed loud and long,
Each in his own opinion
Exceeding stiff and strong,
Though each was partly in the right
And all were in the wrong!*

The Blind Men and the Elephant

(Ancient Hindu fable, John Godfrey Saxe)

ACKNOWLEDGEMENTS

The following are acknowledged for their contribution to the present work.

Conselho Nacional de Pesquisas (CNPq) for the financial support in this 'well-rounded' education abroad.

Mrs Whitbread and Mr Van Vlissingen for the hospitality in Letterewe during field work.

Professor D.R.Bowes for his supervision and interest in the research and specially his editing skills and persistence in trying to transform my 'bringlish' (Brazilian English) into a more readable (?) language.

Professor B.E.Leake for the extended use of departmental facilities and his faith (?) that the work would be completed.

Douglas McLean for the photographic work, daily Brazilian news and numerous 'sweeties'.

'Big Bob' and Jim for the uncountable and extra 'last thin sections'.

Big George for construction of the 'structurometer' and welding skills.

Roddy Morrison for his assistance as chief technician and his never followed philosophical advices.

Eddie for his mechanical skills and for testing the limits of my patience.

Lou-Anne Nicholson and Lisa Haughton for their efficient light-speed typing of the manuscript.

Pat, Breno, Paul, Gawen, Adrian and specially Richard for discussion and help at several stages of the work.

Richard, Lisa, L-Anne, Paul, Reimi and Morgan are specially thanked for their help with 'last week' modifications and editing of the manuscript.

TABLE OF CONTENTS.

	Page
DEDICATION	i
PREFACE	ii
ACKNOWLEDGEMENTS	iii
TABLE OF CONTENTS	v
SUMMARY	ix
CHAPTER 1	
1.1 LOCATION	1
1.2 PREVIOUS INVESTIGATIONS	1
1.3 OBJECTIVES OF THE PRESENT INVESTIGATION	3
1.4 GENERAL APPROACH	3
1.5 FRAMEWORK OF CONTENTS	4
CHAPTER 2 - ROCK UNITS AND THEIR DISTRIBUTION	
2.1 INTRODUCTION	5
2.2 DESCRIPTION OF ROCK TYPES	5
2.3 DISTRIBUTION OF ROCK TYPES	14
CHAPTER 3 - STRUCTURAL FEATURES, THEIR SEQUENTIAL DEVELOPMENT AND CORRELATION	
3.1 INTRODUCTION	17
3.2 DESCRIPTION	20
3.2.1 DOMAIN I - QUARTZOFELDSPATHIC GNEISSES	20
3.2.2 DOMAIN II - AMPHIBOLE SCHISTS	28
3.2.3 DOMAIN III - METASEDIMENTS	32

	Page
3.2.4 DOMAIN IV - MARBLES	36
3.2.5 D-LATE DEFORMATIONAL PHASES (IN DOMAINS I, II, III, IV)	38
3.2.6 FAULTS	42
3.3 BASES OF CORRELATION AND THEIR APPLICATION TO THE LOCH MAREE AREA	43
 CHAPTER 4	
4.1 INTRODUCTION	70
4.2 DESCRIPTION OF FABRICS	71
4.2.1. S1 FOLIATION	71
4.2.1.1 DOMAIN I - QUARTZOFELDSPATHIC GNEISSES AND AMPHIBOLITES	71
4.2.1.2 DOMAIN II - AMPHIBOLE SCHISTS	74
4.2.1.3 DOMAIN III - METASEDIMENTS	74
4.2.1.4 DOMAIN IV - MARBLES	75
4.2.2 S2 FOLIATION	75
4.2.2.1 DOMAIN I - QUARTZOFELDSPATHIC GNEISSES AND AMPHIBOLITES	75
4.2.2.2 DOMAIN II - AMPHIBOLE SCHISTS	78
4.2.2.3 DOMAIN III - METASEDIMENTS	79
4.2.3 S2a FOLIATION	80
4.2.3.1 DOMAIN I - QUARTZOFELDSPATHIC GNEISSES AND AMPHIBOLITES	80
4.2.3 S3 FOLIATION	82
4.2.3.1 DOMAIN I - QUARTZOFELDSPATHIC GNEISSES AND AMPHIBOLITES	82
4.2.3.2 DOMAIN II - AMPHIBOLE SCHISTS	83
4.2.3.3 DOMAIN III - METASEDIMENTS	84
4.2.4 S4 FOLIATION	85
4.2.4.1 DOMAIN I - QUARTZOFELDSPATHIC GNEISSES AND	

	Page
AMPHIBOLITES	85
4.2.4.2 DOMAIN II - AMPHIBOLE SCHISTS	86
4.2.5 S-LATE	87
4.2.5.1 S-000°	87
4.2.5.2 S-040°	87
4.2.5.3 S-060°/S-090°	88
4.3 DISCUSSION	89
CHAPTER 5 - MYLONITES	
5.1 INTRODUCTION	108
5.2 DESCRIPTION	111
5.2.1 MESOSCOPIC SCALE FEATURES	111
5.2.2 MICROSCOPIC SCALE FEATURES	113
5.2.3 GENERAL CONCLUDING REMARKS	124
5.3 DISCUSSION	125
5.3.1 INTRODUCTION	125
5.3.2 CONDITIONS OF DEFORMATION	126
5.3.2.1. PURE SHEAR VS. SIMPLE SHEAR	126
5.3.2.2. STRAIN SOFTENING MECHANISMS	141
5.3.2.3 MINERAL DEFORMATION MECHANISMS	148
5.3.2.4 BRITTLE VS. DUCTILE DEFORMATION	160
5.4 SUMMARY - MYLONITIC FEATURES IN THE LOCH MAREE ROCKS	169
CHAPTER 6 - INTERPRETATION OF THE STRUCTURES	
6.1 INTRODUCTION	182
6.2 GEOMETRICAL ANALYSIS	182
6.2.1 ANALYSIS OF THE ORIENTATION DATA	182
6.2.1.1. ANALYSIS OF L1-L2 DEFORMATION PATTERNS IN RELATION TO MECHANISM OF FOLDING	189
6.2.2 FOLD GEOMETRY	190

	Page
6.2.2.1 INTRODUCTION	190
6.2.2.2 LATE FOLDS	196
6.2.2.3 F4 FOLDS	196
6.2.2.4 F3 FOLDS	203
6.2.2.5 F2 FOLDS	208
6.2.2.6 F1 FOLDS	223
6.2.2.7 DISCUSSION OF THE KINEMATIC MODELS	227
6.3 STRAIN ANALYSIS	235
6.3.1 INTRODUCTION	235
6.3.2 INTERPRETATION OF THE RESULTS	236
6.3.3 GEOLOGICAL INTERPRETATION OF THE STRAIN ANALYSIS	253
 CHAPTER 7 - METAMORPHIC CONDITIONS	
7.1 INTRODUCTION	259
7.2 P-T CONDITIONS	260
7.2.1 GEOTHERMOMETRY	260
7.2.2 MINERAL ASSEMBLAGES	265
7.2.2.1 ALUMINOUS ROCKS	267
7.2.2.2 MAFIC ROCKS	273
7.2.3 GEOTHERMAL GRADIENTS	279
7.3 CHEMICAL AND MECHANICAL EFFECTS OF FLUIDS	279
7.4 DISCUSSION	286
 CHAPTER 8 - TECTONIC MODEL	
8.1 INTRODUCTION	290
8.2 MODEL	295
8.3 REGIONAL CORRELATION - DISCUSSION	295
 CHAPTER 9 - CONCLUSIONS	301
BIBLIOGRAPHY	307

ANNEX

OUTLINE OF THE MAIN STRUCTURES
S-BANDING - S1 FOLIATION MAP
L1-L2 LINEATION MAP
TABLE 3.1 - STRUCTURAL CORRELATION
TABLE 5.1 - MYLONITES -MICROSCOPIC FEATURES
TABLE 7.4 - GNEISSES-XRF CHEMICAL ANALISES

SUMMARY

Field and laboratory studies of the Lewisian Complex of the Loch Maree district in NW Scotland have confirmed the presence of tectonic interleaving of late Archaean basement gneisses and early Proterozoic volcano-sedimentary cover (Loch Maree Group). Structural analysis of these rocks has demonstrated the presence of four generations of approximately coaxial folds and a relative chronology of events has been established. During D1 a strong NW-SE stretching fabric was developed. At a late stage of this phase the basement was tectonically emplaced over the cover with the widespread formation of mylonites particularly at major lithological contacts. D2 affected both basement and cover giving rise to a large SE-plunging NE-verging structure. This fold which shows perfectly coaxial relations with the D1 fabrics, controls the distribution of the lithological units with gneisses and marbles representing basement and detachment zone, respectively, in the core of the structure. During D_3 - D_4 recumbent and upright folds were formed. These display clockwise relations with the L1-L2 stretching lineation and were formed under conditions of continuous deformation at higher structural levels indicating post-D2 uplift.

Climatic metamorphic conditions were operative during early stages of D1 deformation: middle to upper amphibolite conditions (Barrovian type metamorphism) have been deduced from garnet-biotite and garnet-hornblende geothermometry and coexisting mineral assemblages. The temperature was lower (greenschist facies conditions) during mylonitization. D2 temperatures, also determined by geothermometry (garnet-biotite and garnet-hornblende) corresponded to upper greenschist to lower amphibolite facies conditions. The changes in

P-T conditions are interpreted as being indicative of 'thermal relaxation' associated with thickening of the crust produced by (D1) thrusting.

Structures indicating transient brittle deformation along the main thrust horizons are ascribed to pore fluid effects. Evidence for abundant fluid activity is given by chemical transformations producing mineralogical convergence in ultramylonites. Interplay between metamorphism and deformation was complex and the application of the classical microtectonic approach was not possible. Similarly for the determination of the brittle or ductile character of the deformation in 'fault-related' rocks the recently proposed methods do not seem to be applicable: careful analysis of deformation mechanisms on the grain scale is considered to be essential. Viscosity contrast variations between early D1 and late D4 are ascribed to changes in the strain rate, geometric softening and even variations of the temperature: there is no evidence that mineralogical changes exercised a control.

A model based on simple transpression with a middle crustal flat-lying shear zone formed in the step-over of a left-lateral right-stepping wrench system is capable of explaining the deformation of these rocks in a continuous fashion under conditions of progressive uplift of the crust. If such a model is considered realistic, no reliable correlation of structures based on style is possible over distances of few tens of kilometers where physical continuity of structures is not available. Instead features indicating the predominant kinematic pattern are more reliable.

CHAPTER 1 - INTRODUCTION

1.1 LOCATION

This thesis concerns the structural development of the Lewisian rocks north of Loch Maree in Western Ross-shire (Fig. 1.1). These rocks include the supracrustal Loch Maree group, which is of sedimentary and volcanic derivation, as well as gneisses and amphibolites that typify so much of the Lewisian Complex. In the area mapped (Fig. 2.1) the exposure is excellent (e.g. Pls.3-30,70). The topography, with a rise of about 2800 feet over a distance of about two miles (from the shore of Loch Maree to Beinn Lair), provides much three dimensional exposure. The topography is controlled by the geology, with amphibole schists forming a prominent ridge from Folaís to Coire Broige, the sediments lie on the lower ground near the loch, and the gneisses on the north-eastern side of the ridge.

1.2 PREVIOUS INVESTIGATIONS

The area was mapped by the Geological Survey during the early part of the century, resulting in the publication of the 1 inch to 1 mile sheet 92 (1913), and the unpublished 6 inches to 1 mile sheet 58 (1905). Descriptions were written in the accompanying memoirs (Peach et al., 1907, Clough et al. 1913, Peach and Horne 1930).

Recent views of Lewisian geology include the work of Bowes (1978), Park (1980), Bowes and Gadh (1981) and Watson (1983); these also include extensive lists of references relating to Lewisian geology. Results of very recent investigation of several aspects of Lewisian geology are put together in Park and Tarney (1987). Most of the geochronological data of these rocks are summarized by Bowes (1978), Hamilton et al. (1979) and Aftalion et al. (1984).

Radiometric studies specifically relating to the metasediments and gneisses of Loch Maree district have been carried out by Birkeman et al. (1975) and Aftalion et al. (in preparation).

Following the outstanding quality of the detailed lithological mapping by the Geological Survey, Keppie (1967) was the first to

deal with structural mapping of the Loch Maree rocks. This work covered almost exactly the same ground dealt with in the present study.

Stratigraphic relationships in the Lewisian Complex are still subject of much debate (cf. Bowes 1969, 1978, Bowes and Gaál 1981, Watson 1983, Wright 1987). Of particular interest to the present study is the relative position of the Loch Maree supracrustals. Table 1.1 presents an up to date summary of the Lewisian stratigraphy as proposed by Wright (*op. cit.*). Wright places the "Loch Maree Protolithic Succession" at the beginning of the early Proterozoic Laxfordian Cycle, *i.e.* basically consistent with the isotopic data and arguments presented by Birkeman et al. (1975).

The "Loch Maree Protolithic Succession" was considered by C.E. Tilley (in discussion of Sutton and Watson 1951, p. 297) to be critical in the elucidation of the Lewisian stratigraphy. The undoubted metasedimentary origin of these rocks, and the absence of associated basic minor intrusions (which Sutton and Watson 1951, correlated with Scourie dykes), in marked contrast with the juxtaposed quartzofeldspathic gneisses, suggests that the metasediments post-date the igneous event. This indicates a major break in the stratigraphy between these two units. Interpretation of this relationship has been a major source of controversy since the pioneer work of the Geological Survey. Differing views concerning the origin and stratigraphic relations between gneisses and metasediments were taken by C.T. Clough (lithological transition between schists and gneisses) on one hand and B.N. Peach and W. Gunn (thrust contact) on the other (cf. Peach *et al.* 1907, Peach and Horne 1930). Although the idea of thrusting has prevailed, some doubts still persist and are illustrated by the following extract from Peach *et al.* (1907, p. 221): "It is not certain that this superposition was originally brought about by thrusting, for the present synclinal arrangement of the rock masses is later than most of the mylonising, and it cannot be determined how the mylonites were inclined before the syncline was formed".

Describing a sequence of folds and metamorphic events affecting these rocks, Keppie (1967) confirmed the allochthonous nature of the

Table 1.1 LEWISIAN STRATIGRAPHY

TIME	DATES		EPISODE	PHASES AND EVENTS	ROCKS
EARLY PROTEROZOIC	1750-1650	LAXFORDIAN CYCLE	HARRIS	Pegmatite Intrusion Granite Intrusion	South Harris Injection Complex North Harris Granites Laxford Granites
	1900-1700		DURNESS	Metamorphism and Deformation	Loch Maree Division Laxfordian Gneisses
	c.2200-1850		CAIRLOCH	Rodil Metamorphic Phase South Harris Intrusive Phase Loch Maree Phase	South Harris Protolithic Intrusions Letterewe Basaltic Suite Loch Maree Protolithic Succession
	2400-2200		INVERIAN	Scourie Dyke Suite Loch Roe Metamorphism and Folding Intrusion of Sodic Pegmatites	Scourie Dyke Suite Inverian Schists Achmelvich Pegmatites

TIME	DATES		EPISODE	PHASES AND EVENTS	ROCKS	
(LATE) ARCHAICAN	c. 2450 c. 2550	SCOURIAN CYCLE	BARRA	Intrusion of potash pegmatites Intrusion of ultra-basic and intermediate plutons	Kirkaig Pegmatites	
	2600-2650		BADCALLIAN	Badcallian deformation and metamorphism accompanied by partial melting to form granitic gneiss	Badcallian Granulite Kirkaig Granitic Gneiss	Gaelic Assemblage Drumbeg Division Claisfearn etc. Division Kylesku Division Rhiconich Division Sheildaig Division Uist Division
	2920 ± 50		Gaelic	Uamhaig Metamorphism and Deformation (Amphibolite Facies)	Clach Boga Protolithic Intrusions Shios Dykes Uamhaig Gneisses Drumbeg Protolithic Layered Intrusions. Langavat, Leverburgh, Tirez, Ness and Claisfearn Protolithic Successions Hebridean Protolithic Intrusions	

(after Wright 1985)

quartzofeldspathic gneisses. However, the thrusting phase was placed quite late in the structural sequence ('mid-phase', p. 179), and hence no explanation could be given of the structural concordance between features formed in both units before the thrusting. In addition many other important questions remained unanswered, including (i) the geometry and relative age of the 'Letterewe synform' (see Fig. 8.2), and (ii) the interplay between metamorphism and deformation. With the advances made in the field of structural geology over the past two decades, these and other related questions can be tackled and this thesis addresses itself to these matters.

1.3 OBJECTIVES OF THE PRESENT INVESTIGATION

The following are the main aspects of this study.

1. The geometry and relative age of the Letterewe synform.
2. The polyphase deformation shown by the metasediments, gneisses and amphibolites.
3. The variable expression of the deformational phases in different lithologies under non-homogenous strain conditions, and the resulting problems for structural correlation.
4. The age, deformation, and kinematic histories of mylonitic rocks.
5. Mechanisms of deformation, and kinematic significance of fold structures.
6. Metamorphic history, and the interplay between metamorphism and deformation.
7. Significance of the rocks in the interpretation of the stratigraphy and evolution of the Lewisian Complex.

1.4 GENERAL APPROACH

This work is largely based on field study (over six months) and detailed examination of more than five hundred thin sections. Accordingly, discussion and interpretation is mainly based on the comparison of the observed and analysed features, with the results and interpretations reported in the literature. In addition some microprobe and S.E.M. studies, together with XRF analyses of minerals and rocks were undertaken, but the amount of data obtained was limited. Accordingly, the geological significance of some of the presented data will be much enhanced when a more complete

laboratory-based investigation is carried out.

A radiometric analysis of some gneisses and ultramylonites (U/Pb and Rb/Sr) has been carried out by the staff of the Scottish Universities Research and Reactor Centre in conjunction with the present study. The preliminary results are used in this work (cf. Chap. 8) but they are not presented here and instead will be the subject of a joint publication.

1.5 FRAMEWORK OF CONTENTS

The following is an outline of the topics covered.

The rock units, their distribution, and the evidence of their pre-metamorphic origin (Chap. 2).

The sequential development of the structures, followed by a discussion of the problems involved and the criteria used in correlation (Chap. 3).

The microfabrics associated with the development of the folds (Chap. 4).

Mylonitic rocks, their structures and textures (Chap. 5).

Structural interpretation, with particular emphasis on mesoscopic scale features (folds), some strain data and discussion of their kinematic significance in fold belts (Chap. 6).

Metamorphic conditions using geothermometres and petrogenetic grids, with a discussion of geochemical transformation and the possible role played by fluids during overthrusting and mylonitization (Chap. 7).

This study provides constraints on regional correlations and existing models of evolution of the Lewisian Complex, particularly in early Proterozoic times (Chap. 8).

CHAPTER 2 – ROCK UNITS AND THEIR DISTRIBUTION

2.1 INTRODUCTION

2.2 DESCRIPTION OF ROCK TYPES

2.3 DISTRIBUTION OF ROCK TYPES

2.1 INTRODUCTION

In this chapter a brief description of the principal lithologies and of their distribution is presented. The objective is to familiarise the reader with the principal characteristics of the studied rocks in order to facilitate the understanding of the forthcoming chapters.

The first section includes a short account of the lithological compositions, the mesoscopic scale features, and comments about the possible pre-metamorphic origin of the main rock types.

The second section deals with the distribution of the lithological units. It includes a brief explanation of the structural and topographic control on the configuration of these units on the map.

The adopted nomenclature follows the work of Keppie (1967), which is largely based on the mapping of the Geological Survey (Peach *et al.* 1907). A more detailed account of the structural and topographic control on the configuration of these units at the map scale will be presented in chapter 8, after the geometry of the large structures has been discussed (Chaps. 3, 5 and 6).

2.2 DESCRIPTION OF ROCK TYPES

The mineral composition of the principal rock types, as determined by optical microscopy, is presented in Table 2.1 which is slightly modified from Keppie (1967, Table 3.1). Modifications comprise the inclusion of the "Beinn Airigh Charr band" (Fig.2.1) amongst the general heading 'Amphibole Schists' (corresponding to the northeastern limb of the Letterewe synform), and the distinction of the different amphibolites according to their field characteristics. In this way, although the correspondence between

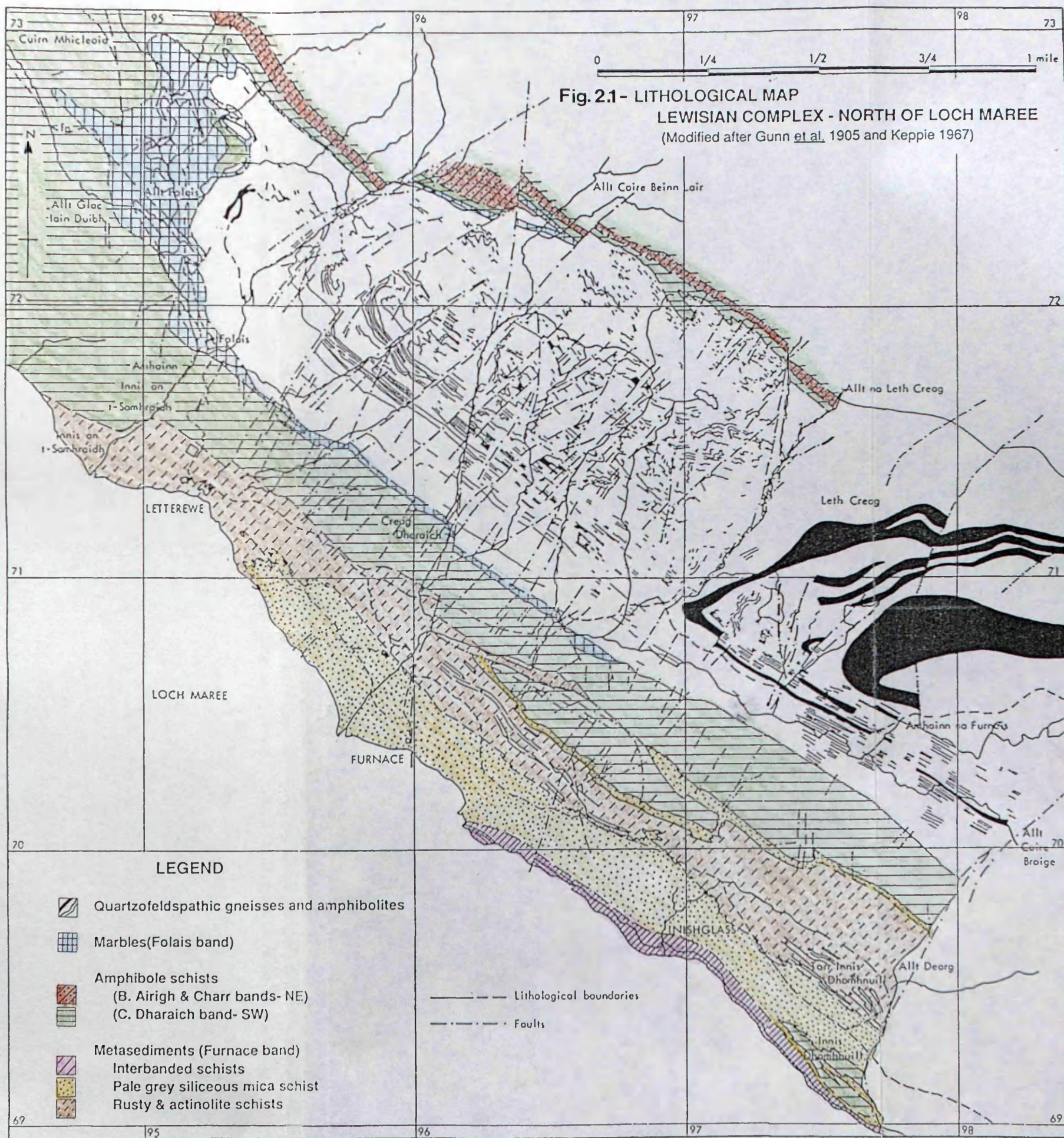


TABLE 2.1 Mineral constituents of the rock types in the area. Musc = muscovite; Bt = biotite; Pl = Phlogopite; Qtz = Quartz; Chl = Chlorite; Tourm = Tourmaline; Sp = Sphene; Mt = Magnetite; Il = Ilmenite; Pyr = Pyrite; Haem = Haemetite; Hbd = Hornblende; Act-Trem- = Actinolite-Tremolite; Calc = Calcite; Apat = Apatite; Zr = Zircon; Gr = Graphite

	Mica			Felspar		Epidote Group			Chl.	Tourm.	Sp	Mt	Il	Pyr	Haem.	Amphibole		Garnet	Staurolite	Calc.	Apat.	Zr.	Gr
	Musc	Bt.	Pl.	Qtz	Potash	Plagioclase	Allanite	Epidote								Clinzoisite	Hbd.						
DOMAIN III	METASEDIMENTS																						
	SCHISTS etc. (Furnace band)																						
	X	X	X	.	x Ab ₆₆₋₈₅	
	X	X	X	.	x Ab ₆₆₋₈₅	
	X	X	.	.	x Ab ₆₆₋₈₅	
	X	.	X	.	x Ab ₆₅₋₈₅	
		.	.	.	x Ab ₅₄₋₆₅	x	.	x	x	.	.	.	X	.	.	
	X	X	X	.	x Ab ₆₆₋₈₅	
	.	.	X	.	X Ab ₄₅₋₈₅	X	
	.	X	.	.	o Ab ₆₆₋₈₅	x	.	x	x	
		.	.	.	x Ab ₅₅₋₇₈	X	
	x	.	X	.	X Ab ₇₀₋₇₆	
		.	.	.	x Ab ₅₉₋₈₁	
	x	.	X	.	x Ab ₆₅₋₈₀	
	X	.	X	X	X Ab ₇₀	
DOM. IV	MARBLES (Folios band)																						
	x	PhL	
		X	.	.	x Ab ₆₄₋₇₆	
DOMAIN II	AMPHIBOLE SCHISTS (B.A. Char band-'NE')																						
	X	X	X	.	x Ab ₆₄₋₇₅	
	.	.	X	.	x Ab ₆₄₋₇₅	
	X	
	X Ab ₆₅₋₇₅	.	.	x	X	
	.	.	X	X	
DOMAIN II	AMPHIBOLE SCHISTS (C.Dharaich band-'SW')																						
	x Ab ₆₀₋₈₀	X	
	x Ab ₆₀₋₈₀	X	
	x Ab ₆₀₋₈₀	X	
	x Ab ₆₀₋₈₀	X	
	o Ab ₆₀₋₈₀	X	
DOMAIN I	LETH CREAG GNEISS																						
	x	x	X	x	X Ab ₆₅₋₇₅	x	x	
	x	.	X	x	X Ab ₆₅₋₇₅	x	x	
	.	.	X	x	X Ab ₆₅₋₇₅	x	x	
	x	x	X	x	X Ab ₆₀₋₇₅	x	x	x	
DOMAIN I	AMPHIBOLITES																						
	X Ab ₆₀₋₇₅	x	x	X	
	X Ab ₆₀₋₇₀	x	x	X	
	X Ab ₆₀₋₇₀	x	x	X	

TABLE 2.1

Figure 2.1 and Table 2.1 is kept here, it will not be maintained in following chapters where most of the detailed lithological subdivisions are incorporated into larger units, corresponding to the adopted domains (cf. Figs. 2.1 and 3.1). The latter are thought to represent the lithologies with enough detail to solve the geometry of the macroscopic structure (see Sects. 3.2 , 6.2). More detailed petrographic descriptions of several of the Loch Maree rock types are given in the Memoirs of the Geological Survey (Peach et al. 1907, Chaps. IV, VI and XII). Analysis of major and trace elements of the gneisses, and mineral (microprobe) analyses of several rock types are presented in Chap.7.(Metamorphism).

DOMAIN I

Quartzofeldspathic gneisses

The quartzofeldspathic gneisses (Leth Creagh gneiss of Figs. 2.1 and 3.1) constitute a sequence of coarse reddish crystalline rocks varying from massive biotite-muscovite gneiss to augen to 'papery or granulitic' gneiss (Peach et al. 1907). The reddish outcrop colour of these rocks does not reflect their composition (see Table 2.1); it is mainly an oxidation feature related to the once overlying Torridonian sediments. The appearance of these rocks is very much dependent on the type and intensity of deformation they have suffered, so that the division in three units with gradational contacts (Fig. 3.1) made by Keppie (1967, p.15), and also recorded by Gunn, Clough and Greenly on the six inch map of the Geological Survey (published in 1905), is attributed here to a transition from rocks with a 'L' fabric to rocks with a 'S' fabric (see 'zones of high strain' on the structural map and in Sect. 6.3). Compositional variants include muscovite, biotite, and calc-silicate gneiss (biotite-hornblende-bearing), the latter being more frequent along the contact between domain I and the carbonate-bearing lithologies of domain IV.

At some localities, biotite gneiss shows large (up to 5cm) K-feldspar crystals (Pl.5.1), which in few places are concentrated into 'bands' (Pl.2.1). Individual crystals at hand specimen scale are observed under the microscope to be composed of several smaller grains presenting a well-developed granoblastic polygonal texture.

This feature corresponds to that shown by the porphyritic amphibolite produced by M1 recrystallization (see Chap. 4).

The pre-metamorphic origin of this sequence is not clear, but the above described features can provide some indication of their pre-metamorphic nature. The large pre-D1 K-feldspars could represent recrystallised phenocrysts and this together with the occasional presence of microgranodioritic 'xenoliths' in these rocks (Pl.2.2) suggest an igneous origin. This interpretation seems to be confirmed by the work of Weaver and Tarney (1980) and by preliminary results of the analysis of major and trace elements of 50 samples of quartzofeldspathic gneiss from domain I. Thus the more frequent occurrence of calc-silicate gneiss along the contact with the carbonate-bearing lithologies of Domain IV, if geologically significant, would be best interpreted as a result of element mobility during the peak of Laxfordian metamorphism affecting the rocks (M1). An age constraint is given by the observation that minerals characterizing the calc-silicate paragenesis also show the well-developed granoblastic polygonal texture typical of the M1 phase. As is shown in chapter 4 ('Fabric Studies'), this same (M1) event is responsible for the recrystallization of the phenocrysts of porphyritic amphibolites, which represent intrusions younger than the gneissic banding (see Chap.3), confirming that the strong shape fabric is mostly a product of deformation younger than the banding (but see Wheeler *et al.* 1987, p.160, for a discussion of similar fabrics developed during the Inverian and Laxfordian episodes at Torridon). Evidence from U/Pb and Rb/Sr dating of these gneisses (Bikerman *et al.* 1975) has suggested that the 'material' was formed during late Scourian times (U/Pb zircon $\underline{c.}$ 2.6 Ga) and re-homogenized during the early Laxfordian (Rb/Sr $\underline{c.}$ 1.9 Ga). These dates are the only constraints on the age of deformation of the segregation banding of the gneisses (*cf.* Sect. 8.3). Although no such data are available for the carbonate-bearing lithologies, the bulk of the structural and stratigraphic evidence (see Chap. 8) suggests that a late Archean age for this unit is unlikely (but see Rock, 1987). This would also indicate that the modification of the basement gneiss occurred at a relatively early stage in the deformational history of these rocks (see Chap.6) and under the highest recorded P-T conditions (see Chaps.7 and 8). Accordingly evidence for widespread mobility of several elements is ubiquitous,

particularly at the late stages of D1 and D2 déformation, and will be discussed in more detail in chapter 7.

Amphibolites

There are three types of amphibolite; banded, porphyritic and mafic varieties. They have similar mineralogical composition (Table 2.1), but can be distinguished in the field. The banded amphibolites have suffered the same metamorphic segregation event that produced the gneissic banding (Pls. 3-8, 3-9, 3-20). The relative age of the other two amphibolite types is unknown; they were distinguished on the basis of structural relationships and the presence of relict igneous features such as phenocrysts (Pls 2-3/4) and intrusive contacts (Pl.2-5).

The **banded amphibolites** are of very restricted occurrence. They show a well-developed irregular banding with feldspathic layers, 1-10cm wide, surrounding thicker mafic 'pods' or boudins (Pl. 3-8), some of which have very small feldspar phenocrysts (Pl. 2-4). The interbanding of these amphibolites with the quartzofeldspathic gneisses is so intimate that it was difficult to distinguish between the felsic bands of the basic rock and some of the leucocratic gneisses in the field, a problem also reported by Clough (in Peach et al. 1907) and Keppie (1967). Ultramafic layers are commonly observed and although the thin bands were probably formed by metamorphic segregation processes (cf. Bowes and Park 1966), the thick layers are more likely to represent inherited igneous features (cf. Bowes et al. 1964).

This type of amphibolite is part of the "early basic rocks" mapped by Clough (in Peach et al. 1907, p.198; 1913, p.24; Survey sheet 92, 1913) between Leth Creag and Loch Garbaig (NG 976708). It is a large body (or several connected small bodies) which marks the hinge zone of the Letterewe synform in domain 1. Although represented on the lithological map (Fig.2.1) as a continuous drop-shaped body this is mainly an effect of the scale of interbanding and structural control (cf. Section 2.3).

The **porphyritic amphibolites** are also regarded as intrusions, and are of probably of the same as the mafic amphibolites. They

frequently occur as lens shaped bodies amongst the banded and mafic mylonites, showing concordant contacts with the gneissic banding. The porphyritic amphibolites are sparsely distributed, and their deformation is described in chapters 5 and 6.

The mafic amphibolites form the great majority of the bodies shown in domain I (Fig.2.1). With the exception of one large body that marks the hinge of the Letterewe synform (together with the banded amphibolite, NG970708) they are less than a metre thick and are only schematically represented in the lithological map (cf. Section 2.3). In a few instances discordance to the gneissic banding was observed (e.g. Pl.2-6) along the SW limb of the Letterewe synform, where the composite banding is steeply-dipping. Intrusive features include irregularities of the contact (Pl.2-5), and in some cases fragments of the country rock within the intrusion. However, these are not simply igneous features and their partial modification by superimposed deformation can be illustrated by the presence of a system of shear 'fractures' (Pl.2-5). These structures, initially established in the irregularities along the contact between amphibolite and gneiss, bend progressively into parallelism with the amphibolite-gneiss margin on the opposite side of the intrusion, where the deformation is dissipated within the dyke (cf. Pl.2-5).

The state of deformation of these amphibolites is difficult to evaluate in the field due to their fine grained, homogeneous nature. This has probably been the cause of their misinterpretation as undeformed Scourie dykes (Daly et al. 1985). However, the well-developed character of the amphibole lineation, and the good planar fabric they show in most places (e.g. Pl.2-6/7), give enough indications about their deformed nature. In addition, the presence of isoclinal intrafolial (F1) folds affecting thin feldspathic veins within these amphibolites, together with the frequent presence of basic mylonites along their contacts with the host rock, are unequivocal indications that several of these bodies have suffered high deformation.

DOMAIN II

Amphibole schists

This unit consists mainly of finely banded hornblende schists, with varieties including garnet-hornblende schist, clinozoisite-hornblende schist, and chlorite-hornblende schist (Table 2.1). The banded variety is the predominant type along the southwestern limb of the Letterewe synform (the so-called 'Creagh Dharaich hornblende-schist' of Keppie 1967, p.14), while most of the hornblende-schist along the northeastern limb of the fold (the 'Beinn Lair hornblende schist', Peach et al. 1907, pp.239-244) is composed of the non-banded variety.

Interbanded with these hornblende schists is a sequence of extremely mylonitized and discontinuous lenses of metasediments including quartz-mica schists, quartz-feldspar schists, chlorite-tremolite schists, chlorite-hornblende-clinozoisite schists and garnet-quartz-hornblende schists. These lithologies are finely interbanded and occur as discontinuous 'lenses' which were probably produced by the strong mylonitization.

Mylonitization of these amphibole-rich rocks is localized along their contacts with the carbonate-bearing lithologies of domain IV and the gneisses of domain I (where the carbonate-rich rocks are absent).

Evidence for the pre-metamorphic nature of these rocks includes (1) lenticles of saussurite mapped by the Survey (Peach et al. 1907, p.243) and interpreted as igneous concretions and (2) lithogeochemistry. Field evidence and geochemistry (Park 1966, Powell and Park 1969, Johnson and Winchester 1985) suggest the predominance of lava flows, with tholeiitic and composite magma parentage for some of the large units. The possible presence of sills is indicated by high level fractionation patterns (Johnson and Winchester 1985). On the basis of rare earth element patterns these authors have also ruled out the possibility of amphibolite 'dykes' (similar to the ones present in domain I - their 'Scourie dykes') to be representing feeders for the large mass of amphibole schists, and suggest that they represent separate magmatic activity.

DOMAIN III

Metasediments (Furnace band)

These rocks were divided into three broad units corresponding to NW-SE elongate bands (Fig. 2.1): (1) **interbanded schists**, (2) **pale grey siliceous mica schist**; and the (3) **mixed rusty and actinolite schist** (Keppie 1967, pp.10-12, survey sheet 58, 1905).

The interbanded schists include quartzofeldspathic schists with bands of hornblende and chlorite schists, some of which are strongly mylonitized (in particular the quartzose mica schists and graphite schists). These are finely banded rocks with light quartzose layers less than 1-10mm thick (Pl.2-8), where mylonitic features are ubiquitous and large, idioblastic, post-mylonitic garnets are commonly observed.

The pale grey siliceous mica schist is a more uniform unit, with few interbanded layers of mica-schist within the massive fine-grained siliceous mica schist (Clough in Peach et al. 1907, pp.222-224; Keppie 1967, p.11). In some places, for example NE of Inishglass (Fig. 2.1), D1 mylonitization of these rocks is very strong (Pls 3-55, 3-56).

The mixed rusty and actinolite schists are a sequence of brown (ferruginous) quartz-mica schist, graphite schist, mica schist and actinolite schist (Teall and Clough in Peach et al. 1907, p.79 and pp.31-32 respectively; Keppie 1967, pp.11-12). The weathering of these lithologies produced the typical rusty colour as a result of oxidation of their abundant iron sulphide content. A single body of a mesocratic coarse-grained amphibolite was mapped at one locality (NG 960698). It is a thick sill-like body, but no contact with the composite schistosity was observed. Transposed folds within this body are marked by fibrous amphiboles. This amphibolite does not resemble in any way the amphibole schists or the amphibolites amongst the gneisses.

Similar lithologies in the Gairloch region contain small

stratiform sulphide mineralisations with 15-20% of sulphides (pyrite, pyrrhotite and chalcopyrite with native gold: Rice *et al.* 1985). Strong mylonitization of these rocks is observed in Torr Innis Dhomnuill (see Fig. 2.1 - NG 976695) where mylonites along attenuated localized limbs of recumbent folds affecting quartzose bands indicate D3 age for the thrusting (see Chap.3). There are few doubts that these rocks represent metamorphosed sediments. Unequivocal evidence for their early Proterozoic age is presented by Birkman *et al.* (1975) and O'Nions *et al.* (1983, fig.2), where the closeness between crustal residence age and depositional ages of these schists is demonstrated by Nd isotopes.

The similarities between some of the quartzofeldspathic schists and the mylonitized gneisses led Clough *et al.* (1913) to suggest that some of the schists of the Furnace band might be mylonitized tectonic slices of basement gneisses. Despite their similar outcrop appearance, petrographic data shows that (1) K-feldspar (a resistant mineral to mylonitization - see Chap.5) is not present in the mylonitized metasediments (see Table 2.1) and (2) they contain different epidotes - clinozoisite in the sediments and epidote *sensu stricto* in the gneisses (Keppie 1967, p.10). Park (1964), facing this same problem in the Gairloch district, interpreted some of the gneisses (Ard and Mill na Claise gneisses) as modified sediments. However, in more recent work based on geochemical evidence Holland and Lambert (1973) and Park *et al.* (1980) propose that these gneisses are in fact mylonitized basement rocks. The conspicuous layering in the mylonitized siliceous mica schists (produced by variable degree of grain-size reduction), has such striking similarities with sedimentary structures (Pls. 5-4, 5-4a) that if ^{not} observed in association with the ultramylonite rocks and quartz segregation bands could be very misleading (cf. Wheeler *et al.* 1984, Daly *et al.* 1985).

DOMAIN IV

Carbonate-bearing rocks (Falais band)

These include grey, greenish-grey, dark-green or brown impure marbles and dolostones. The most abundant type is the compact

cream coloured Letterewe Limestone (Peach *et al.* 1907, pp.233-235). There is a complete gradation in composition and intensity of deformation between pure crystalline marble, and the dark schistose types where biotite, actinolite, hornblende and plagioclase are abundant. Fragments of banded amphibolite, gneisses and several types of amphibole schist, some of which were not observed *in situ*, are common in the dark marbles and dolostones. These were interpreted by Peach *et al.* (1907, p.234) and Keppie (1967, p.13) as representing tectonic inclusions (but see also Sect. 5.3).

The petrographic and chemical characteristics of these and other marbles in the Lewisian complex are discussed by Rock (1987), who suggests that most of them might have been deposited contemporaneously (see also Chap. 8).

2.3 DISTRIBUTION OF ROCK TYPES

The **quartzofeldspathic gneisses** of domain I occupy the core of the Letterewe synform. The outcrop is tongue-shaped, and is elongate in a northwest-southeast direction (Fig. 2.1). With exception of the SE boundary, which is covered by Torridonian sandstones (Stoer Group), all the others are delimited by the marbles of domain II (Folais band) or the amphibole schists (where the marble band is tectonically disrupted), and represent tectonic boundaries of late D1 age (see Chap.8). There are many thin (1-3 m) bands of amphibolite amongst the gneisses. They show discordance to the dominant gneissic banding fabric (Pl. 2-8). While it is not possible to put individual masses of this size onto the lithology map, the representation shown depicts their overall abundance from place to place and their overall disposition. This shows them folded around the hinge of the large SE-plunging synform, particularly NE of Letterewe and NE of Furnace. In addition there are many other smaller folds which are schematically represented on the lithological map (Fig. 2-1).

The **marbles** crop out along most of the rim of the gneisses, and consist of a unit sandwiched between the gneisses and the amphibole schists. The largest exposures are in the hinge zone of the Letterewe synform. The thickness of this unit along the limbs is greatly reduced or completely attenuated, (mainly) by tectonic processes. Similar to the thin amphibolites of domain I, the representation of these marbles along the limbs of the large synform in the lithological map (Fig. 2.1) is essentially schematic.

The **amphibole schists** comprise the most abundant lithological unit of the Loch Maree supracrustals, and outline the shape of the Letterewe synform in small scale maps (Fig. 1.1). However, most of this unit is located outside the presently studied area, so that the shape of the synform in the mapped ground is marked by the amphibolites of domain I and the marbles of domain IV.

The **metasediments** occur in relatively thin NW-SE elongate bands along the shore of the loch, and form part of the southwestern limb

of the large synform. The nature of their internal contacts is uncertain, being either tectonic (interbanded schist and pale grey siliceous mica schist), or possibly gradational (pale grey siliceous mica schist and mixed rusty schist and actinolite schist). A continuous band of quartz-mica schist and garnet-mica schist borders the Creag Dharaich hornblende schist along much of its length (Fig. 2.1).

In addition to the originally variable thickness of some of the rock units (e.g. some of the amphibole schists; cf. Peach *et al.*, 1907, Fig. 10), the distribution of the rock types and their appearance on the lithological maps (Figs. 2-1, 8-1) is a function of structural control by the Letterewe synform. The asymmetry, interlimb angle and low plunge of this fold (cf. Section 6.2) has partially controlled the width of outcrop of the amphibole schists and marbles, increasing the original pre-fold thickness variations (amphibole schists of NE limb were calculated to be ~3 times thicker than the SW limb before the F2 folding).

The area is cross-cut by several sets of faults, most of which strike NE-SW.

FIGURE CAPTIONS - CHAPTER 2

With the exception of Pl. 2-4 which faces NW, all other photographs were taken from subhorizontal surfaces.

Plate 2-1 Concentration of feldspar megacrysts along a band in protomylonitic gneiss; note the slightly better foliated nature of this band; pen 15cm.; see Map 3.1 [NG 975 704].

Plate 2-2 One of the rare microgranodioritic intrusions observed in the quartzofeldspathic gneiss; pen parallel to composite foliation [NG 966 715].

Plate 2-3 Plagioclase phenocrysts in porphyritic amphibolite; note the incipient development of S₂; coin 2.5cm. [NG 978 712].

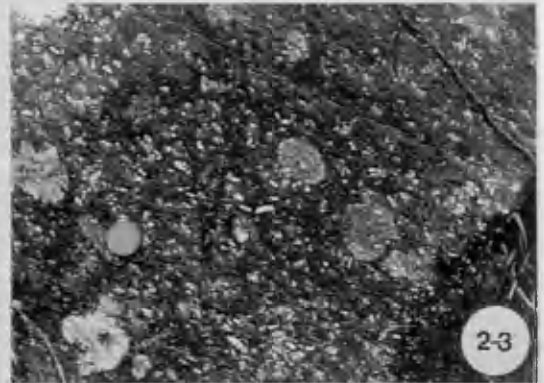
Plate 2-4 Lens of fine porphyritic amphibolite (white dots are plagioclase phenocrysts) within a large banded amphibolite interlayered with gneiss; note the well-developed nature of the felsic bands and the concentration and larger size of phenocrysts along the contacts [NG 978 709].

Plate 2-5 Irregularities of the contact between mafic amphibolite and quartzofeldspathic gneiss; note the swing of the shear 'fractures' (marked by pen) into parallelism with the (top) margin; see Map 3.1 [NG 975 704].

Plate 2-6 Detail of mafic amphibolite discordant to the composite banding (parallel to hammer) in quartzofeldspathic gneiss; note S₁ foliation marked by deformed quartz band within amphibolite; detail of Pl. 3-36; see Map 3.1 [NG 975 704].

Plate 2-7 Well-foliated mafic amphibolite affected by F₂ fold [NG 971 707].

Plate 2.8 Finely interbanded (mylonitic) siliceous and graphite schists; see Map 3.4 [NG 970 696].



CHAPTER 3 STRUCTURAL FEATURES: DESCRIPTION AND CORRELATION

3.1 INTRODUCTION

3.2 DESCRIPTION

3.3 BASES OF CORRELATION AND APPLICATION TO LOCH MAREE AREA

3.1 - INTRODUCTION

Evidence for polyphase deformation is evident at almost every outcrop. Consequently, chronologies of structural events could be established from outcrop to outcrop using criteria that are the general basis of the determination of any local sequence of geological events; namely that (1) deformed structures are older than those that deformed them, and (2) cross cutting features are later than those which they cross-cut (but see Sections 3.3, 6.3, 8.3). There are, however, differences in expression of various structural features, due to variation in rheological properties of different lithologies observed at individual outcrops. This meant that correlation of chronologies from place to place throughout the area could not be treated as straight forward. In addition, variations in expression resulting from the superimposition of structures on to multi-layered assemblages with diverse disposition (e.g. shallowly dipping and steeply dipping limbs of F2 folds) had to be taken into account. To deal with such factors, the area was divided into four domains (Fig. 3.1). The boundaries of these domains coincide approximately with the limits of the main lithological units, so that each domain contains rock assemblages that are not widely disparate in rheological characteristics. Domain I consists mainly (80%) of quartzofeldspathic gneisses and amphibolites. Domain II is composed almost entirely of a variety of amphibole schists, and domain III consists predominately of metasediments with minor bands of amphibole schists. Domain IV consists

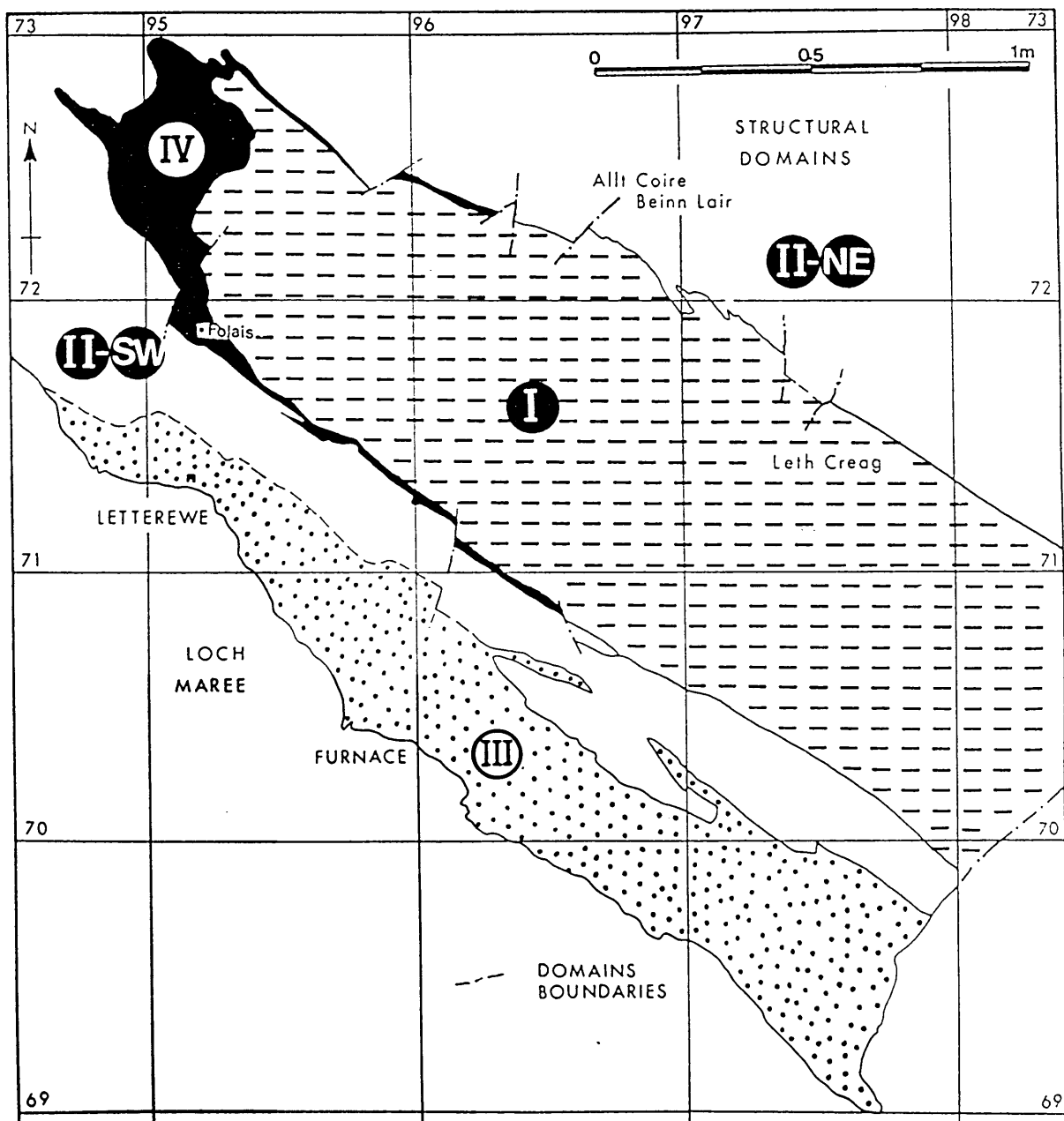


Figure 3.1 STRUCTURAL DOMAINS

- I - Quartzofeldspathic gneisses
- II - Amphibole schists
- III - Metasediments
- IV - Marbles

predominately of marble (see Chapter 2).

The subdivision into these domains was a result of constant reassessment of an initially formulated hypothesis, so that the understanding of the geometry of the area was progressively built up through the repeated examination of the outcrops. With the help of microfabric studies and the progression of mapping a model of the geometry of the whole area was set up. The procedure was similar to the one discussed by Hopgood (1980, p.64), with the difference that in this case the area studied was dominated by a single major structure, the large F2 Letterewe synform. Demonstration of its shape resulted mainly from mapping the distribution of amphibolites interbanded with gneisses (cf. Peach et al. 1907, p.193), and this in turn meant that the control of the major fold on the geometry of the younger structures could be established.

The influence of the Letterewe synform on the distribution of the lithological units was an important factor in the choice of the domains (see Chaps. 2 and 8). The choice was also influenced by the way that it permitted a rational presentation of both description and analysis of the distribution, orientation and geometry of the structural elements that developed during the several phases of deformation which affected the rocks in this area (Chaps. 2 and 6). The order in which features are described clearly implies that a correlation of structures has been made (bearing in mind all the aspects discussed in section 3.3).

An outline of the principal structures that were mapped at the scale of 6" to 1 mile is presented below, and a summary of the characteristic features of the structures in the four domains is set out in Table 3.1. This presents a sequential development for each of the different domains, correlations made between domains, and how each domain is considered to

fit into an overall scheme of structural evolution. An outline of the spatial correlation of structural features is given in Table 3.2. This is a schematic representation showing correlations made in the various domains across the major F2 composite fold (Fig. 8.2). The detailed evidence and the philosophical arguments which form the bases of the correlations made are set out in sections 3.2 and 3.3, respectively. Since the relationships are best shown in domain I, the structural sequence recorded for this domain is more extensively documented than those of domains II, III and IV.

In Table 3.1 the structural features and structural sequences for the different domains are labelled with subscripts a,b,c, etc. These only have sequential significance for the domain for which they are used; there is no implication that structures labelled 'a', or 'b' etc. in one domain correspond to structures 'a' or 'b' etc. in a different domain.

In the text descriptions and on the diagrams subscripts 1,2,3 etc. (F1, F2, F3 etc.) are used to avoid confusion of multiple notation systems. This numbering corresponds to the last column of Table 3.1 (general sequence for the area), which indicates the conclusions drawn from correlation of the more local sequences (Table 3.2) with reference back to the local sequences possible using this table.

The correlation of these local sequences (Table 3.2) has been made with a considerable degree of confidence. It shows only the structural features used for correlation and the subscripts a,b,c, etc. correspond to the local sequences presented in Table 3.1. Since this table represents a cross-section of the area (from NE to SW) the amphibole schists are shown twice corresponding to both limbs of the major synform. The following features or groups of features are important in making correlations between domains (see section 3.2):

TABLE 3-2 -- DIAGRAM OF CORRELATION IN A CROSS-SECTION (NE-SW) OF THE LOCH MAREE AREA

DOMAIN I (NE)	DOMAIN I	DOMAIN IV	DOMAIN II (SW)	DOMAIN III
AMPHIBOLE SCHISTS	GNEISSES AND AMPHIBOLITES	MARBLES	AMPHIBOLE SCHISTS	METASEDIMENTS
STRETCHING LINEATION + FB - MYLONITES	STRETCHING LINEATION + FB - MYLONITES	MYLONITES	STRETCHING LINEATION + MYLONITES	STRETCHING LINEATION + FB - MYLONITES
	BOUDINS	BOUDINS	BOUDINS	BOUDINS
F _c FOLDS	F _c FOLDS		F _c FOLDS	F _c FOLDS
	F _e FOLDS		F _d FOLDS	F _d FOLDS
F _e FOLDS	F ₁ FOLDS	F - 'mid' FOLDS	F _e FOLDS	F _e FOLDS

1. The stretching lineation and/or mylonites in domains I(NE), I, IV, II(SW) and III.
2. The boudins in domains I, IV, II(SW) and III.
3. The reclined to upright buckles with strong axial planar foliation in domains II(NE), I, II(SW) and III.
4. The recumbent chevron folds in domains I, II(SW) and III.
5. The upright buckles in domains II(NE), I, IV, II(SW) and III.

3.2 DESCRIPTION

3.2.1 Domain I - Quartzofeldspathic gneisses

D-banding deformational phase.

The most prominent foliation in this domain is defined by an alternation of quartzofeldspathic and mafic-rich bands (biotite and hornblende), in which there is a dimensional alignment of the minerals. The bands^(Sb) are generally 5-10 cm across (Pls 3-1, 3-20, 3-30), but locally are 40-50 cm. These fabric elements are folded, boudinaged and off-set in dissected fold hinges (F1), and are subjected to partial or complete obliteration as a result of intense mylonitization late in the D1 phase. The superimposed features account for much of the irregularity of the banding throughout the domain.

In addition to this banding, which is interpreted as the result of metamorphic processes, there are thin anastomosing masses of quartzofeldspathic material that now show an

irregular network pattern (Pl.3-2). These bands are discordant to the metamorphic banding and show no evident S1 foliation. Accordingly, the characteristics of the lithological layering are the result of more than one process, acting at more than one time, but with the earliest recognized banding being the dominant feature in much of the domain.

The banded amphibolite bodies show a well-developed grain shape fabric and compositional banding (Pls. 3-3, 3-4, 3-9), some of the layers being of ultramafic nature (Pl. 3-20). These basic rocks are so intermixed with the quartzofeldspathic gneisses that unique separation of the two types in the field is difficult (cf. Peach et al. 1907, p.195).

A common feature within the large units (NG 970 709) is the partial remobilization of feldspar from the felsic bands, giving a geometry resembling several 'imbricated boudins' due to the anastomosing fashion in the distribution of these feldspathic veins (Pl.3-8).

No folds were seen associated with this phase of deformation, but their unequivocal identification would be a very difficult task due to the characteristics of the D1 deformation phase (see also section 4.3.7)

D1 deformation phase

The folds developed during this phase are tight to isoclinal, and show long limbs (usually attenuated) with thickened noses affecting both the S-banding and the (anastomosing) quartzofeldspathic material (Pls. 3-1, 3-2). Folds having amplitudes of 2-3m are rare; they are seen only where there are interbanded lithologies. Their attitude varies from upright to recumbent (Pl.3-7), being generally controlled by the geometry of the later folds.

Where affecting the banded amphibolites and interbanded gneisses, the F1 folds in places show sheath-like shapes (Pl.3-6). In the mafic amphibolite bodies the F1 folds are isoclinal, with long limbs and thickened hinges, usually affecting thin (<1 cm) syn-D1 white feldspathic veins (Pl.3-5). These amphibolites show discordant intrusive relationships to the gneisses. However, no set of F1 folds deforming these contacts was observed in the area mapped (see Chap.6).

Linear structures developed during the D1 phase include fold axes (sometimes plunging to opposite quadrants - see Chap. 6), irregular mullions and fold mullions (Pl.3-10), strong amphibole mineral orientation, and also deformed phenocrysts of feldspar in the gneisses and porphyritic amphibolites (these feldspars assume a prolate or oblate shape when seen at a section which does not contain the extension direction: see Sect. 6.3). In some of the amphibolite bodies, the deformation of the phenocrysts gave rise to a fine and continuous to semi-continuous banding (see Chap.7). All stages from undeformed phenocrysts to a prolate and then an oblate shape are observed. This is interpreted as indicating progressive deformation as D1 zones of high strain are approached (Pls 3-11, 3-12, 3-13). The principal zones of D1 deformation and mylonitization correspond to the boundary between domain I and the amphibole schists. This zone is occupied by the marbles of domain IV, and is referred to in this study as 'Letterewe or Loch Maree thrust zone'.

Boudins that affect S1 and that include F1 folds are seen in a few places (Pl. 3-9). As the fabric axial planar to F2 (S2) cuts across the boudins, (a feature best observed in the more mafic lithologies), the boudin development is interpreted as a late D1 feature that developed after the most intense phase of F1-S1 formation. Corresponding features and relationships in domain II indicate that boudin formation was not just a local phenomenon confined to domain I.

Where affected by strong mylonitization the gneisses and the various types of amphibolite exhibit a small-scale banding, with the feldspar-rich portions showing a porcelain-like appearance. Some of these bands also show more than one set of intrafolial folds affecting white fine siliceous bands (Pl. 3-15). Outcrops where (F1) folds are refolded by a later set (F2) are common in these mylonitized gneisses. Although in several examples the F2 folds do not show their typical attitude, the presence of associated features such as (1) folding of the L1 stretching lineation, (2) hinge detachment, and (3) parasitic minor folds (Pls. 3-16, 3-16a, 3-17, 3-18), together with a comparison of nearby outcrops was considered sufficient for their identification (see sect. 6.3).

D2 deformational phase

In the southeastern portion of this domain a large F2 fold affects the gneisses and a large banded amphibolite body (see structural map), and is partially responsible for the geometry of the 'Letterewe synform' (Peach et al. 1907, p. 193). Clear F2 refolding and S2 cross-cutting has affected D1 features (F1-S1) and late D1 boudinage. This is observed mainly in the outcrops along the hinge of this fold (Pl. 3-4). The fold is an asymmetrical and reclined synform with NE vergence, SE plunging axis and an almost E-W striking axial plane (see sect.6.2.1). The subvertical attitude of the southwestern limb has favoured overprinting by the recumbent F3 folds, whilst the relatively shallow dip of the northeastern limb ($45-30^\circ$) has favoured overprinting by the upright F4 folds (see Chap.8). The development of the cogenetic small-scale folds is very much dependent on the nature (composition and thickness) of the affected lithology (Pl.3-20). Over most of the domain they are tight, concentric, and upright (Pl. 3-19) to reclined (Pl. 3-20a) structures with parasitic minor folds, sinusoidal shapes,

and wavelength all depending on the multilayer assemblage they deform. Where affecting quartzofeldspathic and biotite-rich bands they show thick hinges and attenuated limbs (Pl.3-21). The axial-planar foliation (S2) in the gneisses of the northern part of the domain is a finely spaced cleavage showing a sinistral displacement sense of the affected banding, whether mylonitic (Pl. 3-23) or not (Pl. 3-22). Some of these planes seem to be preferential sites for movement, sometimes causing shearing-out of the limbs of small folds (Pl.3-23). In the northern part of this domain, where gneisses affected by D1 mylonitization have been deformed, the F2 folds are polyclinal and show strongly curvilinear hinges and very complex structural patterns which do not show any kind of regularity (Pl.3-18). However in some nearby outcrops where this lithology is deformed there are F2 folds with geometries similar to F2 folds elsewhere (Pl. 3-19). In these zones of high D1 and D2 strain the F2 folds have no associated axial planar foliation, the deformation being similar to that operative in the development of conical and pygmatic structures.

In the banded amphibolite S2 is a distinct biotite-amphibole growth axial planar to F2 folds; it is best seen in the mafic units in the hinge zone of the Letterewe synform (Pl.3-20). However, in places where the gneisses or feldspathic bands are interlayered with thin bands of mafic amphibolite this mineral growth is not prominent, partially due to the relative lack of phyllosilicates (biotite mainly) in relation to amphibole crystals that show the structures of an "L"-tectonite (see Chap.4).

The perfect coaxiality of F1 and F2 folds is a remarkable feature and makes it practically impossible to distinguish between an L1 and an L2 amphibole lineation. However, in the porphyritic amphibolites the L1 lineation can be distinguished because of the characteristic presence of stretched feldspar phenocrysts.

Coaxial refolding of small F1 intrafolial and cylindroidal F2 folds, as well as white quartz and quartzofeldspathic veins discordant to the composite banding (S-banding & S1), resulted in the development of type 3 interference structures of Ramsay (1967).

D2a deformational phase

Several narrow NW-oriented shear zones (usually less than 1 metre in width) are developed mainly in the eastern half of this domain. They generally show a subvertical attitude, dipping either to the SW or the NE; their observed length is usually limited by the exposure (map 3.1). The associated folds that are restricted to the margins of these shear zones are concentric, relatively tight, and have steeply plunging axes and sub-vertical axial planes (Pl. 3-24) which in places curve along the profile of the fold. The axial planar foliation is a spaced cleavage, crenulating a composite banding (Pl. 3-24). This banding clearly contains components of S1 and S2, but because these outcrops are sub-horizontal surfaces localized along the limb of the major F2 fold, the traces of all these foliations are parallel (Pl. 3-26).

The emplacement of narrow veins of granitic pegmatite and quartz along this zone is a common feature, sometimes at high angles to the composite banding (Pls. 3-26, 3-26a, 3-27). Although cataclastic features are shown by the pegmatites at some places these were not produced by brittle reactivation of the shear zones. They are thought to represent original features produced by the building up of fluid pressure during D2a deformation. Accordingly, the presence of relict fragments of gneisses with the distinct L1 lineation within pegmatites (and showing various stages of 'pegmatitization'), suggests that fluids played an important role in pegmatite development and emplacement.

This is also indicated by the existence of diffuse as well as sharp contacts (Pl.3-27) between the host rock and pegmatites.

The development of phyllonite and pseudotachylite along these zones is a very localized feature being restricted to some of the wider zones in the gneisses (Pl.3-24), where the brittle behavior was favoured at a particular time. Where these shear zones affect the porphyritic amphibolites the features produced show evidence of more ductile deformation than in the gneisses (Pl.3-25).

D3 deformational phase

The refolding of F1 rootless folds by the recumbent F3 folds is sometimes observed (Pl.3-29), but this is a rather rare feature because the development of the recumbent folds occurs only on a localized scale. More commonly a spaced cleavage (S3) is seen to cut across the composite (Sb+S1+S2) banding (Pl.3-1, 3-2). As F3 folds commonly have a large interlimb angle and a wavelength in the order of metres, they are almost exclusively observed in the outcrops with a deep topographic profile (particularly in the southern part of this domain, where they affect the steeply dipping SW limb of the F2 major synform). This has resulted in the occasional sub-horizontal attitude of the composite banding. F3 folds are usually concentric buckle folds with a sub-horizontal axial planar crenulation cleavage (Pl.3-28) or spaced cleavage (depending on the lithology affected), and have curvilinear hinges that plunge NW at low angles. Where they deform alternating biotite-rich and thin (10cm) quartzofeldspathic bands they have a smaller interlimb angle, a smaller wavelength, and show detachment along the lithological boundaries and well developed parasitic folds with an associated axial planar gradational crenulation S3 cleavage (Pls 3-21, 3-29). In the massive quartzofeldspathic bands S3 is a set of sub-horizontal finely spaced fractures; offsets of the composite

banding indicate that movement has taken place along these fractures.

D4 deformational phase

The F4 folds deform F1 and F2 folds and their associated structures. In this domain they were seen affecting the F3 recumbent folds possibly due to the large interlimb angles and dimensions of the F3 structures. The F4 folds affect the L1-L2 lineation (Pl.3-33) and this is one of the principal causes for reversals of L1-L2 plunge direction (see sect.6.2.1.1). In some places, where the F2 and F4 folds are of almost equal dimensions, the later set modified the geometry of the F2 folds and caused widening of the spaces between the folded bands as well as partial refolding of detached bands (Pl.3-34).

The F4 folds are not evenly distributed throughout the area, being best developed in the gneisses and amphibolites of the northern portion of domain I. They are concentric, upright (or steeply inclined) 'buckle' folds with steep axial planes and moderate SE - plunging axes. Sinusoidal shapes, parasitic minor folds and development of 'shoulders' are common features (Pls 3-30, 3-31). Nose detachment is frequent, with the gaps sometimes 'mechanically' in-filled with a 'melange' of more ductile material (Pl.3-32). Such features are usually shown in bands differing in competence and thickness from adjacent bands, where slickenside^{lineations} at high angles to fold hinge are sometimes observed on the folded surface. Disharmony of the folds, inversion of the sense of closure and cusped and lobate contact features (Ramsay 1967, p. 383) between quartzofeldspathic and mafic-rich bands are sometimes observed (Pl.3-30). Rarely, an S4 crenulation cleavage is seen, and the complete absence of any feature suggesting movement along this foliation makes it easily distinguishable from the S2 cleavage in places where the geometry of both F2 and F4 folds is similar. Where

F1 or F2 folds were folded into an upright position by D4 deformation, e.g. at [NG 966718], they can be distinguished from F4 folds in most cases on the basis of the S1 mineral growth and the nature of the associated L1 stretching lineation.

Structures formed in the late deformational phases in this and other domains are described in Section 3.2.5

Basic igneous intrusions

Basic igneous intrusions are usually seen emplaced along the metamorphic segregation banding (Pl.3-35). In some places discordant relations between these 'mafic' and 'porphyritic' amphibolites and the old gneissose banding are observed (Pl.3-36). Although of clear intrusive nature (see Chap.2), these amphibolites show all the D1 fabrics including the mylonitic features (Chap.5). This shows that they have been emplaced after the formation of the segregation banding (S-banding), but during or before the development of D1 fabrics. Features developed during D1 include (1) a foliation (S1) oblique to the margins of the discordant bodies, (2) a pervasive amphibole lineation observed even in the low strain parts of the rock (3) boudinage and other late D1 features indicating shortening parallel to their lengths. A compositional variation parallel to their margins is ascribed to mimetic recrystallization of a flow banding (Pl.3-35). However a schistosity also parallel to the intrusion margins is more difficult to interpret (cf. Talbot 1982).

3.2.2. DOMAIN II - AMPHIBOLE SCHISTS

D-banding deformational phase

The uncertainties about the nature and identification of

the composite banding (S banding + S1 + S2) in this unit is due to: (1) the strong transposition during D1 and D2 phases, and (2) the presence of fine-grained feldspathic bands along the foliation which may be axial planar to folds as late in the sequence as F2 (Pl.3-38).

The oldest identified feature in the amphibole schist on the southwestern limb of the Letterewe synform is a boudinaged feldspathic 'segregation' banding folded by the F2 folds (Pl.3-39). Although unlikely, it is possible that this banding could have been developed during the D1 event, since the boudinage (assumed to be of the same age throughout the area) is of late D1 age. However, along the northeastern limb of the major synform where mylonitized garnet-quartz-mica schists locally crop out in the core of one of the F4 upright buckles (Pl.3-41), it is possible to identify both F1 and F2 folds showing their typical features. This is interpreted as an indication that, at least in that part of domain II, the banding predates F1 folds. Unfortunately however, at most localities it is very difficult to be sure about the age of the banding in the amphibole schists (sensu stricto) which make up most of the lithologies of this domain. Problems of correlation could arise depending on the preferred interpretation of this evidence. They will be discussed in more detail in Section 3.3.

D1 deformational phase

Folds which deform the earliest recognized banding in the interbanded amphibole schists and quartz-mica schists occur on the northeastern limb of the major F2 synform. They are isoclinal, with thickened hinges (Pls. 3-41a, 3-41c, 3-43), long limbs, and generally are of small dimensions. There is an axial planar muscovite-biotite growth which defines a foliation (S1), and its intersection with the lithological banding results in an intersection lineation. This has a NW

trend but its original attitude is difficult to assess due to the unusual geometry of some of the F2 folds (see below).

In the amphibole schists, the only feature which could be attributed to the D1 deformational phase is the boudinage of feldspathic bands which is folded by F2 folds (Pl.3-39).

D2 deformation phase

The F2 folds that are particularly well shown in the crags behind Letterewe house [NG 952 717] deform the lithological banding (Pl.3-37) and the features developed during D1 (F1+S1) deformational phases (Pls 3-41b, 3-41c, 3-42, 3-43). They are small, tight to isoclinal, cylindrical with sinusoidal shapes in profile sections; 'parasitic' minor folds are frequently seen (Pls 3-37, 3-38). Thickening of the hinges and attenuation of limbs is also common, being observed particularly well in units of contrasting composition (Pl.3-40). The folds have subvertical axial planes and shallowly SE-plunging hinges. Linear structures associated with these fold include small scale feldspathic mullions and an amphibole mineral lineation which is commonly difficult to identify even in the mafic units.

The axial planar foliation is a fine amphibole growth that, although not very pervasive, can be observed in the more mafic units (see Chap.4). Thin feldspathic veins showing folds consistent with F2 folds but which, in parts, seem to cut the S2 foliation are sometimes developed (Pl.3-38). Some white quartz veins that are also discordant to the banding show folds with geometry compatible with the structures developed during D2 (Pl.3-37a).

In places [e.g. NG 971 722] the transposition of the

structures in amphibole-bearing rocks during D2 seems to have been particularly strong. The F1 and F2 folds in micaceous quartz mylonite are folded by upright F4 folds, but the juxtaposed amphibole schist shows only a single banding affected by the F4 buckles (Pl. 3-41). The geometry of the F2 folds in this outcrop is of crucial importance for the understanding of the kinematic processes that have affected the rocks during the D2 deformation phase (see Chap.6). The folds are tight to isoclinal, with two contrasting geometries. Most of them have exceptionally rectilinear hinges with the development of 'fold mullions', while others have curvilinear hinges with internal angles of dispersion usually greater than 90° . Some of these acylindrical folds clearly show refolding patterns of F1 structures (F1+S1+L1, Pls 3-41c, 3-42, 3-43). The curvilinear-hinged folds show the initial stages of the development of a stretching lineation; this permits the direction of tectonic transport during part of the D2 deformation to be established (Pl. 3-42). Some of the F2 cylindrical folds affect L1 which is disposed at about 30° to the F2 fold hinges. Discussion of the angular relationships between these two structural features, and of the unusual geometry of the F2 folds is given in Chapter 6.

D3 deformational phase

The F3 folds are almost exclusively seen in the amphibole schists on the steeply-dipping southwestern limb of the major synform. There they deform F2 folds in a nearly coaxial fashion, giving rise to type 3 interference patterns (Pls 3-40, 3-45, 3-46). They are open to tight chevron folds with angular to round hinges (Pls 3-44, 3-46); some are asymmetrical (Pl.3-51a). In many instances a remarkable variation of interlimb angle along the trace of their axial planes is shown (Pl.3-44). Where little affected by later phases the axial planes and axes present a sub-horizontal attitude. Their trend is controlled by the attitude of

the previous structures. Features such as curved axial planes (Pl.3-47), hinge detachment with the spaces filled with white quartz, and "parasitic" minor folds are common (Pls. 3-50, 3-52). Minor thrusts (Pl.3-49) occur along the limbs of some asymmetrical folds, indicating in most cases a southwesterly direction of tectonic transport, though displacement towards the NW was not rare (see Chap.6).

The axial planar foliation to these folds (S3) is a gradational crenulation cleavage usually best developed in the more finely interbanded units (Pl.3-48). In the more competent bands it is a spaced cleavage (Pl.3-45) with quartz infill. A pod-like crenulation lineation is sometimes developed on the composite banding(S banding+S1+S2) surface.

D4 deformational phase

Upright SE-trending open buckle folds deform the F3 (asymmetrical) folds and their associated structural features (Pl.3-51). Generally they are concentric, with shallow plunges and interlimb angles of 90-120°; the angle is related to the degree of development of banding shown by the lithology, as well as the interlimb angle of the affected folds. Where the amphibole-bearing rocks are distinctly schistose the folds assume chevron shapes with the frequent development of a single fracture along the axial plane. Where F2 folds are refolded the interlimb angle of the F4 folds reaches its highest values, e.g. along the hinge of the major synform as well as along its southwestern limb.

3.2.3. DOMAIN III-METASEDIMENTS

D- banding deformational phase

The banding in this unit is a composite feature, probably resulting from modification of lithological layering (in sediments) during D1, D2 and D3 deformational phases. The

sedimentary component of this structure is best demonstrated on a large scale by the lithological variation (see Chap. 2). At outcrop and microscopic scales this structure is difficult to unequivocally identify due to the effects of D1 transposition and superimposed M1 metamorphic segregation (see Chap. 7). This modified lithological layering is observed as remnants of mica-and feldspar-rich bands along hinges of small (F1) folds in more competent units such as micaceous quartzites and siliceous mica schists (Pl.3-53).

D1 Deformational phase

D1 structures are represented in this domain by decimetric scale folds which deform relics of the 'banding' and were deformed during the subsequent folding phases (Pl.3-53). Usually they are best preserved in the more competent quartzofeldspathic and quartz-rich units, being in most cases isoclinal with thickened noses and attenuated limbs (Pl.3-54). Geometrical reconstructions of L1 disposition indicates a NW-N trend for this lineation; unfolding technique assumes that there was no rotation of F2 folds.

Away from zones of high D1 strain the axial planar foliation (S1) is not particularly strong muscovite-biotite growth. In high strain zones mylonites are developed, their most prominent expression being in the siliceous mica schists and feldspathic schists with the more feldspathic bands showing a porcelanic appearance very similar to that seen in domain I (cf. Pls 3-15 and 3-56). White quartz bands showing the L1 lineation, in general refolded by strongly non-cylindrical (F2) folds are a prominent feature in certain lithologies (Pl.3-55).

Plots of axial planes and axes of the few identified F1 folds show a large dispersion with predominantly NW strikes and shallow dips for the former and shallow plunges and N-NW trends for the latter (see Chap.6).

D2 deformational phase

The deformation of F1 folds (and their associated elements) by approximately cylindrical F2 folds gave rise to type 3 interference patterns (Pl.3-53). Where the F2 folds are dominant in an outcrop they generally have steeply dipping limbs affected by smaller F3 folds and axes that are bent by the 000° and 040° phase (map 3.4). The F2 folds are isoclinal to tight with thickened hinges and associated minor folds. Some show reverse sense of closure of the hinges (Pl.3-57), and sometimes local transposition of the folded composite banding (Pl.3-57a). In the siliceous mica schist, and in some other lithologies in which a mylonitic banding was developed during D1, the F2 folds are convolute (Pl.3-56). Because of this, in some places F1-F2 relationships cannot be demonstrated unequivocally. However, some F2 folds clearly deform L1 which is prominently developed in the white quartz-rich bands of mylonitized sediments. There the F2 folds assume conical shapes, and there is a reasonably well-developed S2 foliation (Pl.3-55).

The S2 axial planar foliation, which is a fine mica growth, is better developed in the cylindroidal folds than in some of the conical ones, being represented in the latter by a fine cleavage (Pl.3-55). In the convolute folds this foliation (S2) is difficult to identify but an intersection lineation is sometimes visible on the banding surface; whether it is a D1 or D2 feature it is difficult to determine. Like the F2 folds these structures have NW-trending axes and NW-striking axial planes, the dip of which is variable.

D3 deformational phase

In the few places where refolding relationships between F1, F2 and F3 can be demonstrated with confidence, the successively formed folds are almost coaxial, forming type 3 interference patterns (Pl.3-54). However, perfectly coaxial relationships are less common than in domains I and II (Pl. 3-58). F3 refolding of L1 and L2 at variable angles (Pls. 3-61, 3-62) is very frequently expressed, variation in attitude being attributed to deformation of pre-existing curved features, as well as to type of mechanism of deformation active during the D3 phase (see Chap.6). Stereonets in Chapter 6 show the higher dispersion of axes and distribution of axial planes of these folds.

F3 folds are generally tight to isoclinal, some with amplitudes in the range of 5-10 metres. The existence of long limbs, frequently attenuated where there are ductility contrasts, makes the expression of these folds different from the F3 folds in domain II. In places, attenuated limbs pass into thrust planes (Pl.3-59a) showing a southwesterly, or more frequently, northeasterly direction of tectonic transport. Parasitic minor folds and bifurcation of the hinges producing axes with quite variable trends (Pl.3-60) are common features. Slickenside ^{lineations} and quartz fibre growths at high angles to the F3 fold axes are sometimes seen on the composite banding surface (Pl.3-61), indicating the active character of this banding during the D3 phase. Extension of the composite banding along the outer layers and small thrusts in the core of the folds are sometimes observed (Pl.3-59).

An axial planar gradational crenulation cleavage (usually tight) is generally restricted to the hinge zones; where little affected by later phases it has a sub-horizontal attitude. In the more siliceous units this cleavage shows a transition to a finely spaced cleavage. Where this intersects white quartz bands rods are formed. L3 is frequently seen in the more micaceous units as a 'pod-like' crenulation lineation (Pl.3-62)

D4 deformational phase

The F4 folds (best developed in the metasediments along the shore of Loch Maree but poorly shown in the siliceous mica schists), deform F3 folds. Due to their large wavelength compared to F1 and F2 folds, the effects of these open buckles are most prominently shown in the field by the modifications they cause to the dip of the axial planes of the older F3 fold phases. Since the refolding is almost coaxial (type 3 interference patterns) the attitudes of axes of phases earlier than F3 are virtually unmodified (see Chap.6). The F4 folds are open upright (or steeply inclined) warps with shallowly plunging axes (Pl.3-63). Most are concentric but in some places they show chevron style. There is an axial planar spaced cleavage in most of the units but in some mica schists a gross crenulation cleavage is developed. Their trends are NW-N and most of the axial planes dip towards the northeast.

3.2.4 DOMAIN IV - MARBLES

D-banding deformational phase

It is as difficult to assess the nature of the 'early' banding in this domain as it is in domain II. It consists of an alternation of pure and impure (amphibole-bearing) bands of variable thickness, together with occasional bands of amphibole schists (Pl.3-68) and white quartz (Pl.3-65). Patches rich in garnet are sometimes observed amongst the impure marble.

The uncertainty in the correlation of the folds and foliations in this domain with those in other domains, and the rheological properties of the lithologies mean that the development of the banding cannot be ascribed to a specific phase of deformation. It could be the result of sedimentary

layering, D1, D2, or even a combination of these. The mylonitic component is strong, so that D1 deformation played a significant or major role in its development (see Chap.5).

D-'early' deformational phase

The earliest recognized set of folds show the widest range of styles, from intrafolial and isoclinal (in which attenuation of limbs, thickening of hinges and nose detachment are common: Pl.3-66), to concentric (Pl.3-68) and box folds (Pl.3-64). They fold the 'early' composite banding and are usually non-cylindrical plane (Pl.3-67) to non-cylindrical non-plane in places.

Axial planar fabric is not common, but where seen is a fine and closely-spaced cleavage which gives rise to an intersection lineation on the surface of the banding. Where amphibole-mica schists are affected there is a local development of a gradational crenulation cleavage (Pl.3-68). The existence of much tighter folds in thin siliceous layers interbanded in the dolomitic marble (Pl.3-65) provides evidence concerning the magnitude of the layer parallel shortening suffered by the thicker carbonate-rich bands. Apart from the banding, small boudins and mullions are the only refolded structures observed. The boudins seem to be imbricated at the cores and stretched out (along the banding) in the outer parts of the folds (Pl.3-68). The mullions, which were observed only at one locality in this domain [NG 952 720], are at high angle to the fold axes.

D4 deformational phase

Very open upright warps affect the folds and fabrics described above. Their axial planar fabric is a convergent

fanning spaced cleavage which is sometimes difficult to identify (Pl.3-66). This is due to both (1) the superimposition of fractures associated with the development of the NW-trending faults and (2) the large wavelength/height ratios of the F4 warps that make it difficult to relate the position of the cleavage to the geometry of the folds.

3.2.5 D-LATE DEFORMATIONAL PHASES (in DOMAINS I, II, III, IV)

A number of sets of upright open warps that postdate the D4 structures retain a regularity of attitude, interlimb angle and dimensions throughout the whole area. Accordingly they are described collectively as sets, and not domain by domain. The strike of axial planes (and trend of axes) remains fairly constant for each set (see Chap.6) and for convenience they are referred to according to the strike of their axial planes as measured in the field; 000°, 040°, etc. The warps are usually of small amplitude and large wavelength and are commonly confined to relatively narrow belts. Axial planar fabrics are generally spaced cleavages and the relative ages of some of the phases was established on the basis of cross-cutting cleavages in the few places where relationships were observed (Pl. 3-71, maps 3.1, 3-3.4).

The oldest of these late deformational phases are the 000° and 040° sets, but direct evidence to establish which of these two is the older has not been obtained. The 060° and 090° sets are even younger (000° and 040° were affected by 060° and 090°), but once again, mutual relationships of these two sets could not be established with confidence. However, based on factors such as a general decrease in the ductility of the affected rocks (indicated by an increase in

the interlimb angle, wavelength/height ratios and pervasiveness of the axial planar foliations), it was assumed that the D000° was the oldest phase of deformation followed by D040°, D060° and D090°. Although it seems obvious that factors such as (1) variation of strain magnitude, (2) nature of the affected lithology, and (3) previous attitude of the folded structure, could all produce similar features, this sequence is consistent with the few pieces of evidence for the relative age of the fold sets (see above), and also provides an initial working hypothesis without materially affecting the overall correlation of deformational phases.

Reactivation of these late-formed cleavages associated with brittle deformation is very common. It is particularly strong along the 000° and 040° directions giving rise, in several instances to fault zones. In some places where these zones of fractures intersect each other the fragmentation of the affected lithology is remarkable giving rise to 'chess board' patterns (Pl.3-72). In many localities fractures trending 060° and 090° cut across late crush zones, suggesting that they represent reactivation after the development of the Loch Maree fault set with which the crush zones are probably associated.

The folds of these late deformational phases have sub-vertical axial planes, are not cylindrical, and show variable orientation of axes mainly due to the control by the geometry of the previous structure. These 'cross folds' were probably responsible for changes in orientations of D4 and earlier formed structures. However any such changes would only be slight because of the large interlimb angles and small amplitudes of these concentric folds which die out along their axial planes.

D 000° deformational phase

Folds (F000°) which deform F4-S4, and particularly the trend of older lineations (L3, L2-L1), vary from being concentric

asymmetrical (sinistral) with parasitic minor folds in some of the more massive units (e.g. the amphibole schist of the southwestern limb of the major synform, Pl.3-69), to symmetrical upright chevron folds and kink bands in some of the chlorite schists interbanded with the marbles. Most are open structures, with variable plunge of axes but fairly constant trend and strike of the axial plane (000°). The interlimb angle varies from 70° to 150° and the folds usually show round hinges and variable wavelength to height ratios (but frequently about 8) (cf. Hansen 1971). The axial planar foliation is a steeply dipping convergent spaced cleavage ($S000^\circ$) but in more micaceous units a zonal crenulation cleavage is not uncommon. Evidence of reactivation of this cleavage is shown by the common development of brittle features which contain calcite, quartz and chlorite.

The $F000^\circ$ folds are irregularly distributed. Their best development is where the composite banding was steeply dipping (Pl.3-69).

D 040° deformational phase

The 040° folds are usually upright symmetrical gentle warps with round hinges, interlimb angles of 90° - 160° , and large wavelength to height ratios (10 upwards; Pl.3-70). They are best developed where affecting a sub-horizontal composite banding, and frequently deform L1-L2 and associated folds (Pl.3-70). There is an axial planar spaced cleavage ($S040^\circ$) in most of the lithologies but in more micaceous units a wide crenulation cleavage is sometimes observed. As in the case of $S000^\circ$, brittle fractures parallel to $S040^\circ$ indicate reactivation; in some cases these fractures appear to cut and displace 000° -oriented fractures. The presence of quartz, opaque minerals, calcite and sometimes the presence of fresh-looking plagioclase along zones cut by these fractures indicates they were channel ways for fluids. In

places, reactivation has given rise to fault-breccia, for example in the marbles on the northwestern limb of the major synform [NG 958 724]. Pyrite crystals up to 5cm across occur in a pure calcite 'matrix' produced by fragmentation and remobilization of the host rock.

The fairly constant strike of axial planes and trend of axes of these folds is one of their principal characteristics.

D 060° deformational phase

The folds (F060°) developed during this phase are rarely seen in most of the lithologies, being restricted to the marbles and some of the mica schists where S composite is flat-lying. There, warping of the axial plane of F early recumbent folds (S3) and of 'L-early' lineations are the most common features. They are expressed as a set of gentle warps with a very spaced axial plane cleavage (S060°). The brittle overprinting is manifest as fault zones showing either sinistral or dextral sense of movement (Pl.3-73). Some such zones which show intense cataclasis, cross-cut crush belts associated with the Loch Maree fault set. This indicates that reactivation took place more than once.

D 090° deformational phase

Like F060° folds, F090° folds are very rare. They are upright gentle warps and spaced kinks that affect the older structures, particularly the most pervasive like L1-S1. In very few localities S090° cuts across S000°, and in places it can be seen to be an axial planar spaced cleavage associated with the few folds of this phase developed in carbonate-bearing units and in mica-schists. Reactivation of this structure gave rise to small faults with dextral displacement, some of which cut across crush belts associated with the Loch Maree fault set.

3.2.6 FAULTS

Normal faults

This set of structures is only seen on the northeastern limb of the major synform where it is apparently cross-cut by steeply-dipping crush belts (Pl.3-77). It consists of a set of NW-striking normal faults with low dips (around 45°) and movement of the hanging wall towards the SW.

Crush belts

Structures associated with the Loch Maree fault comprise relatively narrow (10-50m) crush belts developed in the northern part of the area. Their attitude generally corresponds to that of the axial planes of F4 folds but detailed observation shows there to be a discordant relationship (Pl.3-74). The interdigitation of the amphibole schists and associated lithologies with the gneisses along the NE limb of the large synform is produced by these faults which cut across (at low angles) the lithological boundaries and the normal faults. The dip of the crush belts is usually c. 80° to variable quadrants (normally to SW). In the few instances where their sense of movement, on a sub-horizontal surface, could be determined, it is sinistral.

The development of fault-breccia is a distinct although localized feature (Pl.3-78). Generally the fault zone consists of blocks of relatively less affected rocks (with F4 folds still preserved) surrounded by zones of more severe cataclasis. When affecting the iron-rich schists of the 'Charr band' (see Fig.2.1) the brecciated zones are cemented by limonite which in places shows planar structures looking like a foliation (Pl.3-75). On the other hand where the finer grained gneisses and amphibolites are the affected rocks of the fault zone they show a whitish colour and look massive at a distance.

Reverse faults

A very few examples of reverse faults were seen on the northeastern limb of the major synform. They show steep dips (60-70°), approximately E-W strikes and a N-NE direction of transport with displacements in the order of few centimetres (Pl.3-77). Although they seem to affect existing cataclastic rocks, unequivocal determination of their position in the overall sequence or of their primary or reactivated nature has not been made.

3.3 BASES OF CORRELATION AND THEIR APPLICATION TO THE LOCH MAREE AREA

The application and validity of the methods of structural analysis has been an integral part of the systematic study of orogenic belts over the past 25-30 years (e.g. Ramsay 1958, 1967, Turner and Weiss 1963, Hobbs et al. 1976). Much of the earlier work (e.g. Clough 1897, Wilson 1951) was generally of local nature but the past quarter of a century has seen a constant reassessment of the significance of structural features in regional studies, not least in relation to their value as criteria for correlation. As an example, fold style which Park (1969, pp.336,329) considered to be of 'little value in correlation' and its use 'should be abandoned' is considered by Hopgood (1984, p.233) as being of fundamental importance in correlation and by Williams (1985, p.270) as 'the best single characteristic for meaningful grouping or correlation of structures' (but see also Williams 1970). Likewise assessment of other individual structural characteristics has resulted in similarly divergent opinions. What are considered the more secure criteria for correlation such as overprinting relationships (Hobbs et al. 1976, McLellan 1984) or even the application of results of experimental work in structural analysis, can be criticized if individual aspects are taken in isolation. It is possible to use factors like the non-

coaxial nature of the strain (Borradaile 1972,1978, Bayly 1974, Ramsay 1976, Gray 1981) or the difficulties involved in the extrapolation of laboratory results to geological conditions (Paterson 1976) to pose problems in any interpretation. However, use of the combination of as many structural features as possible would appear to result in providing an integrated group of criteria that can be used with considerable confidence and lead to self consistent interpretations (cf. Huber et al.1980, Park and Bowes 1983, Williams 1985). Where isotopic data can be integrated (e.g. Black et al. 1979, Hoggood et al. 1983, Cliff 1985) correlation can be established across larger areas with reasonable certainty (see Hobbs et al. 1976, p.355 and Chap.8).

Although the presence of well-bedded units (e.g. quartzites which delineate the geometry of large folds) and the preservation of primary features (e.g. graded bedding) in low grade terranes lead to a higher confidence level in correlation, the criteria utilized in the analysis of these rocks are the same as those applied in higher grade and more intensely deformed metamorphic terranes such as in the Loch Maree area. Accordingly any criticisms of the use of structural analysis as a basis for correlation in the latter (cf. McLellan 1984) have to be viewed in the light of their application to the former. Such critical assessment of the method and of its limitations provides the basis for both an improvement of its application and the development of a better technique (cf. Popper 1959). Such advances could not only play a role in relation to the advancement of understanding of processes operative in the deep levels of orogenic belts but also in the search for and exploitation of the commonly occurring sulphide ore bodies in multiply deformed high-grade metamorphic terranes, particularly in Precambrian Shield areas (see Koistinen 1981).

As the technique of structural analysis is essentially based on field observation it should not be subject to the type of variations that are inherent in methods that rely on

interpretation (Hopgood 1980, p67). However, even in this case some sort of bias can be expected to be part of the process. This problem of 'perceptual experiences as empirical basis', was discussed by Popper (1959, pp. 93-111) and shown by Chadwick (1975) to be a common distortion in structural geology. Another example of bias is the tendency to emphasize the regularity and periodicity of structures and to simplify and classify. In addition a desire for order may result in the selection and description of only the best developed examples of structures (cf. Cobbold and Ferguson 1979, p.93). Such factors can lead to the representation of an oversimplified picture of a complex geometry. Accordingly, any interpretation presented here should be regarded as a simple model.

Assessment of the use and validity of the various structural features used in correlation in metamorphic terranes are set out by Hopgood (1980, 1984) and the work in the Loch Maree area generally reinforces some of the principles set out and their application. The main exception relates to whether mechanisms of deformation are of importance in any correlation. Hopgood (1984, p.235) considers that deformation mechanisms are not, but it now seems well-established that simple shear mechanisms can generate several sets of folds and banding (on various scales—see Chap.8) in a continuous fashion (Cobbold et al. 1980, La Tour 1981, Coward and Potts 1983, Platt 1983, Williams and Campagnoni 1983, Bell and Hammond 1984). This must be taken into account when applying refolding criteria particularly where there are zones of high deformation, such as the (D1) zones of mylonite which are common in the rocks of the Loch Maree area; correlation of the products of progressive refolding in such zones with multiply deformed rocks outside these zones must be applied with extreme caution (see below). However, this same factor which precludes the correlation based on style, orientation, etc. of folds, can allow the correlation of features indicating the same kinematic evolution such as the stretching lineation (cf.

Sect. 8.3) In addition, the predominant mechanism of deformation (as assessed on the mesoscopic scale) appears to change with the initiation of D2 structures, corresponding to the development and preservation of more abundant structures with geometry suggesting the action of buckling during at least the early part of their development (see Chaps. 6,8). This criterion, can be used as a diagnostic structural feature in the local structural sequence when used in association with the following factors:

(1) the relatively low strain (as compared to F1 folds) suggested by the geometry of most 'F2' folds, (2) the presence, nature, geometry and orientation of the F2-S2 structures (see Sect.6.2.1)) over most of domains I and II, (3) the 'intrafolial' nature (in relation to the mylonitized zones) of 'multiple' sets of F1 folds when compared to the F2 structures which also affected the surrounding rocks, and (4) the fact that the present investigation was restricted to a single major fold which occupies a relatively small area. In this way, the structures referred to in the field as F2 folds did not receive this denomination based only on the fact that they were seen folding one (or more) set(s) of folds, but also on the observation that they showed shortening equivalent (in orientation and magnitude ?) to the folds outside the mylonite zones. Although this seems a highly subjective criterion, it is not unreasonable if the expected D2 shortening affects ^{on} a pile of tectonically juxtaposed rocks are considered. Thus if the strain necessary to produce ('normal') F2 folds on non-mylonitized rocks a few metres away from a mylonite zone was roughly homogeneously distributed over this short distance, then it is considered legitimate to make some predictions about its effects upon these, e.g. thin competent quartzofeldspathic bands in a fine mica-rich matrix (see sect.6.2.2.5). Although there is always the possibility that some of these effects could have been produced by the shortening which gave rise to F4 folds, this was considered unlikely since where F2 folds are dominant no significant

development of F4 folds was observed (Maps 3.2/3.3). The convolute and polyclinal F2 folds were interpreted as representing an interference pattern produced mainly during D2. This is not based only on the criteria set out above (refolded folds, etc.), but also on theoretical predictions of how high viscosity quartzofeldspathic bands enclosed in a 'soft' medium like a mica-rich matrix would behave under high deformation (compression). The pygmatic geometry frequently shown by these and associated folds (in quartz bands) indicate the importance of buckling during their development. This sort of structure is particularly common in migmatitic rocks, where an analogous situation is observed (where high competence leucosomes within ductile melanosomes are strongly shortened). Similar geometry of structures has also been produced experimentally by buckling of a competent layer in air (the 'elastics' of Ramsay and Huber 1983, p.12), so that there is no need to postulate a special melting-dominated deformational mechanism ("viscous folding") to explain their origin as proposed by McLellan (1984, p.340). Accordingly, in the case of the Loch Maree mylonites, as in many other situations where these structures are observed, there is no evidence for partial melt. The absence of a coherent refolding geometry or cross-cutting relationships is not indicative of an unusual controlling mechanism of development of these structures (since 'normal' relationships can be observed in the surrounding outcrops) but instead, it reflects the high competence contrast and perhaps high strains produced in mylonitic zones. A more detailed discussion of the evidence for D2 deformation processes, which in some way can constrain the proposed 'correlation', is developed in chapters 6 and 8.

As there is no individual structure, or no set of structures, that is pervasively developed and uniquely recognizable throughout the Loch Maree area, the simple application of the 'key structure' concept of Hopgood (1980, p.63) was not used. Instead several sets of features are

used together (cf. Huber et al. 1980, Park and Bowes 1983); those used show both physical continuity across domains and have similar characteristics and positions in the local sequences. In particular the open upright SE-trending warps (Ff, Fe, Fe, F'mid' in domains I, II, III and IV respectively - Table 3.1) are consistently separated from boudin development by fold sets (one fold set in domain IV) and these, in turn, precede the development of isoclinal folds (Fb) associated with mylonite formation in domains I, II (NE) and III (see Table 3.2). Similarity of structural expression of these features in the different domains and their consistent sequential development permits both an overall correlation to be made and other structural elements to be integrated within this framework.

Because of the wide range of lithological types or association of types special attention was paid to competence control. This ensured that (1) the use of 'style' was restricted to local sequences, (2) consideration was given to location in relation to the large F2 synform and (3) the assessment of D2 deformation of multilayer assemblages in small areas could be considered as having been subjected to an approximately identical stress history (cf. Ramsay 1982). In this way extrapolation of fold geometry was made between outcrops of similar lithological types taking into account the thickness of the bands and the interbanded nature of the sequence. As a corollary of this and based on both the geometry of the folds and a consideration of the size of these small areas, it has been possible to make a general assessment of the mechanical behavior of a particular lithological layer under given physical conditions (Ramsay 1982). Such assessment in relation to the D2 deformational event is based on the assumption that the D2 structures were superimposed on fairly regular and approximately planar D1 structures (see Chaps. 5 and 8).

The presence or absence of ^{an}axial planar foliation, as well as its nature (see description of S2 in all domains), was used as part of the overall concept of 'style' (cf. Hopgood

1984, p.233). In most places the S₂ foliation could be used as an important marker due to its regularity and characteristic features. However in some units of domain III (e.g. siliceous mica schist) where quartzofeldspathic bands and micaceous units were folded in convolute or polyclinal styles, the absence or poor development of the S₂ foliation was interpreted in terms of the rheological characteristics of the interbanded assemblage and the dominant mechanism of deformation in these rocks (see Chap. 6). In such instances and also where interbanded mylonitized gneisses and amphibolites were deformed concepts like 'the associated metamorphic facies' and 'vergence' were of no practical use.

Generally any use of foliations in the correlation needs to bear in mind the possibility of the existence of undetected transpositions (Park 1969, p.322, Hobbs *et al.* 1976, p.351, Williams 1985, p.277). However in the Loch Maree area, extensive transposition was confined to D₁. The effects of superimposed events were retrogressive and the expressions progressively less penetrative. Accordingly, in such a relatively small and well-exposed area it is possible to be confident that any post-D₁ transposition of any noticeable amount was only during D₂, and then localized (see description of D₂ in domain II). In this way mistaken identification of foliations is not considered to be a factor in correlation of local deformational sequences. In addition, although overlapping ranges of varying styles was not a problem in domains I and II, it was a serious problem in domains III and IV (Sects. 4.3.1 and 4.3.2 below).

Although the small size of the area studied means that factors like tectonic level and metamorphic grade cannot play important roles (cf. Hopgood 1980), there are specific features and problems that had to be considered in the setting up of the correlation shown in Table 3.1.

1. There is no single continuous lithological unit that

defines the shape of the major folds, although the amphibole schists and some of the large banded amphibolites played this role in domain II and part of domain I. Over most of the area the banding is of small scale and of irregular expression so that it could not be used to trace out structures of considerable size (see also Chap. 2).

2. The uncertainty about the position in the overall structural sequence of the first recognized set of folds in the marbles is due both to the absence of distinct features of these structures and to the lack of more than one generation of tight folds in any single outcrop of this domain. The folds affect the composite banding and are usually very well-developed (see domain IV) but they show characteristics which are common to both F2 and F3 folds. The fact that in places they show a symmetry compatible with the major F2 synform in domain I [NG 951720] has to be put against their having geometry consistent with that of the F3 folds in domain II [NG 976704 & NG 965709]. With folds well-developed in practically every outcrop of this unit, it seems unlikely that refolding relationships would not somewhere be shown if there were representatives of more than one phase present. In addition only one cleavage is seen associated with the folds in rocks not conducive to the development of distinctive mineralogical assemblages. The fact that the folds affect small boudins could suggest that they belong to the F2 set; such a conclusion is based on the assumptions that (1) the boudins are of late D1 age as they are in domain I, and (2) the folds represent the first phase of deformation to affect the boudins. However the discontinuity of the marble unit (domain IV) along the boundary between the gneisses of domain I and the amphibole schists of domain II, as well as the relatively clear picture of the structures and their relations in these two domains, means that lack of unequivocal demonstration of the relative time of development of this set of folds (whatever they are - F2 or F3 folds) was not an obstacle to the overall correlation within the area as a whole. The local

correlation could be established between domain IV and other domains in the later parts of the sequence as the upright open buckles which refold the 'tight folds' have both attitude and characteristics of F4 structures.

3. Distinction in the field between F2 and F3 folds is difficult in several of the outcrops of the metasediments (domain III), particularly in the siliceous mica schist unit because of (1) the coaxial nature of the lineations, (2) the problems of distinguishing between a very tight zonal crenulation cleavage (S3) and the S2 cleavage as both are retrogressive and show the beginnings of transposition, (3) the lack of continuous exposures and (4) the convolute geometry of the folds. Microfabric studies provided answers for a limited number of outcrops but those required a large number of thin sections and much time. Where exposure was good, and the whole sequence of structural features well-developed, it was generally possible to identify earlier and later structures. However, in many localities where several sets of folds were developed there was no confidence about which fold phase was being dealt with. Data from these places were not further analysed.

Despite this uncertainty, deriving from the commonly colinear geometry of the structures, the interpretation of the lineations as indicating the stretching direction provided a valuable element for the (kinematic) correlation between these early structures in the metasediments and the equivalent ones in the gneisses of domain I (cf. Chap. 8).

4. The F3 recumbent folds played an important role in the correlation between the domains I, II and III. Useful aspects were (1) the way the folds controlled outcrop shapes, (2) the continuity of the folds across the domain boundaries along the southwestern limb of the large F2 synform, (3) their regular geometry and orientation along most of the boundary between domains II and III where there are few effects of the D4 phase, and (4) prominent

development in most of the outcrops of mica schists of domain III where isoclinal folds with amplitudes of 10-15 metres are not rare [NG 960707].

5. The almost constant strike of the axial planes of the F4 and F-late folds makes these structures useful in the correlation regarding the late structural history. However both their sporadic distribution and the variation in the angle (but not direction) of plunge, because of the control of previous structure, mean that they cannot be used in isolation. In addition while these late buckles are best developed on sub-horizontal parts of any previous folds (F1, F2, or F3), it is not common to find them deforming massive units, hinges or steeply-dipping limbs of older structures.

6. The extremely localized distribution of D2a ductile shear zones (only seen in parts of domain I) as well as the limited relationships shown with other structures meant that determination of their position in the overall sequence of events was not straightforward. They show, (1) relatively constant orientation across the major F2 fold, (2) folding of the composite banding and a discordant relationship, in some places, of the associated pegmatites to the composite banding (Pl.3-26,26'), (3) ductile deformation of the porphyritic amphibolite (Pl.3-25) and (4) a generally more 'ductile appearance' than D-late structural features. This evidence points to the shear zones, folds and pegmatites as representing a post-D2 event (the subscript 2a is used because of their extremely localized nature and post-D2 age). There is no direct evidence to place these structures before or after the D3 phase. The folds that affect the pegmatites have characteristics in common with F3 folds elsewhere. F4 folds also show a geometry compatible with NE-SW shortening (see Chap. 6). The localized nature of the shear zones and pegmatites in domain I and their absence in the other domains suggests a lithological control of their development (Ramsay 1982) as well as a weak expression of the operative conditions.

7. With the qualifications attached to the criteria used for assigning a set of folds to a particular deformational phase, the possibility of an erroneous correlation is always present. This is illustrated by the set of folds shown in Plates 3-30, 31 and Figure 6.3, interpreted here as F4 folds. During field work the possibility that they were developed during D2 rather than during D4 was considered. Assigning them to D4 was preferred not only on the basis of the absence of an axial planar foliation showing the typical features of S2, but also due to the fact that they fold a well-developed lineation (10° to 30° clockwise to the fold axis) with the characteristics of L1-L2. However, it should be borne in mind that other possibilities exist, including (a) that these folds are F2 with lack of expression of S2 foliation being due to the properties of the high competence contrast of the interbanded sequence (quartzofeldspathic gneisses with decimetre thick biotite-rich bands) and (b) that the refolding of the L1-L2 lineation was produced by migration of the fold hinge during a possibly later shortening (which could be the D4 event). While the interpretation of these structures as F4 folds seems to be the most likely one in the light of the present evidence, some questions still remain unanswered, e.g. why F2 folds were not developed in such a well-interbanded sequence when they are observed in the surrounding rocks and also show features indicating buckling.

8. There are limitations to the use of structural analysis in the elucidation of basement-cover relationships, something which has been a matter of debate in the Loch Maree area since the pioneer work of Peach et al. (1907). One major question is whether the gneisses and amphibolites (domain I) are a slice of basement rocks tectonically emplaced above a younger volcano-sedimentary assemblage domains II and III (cf. Peach and Horne 1930). The structural concordance of the D1 mylonitic fabric and associated features in the gneisses and metasediments is evidence that these units were juxtaposed during at least

part of the D1 episode. While this does not demonstrate that the deformed banding in the gneisses is of the same age or origin as the deformed (and largely transposed) banding in the metasediments, the possibility of such correspondence cannot be excluded on the basis of structural analysis only.

The presence of extensive effects of D1 mylonitization, particularly in localized zones, means that strong transposition has been operative. In addition there is the possibility of both (a) the localized development of deformational phases and (b) the complete obliteration of others resulting in the juxtaposition of assemblages showing different structural histories (cf. McLellan 1984). However, in the Loch Maree area both the juxtaposition of schists and gneisses and the presence of mylonites along the main lithological boundaries suggests a tectonic junction between these units. However the possibility that the rocks were part of the same assemblage whose varying rheological properties resulted in differences in mechanical behavior during deformation had to be borne in mind until radiometric data were obtained.

Tectono-stratigraphic markers like the basic intrusions locally discordant to the banding (but also presenting D1 features) in domain I could not be used due to their absence in the metasediments and uncertainties of their unique origin. U-Pb zircon and Rb-Sr whole-rock isotopic data for some of the gneisses and mylonites indicate the superimposition of early Proterozoic tectonothermal activity on rocks of late Archaean age (see also Chap.8). The consideration of initial $^{87}\text{Sr}/^{86}\text{Sr}$ in the metasediments whose metamorphism was c.1.9 Ga indicates that crustal history did not go back beyond c. 2.1-2.2 Ga (Bikerman et al. 1975, O'Nions et al. 1983). This together with the evidence for the repetition of the marble unit (between the domains I and IV) along the boundary between the gneisses and the amphibole schists in the hinge zone of the major fold (see Chap.8) points to the existence of a major

stratigraphic break between the gneisses and the amphibole schists and metasediments marked mainly by the mylonitized carbonate-rich rocks. Unfortunately due to the present state of development of the radiometric dating techniques they are of limited use in correlation where detailed sequences of fold phases and related structures are concerned. This is due to the possibility that two or more deformation episodes take place in a period of time within the error of the method. As pointed out by Pfiffner and Ramsay (1982) longitudinal strains (ϵ) as measured in many rocks, often range from 1 to 40 and 1 to 0.025, so that the time span available to produce such strains in orogenic belts can be as short as or even less than 1 Ma. Although Hopgood *et al.* (1983) have obtained shorter time intervals between tectonic and magmatic events than most authors (cf. Black *et al.* 1979) these are still regarded as crude approximations of the natural conditions. This situation will remain unchanged until high resolution radiometric techniques become available. On the other hand, as demonstrated by Tobisch and Fiske, (1982) features showing a consistent geometry between structural elements (orientation, style, etc.) could have been developed at successive deformation episodes separated by time intervals of several million years. Thus, the following paragraph from Tobisch and Fiske (1982) seems to give useful guidelines to be followed by any structural investigation, being also very adequate to close this section. "To establish a rigorous and detailed structural succession for any given area it may be necessary to gain a thorough understanding of the stratigraphy, the relative and absolute age of the units, as well as carrying out radiometric dating of rock bodies which have key relationships to structures involved. Until one arrives at this level of understanding, it will be possible only to delineate the broadest of time sequences for the structures involved" (p. 194).

Correlation problems involving large scale structural features will be further discussed in section 8.3.

CHAPTER 3 - CAPTIONS OF PLATES

- DOMAIN I - Plates 3-1 to 3-36
DOMAIN II - Plates 3-37 to 3-52
DOMAIN III - Plates 3-53 to 3-63
DOMAIN IV - Plates 3-64 to 3-68
LATE PHASES - Plates 3-69 to 3-78

Unless otherwise stated all pictures were taken of outcrops facing NW.

DOMAIN I

Plate 3-1 Tight F1 folds with thickened noses and attenuated limbs affecting S banding shown by varying proportions of quartz, feldspar and mafic minerals in gneiss; note the subhorizontal S3 spaced cleavage. [NG 960 721]

Plate 3-2 Quartzofeldspathic neosome (Sb') discordant to the older banding (Sb) in gneiss and marking F1 folds; scale 2.5cm. [NG 956 718]

Plate 3-3 F1 'flame' fold in banded amphibolite amongst quartzofeldspathic gneisses, affected by open F2 antiform. [NG 974 718]

Plate 3-4 Detail of Plate 3-3 showing the S2 mineral growth (parallel to pen) and F2 minor folds. [NG 974 718]

Plate 3-5 Feldspathic vein (Sb') showing tight F1 fold in mafic amphibolite; lens cap 5 cm. [NG 961 711]

Plate 3-6 Sheath-like F1 fold in banded amphibolite; coin 2.5 cm. [NG 976 708]

Plate 3-7 Large F1 folds in banded amphibolite slightly affected by F2 and possibly F3 folds; arrow indicates hammer handle (~ 70cm); sketch from photograph. [NG 964 718]

Plate 3-8 D1 'imbricated boudins' of mafic material (ornamented and black) permeated by feldspathic material (v) in banded amphibolite; scale 6 cm; sketch from photograph. [NG 975 710]

Plate 3-9 Late D1 boudins affecting S composite in banded amphibolite; note small intrafolial F1 fold to the left of pencil tip. [NG 973 708]

Plate 3-10 SW-plunging L1 fold mullions in mylonitized quartzofeldspathic gneiss near the contact with marbles. [NG 973 704]

Plates 3-11,12,13 Three examples of the progressive change of phenocrysts from undeformed to prolate (L1) to oblate (S1) shapes in porphyritic amphibolites; lens cap 5cm, scale 2cm, pen 15cm respectively; exposure (3-11) faces SE. [NG 978 712]

STRUCTURES IN MYLONITIZED GNEISSES

Plate 3-14 Isoclinal F1 fold with limb affected by F2-S2 in mylonitic gneiss; note the convolute geometry of the folds affecting the thin bands at the core of the F1 synform; the similarity of these structures with larger scale examples is striking (see Plate 3-15).[NG 971 716]

Plate 3-15 Small intrafolial F1 fold and 'convolute' F2 folds affecting mylonitized gneiss; the darker bands correspond to mafic layers of the original rock; width of photograph 50cm. [NG 971 716]

Plate 3-16 F1 fold with reverse sense of closure of the hinge (coin) folded by F2 fold with parasitic minor structures (synform at the top) and hinge detachment (antiform at the bottom); the dark layers are mylonitized mafic bands; pencil = 15cm long.[NG 971 716]

Plate 3-16a Detail of Plate 3-16.[NG 971 716]

Plate 3-17 Mylonitized gneiss showing the late D1 mylonitic banding affected by F2 folds with detachment of hinges and wavelength controlled by layer thickness; length of scale (above detached hinge of antiform) 10cm.[NG 971 716]

Plate 3-18 L1 stretching lineation folded around flattened non-cylindrical F2 folds in mylonitic gneiss; coin 2cm; exposure faces SW.[NG 972 716]

Plate 3-19 Large upright F2 folds affecting interbanded gneiss and mafic amphibolite (dark layers); hammer (just above F2 label) 40cm long.[NG 972 715]

Plate 3-20 F2 antiform in banded amphibolite; thin ultramafic layers show pinch-and-swell structures folded at small wavelength; compass 10cm long.[NG 975 708]

Plate 3-20a Well-developed S2 biotite and amphibole foliation axial-planar to asymmetrical (towards NE) F2 fold in banded amphibolite (same unit as in Plate 3-20).[NG 975 708]

Plate 3-21 Large F2 folds in gneiss with quartzofeldspathic and biotite-rich bands; note fold geometry and good development of S3 crenulation cleavage (see also Plate 3-29); sketch from photograph; scale 150cm.[NG 968 716]

Plate 3-22 Sinistral displacement of granitic neosome (Sb'-marking F1 folds) along S2 in quartzofeldspathic gneiss; in hinge zone of F2 fold; hammer 40cm long.[NG 975 704]

Plate 3-23 Sinistral shear and pressure solution effects of S1 quartz bands along S2 foliation in mylonitized gneiss; coin 2.5cm (see map 3.2) [NG 971 716]

Plate 3-24 S2a crenulation and spaced cleavage axial-planar to F2a fold affecting composite banding of gneiss; note the cataclastic aspect of the rock in the discrete part of this sinistral shear zone (top of photograph); horizontal surface (see map 3.1) [NG 975 704]

Plate 3-25 Narrow ductile sinistral D2a shear zone affecting feldspar phenocrysts in porphyritic amphibolite; coin 2.5cm [NG 975 704].

Plate 3-26 F2a folds in pegmatite (pg) discordant to the composite banding (Sc) which is deflected around fold hinges in quartzofeldspathic gneiss; horizontal surface (see map 3.1) [NG 975 704].

Plate 3-26a Sketch of Plate 3-26; scale 15cm.

Plate 3-27 Thick irregular pegmatite body (peg) with sharp contacts with composite banding of interlayered gneiss and amphibolite (black bands); sketch from photograph; scale 40cm; horizontal surface.[NG 975 704]

Plate 3-28 F3 recumbent fold affecting composite banding in gneiss; hammer 40cm.[NG 961 711]

Plate 3-29 Widely spaced S3 crenulation cleavage in chloritized biotite-rich band of quartzofeldspathic gneiss (detail of lower part of Plate 3-21); hammer 40cm.[NG 968 716]

Plate 3-30 F4 buckle folds affecting composite banding which is an alternation of quartzofeldspathic and biotite-rich layers (more eroded spaces); S000° affects long limbs of these folds (see also Fig. 6-3); hammer 40cm.[NG 966 718]

Plate 3-31 Shoulder development and hinge detachment of F4 buckle folds in banded quartzofeldspathic gneiss; the spaces correspond to more weathered biotite-rich bands; hammer 40cm. [NG 966 718]

Plate 3-32 'Melange' of more ductile mica-rich material along the hinge of F4 folds affecting quartzofeldspathic gneiss and mafic amphibolite; note the S4 zonal crenulation cleavage at the core of the fold.[NG 962 722]

Plate 3-33 Concentric slightly reclined (to SW) F4 fold refolding the L1-L2 composite lineation in quartzofeldspathic gneiss; exposure faces W.[NG 964 712]

Plate 3-34 F4 refolding of detached hinge of F2 fold in biotite (black layer) gneiss; sketch from photograph; scale 20cm. [NG 966 721]

Plate 3-35 Concordant mafic amphibolite with internal compositional (flow?) banding; note deflection of amphibolite margin (lower) around coarse-grained quartzofeldspathic band with pinch-and-swell structure. (see map 3.1) [NG 975 704]

Plate 3-36 Discordant mafic amphibolite cutting across banding but presenting a well-developed S1 foliation (see Plate 2-6 for detail); hammer 40cm. [NG 975 717]

Plate 3-37 F2 fold affecting feldspathic banding in amphibole schist; note the geometry of the antiform (class 2 fold) and reverse sense of hinge closure of fold in thin layer above thickest band; coin 2.7cm. [NG 952 717]

Plate 3-37a F2 folds in discordant quartz vein in amphibole schist; coin 2.2cm. [NG 952 717]

Plate 3-38 Discordant feldspathic veins (fdp) folded by F2 in amphibole schist; note the development of fine feldspathic segregation bands along S2; coin 2.2cm. [NG 952 717]

Plate 3-39 Low ductility contrast D1 boudins in feldspathic bands affected by NE-verging asymmetrical F2 fold. [NG 954 715]

Plate 3-40 Coaxial refolding of F2 by F3 fold in banded amphibole schist. [NG 960 710]

Plate 3-41 Block diagrams and sketches showing relationships between D1, D2 and D4 structures in mylonitized quartz-mica schist interbanded with amphibole schist. (a) Tight F1 refolded by F4 fold; note angle L1-L4; sketch from sample; scale bar 5cm. (b) Coaxial refolding of F1 by F2 fold; note curved axial plane of F2; sketch from photograph; scale 3cm. (c) Interference structure between isoclinal F1 fold and curvilinear hinge F2 folds; sketch from part of Plate 3-43; scale 5cm. [NG 971 722]

Plate 3-42 Non-cylindrical F2 fold affecting isoclinal F1 fold in quartz-mica schist; note folded L1 and developing L2 stretching lineation; sketch from sample; scale 8cm. [NG 971 722]

Plate 3-43 Interference structures between isoclinal F1 folds and several non-cylindrical F2 folds in quartz-mica schist; coin 2cm. [NG 971 722]

Plate 3-44 Variable interlimb angle of F3 chevron fold along fold profile in banded amphibole schist; sketch from photograph; scale 15cm. [NG 956 714]

Plate 3-45 Tight F2 folds with sharp hinge affected by open chevron F3 fold; the F3 fold is the continuation (towards the core) of the structure shown in Plate 3-44; note the S3 spaced cleavage. [NG 956 714]

Plate 3-46 Type 3 interference pattern between tight F2 folds and open F3 with round hinges in amphibole schist; sketch from photograph; scale 10cm. [NG 961 702]

Plate 3-47 Asymmetrical F3 fold with curved axial plane in finely banded amphibole schist. [NG 961 702]

Plate 3-48 S3 crenulation cleavage affecting finely banded micaceous amphibole schist; coin 2cm. [NG 970 704]

Plate 3-49 Minor thrust along F3 fold limb in finely banded amphibole schist; coin 2cm. [NG 956 714]

Plate 3-50 Concentric to chevron F3 folds with hinge detachment; the spaces are left by dissolved material; coin 2.2cm.[NG 956 714]

Plate 3-51 F4 open fold affecting asymmetrical F3 folds in banded amphibole schist ; sketch from photograph; outcrop is 10m wide and faces SE.[NG 964 707]

Plate 3-51a Detail of F3 fold - S4 cleavage relationship; sketch from photograph. [NG 964 707]

Plate 3-52 Concentric to chevron F3 folds with quartz saddle reefs in banded amphibole schist; coin 2.2cm.[NG 956 714]

Plate 3-53 F1 coaxially refolded by F2 fold in mica schist; the F1 affects an older schistosity (D banding); see map 3.4. [NG 970 696]

Plate 3-54 Coaxial refolding of isoclinal F1 folds by recumbent F3 folds in quartz mica schist; note the thick nose of the early folds and the well-developed crenulation of the mica-rich lithology; exposure faces SE. [NG 963 703]

Plate 3-55 Non-cylindrical F2 folds in lineated (L1) quartz-rich bands of mylonitized siliceous mica schist; note the fine S2 cleavage inclined toward NE. [NG 975 695]

Plate 3-56 Convolute F2 folds in feldspathic bands of mylonitized siliceous mica schist. [NG 975 695]

Plate 3-57 Hinge of F2 fold in mica schist; ornamented bands are more siliceous; circled area is Plate 3-57a; sketch from photograph; horizontal section. [NG 973 693]

Plate 3-57a Detail of transposition of composite banding and quartzose layers by S2; large pre-D2 garnet in outlined diamond shape. [NG 973 693]

Plate 3-58 Relationships between F2, F3 and F040° folds in mica schist; black layers are just markers and coarse dots represent the surface of composite banding; sketch from photograph; exposure faces SE; scale 1m. [NG 973 693]

Plate 3-59 Reclined F3 fold in siliceous mica schist, with boudinaged quartz bands along the outer layers and inverse fractures in the core (just above label).[NG 963 704]

Plate 3-59a Mylonitic band along lower limb of asymmetrical F3 fold (vergence towards SW) affecting quartzose band (nose) in rusty schist.[NG 960 698]

Plate 3-60 Hinge bifurcation of F3 recumbent fold in rusty schist; sketch from photograph.[NG 953 718]

Plate 3-61 Acylindrical F3 fold affecting L1-L2 lineation at very low angle to slickensides (parallel to hammer handle) in rusty schist; sketch from photograph.[NG 966 702]

Plate 3-62 Angular relationship between low/plunging L3 and fine L2 lineations in mica schist; exposure faces SW.[NG 971 701]

Plate 3-63 Open concentric upright F4 affecting mica schist.[NG 964 700]

Plate 3-64 Detachment surface between massive (bottom left) and banded marbles producing an F-'early' box fold. [NG 965 709]

Plate 3-65 Buckling of competent quartz band within more massive marble; sketch from right hand side of Plate 3-64. [NG 965 709]

Plate 3-66 Tight F-'early' fold with hinge detachment affected by open F-'mid' (F4) warp with spaced cleavage (parallel to hammer) in marbles.[NG 951 721]

Plate 3-67 Tight non-cylindrical plane F-'early' fold cut across by S4 spaced cleavage in white marble; exposure faces SE; width of photograph ~50cm.[NG 951 721]

Plate 3-68 F-'early' fold affecting interbanded marble (white bands) and micaceous amphibole schist; horizontal surface. [NG 952 720]

Plate 3-69 Open F000° folds in amphibole schist showing wavelength thickness relations in bands of variable thickness (tip of pen); horizontal surface.[NG 953 716]

Plate 3-70 Open F040° folds in quartzofeldspathic gneiss affecting the L1 stretching lineation; some of the vertical fractures might have been produced by reactivation. Outcrop faces SW; hammer 40cm [NG 961 714]

Plate 3-71 Interference between F4, F000° and F040°; detailed examination reveals several differently oriented crenulation cleavages in this quartzofeldspathic gneiss.[NG 963 723]

Plate 3-72 Pattern produced by interference of S000°, S040° and S090° in quartzofeldspathic gneiss; horizontal surface; scale 30cm.[NG 959 722]

Plate 3-73 Dextral displacement along $S060^\circ$ of a quartz vein (black) in quartzofeldspathic gneiss; horizontal surface; scale 20cm.[NG 965 713]

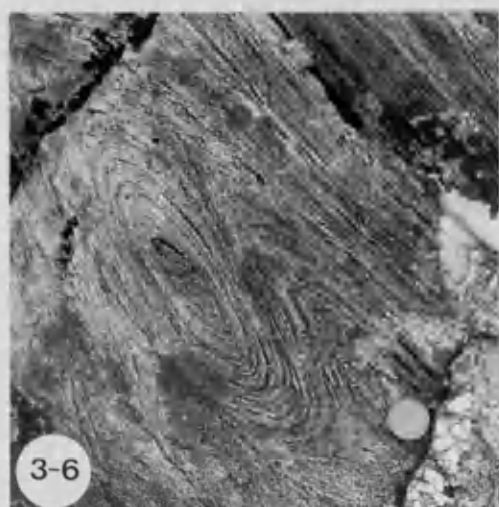
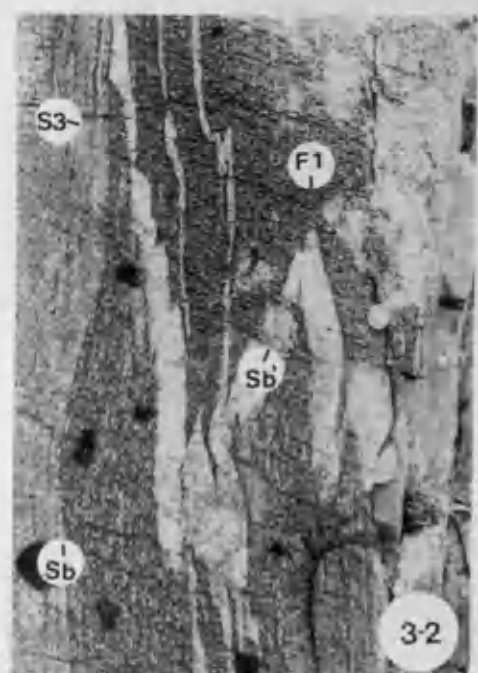
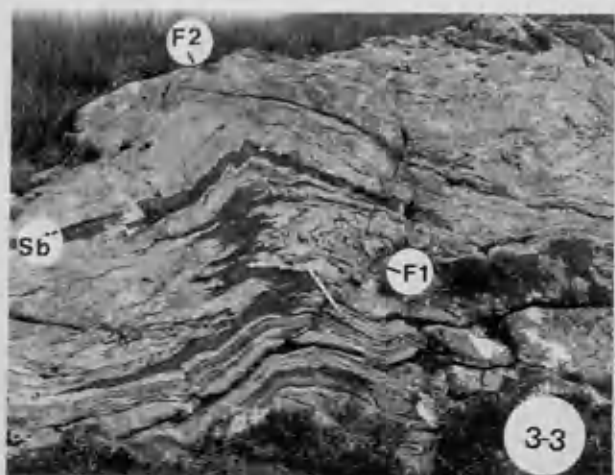
Plate 3-74 Crush belts (cb) oblique to $S4$ foliation in quartzofeldspathic gneiss; sketch from photograph; exposure faces SE.[NG 969 722]

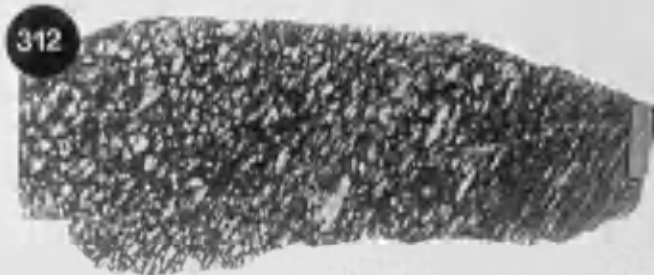
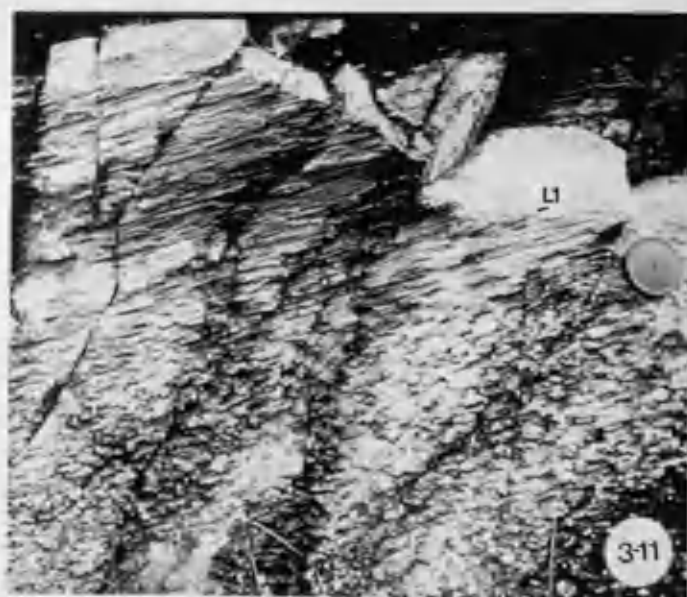
Plate 3-75 Structure resembling foliation formed by limonitic material precipitated along fault zone; in iron-rich schist of Charr band; width of block diagram 150cm.[NG 971 722]

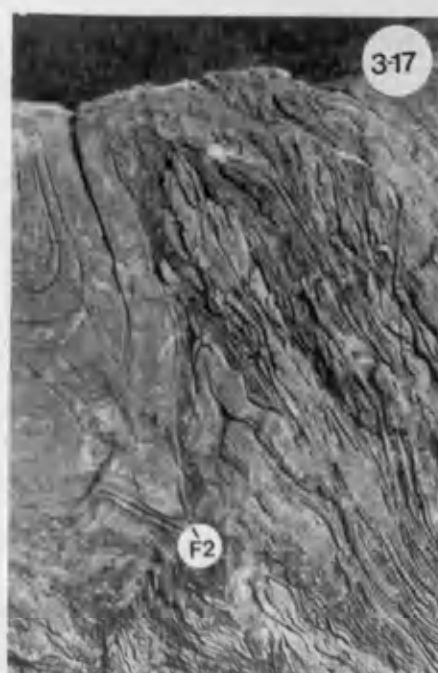
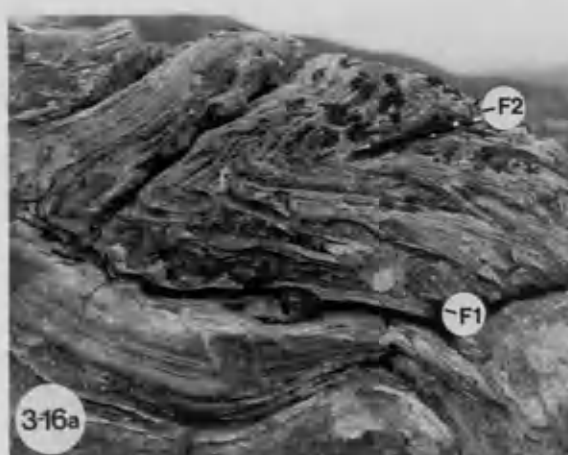
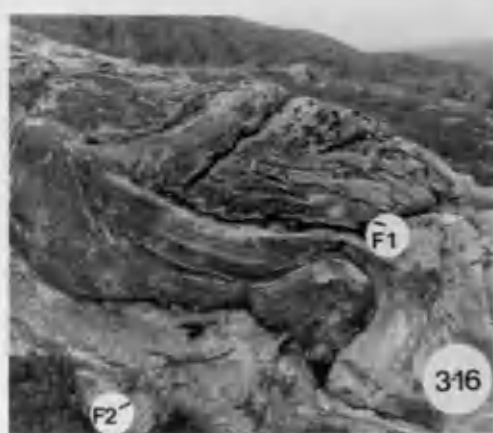
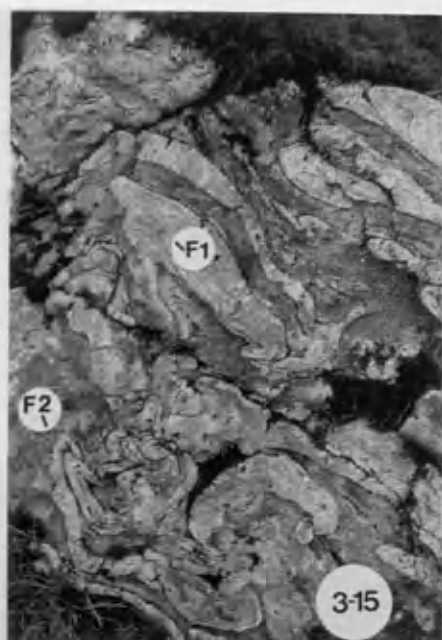
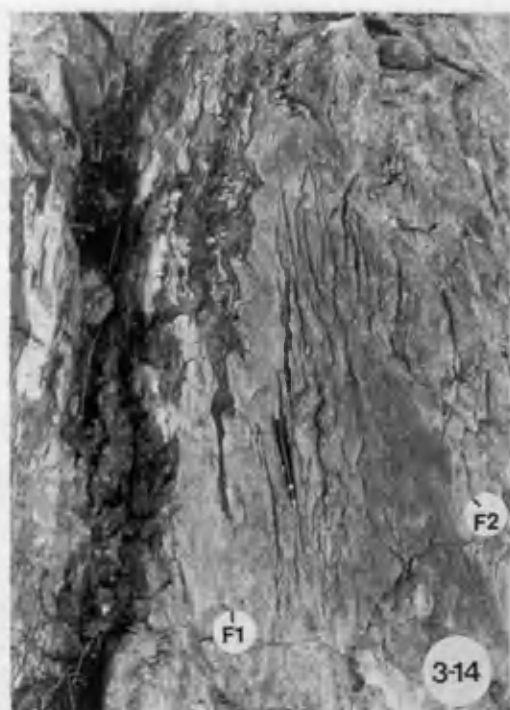
Plate 3-76 Steeply dipping crush belt (cb) cutting across SW-dipping normal faults along the contact between mylonitized gneisses and amphibole schists; sketch from photograph; height of cliff ~20m.[NG 969 722]

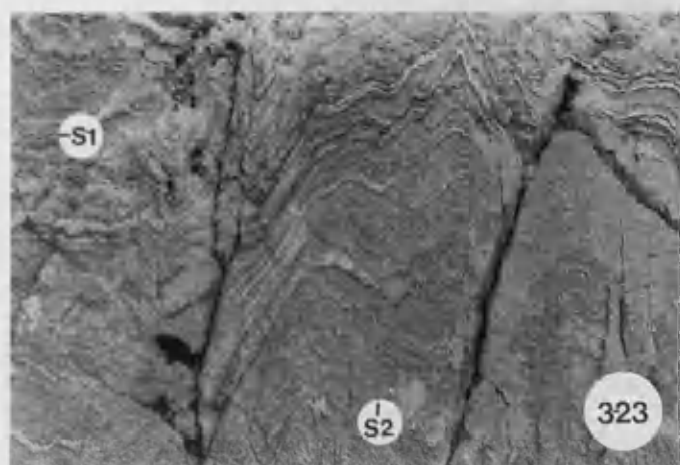
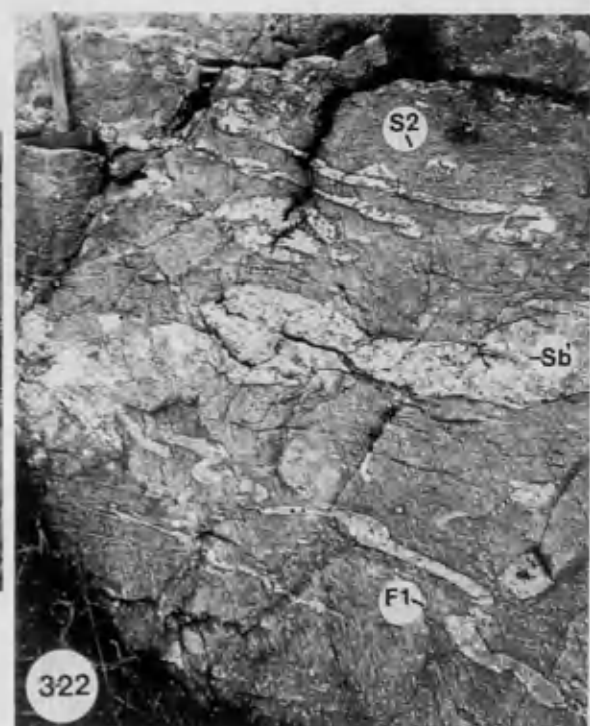
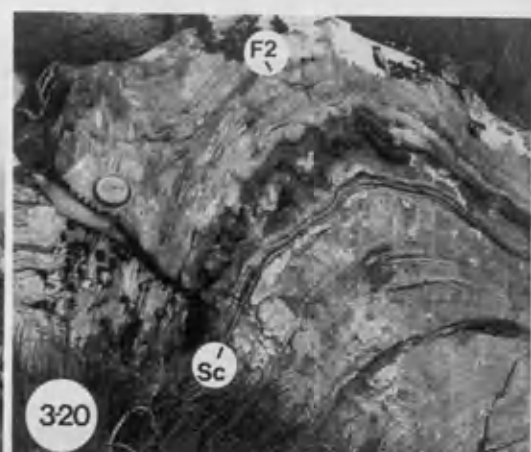
Plate 3-77 Late 'en echelon' reverse faults with a northward movement of the hanging wall affecting quartzofeldspathic gneisses; scale 25cm.[NG 977 711]

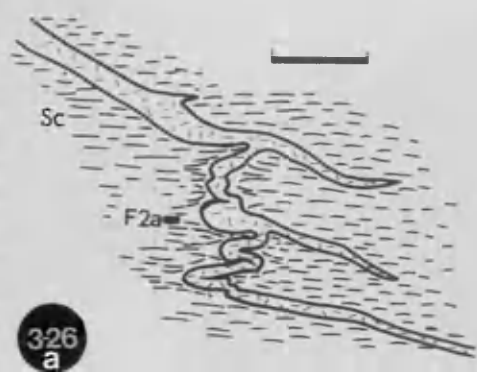
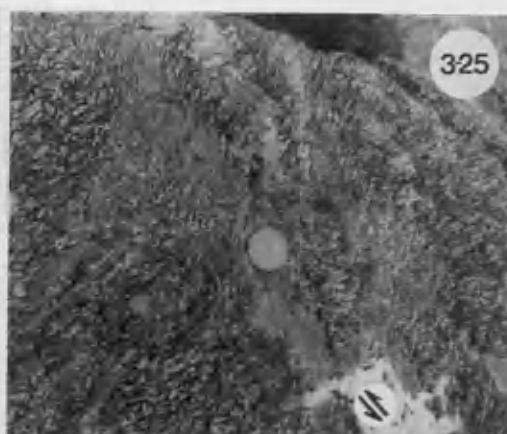
Plate 3-78 Fault breccia in crush belt (parallel to pen) affecting quartzofeldspathic gneiss.[NG 967 722]

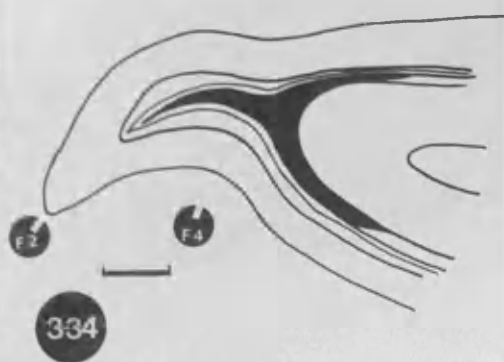
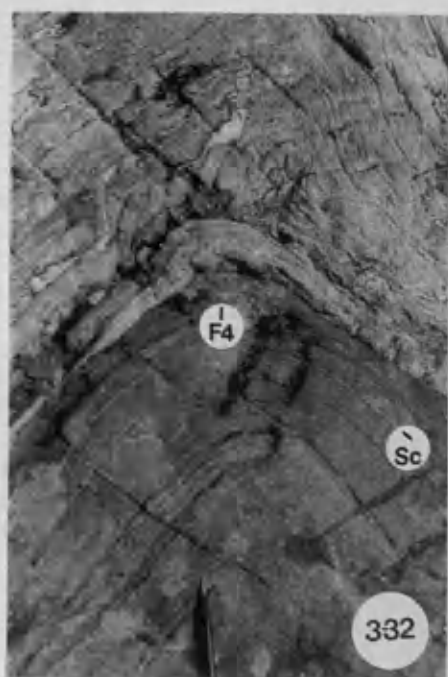
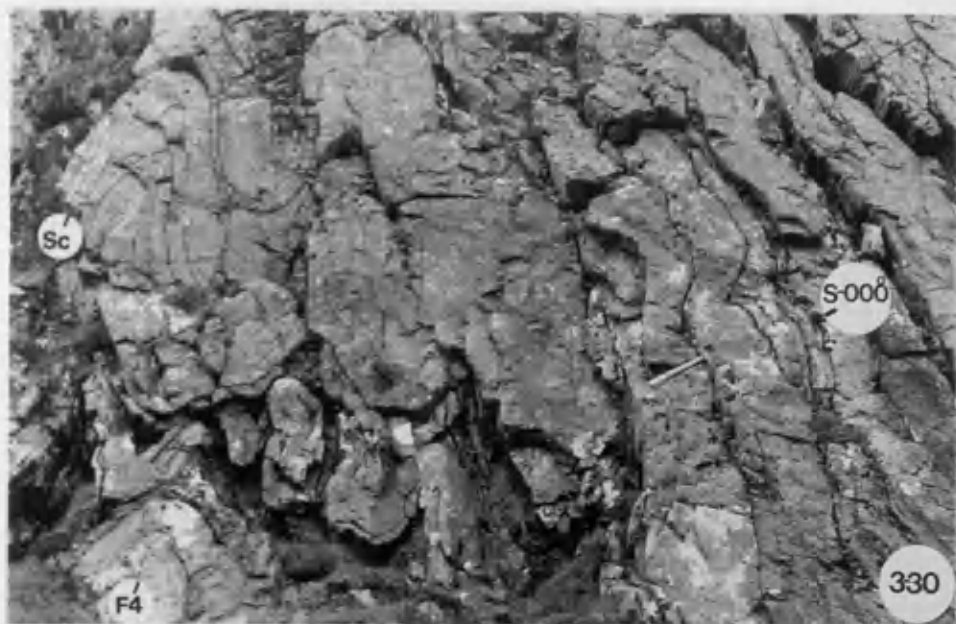


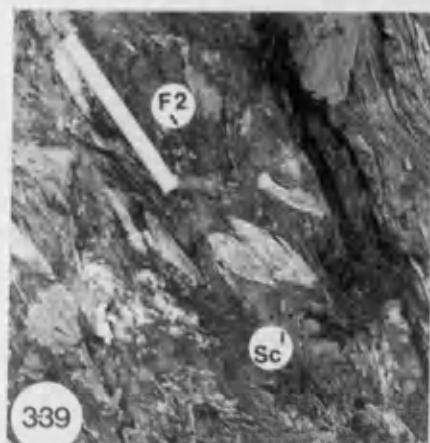
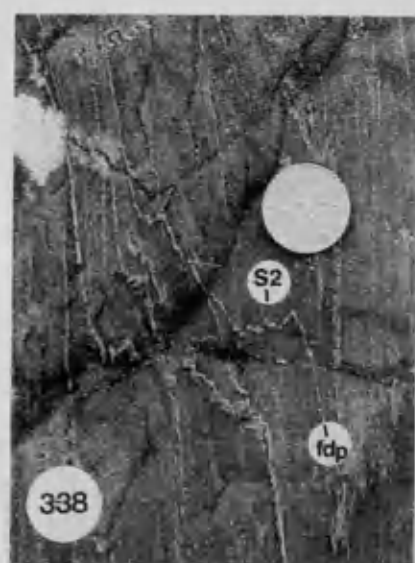
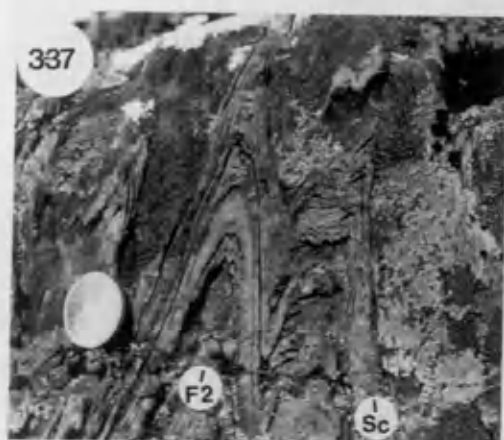
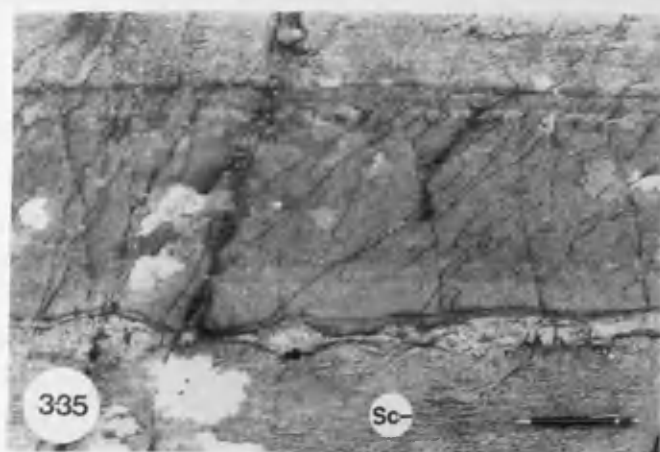


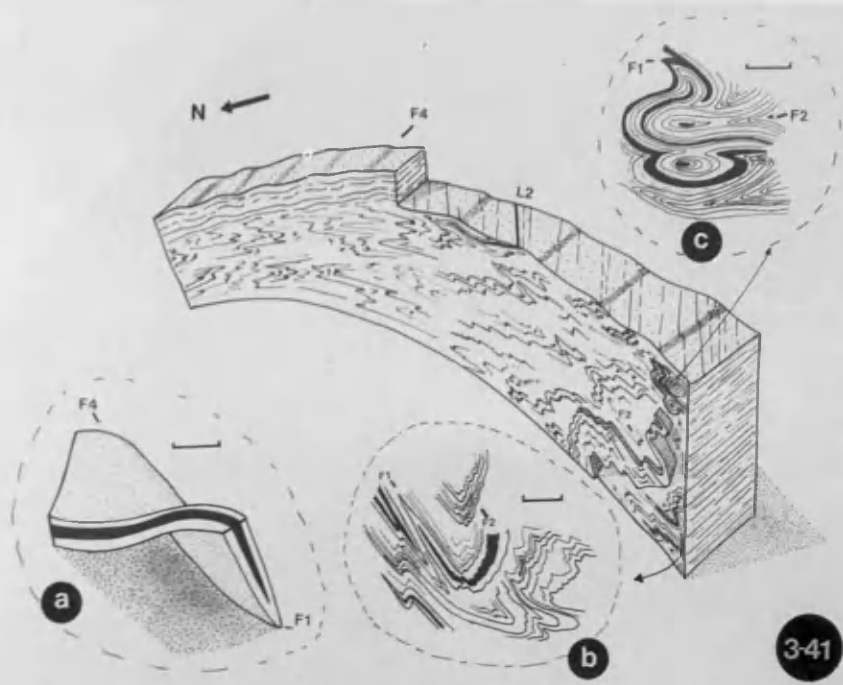




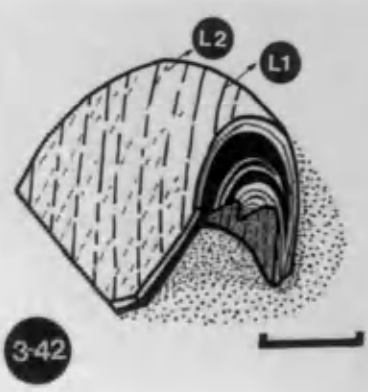




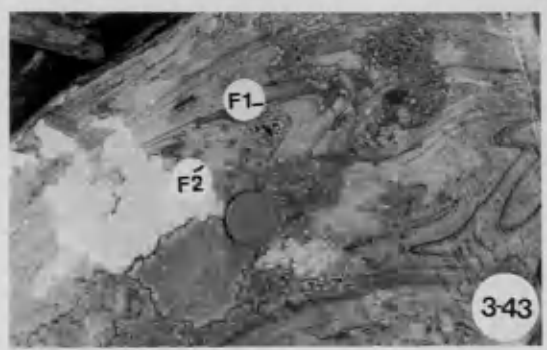




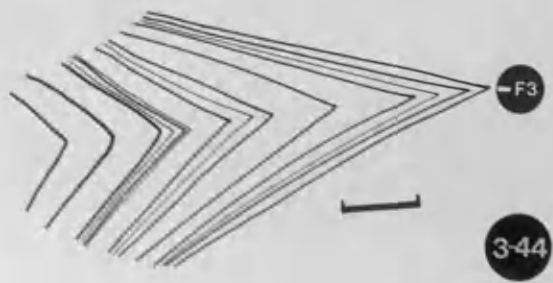
3-41



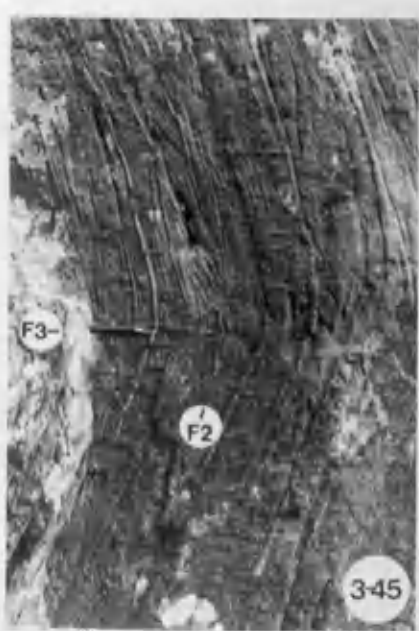
3-42



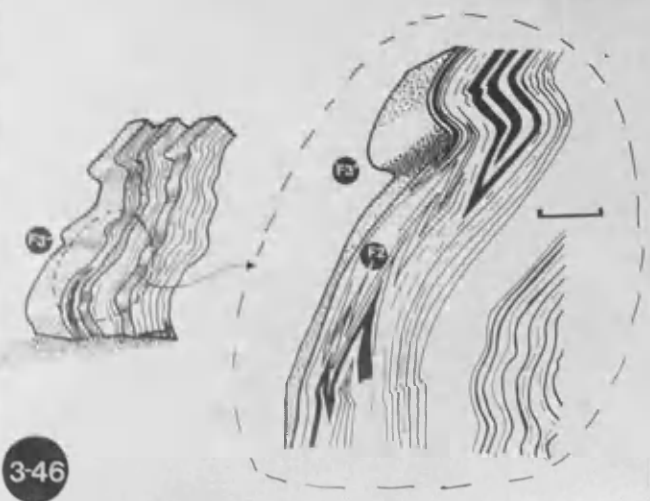
3-43



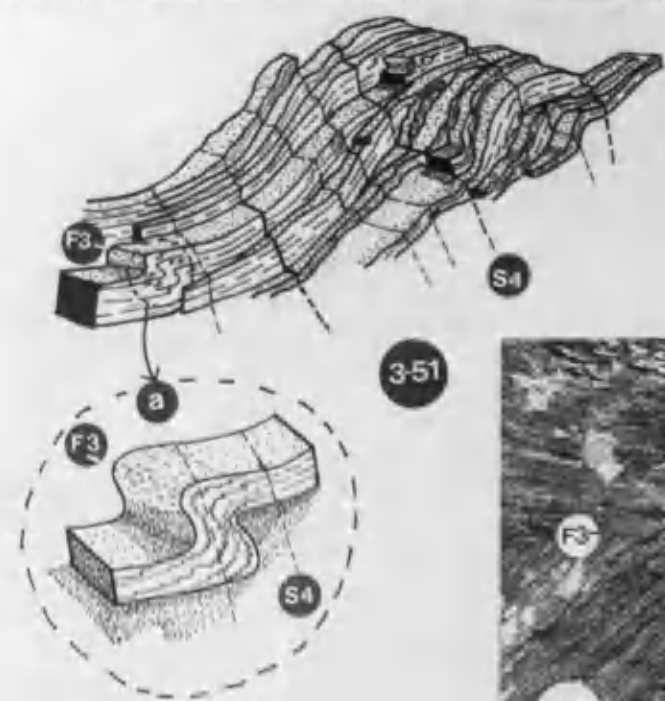
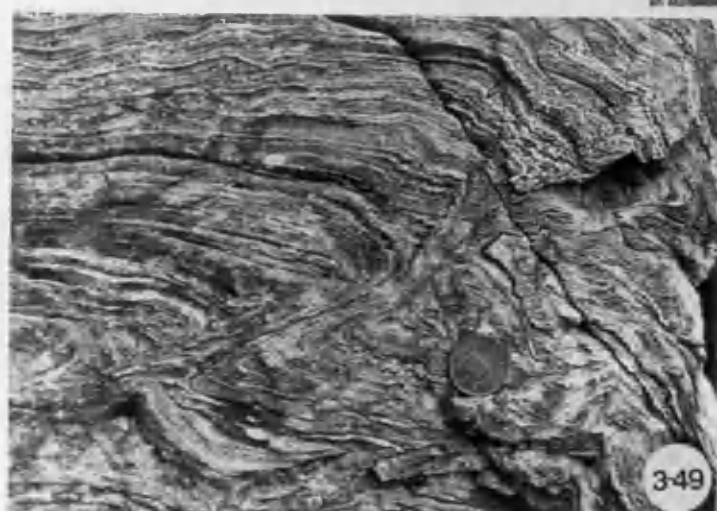
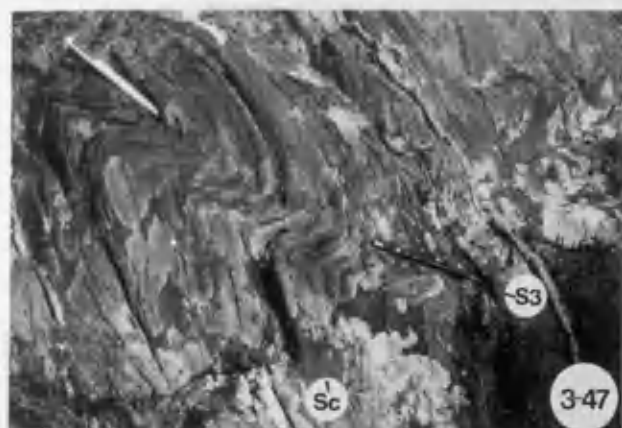
3-44

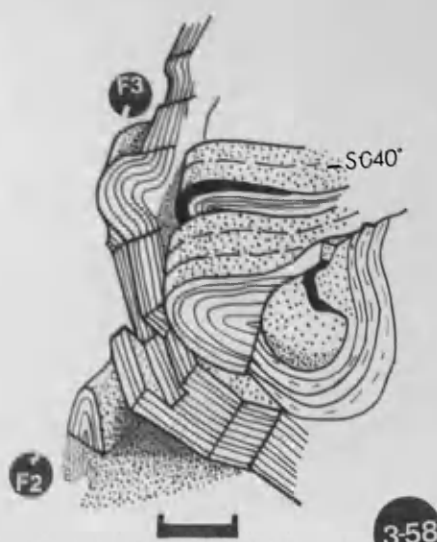
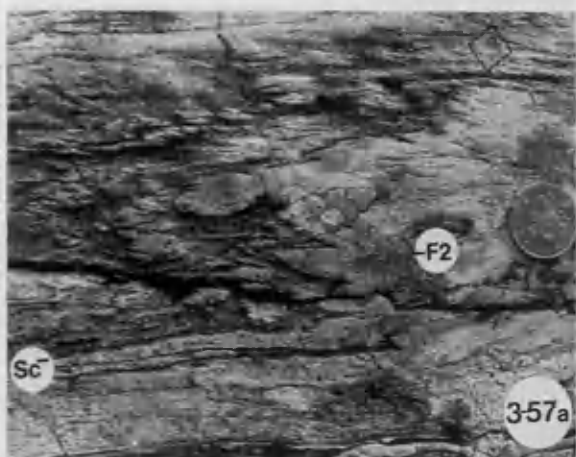
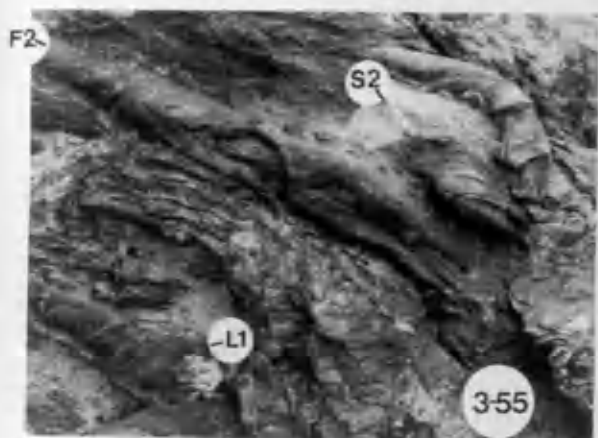
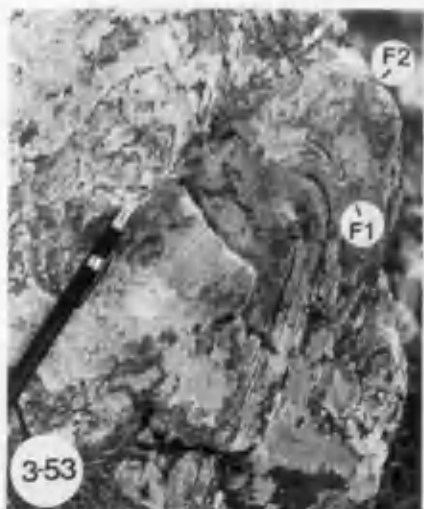


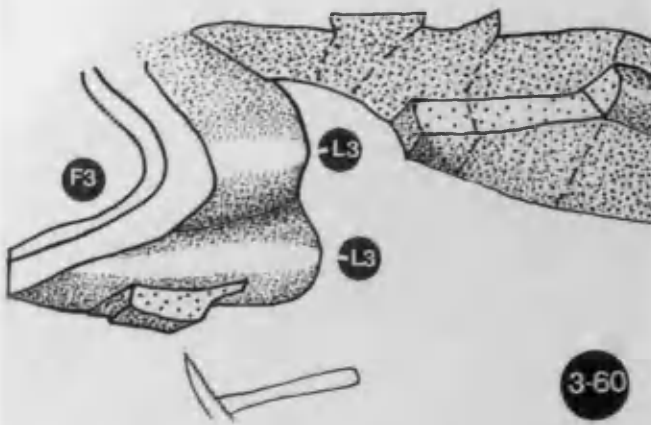
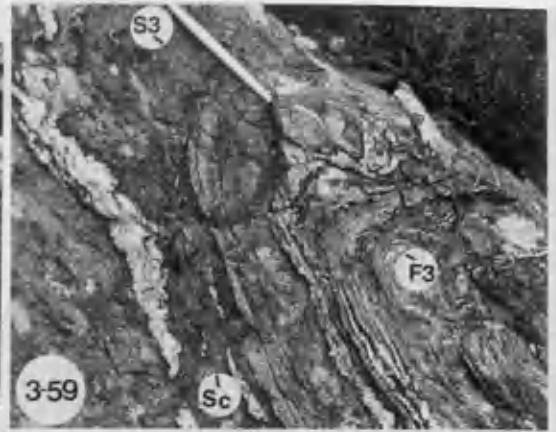
3-45

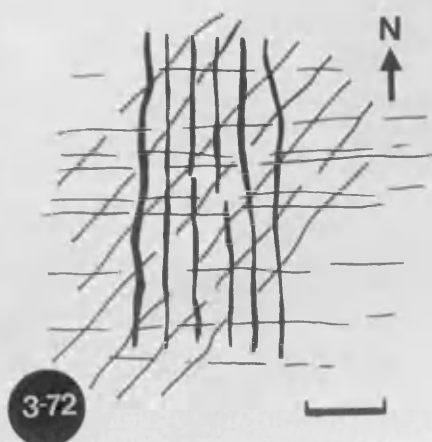
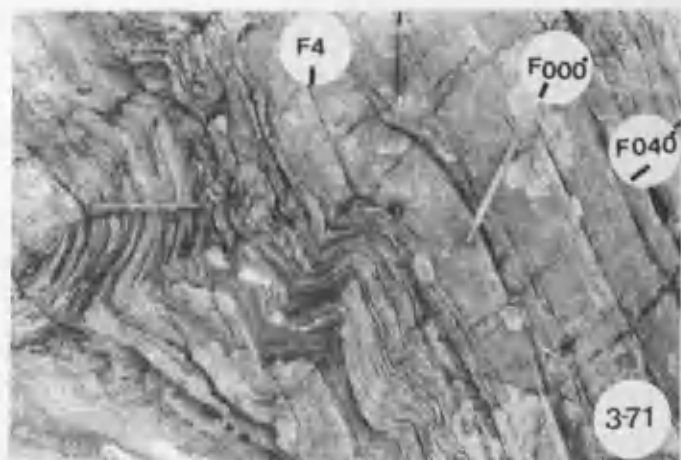
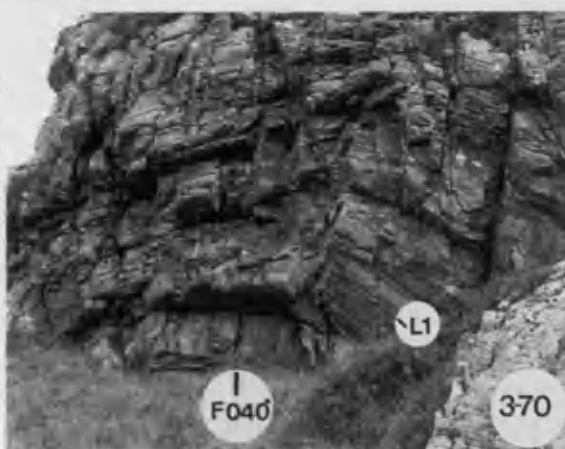


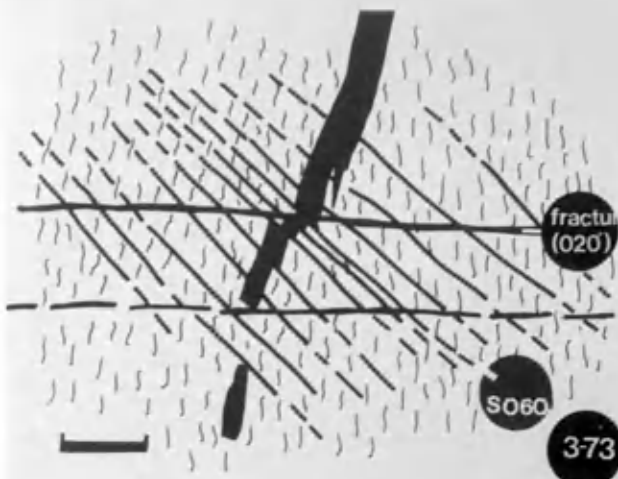
3-46







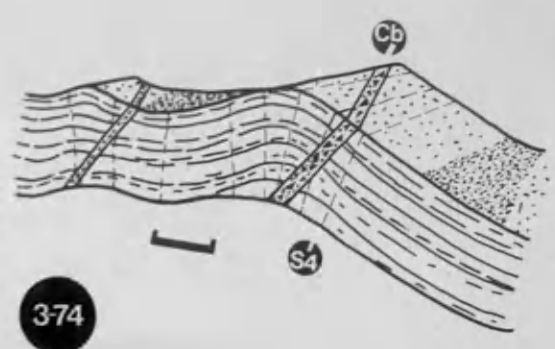




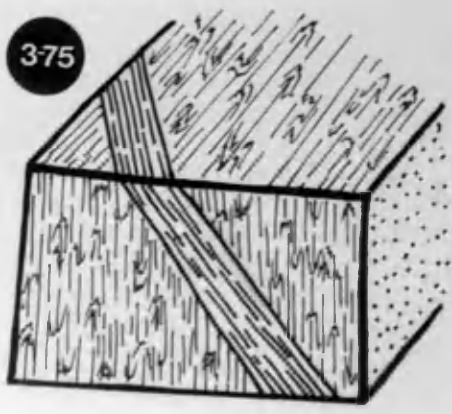
fractur
(020)

S060

373



374



375



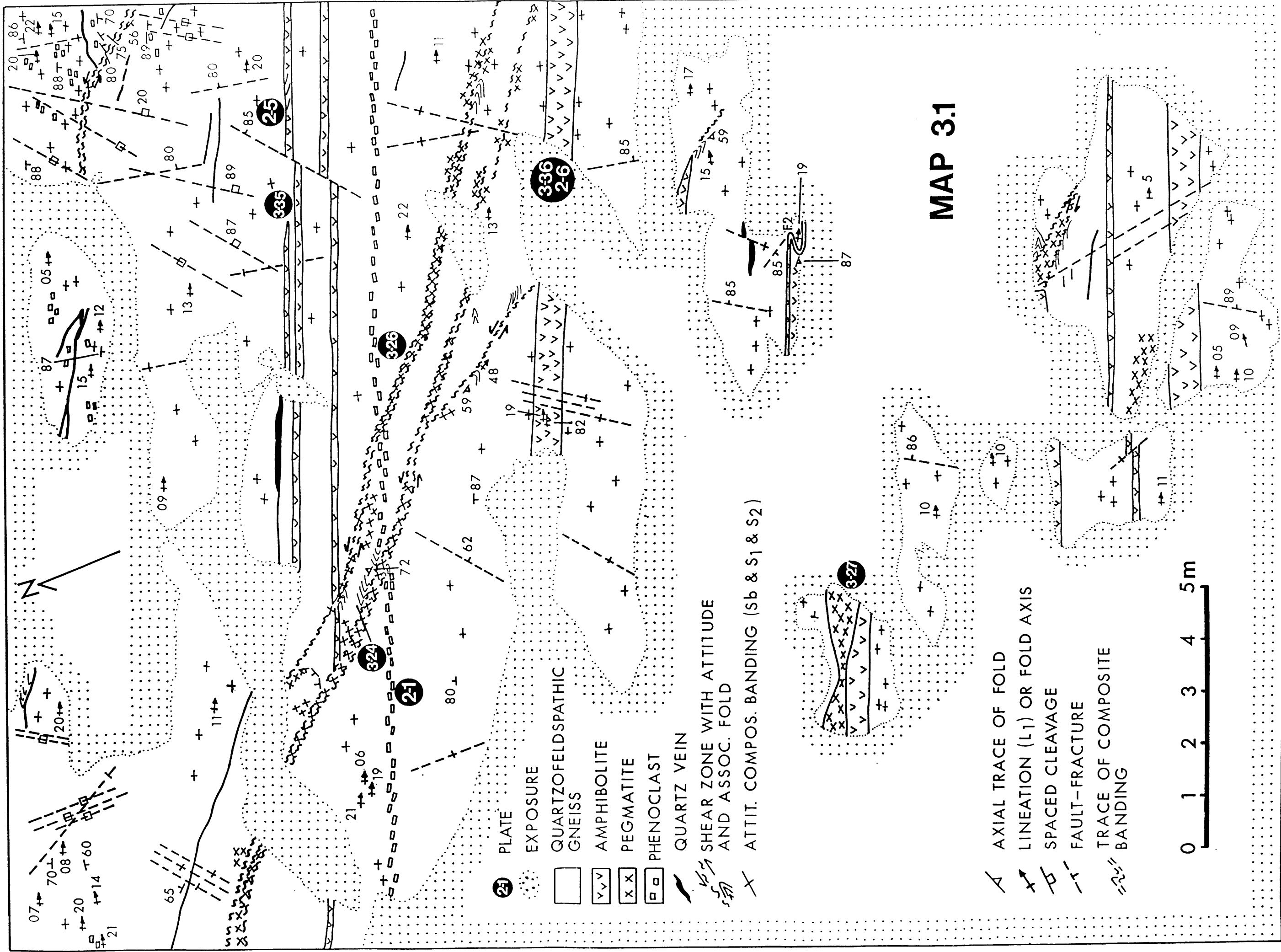
376



377



378



MAP 3.1

- 21 PLATE
- EXPOSURE
- QUARTZOFELDSPATHIC GNEISS
- AMPHIBOLITE
- PEGMATITE
- PHENOCLAST
- QUARTZ VEIN

- SHEAR ZONE WITH ATTITUDE AND ASSOC. FOLD
- ATTIT. COMPOS. BANDING (Sb & S1 & S2)

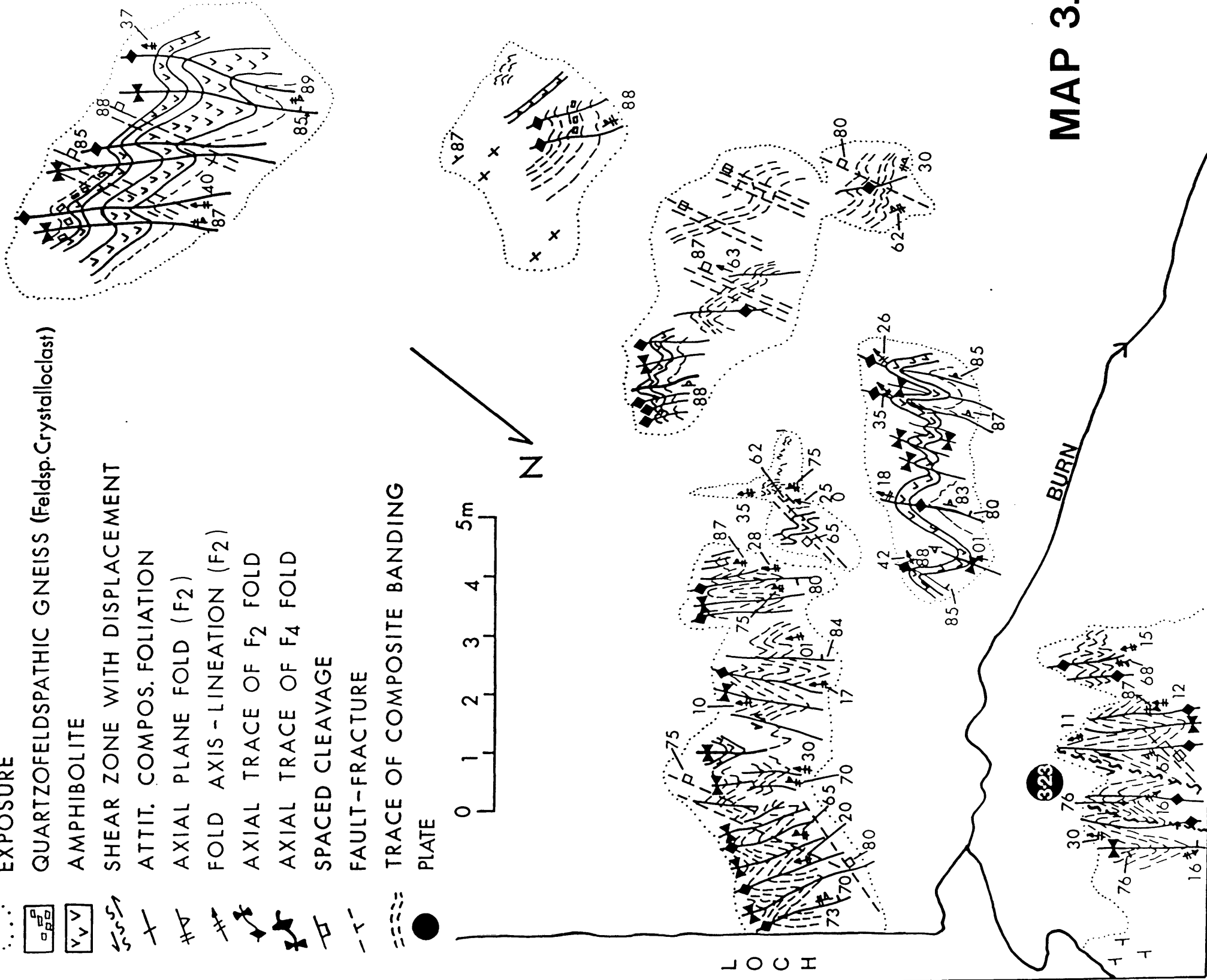
- AXIAL TRACE OF FOLD
- LINEATION (L1) OR FOLD AXIS
- SPACED CLEAVAGE
- FAULT-FRACTURE
- TRACE OF COMPOSITE BANDING



- EXPOSURE
- QUARTZOFELDSPATHIC GNEISS (Feldsp. Crystalloclast)
- AMPHIBOLITE
- SHEAR ZONE WITH DISPLACEMENT
- ATTIT. COMPOS. FOLIATION
- AXIAL PLANE FOLD (F2)
- FOLD AXIS - LINEATION (F2)
- AXIAL TRACE OF F2 FOLD
- AXIAL TRACE OF F4 FOLD
- SPACED CLEAVAGE
- FAULT-FRACTURE
- TRACE OF COMPOSITE BANDING
- PLATE

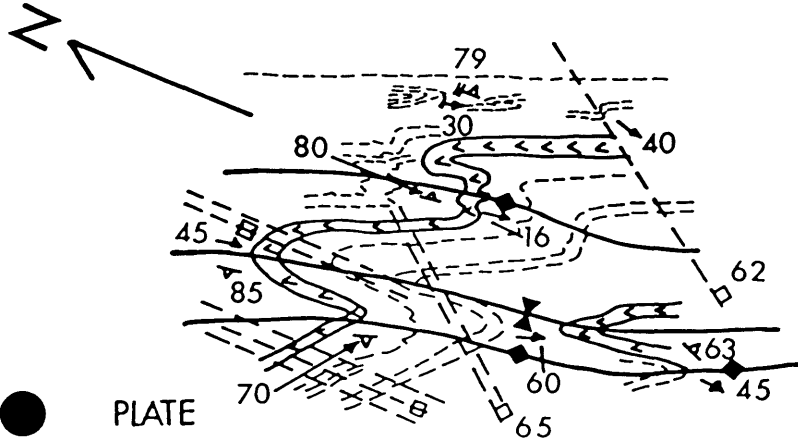
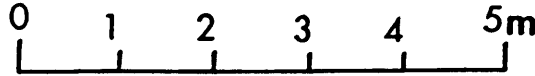


N

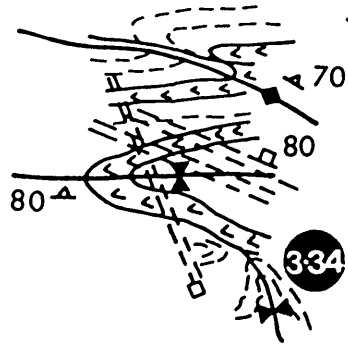


MAP 3.2

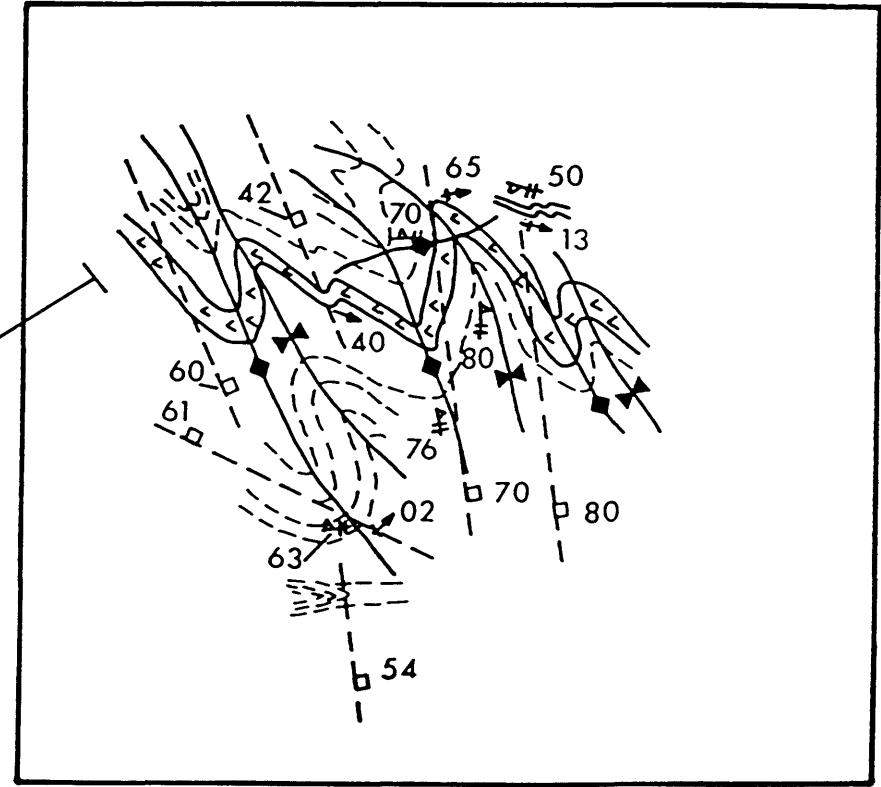
MAP 3.3



- PLATE
- QUARTZOFELDSPATHIC GNEISS
- ▣ AMPHIBOLITE
- ATTIT. COMPOS. FOLIATION
- # AXIAL PLANE FOLD (F₂)
- + FOLD AXIS & LINEATION (L₁)
- ⋈ AXIAL TRACE OF F₂ FOLD
- ⋈ AXIAL TRACE OF F₄ FOLD
- SPACED CLEAVAGE



35m
(110°)

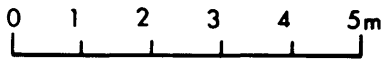


- - - FAULT-FRACTURE
- ≡≡≡ TRACE OF COMPOSITE BANDING (S_b & S₁)

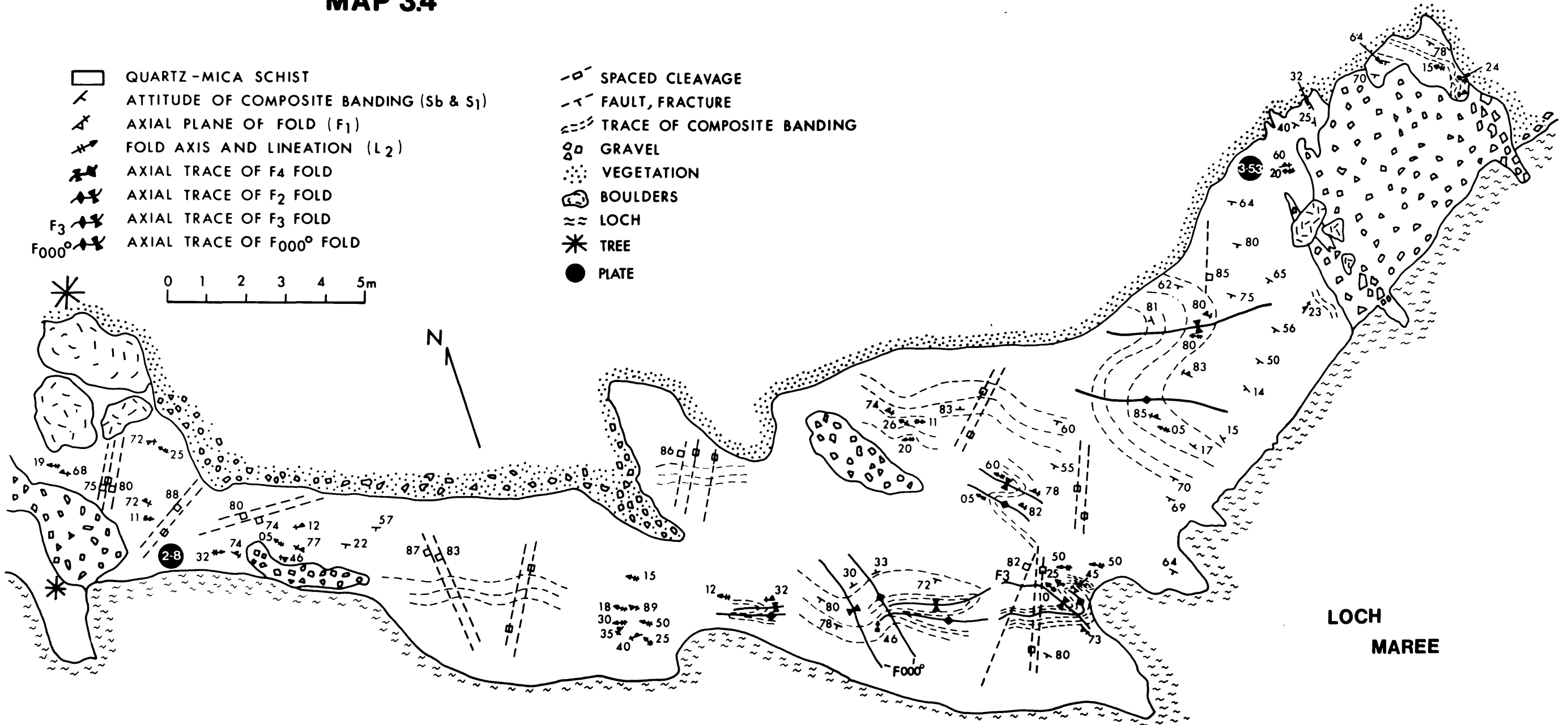
MAP 3.4

-  QUARTZ-MICA SCHIST
-  ATTITUDE OF COMPOSITE BANDING (S_b & S_1)
-  AXIAL PLANE OF FOLD (F_1)
-  FOLD AXIS AND LINEATION (L_2)
-  AXIAL TRACE OF F_4 FOLD
-  AXIAL TRACE OF F_2 FOLD
-  AXIAL TRACE OF F_3 FOLD
-  AXIAL TRACE OF F_{000}^0 FOLD

-  SPACED CLEAVAGE
-  FAULT, FRACTURE
-  TRACE OF COMPOSITE BANDING
-  GRAVEL
-  VEGETATION
-  BOULDERS
-  LOCH
-  TREE
-  PLATE



N



LOCH
MAREE

CHAPTER 4 - FABRIC STUDIES

4.1 INTRODUCTION

4.2 DESCRIPTION

4.3 DISCUSSION

4.1 INTRODUCTION

The microstructures present in these rocks vary between lithologies in both their expression and the extent of their development: no individual domain shows a complete record. For example, while the gneisses of domain I preserve the early fabrics these have been obliterated or only comprise fragments or relics in the marbles. In addition, as with the mesoscopic features, microstructures display transitional characteristics reflecting the diverse nature of the affected lithologies and the heterogeneous character of the deformation. This presents a number of problems in the classification and interpretation of the microstructures.

The approach which produced the most coherent representation of the microstructural features was the description of microfabrics in sequential order of development (D1 to D-late) and from the least to the most deformed representatives of the several phases in the different domains. It permitted the grouping of similar features superimposed on the same mineral assemblage (e.g. the grain size reduction taking place during D1, D2, etc.).

Due to the structural complexity of the rocks, sampling, in most cases, had to be done separately for each fabric in those places where the features were best expressed. Generally the individual fabric elements were followed in the field to establish the extent to which morphology (usually lithology-dependent) and geometry changed. This approach increased the confidence with which the various microfabrics described could be considered to be representative and with which the effects of deformation were interpreted. However, even when this procedure is followed the age and affinity of several deformational features remain ambiguous. This ambiguity is most problematic in the marbles of domain IV (see Chap.3) so that with exception of S1 (mylonitic), no other

microfabric of this domain will be described here.

The most useful sections were those that were cut at an angle to the planar and linear fabrics. The 'L'-tectonite fabric of most of these rocks mean that a section along the fold profile did not permit discrimination between the folded and the newly formed minerals of each fabric (e.g. S-banding and S1). Resolution of this problem has often relied on indirect evidence, e.g. structural and stratigraphic relationships (see below).

The terminology used in the classification of the foliations was that of Borradaile et al. (1982) which is based on critical assessment, is essentially descriptive and can be amended to incorporate new observations.

4.2 DESCRIPTION OF FABRICS

4.2.1 S1 Foliation

4.2.1.1 Domain I - Quartzofeldspathic gneisses and amphibolites

Quartzofeldspathic gneisses

On the basis of isotopic data (see Chap.8) and structural-stratigraphic criteria, the derivation and age of the banding in the gneisses and banded amphibolites has been shown to be different from that in other domains. Although the rocks of domain I were the least modified during the D1 event (see Chap.3) probably due to their rheological properties, the recrystallation during the early stages of the D1 event (M1) has affected most of the older microfabric. Since it is virtually impossible to distinguish between the products of M1 and the M-banding (which is probably the result of pre-Laxfordian recrystallization-see Sect.8.3) it is assumed that all the fabrics which pre-date the D1 mylonitization

were developed or strongly modified during the early stages of D1 recrystallization (M1). The following features support such an assumption.

1. Where the gneisses and amphibolites are little affected or unaffected by D1 mylonitization, they show a well-developed granoblastic polygonal texture with relatively large grain size (1-2mm, Pl.4-1).

2. Both the mafic amphibolites, discordant to the segregation banding of the gneisses and the porphyritic amphibolites show the same metamorphic 'equilibrium' texture. Even in low strain situations, where the phenocrysts still retain their igneous shape, they show a well-developed granoblastic polygonal texture with several smaller crystals replacing the original large feldspar ('Blastoporphyritic texture', Pl.4-2).

3. The evidence that all the subsequent metamorphic events were retrogressive in nature (see Chap.7) together with the deformation of these recrystallized phenocrysts giving rise to L1 stretching lineation (Pl.3-11) indicates that this texture formed during M1 at the latest (see also Sect.6.3).

In the feldspar-rich portions of the gneisses, a granoblastic polygonal texture, with straight grain boundaries and 120° triple points is a common feature (Pl.4-1). This 'equilibrium' texture is restricted to the phyllosilicate-poor bands. Where biotite and, or, muscovite is present even in subordinate proportions, the texture is controlled by the tectosilicates and there is no preferred orientation. Where quartz, biotite and muscovite are relatively abundant the predominant texture is a grain shape fabric with elongate grains of feldspar and quartz with slightly irregular contacts (Pl.4-3). The phyllosilicates show a preferred orientation and the grain size is in general smaller (c.1mm). There is always a structural control (see Sect. 4.3) and the structures described here are best represented along limbs of microfolds. This recrystallization texture is common in the gneisses (Pl.4-3), grain size being controlled by 'inclusion inhibition' (Hobbs et al.1976,p.112). The rate of crystal growth is

reduced by the attachment of small second-phase grains (e.g. micas) to a large number of grain boundaries, so that these phyllosilicates can control the development of the grain shape fabric (see Pl.4-3). The lateral increment of the deformation across the foliation is indicated by the irregularities of quartz crystal boundaries, strong undulose extinction and even some sub-grain development in most crystals.

In sections along the profile of F1 folds the S1 foliation consists of small biotite flakes aligned parallel to the axial plane of the folds (Pl.4-4). This feature is however an exception since the fabric is, in general, that of a 'L'-tectonite with amphiboles and deformed quartz and feldspar aggregates marking the strong grain shape orientation (Pl.4-5a,b,c). In a few places muscovite and epidote poikiloblasts enclose smaller crystals of feldspar, quartz, biotite etc. (Pl.4-6). Whether their growth was syn or post-tectonic in relation to S1 foliation is something difficult to assess due to the 'granular' fabric of the rock which makes it difficult to establish the relationships between the inclusions and the external (to the porphyroblast) foliation (cf. Vernon 1978, pp.299-302). There is no doubt, however, that all the above described minerals were strongly affected by the late D1 mylonitization (Pl.4-7).

Amphibolites

As in the gneisses, the nature of the S1 fabric in the banded amphibolites is complex, varying between a linear fabric ('L'-tectonite) and a linear-planar fabric ('L-S' tectonite) in phyllosilicate-rich lithologies. Amphibole crystals and elongate feldspar aggregates (in the porphyritic amphibolites) mark the former fabric ('L'-tectonite, Pl.4-8). Even in the hinge zones of F1 folds it is practically impossible in most cases to distinguish (under the microscope) the older mineral growth (banding) and the S1 fabric. This is probably due to the type of strain suffered by these rocks during D1-D2 deformations (see Sect.6.3) as well as to the widespread recrystallization and reorientation of all the

mineralogical components during the associated metamorphism (see Chap.7). Even where feldspar phenocrysts show little or practically no deformation, the linear fabric is well-marked by the dimensional alignment of the surrounding amphibole prisms. However, in some biotite-rich samples a weak planar fabric parallel to the axial plane of F1 folds is sometimes observed (Pls 4-9,10).

4.2.1.2. Domain II - Amphibole schists

Apart from remnants of calc-silicate gneisses, amphibole schists and some amphibolites showing a well-developed granoblastic polygonal texture (average grain size 1-3 mm) preserved within large garnet crystalloclasts; no other mineral growth which could be ascribed to S-banding/S1 foliation was observed. The remnants of these lithologies are in mylonites of an isolated outcrop along the northeastern limb of the large synform [NG 971722]. They were protected from the strong effects of the D1 mylonitization by the armouring effect of the garnet overgrowth (see 'mixed mylonites' in Chap.5).

4.2.1.3. Domain III - Metasediments

The S1 fabric in this domain is represented by a fine (grain size 0.5-1 mm) mica growth along the axial plane of small folds (Pl.4-11) or as remnants of a quartzofeldspathic rock with granoblastic polygonal texture preserved as lithoclasts in some mylonites (Pl.5-4). The former is usually shown as muscovite and biotite flakes still marking the remnants of a lithological layering strongly modified (mainly by D2). The micas generally show grain-size reduction along their contacts and frequently the only observed features are the darker and lighter bands which define the fold forms. In the quartz and feldspar-rich rocks the texture is rather granular with the folds showing no associated axial-planar mineral growth. The fabric is of an 'L'-tectonite type and sections at low angles to the fold axes and lineation (L1) show a marked elongation

of quartzofeldspathic aggregates and dimensional orientation of amphiboles and micas.

4.2.1.4. Domain IV - Marbles

Similarly to domain III the only features of possible D1 age, which have survived the strong effects of the mylonitization in this domain, are few lithoclasts of calc-silicate gneisses with granoblastic polygonal texture, surrounded by the fine carbonate-rich mylonitic foliation (Pl.5-67). The extreme conditions of late D1 mylonitization, probably controlled by the rheological properties of these rocks, meant that no S1 fabric older than the mylonitization has remained in the carbonate-rich lithologies (see Chap.5).

4.2.2. S2 Foliation

4.2.2.1 Domain I - Quartzofeldspathic gneisses and amphibolites

Quartzofeldspathic gneisses

The S2 cleavage in the quartzofeldspathic gneisses is expressed by fine discontinuous zones of shear looking like diffuse 'seams' in polished surfaces of hand specimens (Pl.4-12). Their sinuous geometry is probably controlled by the relative competence of minerals and aggregates (Lebedeva 1982) so that quartzose bands are transected while feldspar and epidote are frequently surrounded by the foliation. The effects of shear in the cleavage 'zones' are evident in all scales (Pls 4-12,13). Such a fabric would be classified by Borradaile *et al.* (1982) as a spaced crenulation cleavage with a 'rough' degree of planarity and an 'anastomosing' pattern of cleavage surface. In terms of the relative width of the cleavage domains it would be classified as 'narrow zonal' and as 'discrete' due to the abrupt transition between the microlithons.

The S2 fabric is best developed in the mylonitized gneisses, but since it also produces grain-size reduction like that seen in S1 (mylonitic) it poses a problem regarding the distinction between deformational features (at microscopic scale) produced during D1 and D2. Since S1 is not everywhere a penetrative structure it is usually possible to observe its effects upon the older fabrics (Pls 4-15 to 4-18). Quartz, muscovite, epidote and microcline suffer further grain-size reduction to that imposed during D1, in places down to a submicroscopic grain sized matrix containing ovoid feldspars produced from lath-shaped crystals. The narrower the S2 shear zone, the smaller the grains (Pls 4-14,15a,16). This reduction continues to the point where there is no evident orientation in the matrix; a feature very similar to that shown by the D1 ultramylonites.

Consistently sinistral sense of movement is shown by rotated crystalloclasts, the asymmetry of muscovite flakes caught by the shear zones and displacement of fine quartzose bands (Pls 4-16,17,18). Although muscovite crystals are usually observed within the S2 zones, they occur as long partially destroyed mica flakes, and practically no biotite is left. The presence of aggregates of chlorites probably accounts for the absence of biotite. These aggregates are particularly common along the axial planar position of small F2 folds where some remnants of biotite still survive and the grain size is frequently sub-microscopic. Where quartz bands (mostly formed during D1 mylonitization) are cross-cut by these shears the deformation bands and other similar structures are well developed (Pls 4-17,18).

Factors determining the more or less penetrative character of S2 include:

1. The grain size of the affected foliation (S1 mylonitic). In places where a fine S1 mylonitic banding is cross-cut by S2, the latter tends to be more pervasive (Pl.4-18).
2. The relative abundance of quartz and feldspars compared to micas. In sections where large and abundant clasts of feldspars are present the S2 foliation presents more brittle features and is less penetrative (compare Pls 4-15,15a). In this way the role

played by the D1 mylonitic processes could have been important not only for the reduction of the grain-size (facilitating the pervasiveness of S2) but also because of the associated mineral transformations (see Chap.7).

Being less pervasive than the D1 mylonitic banding the S2 shear bands tend to wrap around the lithoclasts that survived D1 mylonitization. In general, these fragments display granoblastic polygonal textures and are elongate parallel to S1 where S2 is absent or less developed. In areas where S2 is strongly developed (invariably coinciding with areas of strongly developed mylonitic S1) these lithoclasts seem to suffer further grain-size comminution and rotation of their long axis into parallelism with S2. Small folds are frequently observed in these regions. Along the limbs of these folds shear features are well-developed and the elongation of deformation bands in quartz crystals are invariably aligned parallel to their axial plane (Pl.4-19).

Sections at high angles to the folds axes tend to show larger displacements along the S2 shear bands than other orientations of sections, suggesting that the extension direction ('X') is at^a high angles to the fold axis (see Chap.6).

In the hinge zone of the large F2 synform in this domain, a biotite mineral growth cross-cuts the older composite fabric (S-banding + S1, Pl.4-20). The physical continuation of this mineral growth in pure quartz layers is represented by deformation bands and recrystallization (Pl.4-21).

The relative strength of individual minerals to D2 grain size reduction processes seems to be the same as that during D1 mylonitization, with epidote and feldspars being more resistant than muscovite and biotite (see also Chap.6).

Biotites and amphiboles express the S2 axial-planar foliation in the amphibolites. The biotite is present as small flakes better observed in the feldspar-rich bands than in the mafic ones where epidote amphiboles are the dominant mafic minerals (Pl.4-20). In

the mafic amphibolites interbanded with the mylonitized gneisses S2 is a gradational crenulation cleavage affecting the S1 mylonitic banding. Due to the presence of large porphyroclasts in these rocks plus the small amplitude/wavelength ratio of the crenulation, the microfolds do not show a regular geometry. The presence of a large porphyroclast or a group of porphyroclasts appears to inhibit the formation of folds (Pl.4-22).

Quartz, wherever present, shows well-developed deformation bands, invariably elongate parallel to the axial plane of the crenulation. Amphiboles, where they are folded in a concentric style, have opaque mineral infills in concentric fractures, probably developed during folding. Where the folds are tighter, grain size reduction effects are observed, with the production of aggregates of chlorite, epidote and opaque minerals. Reorientation of amphibole crystals by rotation of crystals towards parallelism with S2 is common.

Generally speaking the size of S2 biotites and amphibolites is smaller than their S1 equivalents.

4.2.2.2. Domain II - Amphibole schists

In the amphibole schists hornblende crystals mark the S2 foliation. While in most samples cross-cutting relationships are not clear (Pl.4-10,23), in some, large prismatic crystals (tremolite?) mark the S2 foliation (Pl.4-24). The absence of a well-defined S2 foliation in some samples is probably due to the mechanism of deformation (see Chap.6) as well as recrystallization during M2. In these samples although the crystals do not show particularly straight contacts, the effects of deformation are very few. Where present, the quartz crystals rarely show deformation bands though the development of sub-grains is not uncommon.

Where late D2 quartzofeldspathic veins are present, well-developed mylonitic features are observed, affecting both the quartz and the feldspar. The adjacent amphiboles look unaltered, with minimal grain reduction along the crystal boundaries. The deformation

features observed in these veins are younger than S1 and were folded by F2 folds, indicating their D2 age with certainty. Likewise, quartz deformation bands within the veins show elongation parallel to S2. The feldspars present features like bent twins and kink bands.

4.2.2.3 Domain III - Metasediments

Probably due to the effects of the mechanism of deformation which formed most of the F2 folds, as well as the nature of the interbanded sequence in which most of the folds recognized as F2 were described (quartz-rich bands 'immersed' in fine mica-rich matrix) the S2 foliation is not well-developed (see Chap.6).

Crystalloclasts remaining from the D1 mylonitic episode are here seen folded around F2 hinges. They comprise feldspars and particularly large muscovite flakes, the latter frequently seen in disrupted hinges of F2 folds (Pl.4-25).

Ptygmatic F2 folds are common in this domain, particularly in the mylonitic mica schists. These folds (Pl.4-26) presenting variable layer thickness and large distances between adjacent fold crests (measured along the layer), when compared to fold wavelength and layer thickness, indicate considerable shortening resulting from buckling (see Chap.6). Although the presence of a faint cleavage and layer thickness control over fold wavelength could also suggest the action of layer parallel shortening (Pl.4-27) most of the rocks show only re-orientation of the old minerals.

In general, the S2 foliation is a gradational crenulation cleavage with broad zones corresponding to the limbs of the folds. Where the folds are very tight it is difficult to distinguish between D1 and D2 features. However, deformation bands in quartz showing elongation parallel to the axial plane of small folds and higher density along the (high strain) short limb of folds and large number of grains along the short limbs of folds are certainly D2 features (Pl.4-28).

Large muscovite flakes, generally show a fan-like (undulose)

extinction (Pl.4-25). In some of these isolated hinges, fractures filled with chloritized biotite are present. The latter is also frequently observed along the cleavage planes of large muscovite flakes probably indicating that these structures acted as channels for percolation of fluids during part of the deformation (folding) of these rocks. In other samples, features indicative of the operation of pressure solution mechanisms are widespread. They consist of dark discontinuous seams along the limbs of most small folds. A strong grain size reduction along these zones as well as along some of the hinges of the crenulations with concentration of opaque minerals and sericitization of the large muscovite relicts is observed (Pls 4-29,30). The dark seams show anastomosing patterns surrounding crystalloclasts of feldspar. In several examples these structures tend to develop along the more competent quartz bands, being slightly deviated from their initial position (Pl.4-30). In very fine-grained samples the folded layers show displacements and/or pressure solution along the F2 axial planes characterizing the initial stages of transposition of the S1 fabric (4-31). Transposition of thin quartz bands is locally observed (4-32). Other common features include remnants of the protolith, usually present as well-rounded 'crystalloclasts' surrounded by the S1 mylonite banding (Pl.4-33). In the cylindrical F2 folds large muscovite flakes are commonly aligned along S2 (4-34). The presence of isolated hinges indicates, in those cases, the advanced transposition the rock has suffered, leaving clear the nature of the mica flakes as old crystals rotated towards alignment with S2. The non-cylindrical and 'supercylindrical' F2 folds show no visible axial planar foliation (Pls 4-35,36) while a foliation can be observed in the 'supercylindrical' folds.

4.2.3. S2a Foliation

4.2.3.1 Domain I - Quartzofeldspathic gneisses and amphibolites

Quartzofeldspathic gneisses

Under the microscope the S2a fabric is marked by a well-developed

crenulation cleavage with long deformation bands in quartz crystals parallel to the fold axial planes. The width of the bands decreases considerably where a porphyroclast of a more resistant mineral is present. Some of these bands show a subdivision (internal deformation lamellae) oblique to the elongation of the large ones (Pl.4-37). However, it is difficult to be sure about the contemporaneity of this feature and the development of the shear zones. In the strongly deformed parts of the rock these small oblique deformation bands dominate with the large ones only preserved in relict outline (Pl.4-37). The restriction of these 'sub-bands' to parts of the rock affected by the shear zones seems to indicate their association (in places where the D2a shear zones are well-developed D1 and D2 mylonitic structures are uncommon). The frequent presence of large perthites in feldspars with orientation parallel to the small deformation bands in quartz could also indicate their association with D2a deformation processes.

The extreme heterogeneity of the D2a deformation is suggested by the development of 'localized' (discrete) shear zones and the presence of both (a) little deformed 'pods' of gneisses surrounded by bands with intense deformation and (b) kink bands in mica flakes showing variable orientation.

Ductile shear of feldspar crystals is marked by bending of twins (Pl.4-38). The shear planes are slightly rotated (clockwise) in relation to the axial planes of the F2a crenulation. The latter is marked by deformation bands in quartz; some of which are aligned parallel to the shear bands. Whether they have been rotated to or formed in that position (marking a 'S'-surface) will be discussed in chapter 6.

More than one set of shear zones with different orientations were observed in a few samples. Despite the fact that some sets show geometry compatible with a conjugate system or show features typical of brittle deformation it is very difficult to assess their relative age, since factors like deformation rate, and type of material affected are very important and can easily determine the nature (plastic or cataclastic) of the produced features (see Chap.5).

In more intensely deformed samples zones of pseudotachylite have developed surrounding and intruding pods of less deformed rock. The grain size reduction is extreme, producing angular fragments of crystals immersed in a sub-microscopic matrix (Pl.4-39). In the least affected parts of the rock well-developed deformation bands in quartz are invariably present with associated feldspars showing internal dislocations. The progressive increase of density of deformation bands towards the zones with pseudotachylite seems to indicate that features of ductile deformation were generated at the same time or on the way to the production of pseudotachylite. The absence of overprinting of these structures by later faults seems to rule out the possibility of reactivation of the once ductile zones during later brittle deformation. The presence of pseudotachylite amongst ductile deformed rocks has been recently identified (*cf.* Sibson 1980; Passchier 1982).

Amphibolites

The microstructural D2a features developed in these rocks were not investigated in detail due to their restrict occurrence (see Chap.3). However the minerals (particularly the feldspars) show evidence of much more plastic deformation than their counterparts in the quartzofeldspathic gneisses.

4.2.4. S3 Foliation

4.2.4.1 Domain I - Quartzofeldspathic gneisses and amphibolites

Quartzofeldspathic gneisses

The S3 foliation is expressed mainly as a spaced cleavage. This is probably a function of the lithological control although in some places, the development of a gradational crenulation cleavage

reflects the interbanded nature of the sequence. The associated folds show convolute geometry with patterns suggesting refolding (Pl.4-40). However, these patterns were probably produced by the complex strain developed in detachment zones in mica-schists immediately above the hinge of a thick, folded, quartzofeldspathic band. Like the structural expression of D2 features, thin layers of quartz with deformation bands are elongate parallel to the axial planes of small F3 folds. These folded layers frequently show smaller grain size along the inner arc than along the outer arc (Pl.4-41). Since most of the microscopic features are probably inherited from D1 and D2 deformational episodes these bands in quartz crystals, with orientation parallel to S3, are the only deformational features at the grain scale which can be attributed to D3 deformation with certainty. In contrast the micaceous bands show more regular features like small box folds and conjugate kinks. Along the fold hinges mica flakes show radial extinction. Carbonate fills the spaces left by décollement along the hinges of folds and radial fractures which are commonly seen cross-cutting quartzose bands.

4.2.4.2. Domain II - Amphibole schists

The S3 foliation in this domain is a gradational crenulation cleavage best developed in schistose units (Pl.4-42). Most of the long amphibole prisms seem to have suffered grain boundary sliding, particularly along the hinges of microfolds where features of grain size reduction are particularly well-developed. The general aspect and position of the grains suggests the active character of the older composite foliation during this phase of deformation (see Chap.6.). Although most of these features are probably inherited (products of D1 mylonitization) the active character of the schistosity is shown by small chevron folds presenting imbrication of crystals in the core of the folds (Pl.4-42) as well as development of fractures and reverse micro faults propagated along the foliation. Detachment of the fold hinges is a very common feature and carbonate usually fills the spaces. Where a single crystal is present in a sharp hinge it shows different parts with diverse crystallographic orientation.

Chlorite is the most common mineral both in those zones where there has been grain size reduction and in fold hinges. Generally it is associated with opaque minerals which are abundant along the schistosity planes and so assists in the identification of fold hinge zones.

Where the proportion of feldspar and quartz to amphiboles and micas is high the mylonitic features are more evident. These are particularly well-developed along the axial planes of the recumbent folds, where narrow (0.25mm) zones with amphibole crystalloclasts are surrounded by a very fine matrix, composed of amphibole fragments, opaque minerals, fine-grained feldspars and carbonate (Pls 4-43,43a). Generally these zones are quite irregular, branching around large amphibole crystalloclasts but keeping an overall orientation parallel to the axial plane of the microfolds.

In some samples where large garnets overgrow the composite foliation the crenulation produces a sort of imbrication of these crystals due to their dimensions (larger than the wavelength of the microfolds).

4.2.4.3 Domain III - Metasediments

As in the case of S₂, the S₃ structure in these rocks is a gradational crenulation cleavage, usually best developed in mica-rich units (PL.4-44). In the more siliceous units the crenulation is less visible and where present it shows a larger wavelength than in micaceous bands, while some of the quartz bands show no crenulation whatsoever. In these layers, deformation bands oriented parallel to the axial plane of the crenulation seem to be the equivalent structures. In addition to the late D₁ garnet porphyroblasts, which do not show evidence of D₃ deformation, large muscovite flakes, where not interbanded with quartz-rich layers, show open kink bands. They are mainly oriented slightly oblique to the S₃ crenulation but in some considerably thicker bands this relationship is not that clear.

The S3 crenulation is less developed in quartz-rich bands where, if present, it shows a considerably larger wavelength than in the pelitic units. In the quartz bearing units interlayered with carbonate-rich layers however, deformation bands are present in the quartz (Pl.4-45). It is surprising that these quartz crystals appear to have been relatively intact before the imposition of D3 deformation. Such an appearance may be the result of recovery probably during the late stages of D2 deformation.

4.2.5 S4 Foliation

4.2.5.1 Domain I - Quartzofeldspathic gneisses and amphibolites

Quartzofeldspathic gneisses

In muscovite-rich bands of the gneisses the S4 foliation is represented by a crenulation cleavage of large wavelength and kink bands (Pl.4-46). Commonly the crystals show strong undulose extinction; deformation bands with elongation parallel to the axial plane of the crenulation cleavage are also seen in many places. 'Retrogression' to sericite occurs particularly along the limbs of microfolds, where S4 is best developed. More resistant minerals like feldspars and epidote show no visible signs of deformation which could be attributed to D4 except when they lie in a fold hinge. Here S4 is generally expressed as a fracture which propagated along the fold hinge in a fashion similar to that seen in hinges of chevron folds. Where it is muscovite that is affected radial extinction is developed.

In samples where a previously developed mylonitic fabric is present it is very difficult to distinguish the effects of D4 from those of earlier deformational phases. This difficulty is illustrated by the sigmoidal shapes shown by some deformational bands which could have been produced either by D4 or D1, the phase during which the bulk of the mylonitic features were developed.

Amphibolites

In the amphibolites, the feature controlling the formation of the microstructures during D4 was the presence or absence of a well-developed schistosity. Where the rock shows a granoblastic texture the crenulation is not very evident and some of the grains are 'imbricated'. Where biotite is relatively abundant a large amplitude and regular (sinusoidal) crenulation is developed. Quartz and biotite display mylonitic features (deformation bands and grain-size reduction) developed during D4. These features are frequently seen along detachment zones invariably developed along quartz-rich bands in fold hinges. In the outer arc of most folds the amphiboles are slightly bent and the micas display radial extinction. In the inner arc these prismatic crystals are imbricated and have irregular and diffuse contacts (Pl.4-47). In some of the folds the detachment zones seem to have propagated along the limbs where grain-size reduction zones with angular crystalloclasts (cataclastic deformation ?) are observed.

4.2.5.2 Domain II - Amphibole schists

The development of the S4 cleavage in this unit is also controlled by the nature of the pre-existing foliation. Where amphibole (and plagioclase) dominate the most frequent structure is a gradational crenulation cleavage (Pl.4-48). Although most of the mylonitic features along the folded foliations have been developed in pre-D4 episodes, the presence of deformation bands in quartz crystals showing elongation parallel to the axial planes of the folds indicates the influence of D4 deformation. The amphibole crystals, on the other hand, show very little signs of deformation. As in domain II, detachment zones are localized along quartzofeldspathic bands, where the quartz crystals are strongly deformed and the feldspars occur as remnants (Pl.4-48A). These bands show the effects of much stronger deformation than the surrounding amphibole-rich layers. Although rare, some bent single crystals of

feldspar are seen surrounded by the matrix. Their geometry suggest they were caught in between crystals with differential relative movement. In other samples fracture zones occur along F4 limbs where the grain size reduction reaches the ultraclastoclastic stage.

Samples with higher percentages of phyllosilicates show a crenulation with large amplitude and small wavelength. Detachment zones in fold hinges frequently occur along chlorite-rich bands (Pl.4-49). This mineral shows elongation parallel to the axial plane of the microfolds that do not show the S4 crenulation (stack of straight flakes). This, together with its constant presence around amphibole crystals is suggestive of its secondary origin. Carbonate is also a common mineral in the saddle reefs formed during D4 folding.

4.2.6 S-LATE

4.2.6.1 S-000°

Depending on the nature of the affected lithology this is an open, gradational crenulation cleavage (pelitic units of domain III) or a variably-spaced set of fine fractures (most domains). Wherever the interbanding shows variable competence both types of foliation seems to be present. No mineral growth is present. In several cases the old composite foliation can be seen to have been rotated giving rise to a relatively tight crenulation cleavage frequently very well delineated by opaque minerals.

4.2.6.2 S-040°

In most lithologies the S-040° is a gradational crenulation cleavage (Pl.4-50). It usually shows large wavelength and associated 'ductile-brittle' features. Along most of the hinges of small folds fractures are present following approximately the

variation in orientation of the hinge. This together with the presence of areas of grain-size reduction along these zones, indicates a possible genetic link between the crenulation formation and the fracture zone. The detachment zones along the fold hinges seem to have been established along biotite-rich bands.

'Imbrications' of crystals at the core of the small folds, where micro-faults are conspicuous point to the compressible nature of these regions. The fact that some of the small faults propagated along the mylonitic banding (folded) indicates the preferential reactivation of this foliation during the development of the S-040° crenulation cleavage.

Bent amphibole crystals are not uncommon. Some of these show patterns of conjugate fractures along the inner part of the fold while the outer zones presents the beginning of kink bands development (Pl.4-50A).

4.2.6.3 S-060°/S-090°

These structures are shown as sets of planar spaced (2-10 cm) cleavages with chlorite and opaque minerals filling the planes.

4.3 DISCUSSION

Microfabric analysis has been considered an essential and reliable technique for the elucidation of relationships between deformation and mineral growth in rocks showing polyphase metamorphism and multiple deformation (cf. Park 1969, Hobbs *et al.* 1976, McLellan 1984). Increased understanding of the processes taking place during deformation and mineral growth caused a multiplication of the number of possible interpretations (cf. Vernon 1977, 1978; Ferguson and Harte 1975; Olesen 1978; Williams and Schoneveld 1981; Williams 1985). Although the criteria first systematized by Zwart (1962), in general hold if care is taken to identify fabric elements, the simplistic application of the 'classic approach' can fail to explain several features, or may lead to a much more complicated history of deformation and mineral growth than is necessary. If interpretations of timing of metamorphism and deformation in the analysis of fold belts are equivocal then mineral paragenesis used to set up the isograd and isotherm patterns, and in turn the determination of geothermal gradients, and finally construction of tectonic models will all be likewise equivocal. In addition, if complexities like the influence of folding, thrusting (Mason 1984, Andreasson 1980, Chamberlain 1986), erosion processes (England and Richardson 1977), faulting and other common structures (of several scales) remain undetected or are misinterpreted (Bell and Brothers 1985) the pattern and nature of the simplistically determined heat flows can even be erroneously extrapolated to other geological periods (see discussion in England and Richardson 1977, p.205).

Recent investigations in the relationships between metamorphism and deformation have posed two major questions (Jones 1981). The first is whether there is any evidence for the control of the deformation by metamorphic phase changes. The second is whether deformation has any direct effect on the rate of equilibria of the contemporaneous metamorphic reactions. The answer for these two questions is intimately related and will be discussed in more detail in chapters 5 and 7 respectively. The objective of the present section is to discuss the difficulties faced during the microtectonic studies emphasizing the deformation aspects of the problem (see also Chap.7).

In spite of the several examples in the literature of metamorphic reactions being controlled by deformation (e.g. Jamieson 1986, Brodie 1981, Max 1981), some of the porphyritic amphibolites in the Loch Maree area show granoblastic polygonal textures in slightly deformed feldspar phenocrysts ('Blastoporphyritic texture'), suggesting that although deformation was not pervasive in this case, recrystallization processes seem to have affected the rock throughout (see section 4.2). Although the contemporaneity between metamorphism and deformation cannot be directly demonstrated in this case, several lines of evidence seem to suggest their close association (see Chap.6). In most lithologies where no primary (pre-tectonic) markers were found, the relationships between mineral growth and deformation remained ambiguous and several problems were faced. These will be discussed below.

Despite the fact that the presence of layers and grains with different mechanical properties seem to be of fundamental importance during deformation, scant attention has been paid to the role played by such heterogeneities in the development of tectonic structures at microscopic scale. Apart from the work of Lebedeva (1979) where the influence of heterogeneities at the grain scale in the modelling of development of rock cleavage is investigated, and the more theoretical analysis of deformation by Bell (1981), Lister and Williams (1983) and Williams and Schoneveld (1981), the author is not aware of any other direct application of this approach to the study of the relationships between deformation and mineral growth until the very recent work of Bell (1985) and Bell et al. (1986). In addition to the implications of Bell's work in terms of the establishment of geothermal gradients, this kind of approach also gives a framework for a self-consistent interpretation of the microstructural features observed in the Loch Maree rocks. It also provides a more consistent synthesis of the microstructural data in relation to the mesoscopic scale structural sequence, being at the same time consistent with other lines of evidence like the radiometric data and the climactic metamorphic conditions (see Chaps 7 & 8). For these reasons the principles of "deformation partitioning" (Lister and Williams 1983) and the role played by "progressive bulk, inhomogeneous strain" (Bell 1981, Bell et al. 1981, Bell and Rubenach 1980) will be briefly reviewed.

From the observation of naturally deformed rocks, Bell (1981) developed a number of strain models and geometries produced by progressive, bulk, inhomogeneous shortening. The models reproduce the inhomogeneities at several scales and shows the strain variations produced by deformation of a rock composed of minerals (and aggregates) of variable resistance to deformation. Figure 4.1 (a,b,c) shows the geometry produced for both, coaxial and non-coaxial deformation paths.

The Loch Maree rocks show localized features indicating the action of both types of deformation, but this is to be expected, since once a strain inhomogeneity is established, within the scale of that inhomogeneity, a specific strain field is developed (Bell 1981, p.281). Thus the concepts of coaxial and non-coaxial strain paths during deformation are scale dependent and could be important on one scale but not on another. In the case of the Loch Maree rocks the presence of mylonites, some of which are marking the locus of a movement zone of tectonic importance (the 'Loch Maree thrust zone' between domains I and II), seems to suggest that non-coaxial deformation has played a major part during the structural evolution of these rocks (see Sect. 5.3).

Heterogeneities present in these rocks include both primary (sedimentary) and secondary (tectono-metamorphic). The latter seems to have played a more important role at macro and mesoscopic scales since the first phase of deformation has progressively affected interleaving of basement and cover. In this section emphasis will be given to the primary (modified by metamorphism) and small scale secondary heterogeneities since they are the most important factors controlling the partitioning of deformation at microscopic scale, from late D1 times onwards.

Notation of the position of the specimens in relation to the mesoscopic scale structures was of great help in the interpretations of the microstructural relationships, since, for instance, different parts of a fold present diverse strain distribution, which were certainly reflected in the relationships between minerals (e.g. porphyroblasts and matrix). Similarly, the

nature of the deformation processes reproducing structures belonging to the same generation at several scales, has permitted clarification of the relationship between folding and mineral growth in most of the thin sections. It was then clear, that minerals like garnets were flattened and boudinaged when occurring along limbs of microfolds while the same mineral could show practically no deformation when present along fold hinges. Deflection of foliation, development of crenulations and several other microstructural criteria were also observed to be dependent on factors like (a) the local composition of the rock, (b) the variation of resistance of different minerals to the deformation processes, (c) the wavelength, (d) amplitude and other characteristics of the microfolds, all these demonstrating the extreme inhomogeneous nature of strain distribution. In this way, at several stages of the deformation history, different portions of the rocks take up (1) no strain, (2) mainly progressive shortening strain, (3) progressive shortening plus showing strain and (4) progressive shearing strain (cf. Bell 1985, p.109).

Figure 4.2 reproduces the strain variation observed in a strongly deformed quartzofeldspathic gneiss, for instance, where the feldspars show little effect of the deformation, which is almost completely taken by the phyllosilicates. The latter anastomose around the feldspar porphyroclasts because of the inconstant character of the progressive shear strain along the foliation due to the presence of these heterogeneities (Bell et al. 1986). The pattern is even more complicated if we consider the effects of factors like (a) the polymineralic nature of the rocks giving rise to 'domains' of variable dimensions (Fig.4.2), (b) the variable degree of pervasiveness of the structures, (c) the polyphase deformation and (d) the interaction of different mechanisms of deformation during the evolution of these rocks. Accordingly, during the microstructural analysis each situation had to be individually assessed bearing in mind that similar microscopic features (e.g. deformation bands in quartz crystals) could have easily been developed during several of the deformational phases. In spite of the large number of possible combinations of these features, in most cases the microstructures followed patterns which agree very well with the ones predicted by the above discussed

models. This, together with careful sampling (for each group of features in all the domains) made possible the identification of the relative age of several of these features.

The timing of garnet growth and development of foliation posed the greatest microstructural analytical problem. The presence of idioblastic and deformed garnet crystals side by side was a common feature. In several cases, the crystals did not show clear signs of deformation. However, the phyllosilicates surrounding these (more competent) porphyroblasts seem to have taken up most of the deformation, showing advanced stages of grain size reduction. In other cases the deformation seems to have been strong enough to affect the porphyroblasts as well, producing 'flattened' crystals. These frequently present features like microboudinage and other extensional microstructures (see Sect.5.3). This was the case of most mylonites, where only in exceptional situations idioblastic porphyroblasts have remained intact (Pl.5-61). However, even in these cases, the possibility of later (M2) reconstitution of the garnet (rims) must be considered (see below). Figures 4.1 and 4.2 reproduce the geometry of most of the observed features of deformation at this scale.

Whether we are dealing with just one (set of) garnet growth or not is difficult to assess (cf. McPowell and Vernon 1979, p.42; Etheridge and Vernon 1981). However, the (a) fairly homogeneous composition and idioblastic shape of these crystals together with (b) the positive correlation between low strain zones and idioblastic crystals as well as (c) the presence of similar inclusion patterns in 'deformed' and 'non-deformed' porphyroblasts seem to suggest that some crystals shapes are a function of strain variation and/or that low strain zones were preferred for post-D1 garnet growth. Accordingly, in interbanded quartzofeldspathic and pelitic rocks the idioblastic garnets are generally preserved in the felsic bands (Pl.5-61) unless high strain was achieved. Also, where these crystals occur in 'sheltered' parts of the rock (e.g. strain shadow of a larger porphyroblast - Pl.5-52, Fig.4.3A) or along the hinge zone of a microfold, they show large dimensions and better preserved shapes. This would imply that different rock types have been through markedly diverse strain histories at the scale of a

thin section, illustrating very well the geometry outlined by Bell's (1981,1985) model. On the other hand, the presence of idioblastic garnet crystals with (a) spiral inclusion patterns and (b) crenulation cleavages usually marked by quartz, feldspar and iron ores in their central zones, indicate that there was another episode of garnet growth in these rocks. The observation that in some cases straight garnet rims overgrow the mylonitic banding in pelitic mylonites (Pls 5-65B,65C), together with the open nature of the crenulation cleavage (in some amphibole schists) suggest that this garnet growth episode was post-D1 mylonitization, possibly taking place at relatively early stages of D2 shortening. This (latter) interpretation is also supported by the weak expression of mylonitic features in the amphibole schists as well as the absence of F1 folds in this unit. Evidence from the metasediments is also dubious. There, idioblastic garnets with spiral inclusion patterns are interpreted as pre-D1 mylonitization (rotated) porphyroclasts which have been used as nuclei for garnet growth during the M2 episode. However due to the possibility of:

(a) recurrence of deformation processes (mylonitic features also well-developed during in D2 and to less extent in several of the deformational phases),

(b) uncertainties about the age of the external foliation at several localities and,

(c) the lack of continuity between the internal and external fabric in most porphyroblasts, the above interpretation was regarded as a working hypothesis until it could be cross-checked with other sources of evidence (see Chap.7).

A number of other (general) problems which had to be faced include:

(a) The variation of wavelength and amplitude of the crenulation cleavages (S2, S3, S4 and S-late) which was also an important factor due to its effects on the deformation of the porphyroblasts. Several large porphyroblasts showed no signs of being affected by crenulation, the latter dying out against the crystal boundary (Figs 4.3A/B). Other smaller or already flattened porphyroblasts were easily crenulated and folded, following the behaviour of the foliation (Fig. 4.3C). Some of the thicker quartzofeldspathic bands show, in the same way as the large porphyroblasts, no effects of crenulation, due either to their thickness or to their positions in relation to the local strain.

(b) The reactivation of the older composite foliation particularly along preferential zones (e.g. hinges of microfolds) of the crenulations, where 'detachments' along the foliation are shown by features like spaces, deformation bands and other ('ductile and brittle') features, developed on minerals marking the foliation (Pls 4-47, 48, 48A, 49). Porphyroblasts of garnet present in these zones show practically no effects of further deformation, probably due to the relative ease of shear along the small-grained crystals marking the foliation. This deformation was localized along narrow zones, where grain boundary sliding is believed to be the principal mechanism (see Chap.6). It represents another form of partitioning of deformation, giving rise to a different strain history for these bands in relation to the bulk deformation history of the rock (Williams and Schoneveld 1981).

In the marbles this situation was particularly critical, due to the widespread character of the reactivation. There, not only mechanical reactivation has occurred, but the action of accompanying fluids (see Chap.7) reacting with the carbonates and most silicates, has destroyed most of the original grain boundaries, so that the determination of the porphyroblasts-matrix relationships is practically impossible.

This study shows the extreme difficulties involved with the application of the classical microstructural techniques to highly and heterogeneously deformed rocks where e.g. mylonitization is a recurring process and grain-size destruction dominates over recrystallization. It seems also to be clear from this above discussion that the partitioning of deformation should receive special attention during microfabric studies, even considering that the confection of a larger number of thin sections in different positions could help to solve most of the previously discussed situations. In addition, the critical analysis of every thin section bearing in mind the particularities involved in the deformation of each mineral and aggregate is thought to be essential for the construction of a self-consistent deformation history, which is also in agreement with the other sources of geological evidence (cf. Chaps 5,6,7).

Figure 4.1. Deformation partitioning around porphyroblasts.

(A) Coaxial strain model constructed at constant area showing a transition from unstrained to strained with a bulk strain ratio of 2.5/1; the model is drawn to represent the XZ plane of strain. However it could equally well represent the YZ if extension occurred in Y. Even if extension did not occur on the bulk scale in Y the strain pattern could still be anastomosing. This model provides a possible solution for the two boundary discontinuities unique to progressive pure shear (reproduced from Bell 1981 fig.7A).

(B) Strain field diagram for a geometry developed by non-coaxial progressive bulk inhomogeneous shortening; three zone types of deformation partitioning are indicated. No strain has occurred within the dashed lines (the elliptical areas outlined by these are not strain ellipses). Between the dotted lines the deformation involved progressive shortening plus shearing strain. This diagram shows no examples of progressive shearing without a component of shortening with shearing strain (reproduced from Bell 1985 fig 1a and Bell et al. 1986 fig. 1a.).

(C) Diagram of the strain field resulting from non-coaxial progressive bulk inhomogeneous shortening (see Sect.5.3) where the deformation has repartitioned around a porphyroblast (dashed lines). Zones of deformation partitioning are delineated as in Fig. 4.1.(B). The shearing component of the deformation is partitioned about the porphyroblast which thus protects and ellipsoidal island of matrix from the effects of progressive shearing (reproduced from Bell fig.1b).

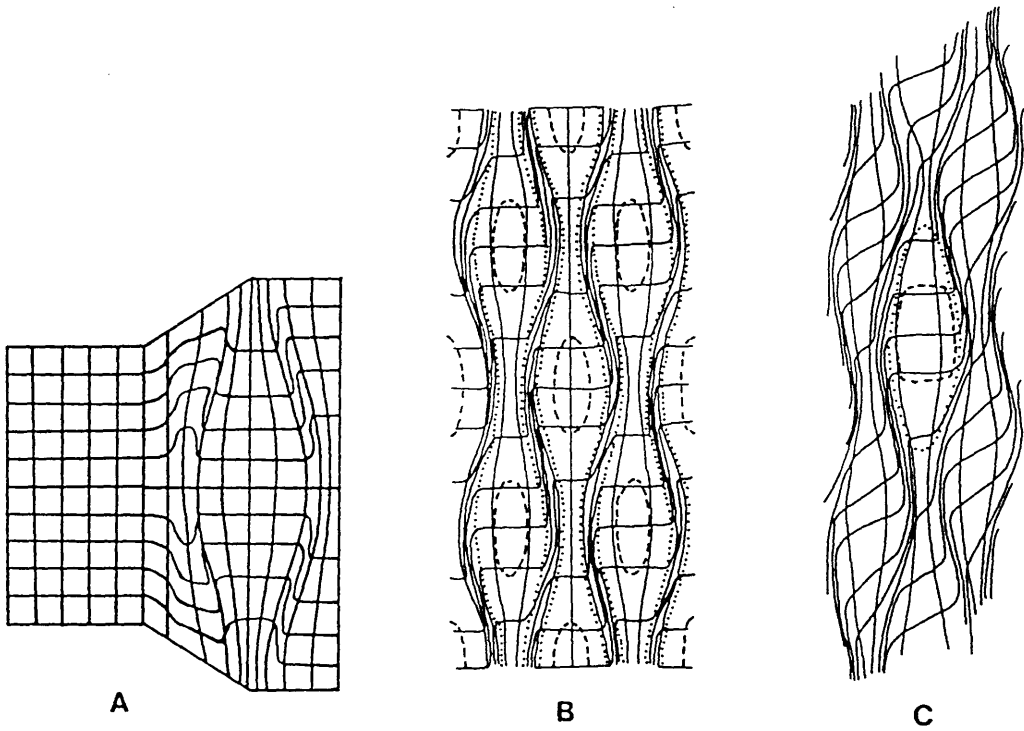


FIGURE 4.1 DEFORMATION PARTITIONING AROUND PORPHYROBLASTS

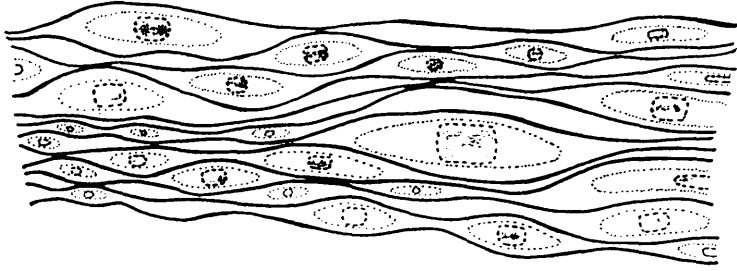


Figure 4.2. Geometry of the strain variation shown by mylonitized quartzofeldspathic gneisses; the matrix (not ornamented) wraps around porphyroclasts of more resistant minerals (grey areas) which show no deformation (area within dashes) or shortening (dots). Most of the shearing is taken by phyllosilicates (black seams) and the fine-grained matrix (modified from Bell *et al.* 1986 fig.1b).

Figure 4.3. Relationships between shape, grain size and orientation of minerals and the wavelength-amplitude of crenulations in mica schists of domain III.

(A) F3 crenulation cleavage dying out against large garnet porphyroblast; note the folded quartz band (top left) and the small idioblastic garnets (bottom left and top right); sketch from thin section of mica schist, scale bar 1mm.

(B) Low-amplitude D2 crenulation cleavage (S2) forming box-fold in small muscovite grain (far left) but dying out against large muscovite crystal (far right); sketch from thin section of mica schist; scale bar 0.5mm.

(C) Boudinaged garnet (D1) with biotite crystallization along extensional fractures folded by F2 crenulation cleavage; quartz layers show deformation bands parallel to axial plane of folds; note also buckling geometry of microfolds and grain size reduction of garnet (inset); sketch from thin section of mica schist; sample 157 X' (see Tables 7.1,2); scale bar 0.5mm.

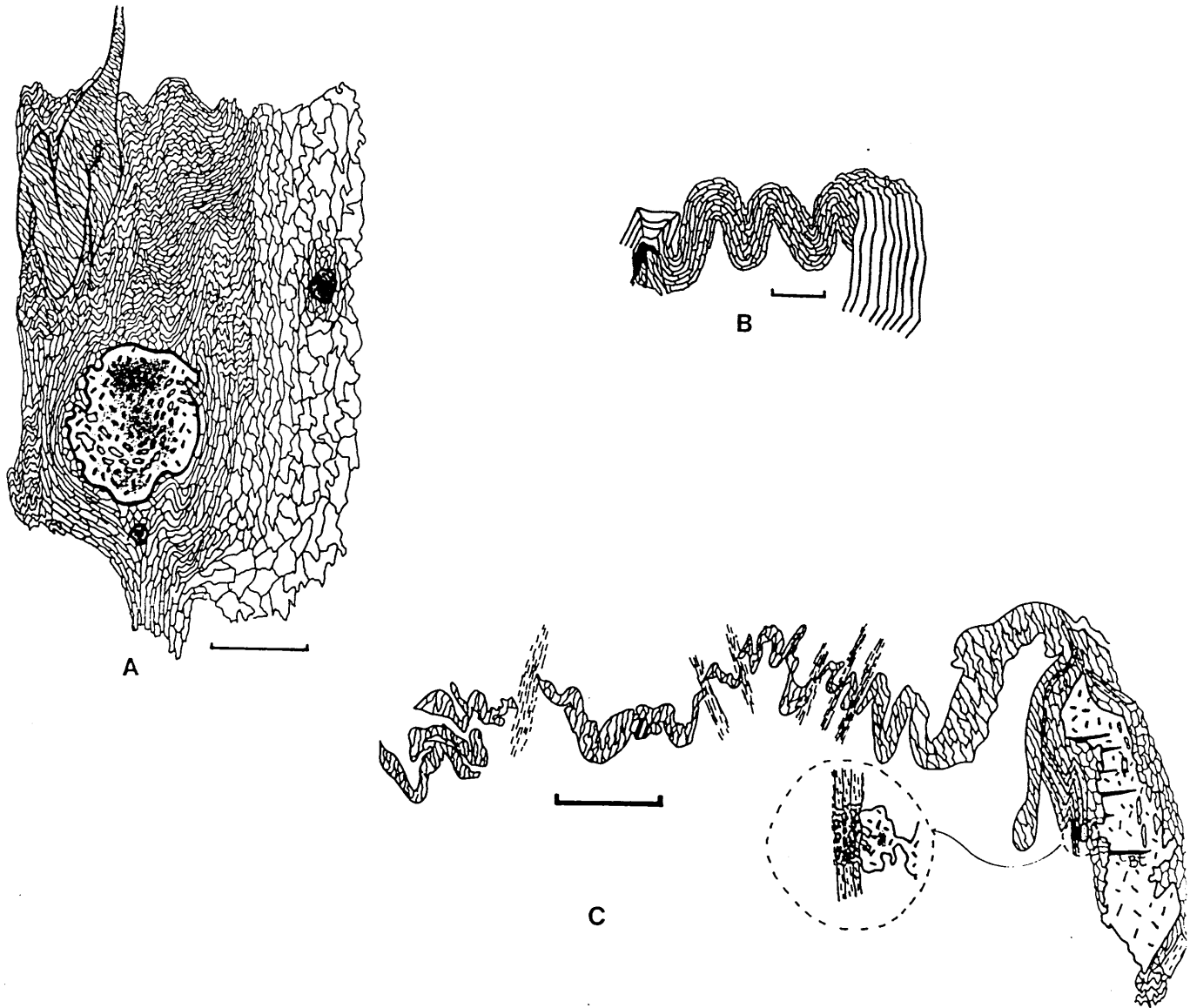


FIGURE 4.3 RELATIONSHIPS BETWEEN MINERAL GROWTHS AND
CRENULATIONS

Plate 4-1 Granoblastic polygonal texture in felsic band of quartzofeldspathic gneiss; note the smaller grain size of the adjacent bands (top right and bottom left corners of picture) where biotite and muscovite are more abundant; section cut perpendicular to stretching lineation (L1), XN, X10 (NG 979 712).

Plate 4-2 Recrystallized (M1) feldspar phenocryst of porphyritic amphibolite (delineated) showing granoblastic polygonal texture in plagioclase crystals ('blastoporphyratic texture'); 'cloudy' appearance is given by fine-grained retrogressive minerals; XN, X10 (NG 967 711).

Plate 4-3 Grain-size contrast between mica-free quartzofeldspathic (top right) and biotite-bearing bands (bottom left) marking S1 in gneiss; XN, X10 (NG 979 712).

Plate 4-4 Chloritized biotite growth marking S1 foliation in mica-rich quartzofeldspathic gneiss; negative print of thin section (perpendicular to fold axis); X6 (NG 973 718).

Plate 4-5 Different types of l1 lineation; defined by (A) grain aggregates (shape fabric); (B) prismatic minerals (amphiboles in particular) and (C) platy grains (micas).

Plate 4-6 Muscovite porphyroblast overgrowing quartzofeldspathic aggregate in gneiss; XN, X10 (NG 960 715).

Plate 4-7 Initial stages of grain-size reduction of a muscovite porphyroblast in quartzofeldspathic gneiss; XN, X10 (NG 972 716).

Plate 4-8 Granoblastic polygonal texture in quartzofeldspathic gneiss affected by late D1 mylonitization; note the more advanced stage of mylonitization around the feldspar aggregate ('matrix'); and the grain-size comminution along the crystal boundaries; XN, X10 (NG 966 721).

Plate 4-9 Dimensionally oriented (chloritized) biotites and amphiboles defining S1 and S2 foliations in banded amphibolite; section perpendicular to fold axis and L1-L2 lineation; arrow marks part enlarge in Pl. 4-10; negative print of thin section; X2 (NG 975 708).

Plate 4-10

S1 biotite growth represented by the large mica flakes with S2 cutting across (SE), represented by fine chloritized biotite flakes; PPL, X10 (NG 975 7081).

Plate 4-11 Isoclinal (F1) fold with fine muscovite axial planar foliation refolded by F2 fold in mylonitized mica schist; negative print of thin section, X2 [NG 971 722].

Plate 4-12 Discrete S2 mylonitic zones cutting S1 of already mylonitic aspect in quartzofeldspathic gneiss; negative print of thin section, X2 [NG 966 720].

Plate 4-13 Grain size reduction effects along S2 in quartzofeldspathic gneiss; PPL, X10 [NG 972 716].

Plate 4-14 Diverse D2 deformation effects of quartz and feldspar crystals in granoblastic gneiss; sketch from thin section; scale bar 0.5mm [NG 972 716].

Plate 4-15 Cataclastic features in feldspar crystalloclasts where S2 cuts mylonitized (D1) quartzofeldspathic gneiss; PPL, X10 [NG 971 716].

Plate 4-15A Detail of D2 grain-size reduction effect in K-feldspar crystalloclast of mylonitized (D1) gneiss; PPL, X25 [NG 971 716].

Plate 4-16 Sinistral shear along discrete S2 cleavage in quartzofeldspathic gneiss; note orientation of deformation bands in quartz which could have been produced during the same deformation episode; sketch from thin section; scale bar 0.5mm [NG 972 716].

Plate 4-17 Penetrative S2 foliation in (S1) banded mylonite; note the magnitude of displacement along S2; XN, X10 [NG 971 716].

Plate 4-18 Penetrative S2 foliation in micaceous finely banded mylonite; note the 'wrong' sense of displacement to be accounted only by pressure solution; XN, X25 (NG 971 716).

Plate 4-19 Progressively detailed features in (D2) deformation bands of quartz layer along the limb of a F2 small fold; sketch from thin section; scale bar 0.5mm (NG 971 716).

Plate 4-20 Relationship between S2 and S1 biotite growths and the compositional banding in amphibolite; PPL, X10 (NG 975 708).

Plate 4-21 Deformation band and sub-grain development expressing S2 in quartz crystal of gneiss; XN, X10 (NG 960 698).

Plate 4-22 D1 crystalloclasts affected by F2 folds; note the effects around large grains and the orientation of the deformation bands of inter-crystalline quartz; sketch from thin section; scale bar 1mm (NG 973 718).

Plate 4-23 F2 fold in feldspathic layer of banded amphibole schist; note the stronger nature of the (NE) oblique foliation (unknown age); negative print of thin section; X3 (NG 952 717).

Plate 4-24 Large amphibole crystals (extinction position) marking S2 foliation in amphibole schist; XN, X10 (NG 962 701).

Plate 4-25 Disrupted F2 hinge mylonitic quartz muscovite schist; sketch from thin section, scale bar 0.1mm (NG 971 722).

Plate 4-26 F2 buckle folds in quartz bands of mylonitized siliceous mica schist; note lithoclast of original rock ('X'); negative print of thin section, X2 (NG 971 696).

Plate 4-27 Layer thickness control of fold (F2) wavelength in mylonitized metasediment; note crystalloclasts at the hinge zone of large antiform; negative print of thin section; X2 [NG 973 693].

Plate 4-28 Deformation bands parallel to axial plane of F2 folds in mylonitic gneiss; note small dimension and high concentration of the bands in the short limb of folds; XN, X10 [NG 973 718].

Plate 4-29 Grain size reduction and pressure solution along S2 (and S1) affecting muscovite flakes in the hinge zone of a F2 fold in metasediment; XN, X10 [NG 973 963].

Plate 4-30 Pressure solution S2 seams affecting quartz bands in mylonitized gneiss; note the sinistral and dextral apparent displacement along each fold limb and the competence controlled (?) deflection of these structures towards parallelism with parts of the folded band (top left); sketch from thin section; scale bar 0.5mm [NG 973 718].

Plate 4-31 Pressure solution and/or displacement superimposed on cusped-and-lobate structures produced during the initial stages of folding of iron-graphite-rich mylonite of the Charr band; PPL, X10 [NG 971 722].

Plate 4-32 Localized transposition of quartz bands along S2 in mylonite of the Charr band; PPL, X10 [NG 971 =722].

Plate 4-33 Hinge of small F2 fold in iron-graphite-rich mylonitized metasediments; note the layer thickness control of the fold wavelength at the hinge zone; lenticular clasts are feldspars; PPL, X10 [NG 964 700].

Plate 4-34 Disrupted hinge of F2 fold affecting large muscovite flake in mylonitized muscovite schist;

Plate 4-35 Non-cylindrical (F2) folds in mylonitized metasediment; section at high angle to the linear fabric; negative print of thin section; X2 (NG 971 7221).

Plate 4-36 Profile section of highly cylindrical F2 folds in metasedimentary mylonite; note the absence of axial-planar foliation and the layer thickness-wavelength relations; PPL, X10 (NG 971 7221).

Plate 4-37 Deformation lamellae (d') within deformation bands parallel to axial plane of F2a folds in quartz of sheared quartzofeldspathic gneiss; XN, X10 (NG 978 7121).

Plate 4-38 'Ductile' deformation of twins in plagioclase of sheared quartzofeldspathic gneiss; note the orientation of deformation bands in quartz (top right); XN, X25 (NG 978 7121).

Plate 4-39 Pseudotachylite in D2a shear zone; XN, X10 (NG 976 7041).

Plate 4-40 Convolute F3 folds of thin quartz bands (dark layers) in chloritized biotite rich layers; negative print of thin section; X2 [NG 962 713]

Plate 4-41 Elongation of deformation bands parallel to axial plane of F3 fold in quartz band of metasediment; note variation of grain size coincident with compressional zones of (buckle) folds; sketch from thin section; scale bar 1mm [NG 961 704].

Plate 4-42 Imbrication of amphibole crystals at the core of F3 chevron fold in amphibole schist; note the absence of sharp contact between grains; XN, X10 [NG 956 714].

Plate 4-43 Discrete zones of (D3) mylonitization parallel to axial plane of F3 fold in amphibole schist; rectangle marks Pl. 4-43A; negative print of thin section; X2 [NG 956 714].

Plate 4-43A Detail of Pl. 4-43 showing D3 mylonitization of amphibole schist along discrete zones (S3); PPL, X25 [NG 956 714].

Plate 4-44 S3 gradational crenulation cleavage in muscovite schist; PPL, X10 [NG 960 708].

Plate 4-45 D3 deformation bands in quartz layers along the hinge of F3 fold in mica schist; XN, X10 [NG 961 704].

Plate 4-46 S2 kink bands in muscovite gneiss; PPL, X10 [NG 960 724].

Plate 4-47 Detachment zone with quartz deformation bands in mafic amphibolite; note reverse of sense of closure of hinge in the core of the fold where grain contacts are mostly destroyed; sketch from thin section; width of plate ~3mm [NG 973 717].

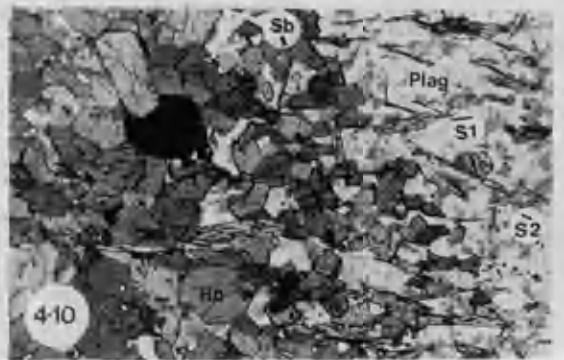
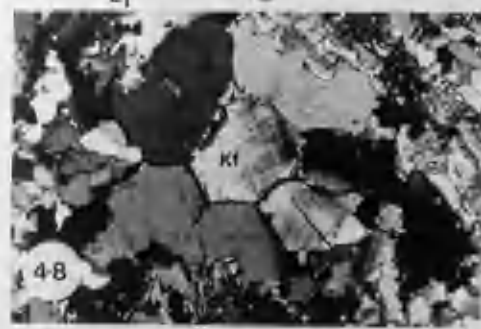
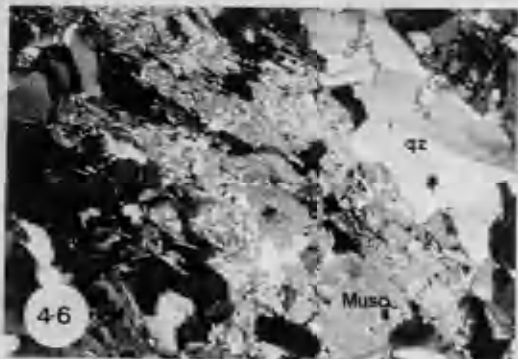
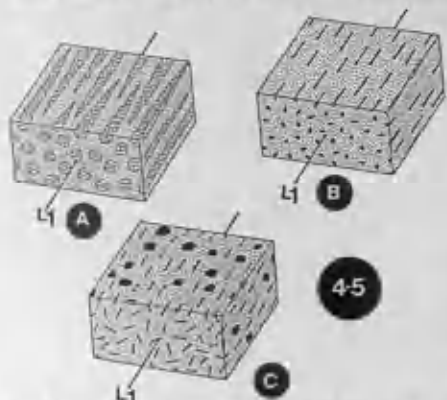
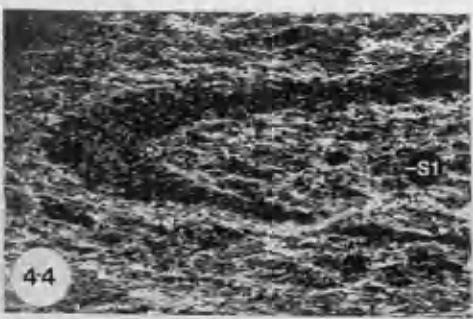
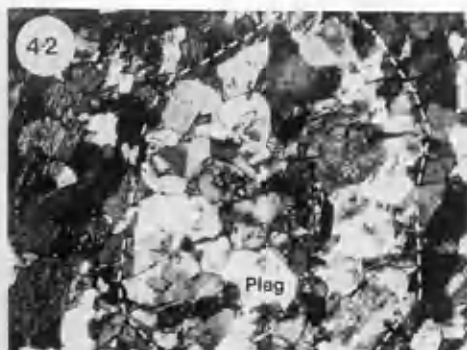
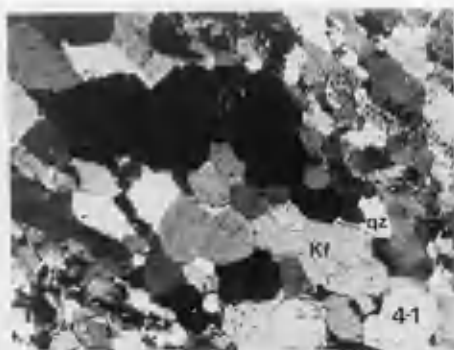
Plate 4-48 S4 gradational crenulation cleavage in mylonitized amphibole schist; detachment along quartz-rich layers where deformation bands are parallel to fold axial plane; negative print of thin section; X1.5 [NG 973 717].

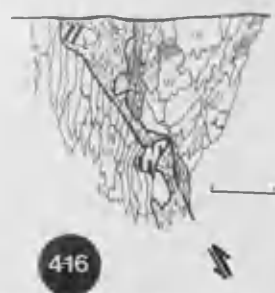
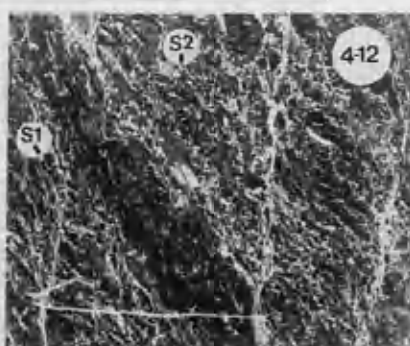
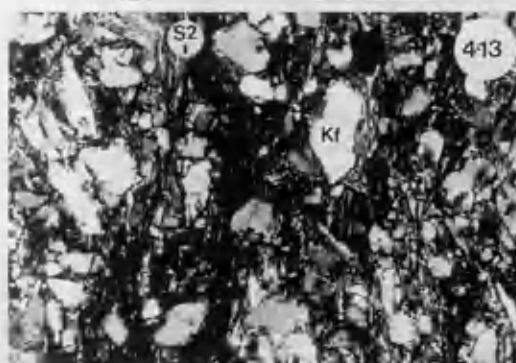
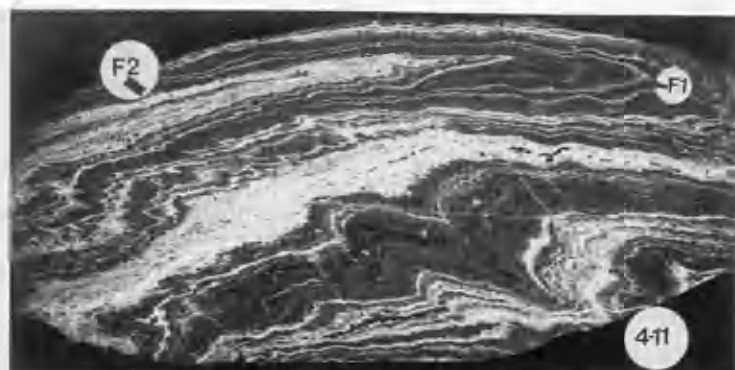
Plate 4-48A Detail of deformation bands in quartz layers of Plate 4-48; XN, X25 [NG 973 717].

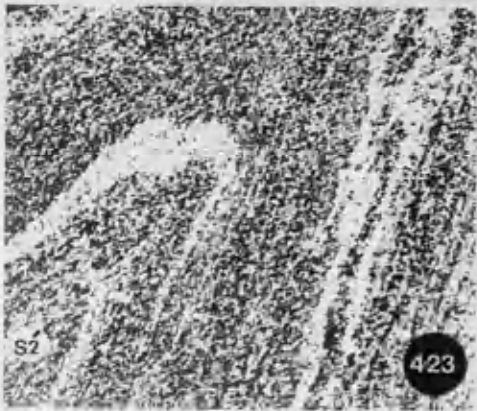
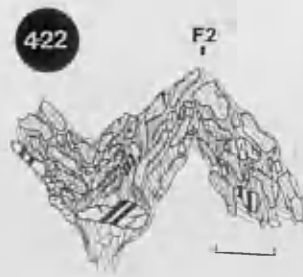
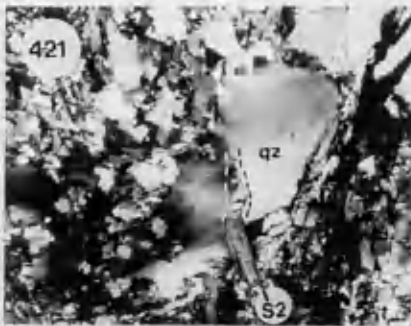
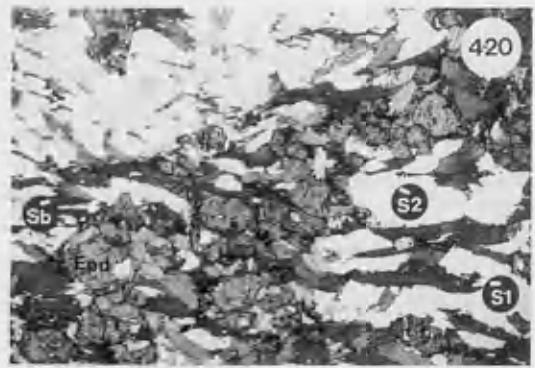
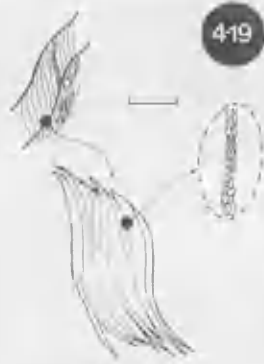
Plate 4-49 Detachment zone along chlorite-rich band in amphibole schist; XN, X10 [NG 953 731].

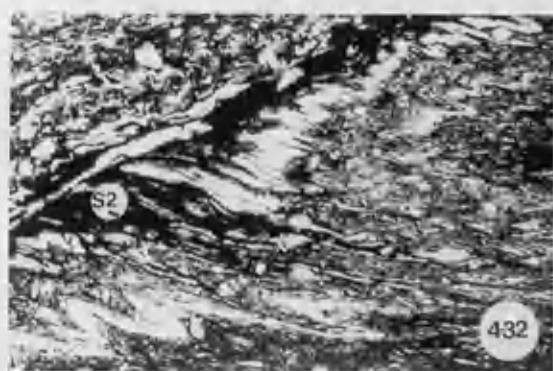
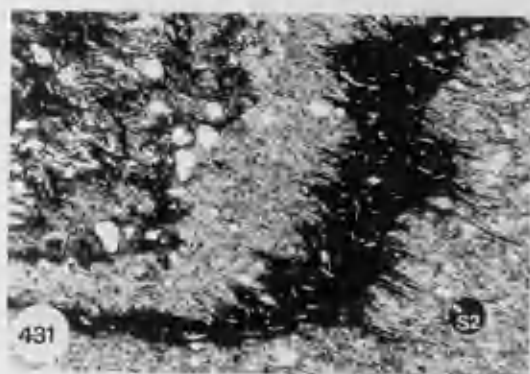
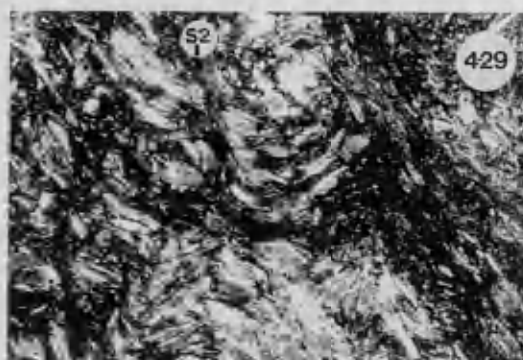
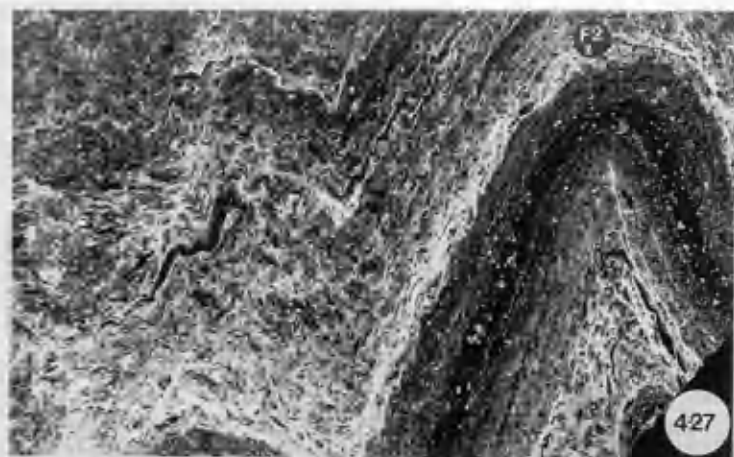
Plate 4-50 S040° gradational crenulation cleavage in mafic amphibolite; fine white bands mark detachment zones; black circle marks position of Pl. 4-50A; negative print of thin section; X2 [NG 968 720].

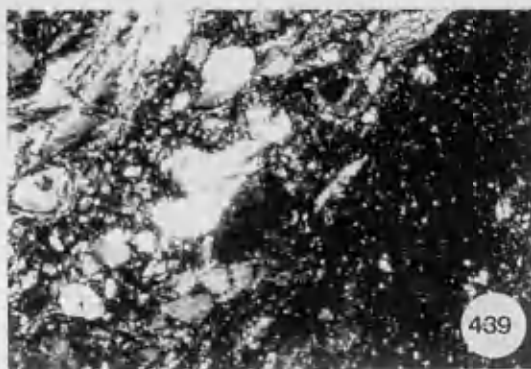
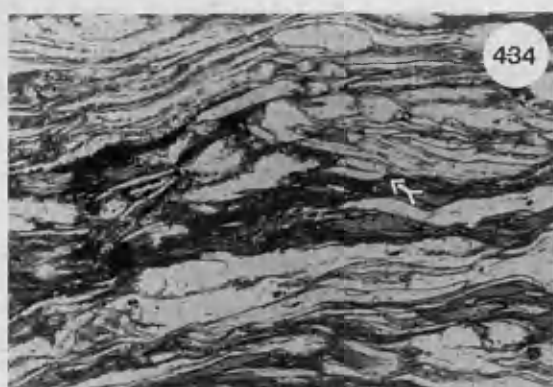
Plate 4-50A Detail of bent amphibole crystal with extensional fractures (in black) along fold nose and compressive structures in the core; sketch from thin section; scale bar 0.3mm [NG 968 720]

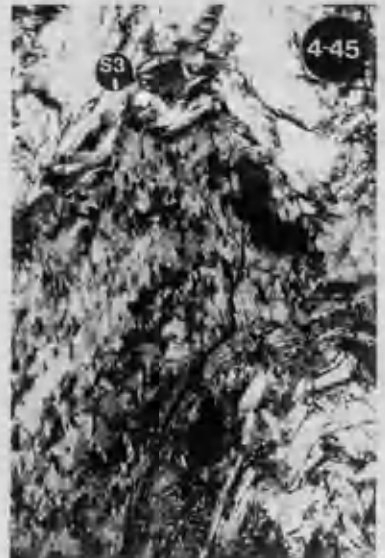
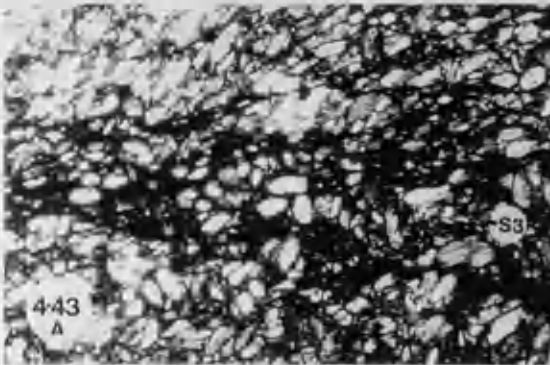
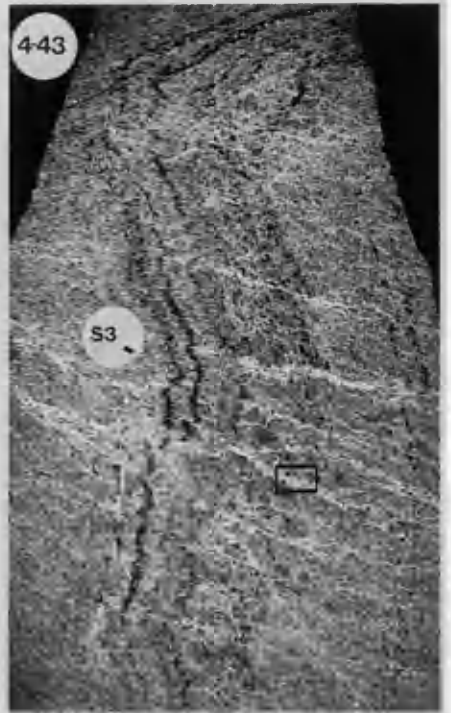
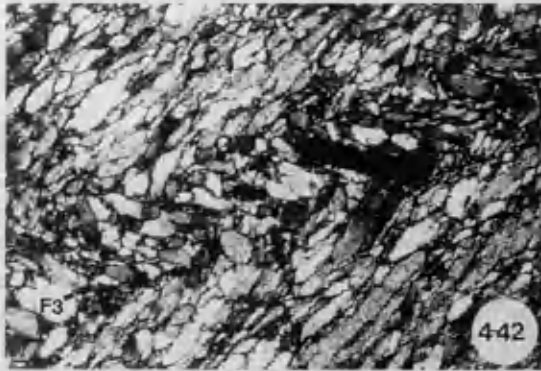
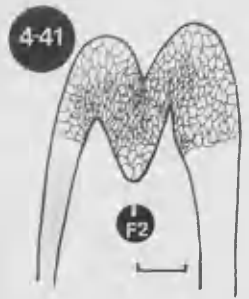
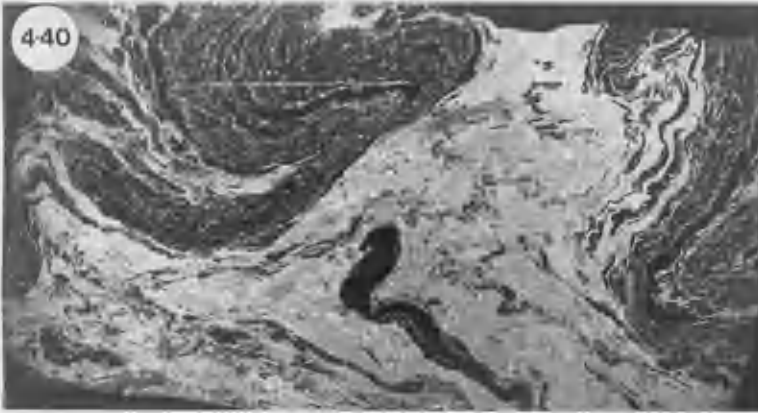


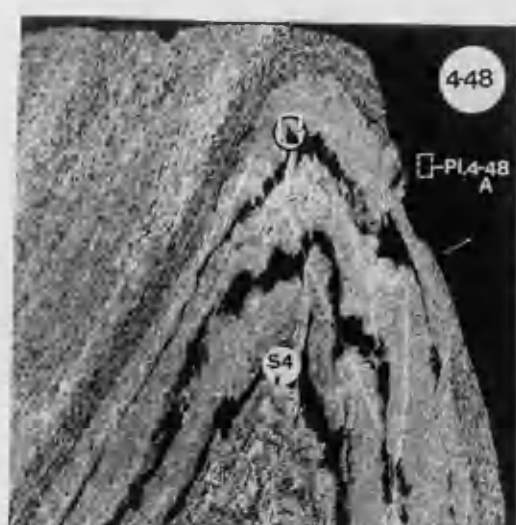
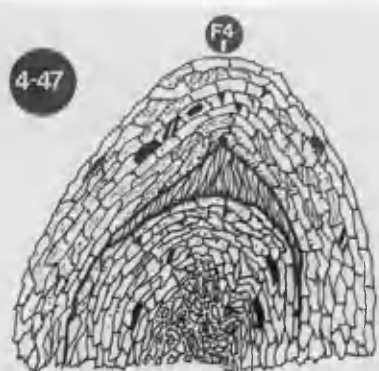
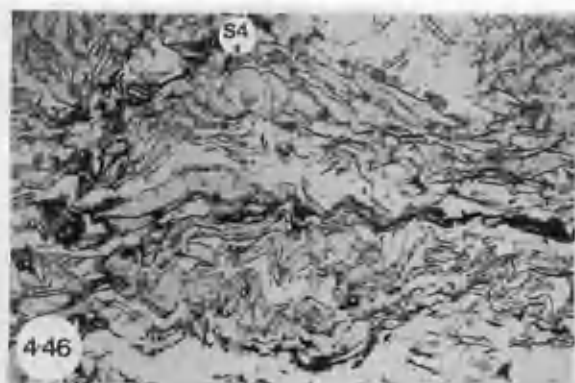












CHAPTER 5 - MYLONITES

5.1 INTRODUCTION

5.2 DESCRIPTION

5.3 DISCUSSION

5.4 SUMMARY

5.1 INTRODUCTION

Mylonitic rocks occur on all scales from centimetres to hundreds of metres in thickness (see structural Map). They are developed from all lithologies and have an originally (pre-D2) irregular distribution throughout the area. Discrete mylonite zones are present at all scales, but protomylonitic developments are evident in most outcrops, and fine seams of ultramylonite are virtually ubiquitous. All degrees of development from proto- to ultramylonite may be visible on the scale of a thin section (cf. Pl.5.36)

While all these features can be explained in terms of strain heterogeneity at all scales, the interaction of P-T-X conditions during metamorphism and the diverse physical properties of the rocks produces a heterogeneity of its own. The most far reaching consequence of this heterogeneity is to make sampling of representative material difficult and its description lengthy.

D1 was the principal period of mylonite generation, but grain size reduction, and relatively localized mylonite development during the D2, D2a, D3 and D4 deformation phases must also be assessed. Given that deformation during D1 was progressive and polyphase itself (see Chap.6), the criteria of analysis must be as rigorously defined as possible.

For practical reasons the following account attempts to describe and interpret the features developed during progressively increasing strain in each of the major lithologies. This is not to imply that the full spectrum of strain states is always seen in any one hand specimen, outcrop or thin section; rather it is an attempt to define all the developmental possibilities of strain morphologies in the major lithologies.

A summary of the principal textural and mineralogical transformation

affecting these rocks with reference to the plates is presented in Table 5.1, where the principal features of deformation are briefly listed, and the main rock types are tabulated against the principal stages of D1 deformation. Since these principal stages are arbitrarily established (Sect.5.3), the listed features describe a progressive increase of deformation for each rock type. Due to the controversy concerning the terminology of fault related rock types (cf. Sibson 1977, Tullis *et al.* 1982, Wise *et al.* 1984) as well as their scale dependency, the 'intensity of deformation' was evaluated in terms of features shown by certain minerals (quartz and micas in particular). For example, features listed at the top of Table 5.1 are considered as having been developed under lower strain conditions than the ones below, as established by the features present in spatially associated quartz and mica grains. The features of deformation for each mineral are **not** described separately. The intention of this procedure was to give an idea of the differential behaviour of each mineral and the influence of their relative abundance and association on the deformation processes during progressive deformation, reproducing more closely the mineralogical control on the deformation and trying to reflect with more fidelity the natural conditions. The descriptive section of this chapter is a good example of the fact that although systematization is essential for description (and understanding) of any natural phenomenon, it can, on the other hand, give a compartmentalized (and sometimes rather simplistic) idea of something which has probably happened in a progressive, continuous and more complex way. This is further illustrated by the difficulties faced during the interpretation of features attributed to 'brittle' and 'ductile' behaviour during deformation of these rocks (Sect.5.3). The present approach is an attempt to examine the deformation at the microscopic scale, and its essence is well expressed by the thought of Orowan (1938, *in* Poirier 1985) reproduced below.

"Creep phenomena have so far been investigated only in terms of old-style technology. For a number of decades, the usual way of tackling similar problems was to apply simple and exact tests (*e.g.* tensile tests) to the very complex and impure materials used in industry and then to subject the results of these tests to a subtle mathematical analysis. As to the prospects of this way of

proceeding, we need only to realize that a piece of iron is far more complicated a structure than, for example, a watch. Now imagine subjecting a watch, without opening it, to a compression test; further trying to draw mathematical conclusion from its undoubtedly very interesting stress-strain curve, and finally dissolving the watch in acids to determine its chemical composition. Although the most accurate experimental tools may be used, and the highest degree of mathematical skill displayed, I doubt whether in this way much valuable information could be obtained about how the watch is working and how it could be improved. A much more promising way is to take the watch to pieces to observe its design and then to study the technological properties of its parts. Translated into terms of our present problem: we must first learn the properties of single crystals, in particular the laws of their plasticity; then we may proceed to a study of polycrystalline metals with more chances of succeeding than hitherto."

In section 5.2, the plates and Table 5.1 are intended to constitute the bulk of the descriptive section, the text being a more detailed commentary. Although mostly dealing with microscopic features, the descriptions include a brief account of the principal characteristics of these rocks at mesoscopic scale reflecting the unusual outcrop aspect of some of these rocks.

In Section 5.3 deformation mechanisms and the physical conditions of deformation are discussed. Macroscopic scale features and their significance will be dealt with in Chapters 6 and 8.

5.2 DESCRIPTION

5.2.1 Mesoscopic Scale Features

Domain I - Quartzofeldspathic gneisses and amphibolites

Quartzofeldspathic gneisses

The mylonitic foliation with fine (mm) quartz bands and cogenetic intrafolial folds is often wrapped around feldspars and amphibole porphyroblasts (Pl.5-1), most of which have lenticular shapes and show strain shadows ('augen gneiss'). With increasing deformation quartz bands are more abundant and porphyroblasts lose their original shape. Grain size is more homogeneous than in the initial stages (Pl.5-2), a feature reflecting the textural and mineralogical 'convergence' produced by high deformation. Where feldspar-rich rock is affected and grain size reduction is extreme, decimetric bands of ultramylonite show a 'porcelanic' appearance. At this stage the rock shows no visible linear fabric and its greenish-yellow colour makes it difficult to distinguish from mylonitized amphibolites. Sheath folds are common and affect the mylonitic banding itself (Pl.5-3). White 'dots' and 'lumps' (Pl.5.3) are lithoclasts of the protolith (gneiss).

Amphibolites (basic mylonites)

These rocks show a higher percentage of phenoclasts to matrix than the quartzofeldspathic gneisses. This together with the frequently unfoliated aspect of the matrix gives the rock a granular aspect resembling a lithic tuff. The association of this rock type with the 'porcelanous' mylonite (Pl.3-15) suggests that the felsic bands have taken up most of the deformation (see Sect. 5.3).

Domain II - Amphibole schists

Mylonites in these rocks are relatively scarce and usually localized

along biotite-rich bands. Whether they were never abundant in these rocks, or whether their rarity is a function of recrystallization during a latter episode is difficult to know, but evidence for strong recrystallization during M2 will be discussed in Chapter 7.

The **'mixed' mylonites** are by far the most strongly deformed rocks in domain II. Similar to the pelitic mylonites (see below), they frequently reach very fine grain size (ultramylonite) with large garnet crystalloclasts resisting grain-size reduction. The matrix is submicroscopic and shows little or no orientation in fresh surfaces. Large amphibolite, amphibole schist and gneiss lithoclasts are fairly common (some with disrupted fold hinges) being wrapped around by the matrix (best observed on weathered surfaces, Pl.5.5).

Domain III- Metasediments

The mylonites developed in these rocks are similar to those with a gneissic protolith. The rock is predominantly light bluish-green with white 'lumps'. 'Spots' (lithoclasts) of a coarse-grained rock that bears microcline and plagioclase (An 32) are ubiquitous (Pl.5-4), as are translucent quartz bands (Pls. 5-6,3-55) and 'porcellanous' bands (Pl.3-56).

Domain IV- Calc-mylonites

The calc-mylonites are generally light green rocks, with large fragments of banded amphibolites, amphibole schists and felsic gneisses chaotically intermixed with crystalloclasts. The grains have widespread variation of shapes and composition across small portions of the rock (Pl.5-7). There is no grain-size sorting, so that almost metre-sized clasts of amphibole schists and amphibolites are intermixed with a much finer 'matrix' of felsic gneiss lithoclasts. Most elongate fragments show orientation of their longest axes parallel to the foliation (Pl.5-8). The rocks look like a heterogeneous breccia which has been subjected to very strong ductile deformation (see Sect. 5.3.2.4) and in this respect they are

very similar to the 'mixed' mylonites.

5.2.2 Microscopic Scale Features

In addition to the principal features displayed by these rocks listed on Table 5.1, several others considered to be important in understanding the deformation of these rocks will be presented below.

Quartzofeldspathic gneisses

Felsic bands

The coarse-grained gneisses with granoblastic polygonal texture (Pls. 5-9, 10B) suffer progressive grain size reduction, initially along crystal boundaries (Pl.5-10C); this extends into individual grains as the deformation progresses (Pl.5-18). Sections at a low angle to the stretching lineation show that perthites in feldspar are oriented parallel to a fine oblique cleavage (Pl.5-12). This is similar to what has been interpreted in the recent literature as an 'extensional crenulation cleavage' (see Sect. 5.3).

Chloritization of fine-grained matrix produced by reduction of mica crystals is widespread and occurs in zones showing anastomosing patterns with variable width. There is an apparent positive correlation between the width of these mylonitic bands and the grain size of minerals within them. With the progression of the deformation, the density of these high strain zones increases until they become the predominant feature and only few isolated 'pods' of the original gneiss are left relatively unaffected.

The relative timing of development of deformation bands in quartz crystals had to be assessed in each case since they could have been produced by (a) flattening of a group of crystals, (b) recrystallization with new grains growing preferentially along planar regions of strong deformation such as deformation lamellae, or even (c) 'normal' grain growth due to inhibition of grain growth migration by a preferred orientation of micas (Hobbs *et al.* 1976, p.117). While the presence of a boudinaged crystal of allanite along the foliation seems to indicate the flattening of these grains (Pl.5-13), the presence of remnants of older and larger grains,

showing several stages of deformation band development, and the presence of a fine crenulation cleavage at $\sim 35^\circ$ to the main shear foliation (Pl.5-12), seems to indicate that these are the main planes of mylonitization ('C'-surfaces). However, due to the non-coaxial character of the deformation and the high strains attained, both mechanisms ('flattening' and simple shear) have probably contributed to the formation of these rocks (see Sect. 5.3).

In sections at a high angle to the stretching direction, the presence of core and rim structure is frequently observed. Large feldspar crystals make up the 'core', while much finer grained quartz and feldspars compose the 'mantle' (Pl.5-14). In this sort of orientation the hinges of disrupted folds are usually best observed, whereas the presence of muscovite crystalloclasts with sigmoidal shapes ('fish-like' of Lister and Snake 1984) with asymmetric tails of fine grained material and asymmetrical pressure shadows around few lithoclasts are best observed in sections at a low angle to the linear fabric.

The contact between still remaining lithoclasts and matrix is sharp along the rim but gradational along the trailing edge. Where a progressive reduction of the grain size is observed it increases away from the centre of the clast (Pl.5-10). Within these fragments and in matrix-surrounded crystalloclasts conjugate fracture systems are developed. Initially fine chlorite and sericite are observed along these fractures (Pl.5-17). With the progression of the deformation a wedge-shaped fracture is formed and the grain-size reduction 'channel way' can be observed (Pl.5-18), affecting even 'isolated' crystalloclasts (Pl.5-21). In other examples fractures displace crystalloclasts but apparently do not affect the matrix (Pls. 5-22,23). These structures are essentially asymmetrical boudins being called 'domino' or 'book-shelf' fractures by analogy with dominos or books sliding past each other, showing a sense of displacement opposite to the bulk shear strain (see Sect.5.3.2.1,d).

The matrix produced along these wedge-shaped fractures is finer than the surrounding matrix, where sometimes aggregates of small quartz crystals show localized development of granoblastic polygonal

texture. 'Ductile' deformation of feldspars included the development of deformation bands in which **no** microperthites can be observed (Pl.5-19), and of ductile faults and pinch-and-swell structures in single feldspar crystals, along which polygonization of small grains can be seen (Pl.5-20). In the latter case a 'right lateral' displacement of the grain is visible but no fracture has developed. Initiation of pericline twinning and development of small grains along the rims of crystalloclasts are also observed. Another common feature in crystalloclasts is the disappearance of the pericline twinning along the margins of the initiating fracture (Pl.5-16). Several of these features are very similar to those developed in quartz crystals that were attributed to plastic deformation (see Sect. 5.3).

Unlike most of the other minerals the only feature observed in epidote at this stage of deformation is the presence of reaction rims along the contact of these crystals with the matrix. Most of these and other (feldspar) round grains when observed under high magnification power show a rather irregular outline (Pl.5-27). Highly deformed zones of these rocks show no distinguishable structure particularly in sections at right angle to the orientation of the linear fabric (in adjacent samples). They have the appearance of a 'crystal tuff' (Pl.5-17,21), and if the geological relations are not preserved it can cause considerable misunderstanding. A good example of this situation can be found in petrographic descriptions of the Torridon group where quartz-feldspar porphyry pebbles in conglomerates described by Williams (1969, Fig.5) have striking similarities with some of the presently described mylonites. His Fig. 5G in particular, shows a banded porphyry with the layers wrapping around deformed phenocrysts. While the banding is interpreted as an original feature (pp.616-619) on closer examination of his plate a fine (NE-SW) cleavage, which a structural geologist would promptly identify as a (oblique) cleavage ('S'-surface?), is clearly visible. It is not the intention to suggest here that there are no porphyry pebbles in the Torridonian, since they have been repeatedly described in the literature (*cf.* Teall *in* Peach *et al.* 1907, pp.281-283; Maycock 1962, pp.51-53) but the identification of part of this material as of mylonitic (and of autochthonous) origin can have important implications for the provenance studies of the Torridonian rocks (see Williams 1969). A

reliable criterion to distinguish porphyry pebbles and mylonites is the state of deformation presented by the quartz crystals. Due to the susceptibility of this mineral to deformation, porphyry pebbles with quartz phenocrysts are unlikely to be mylonitic rocks. On the other hand, banded rocks with feldspar 'phenocrysts' have could well represent mylonites. Accordingly, it is necessary to look for characteristic deformational features of these minerals and other features such as kinematic indicators (see Sect. 5.3).

Mafic bands

As a function of their high content of 'weak' minerals, like biotite, these bands show a rapid variation from coarse to fine grain (Pl.5-36). As in the felsic bands the deformation is initially confined to narrow zones where the grain size reduction has occurred. In contrast with the lack of orientation in the felsic bands, the simultaneous extinction of parts of this fine 'mass' suggests the presence of a localized crystallographic orientation.

Epidote crystals are the least affected, showing little grain-size reduction. The adjacent quartz crystals show well-developed deformation bands, giving an idea about the intensity of deformation necessary to produce the above described features in micas and epidote. However, it should be borne in mind that the weaker mineral bands have probably worked as 'zones of strain softening', localizing the strain along them with the progression of the deformation. The impression of extremely high deformation that these bands give at first sight is perhaps a function of their high proportion of weak (biotite) to strong (epidote, amphibole, feldspar) minerals, producing a picture of few scattered round crystals surrounded by a sub-microscopic matrix (top-right corner of Pl.5-28). The 'micaceous' character of the matrix is difficult to resolve optically, but its nature can be determined by the absence of strain shadows around mica crystalloclasts and their good development at the edges of epidote and amphibole crystals, minerals which have low and high competence contrasts with matrix respectively. Feldspar crystalloclasts present intermediate conditions of deformation with a moderate degree of grain-size reduction.

In marked contrast to the felsic bands where chloritization and sericitization are fairly common, the mafic bands (epidote-biotite-amphibole) of several samples show no evident mineralogical changes. Very few samples of discordance between the compositional banding and the mylonitic foliation were observed. In most cases this was related to fold hinges where a mylonitic foliation develops parallel to the axial planes (Pls. 5-32,35).

Epidote crystalloclasts present more equidimensional shapes than feldspars and amphiboles, probably reflecting their more resistant nature and equant original shapes (Pl.5-37). The more frequent presence of very round feldspar crystals in highly deformed samples seems to indicate the strong control of deformation processes on the shape of these fragments (Pl.5-33, Sect.5.3). Carbonate is relatively abundant in mylonitized calc-silicate gneisses, where it is usually found in fractures (Pl.5-38), a feature probably resulting from remobilization.

Amphibolites (basic mylonites)

These rocks show virtually the same features as the mafic bands of the gneisses with variations introduced by the different proportions of mafic (amphibole instead of biotite) and felsic (plagioclase instead of quartz) minerals. In the low strain specimens the feldspars and quartz already show strong undulose extinction, sub-grain development and deformation bands at the same stage of deformation that biotite crystals show sigmoidal shapes, kink bands and grain size reduction along the edges of the crystals.

The contacts between the lower and higher deformation bands is sharp (Pl.5-42) but no indication of the shear magnitude is observed due to several factors, including the absence of suitable markers (Sect. 5.3). Remnants of the old granoblastic texture (S banding + S1) are still present in felsic lithoclasts (Pl.5-40) but show already advanced mylonitization, mainly along intercrystalline contacts. With the progression of the deformation the proportion of matrix increases, mainly through the 'grinding' of minerals like biotite, quartz and feldspar which starts along the grain boundaries where

deformation bands in (segregated) quartz are observed (Pl.5-41). Epidote, apatite and amphibole seem to be the order of increasing resistance to the deformation. Boudinaged clinozoisite crystals are common where the elongation of the mineral is parallel to the mylonitic bands. Frequently the amount of matrix seems to be increased by the development of later crenulation cleavages which break down large crystalloclasts giving rise to a sericite carbonate-rich matrix.

Evidence for cataclastic deformation of some minerals during this stage is presented by fractures which affect mainly amphibole crystals. They do not seem to propagate into the matrix and their orientations do not fit into any of the identified mesoscopic systems. In some of the samples the presence of an extremely fine-grained rock showing partially intrusive contacts with the surrounding mylonitic ('host') suggests the presence of a pseudotachylite vein (Pl.5-45). The feldspar crystalloclasts are angular to round and strongly cracked, the opaque minerals content is high and the matrix extremely fine (Pl.5-46, cf. Sibson 1975, p.780). Most features are strikingly similar to those described by Passchier (1982, p77) in ultramylonites derived from pseudotachylites. In this case, the locally discordant nature and optical characteristics of the fine bands were the principal features used for their identification.

Amphibole schists

The textural characteristics of these mylonites vary in accordance with their composition. The more amphibole-rich they are the less frequent is the presence of optically visible mylonitic features. Destruction of the intercrystalline contacts is the most common feature with the production of a 'metasediment-looking' rock (Pl.5-47).

Strong mylonitization of this unit is quite rare. The deformation is thought to have been concentrated into narrow biotite-rich zones as well as along the interbanded 'mixed' mylonites. Perhaps the most important factor determining the absence of well developed mylonite in these rocks is the generalized recrystallization they have suffered during M2 (see Chap. 7).

'Mixed' mylonite

A mylonite whose protolith shows a very heterogeneous composition was identified in a narrow zone (Charr band) in the northeastern corner of the area studied [NG 971 722]; this is referred to as 'mixed mylonite'. The preservation of lithoclasts of amphibolites, amphibole schists and quartzofeldspathic gneisses (as well as remnants of these rock types within garnet porphyroblasts (now crystalloclasts Pls. 5-49, 49A) of large dimensions) poses a problem for the determination of the protolith of this mylonite. Some of the aggregates of small ($< 0.5\text{mm}$) quartz crystals have been recrystallized, presenting straight boundaries and very weak deformation features. Isolated lenses of sub-microscopic material with feldspars as remnants are all that is left of the gneissic protoliths. Other common porphyroclasts include well-rounded fragments of amphibole schists of variable size (1mm to 1m), amphibole crystals and garnets (1 to 4mm) being partially replaced by carbonate (Pl.5-49). Flattened, boudinaged and fractured garnets (Pl.5-48, 48A, 48B, 50) as well as amphibole (Pl.5-51), carbonate, feldspars, muscovite and clinozoisite crystalloclasts are still preserved in a matrix of extremely deformed quartz bands. Intrafolial folds are a common feature, particularly in the proximity of large garnet porphyroclasts. They are in general disharmonic, convolute and polyclinal (Pls. 5-52, 53). More than one set of folds is not an uncommon feature and the occurrence of these structures preferentially in the proximity of porphyroclasts has probably been influenced by the complex strain partitioning in these zones (see Sect. 5.3).

Feldspar, garnet and amphibole (most abundant) show good roundness, being wrapped around by the fine matrix which frequently present asymmetrical strain shadows (Pl.5-55) showing variable stages of rotation (Pl.5-54). Some of the elongate crystalloclasts do **not** present orientation of their longest axes parallel to the banding.

Protoliths of these mylonites include

- (a) biotite-plagioclase-quartz-garnet gneiss,
- (b) garnet amphibolite,

- (c) epidote-garnet quartzite,
- (d) carbonate-garnet amphibolite, and
- (e) carbonate-quartz-biotite amphibolite

In general the amphiboles preserved within garnet crystalloclasts are fibrous varieties, and are not found amongst the mapped rocks.

Metasediments

These rocks show variation in composition from quartzofeldspathic to mica-rich units to quartzites. As in the case of other lithologies the mylonitic features developed are very much a function of the original mineralogy (but see Section 5.3).

The quartzofeldspathic mylonites referred to as siliceous mica schists (Chap.2) show 'sedimentary-looking' features with feldspar grains surrounded by a structureless matrix (Pl.5-57) identified as a product of mylonitization processes (Peach *et al.* 1907).

The impression of relict sedimentary structures in outcrop is given by

- (1) porphyroclasts of a quartzofeldspathic rock (Pl.5-58) that have a large grain size (~ 2-3mm) and show remnants of a granoblastic polygonal texture (surrounded by the mylonitic banding), and
- (2) the variable degree of grain size reduction (Pls. 5-4, 4A).

Although in thin sections sections at high angles to the stretching lineation the matrix does not show clear tectonic structures, the presence of metamorphic minerals such as garnets and (sometimes staurolite) showing the same relationship as the feldspars with the mylonitic matrix, indicates the non-sedimentary origin of these features. The white lithoclasts have crystals with corroded boundaries. Their composition is quite homogeneous with plagioclase (oligoclase An₃₂) making up approximately 90% of the lithoclasts. Fine quartz bands as well as a fine grained matrix produced by comminution of biotite, muscovite and surrounding the remnants of the protolith is a widespread feature.

The textures developed in quartz and feldspar crystals generally correspond with those observed in the mylonitized gneisses. With increasing deformation the sequence starts with undulose extinction in deformation bands and ends with strong grain size reduction. The

mylonitization, however, seems to be stronger in parts of the rock where phyllosilicates are intermixed with feldspars and quartz than in mica-rich bands, the presence of (more competent) tectosilicates perhaps enhancing the grain size reduction.

In addition to the usual deformational features in quartz crystals, the more siliceous lithologies also show carbonate grains with sigmoidal fine-grained 'tails' indicating the sense of shear (Pl.5-59,59A). The partition surfaces define the position of the mylonitic banding, which is not obvious because of the almost monomineralic character of the rock. Quartz bands show sub-grain development with prismatic boundaries (Bouchez 1977) at an angle of 70° to the grain elongation (and mylonitic foliation). In these rocks garnet seems to be the most resistant mineral (Pl.5-60). In the protomylonites it is common to find idioblastic crystals growing in more felsic bands and being surrounded by a more deformed matrix. Although the quartz grains show strong undulose extinction, prismatic sub-boundaries and subgrains, the garnets show no visible deformational effects. Most of the deformation seems to have taken place along the phyllosilicate-rich bands where biotite (mainly) and muscovite display a good deal of grain size reduction (Pl.5-61).

Occasionally quartz crystals show recrystallization features with slightly larger grain sizes, more regular contacts, and textures tending to granoblastic polygonal. The biotite crystals are nearly all destroyed, resulting in the formation of aggregates with sub-microscopic grain size some of which show simultaneous extinction. Muscovite porphyroclasts, in contrast, still persist as large lenticular crystals with 'tails' extending into the mylonitic foliation. Resistant minerals include feldspar, garnet and allanite. In thin sections cut at a low angle to the linear fabric the orientation of the matrix is very strong. In more siliceous units quartz aggregates are extremely elongate, with $X:Z > 50:1$. In places these aggregates stretch across a thin section, and show evidence of disruption by boundinage and/or being squeezed against hard inclusions like feldspar and garnet crystalloclasts (Pl.5-62). Despite all the structures shown by minerals around the garnets the latter display fewer internal deformation features: extensional fractures (at high angles to the banding) are the most frequent. It

seems that the bulk of the ductile deformation was taken up by quartz, biotite, muscovite and feldspars. Another possibility is that these idioblastic garnets have recrystallized after D1 mylonitization (see Sect. 5.3). No lithoclasts are visible at this stage but it is difficult to attribute this to the mylonitization processes or to inheritance (feldspathic or quartz greywacke?). The more resistant nature of the feldspars in relation to quartz can also be demonstrated by the indentation caused by crystalloclasts of the former on the quartzose bands (Pl.5-63). The pattern produced is very similar to the features described in deformed polymitic conglomerates (e.g. Borradaile *et al.* 1982, p.478) and reproduced by Gay and Fripp (1976) in experimental deformation of pebbles with different ductility.

Despite the fact that grain size reduction is at an advanced stage, and most minerals show features indicative of plastic deformation, the feldspars and garnets were still deformed in a cataclastic fashion with grain size reduction taking place along fractures restricted to these crystals. Some of the fractures have rectilinear traces, others tend to show convergent patterns similar to fractures presented by boudins developed in high ductility contrast materials (Ramsay 1967, p.106). Where they are present, amphibole crystalloclasts show lenticular shapes with strong flattening and occasional boudinage, with different boudins frequently interconnected by long strips ('tails') of fine-grained material (Pl.5-64). The fact that garnets frequently show idioblastic shapes is not simply a function of their higher resistance to deformation, since it is often difficult to assess whether the crystals have been reconstituted or not (*cf.* Sect.5.3.2.3 e and Chap.7).

In the ultramylonite stage the difference in ductility between the minerals becomes much more evident. While biotite is completely destroyed, quartz grains show X:Z ratios from between 30:1 to more than 80:1 (some of which are impossible to compute at thin section scale). In these samples, despite the strong deformation, the distinction between 'fresh-looking' feldspars and quartz is extremely simple due to their diverse structural behaviour (Pl.5-62). In some cases the deformation bands have the same length as the quartz bands. The prismatic sub-boundaries are at an angle to

the elongation of the bands, and are probably produced by a later deformational episode (cf. Sect. 5.3.2.1 f).

Sheath-like folds are fairly common being usually marked by fine bands of quartz in sections at high angle to the linear fabric (Pl. 5-65). Examination of these structures under the microscope shows that well developed folds affect an already mylonitic banding. Well-rounded feldspar and amphibole crystalloclasts are also seen (Pl. 5-65A), but observation at higher magnification shows the irregular nature of these boundaries (Pl. 5-65B). The heterogeneous behaviour of the different minerals during deformation and their post-mylonitization growth is always evident, so that round crystalloclasts of feldspars and other minerals are seen side by side with idioblastic crystals of amphibole (Pl. 5-65A) and garnet (Pls. 5-65B, 65C).

The extreme stage of grain-size reduction of a feldspathic mylonite is shown by small feldspar crystalloclasts in an extremely fine, structureless matrix.

Calc-mylonites

In the almost pure marbles it is quite difficult to see the mylonitic structures due to the homogeneous character of the rock. Large and isolated crystalloclasts of twinned carbonate and mica are the only minerals which show any sign of deformation. Displacement of twins and pressure solution along cleavage planes (Pl. 5-66) and the occasional presence of a bent mica flake, marking the hinge of an otherwise indistinguishable fold, are some of the few identified features. Isolated crystals of epidote and plagioclase, although less common, are sometimes seen but perhaps the most conspicuous feature of these rocks is the fine grained nature of their matrix. The more impure samples show more evident signs of deformation. Lithoclasts of amphibole schists, amphibolite and carbonate-microcline-quartz-amphibole gneisses as well as microcline-epidote-hornblende-quartz gneisses with well-formed granoblastic polygonal texture are very common (Pl. 5-67). Lithoclasts of a very fine grained feldspathic rock with porphyroclasts of feldspar are observed in some sections, showing advanced stages of reaction with the carbonate-rich matrix (Pl. 5-68). The clasts show embayments and

if the mylonitization processes is responsible for the grain size reduction within the clasts as well as of the carbonate-rich rock, the reaction between the carbonate and the lithoclasts must be a relatively late event in the development of these rocks (cf. Chap.7).

Most of the porphyroclasts display reaction effects with the carbonate-rich matrix. The latter usually shows no visible structures but its orientation is eventually marked by the alignment of the long axes of amphibole crystalloclasts. It is also composed of a considerable amount of chlorite and sericite, probable produced by later reaction with the finer mylonitic material.

In the associated calc-silicate schists folding is a quite common feature, being marked by an alternation of quartz-rich and carbonate-rich bands. These minerals show strong elongation, with deformation bands in quartz, and grain-size reduction tails in carbonate, aligned parallel to the axial plane of the folds (Pl.5-69).

In the ultramylonites crystalloclasts of amphibole and epidote (most common) show well-rounded shapes (Pl.5-70); the matrix is frequently submicroscopic.

5.2.3 General Concluding Remarks

Although the above description might seem to be far too detailed, and the importance of the features dealt with may not be immediately comprehended, they provide valuable information about two broad aspect of the deformation, viz. (a) the predominant type of strain (simple or pure shear) and kinematics of the deformation (translation direction), and (b) the ductility conditions and active grain size reduction processes of minerals and rocks as a function of conditions of P,T,X, strain rate etc. The described features will not only be the basis for the discussion in the next section (5.3), but will also provide valuable elements for a self consistent interpretation of mesoscopic scale features presented in chapter 6. Other important points emerging from the above description include:

- (1) each mineral develops markedly different features under similar conditions of deformation, mainly as a function of its particular physical properties,
- (2) the features presented by each mineral can be relatively assessed by comparison with features developed in minerals whose deformation properties are better constrained (e.g. quartz), and
- (3) lithological variation, although of fundamental importance in the localization of the deformation, was by no means the only factor. Several others are equally important but the more precise evaluation of their role was made difficult by the wide range of rock composition (see Sect.5.3.2.2).

5.3 DISCUSSION

5.3.1 Introduction

This section is an attempt to evaluate the importance and role played by the different mechanisms of deformation which affected these rocks at the grain scale. The discussion presented here has

originated from the difficulties faced when trying to apply the existing criteria and concepts of deformation features in mylonites to the Loch Maree rocks. Although basically supported by the features described in the previous section, it is essentially a critical review of the available literature. Readers well-acquainted with the characteristics of mylonitic rocks are referred to the summary (section 5.4).

Additional evidence from the analysis of mesoscopic and larger scale structures (Chap.6) and metamorphic conditions (Chap.7), both intimately related to the formation of the mylonites, will be given wherever possible.

A reconstruction of the late D1 tectono-stratigraphy is attempted in chapter 8, taking into account estimates of magnitudes and directions of displacement along the main thrust surface, the structural level of deformation (metamorphic conditions), and other sources of evidence.

5.3.2 Conditions of Deformation

5.3.2.1 Pure shear vs. Simple shear

Like most of the mylonite zones described in the literature the mylonites of the Loch Maree area seem to have been developed during non-coaxial deformation. Examples of mylonites formed by coaxial deformation are very rare (see Mawer 1983, Choukroune and Gapais 1983), and as pointed out by Lister and Snoke (1984) in many cases where flattening or coaxial deformation has been claimed to have produced mylonitic rocks, subsequential detailed microstructural studies showed evidence of non-coaxial deformation. In other reported cases, flattening seems to have been restricted to low strain zones delimited by high deformation bands where the strain was found to be non-coaxial. This kind of strain distribution

pattern was explained by Ramberg (1975, p.32) in terms of flattening suffered by the thrust sheets due to their own weight associated with simple shear caused by friction occurring mainly along the sole, parallel to the quasi-horizontal thrust plane. Whether the 'body weight' of the thrust sheet is enough for the production of mylonitic rocks and other microstructural features is still debatable (see Law *et al.* 1984), but it seems evident that pure shear does not seem to be the only or even the principal deformation mechanism in the presently studied mylonite zones.

Due to the likely complex nature of the deformation path involved in the formation of mylonites, as well as the anisotropic character of most metamorphic rocks, the precise determination of the type of strain they suffered seems to be a difficult problem and frequently of impossible solution (see Sect.6.3). This is a particularly important remark for the analysis of the Loch Maree rocks where the application of techniques such as quartz 'C'-axis analysis is impracticable due to the polydeformed nature of the rocks. However, based on the observation of several scales of structural features which can be used as kinematic indicators in the mylonites, a discussion of the nature of the deformation mechanisms which formed these rocks will be presented in this section.

A brief review of the existing strain models from the literature (Bell 1981, pp.275-281) will be reproduced here. It is thought to be necessary for the present discussion not only because it is a good systematization of the modern nomenclature but also enable it to be compared with the geometry produced during deformation of the L.Maree rocks (see Sects 4.3 and 6.3).

The strain models described in the literature include:

- (1) progressive simple shear-non-coaxial plane strain (Fig. 5.1b),
- (2) progressive, inhomogeneous, simple shear non-coaxial plane strain (Fig. 5.1c),
- (3) approximately progressive, simple shear non-coaxial, non-plane strain (Fig. 5.1b),
- (4) approximately progressive, inhomogeneous, simple shear non-coaxial, non-plane strain (Fig. 5.1c),
- (5) progressive pure shear coaxial, plane or non-plane strain (Fig. 5.1d), and

(6) progressive, bulk, inhomogeneous shortening ('flattening'), where the centres of bulk boundaries are displaced relative to the average direction of flattening as shortening occurs (Fig. 5.1f) and where they are not displaced - coaxial on the bulk scale - plane or non-plane strain (Fig.5.1e).

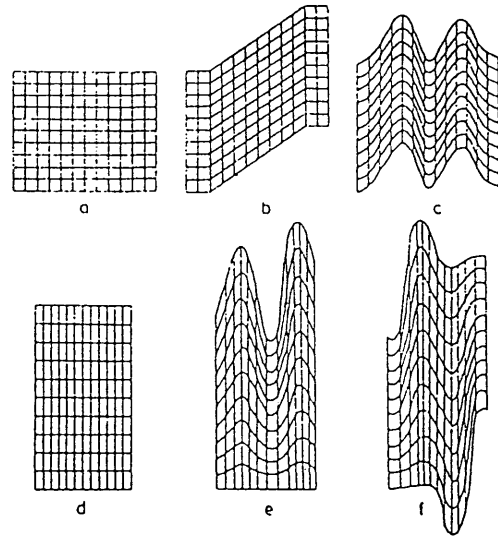


Figure 5.1 Sketches (modified from Ramsay 1963) of strain fields generated in a block of originally undeformed rock (a) by deformational histories which involved, (b) progressive simple shear, (c) progressive, inhomogeneous, simple shear, (d) progressive pure shear, (e) coaxial progressive, bulk, inhomogeneous shortening (Ramsay's 1963 inhomogeneous form of pure shear), and (f) non-coaxial progressive, bulk, inhomogeneous shortening. (reproduced from Bell 1981, fig. 1)

Problems of space and boundary discontinuities associated with bulk shortening (Escher and Watterson 1974, Law *et al.* 1987), together with the lack of most characteristics listed by Bell (1981, p.293) as indicative of a bulk inhomogeneous shortening history of deformation, seems to indicate the unlikeness of the action of this mechanism alone (see Sect. 6.3). The same is the case for simple shear - non-coaxial **plane** strain (1 and 2 above) since this model is neither the most appropriate to explain the pattern of strain variation (Sect.6.3), nor does it fulfill the criteria for the formation of mylonites during ideal conditions of heterogeneous simple shear proposed by Ramsay and Graham (1970), *viz.* the walls of the shear zone are undeformed and volume change is unimportant. The inhomogeneous character of the strain together with the presence of features suggesting ^{the} action of pure shear in addition to simple

shear deformation, indicates the inadequacy of the above presented strain models to accommodate the geometry of features registered for these rocks (cf. Figs 4-1 and 5-1). This reinforces the conclusions made in chapter 4 where the geometry produced by the 'non-coaxial progressive bulk inhomogeneous shortening' model was found to be the closest reproduction of the microscopic scale features of the studied rocks.

Features indicating simple shear deformation were by far the most abundant in these rocks and their kinematic significance will be the subject of the discussion to follow.

Simple Shear Kinematic Indicators

There are six main types of simple shear kinematic indicators observed:

- a) asymmetric pressure shadows
- b) asymmetric microfolds
- c) 'asymmetric augen structures' and 'mica fish'
- d) broken and displaced grains
- e) oblique foliations
- f) oblique cleavages

The presence of **asymmetric pressure shadows ('a')** in garnets, amphiboles and other elongate porphyroclasts (that have high ductility contrast with the matrix) is a common feature in the L. Maree mylonitic rocks (Sect.5.2). Large garnet porphyroclasts in these mylonites show carbonate pressure shadows and microfolds in the foliation at the edges of the rotated crystals. However, the wide spacing and less concave character of the foliation around the porphyroclast (at the site where the most recent deposition of material would occur), considered as diagnostic by Simpson and Schmid (1983, p.283), are not always observed. Grain boundary sliding-dominated deformation of the external foliation, the carbonate-rich composition of the pressure shadows, and the nature of the deformation path are possible responsible factors for the absence of spectacular pressure shadows. The observed ones (e.g. Pl.5-55) register only the last increments of deformation.

Although prismatic sections of amphibole and epidote are aligned parallel to the mylonitic banding, some of these crystalloclasts show oblique or perpendicular orientation in relation to this foliation (e.g. Pls. 5-54,55). Ramberg(1975), Ghosh and Ramberg(1976), Ramberg and Ghosh (1977) and Schoneveld (1979) have studied the behaviour of elongate (and round) rigid inclusions immersed in a matrix undergoing simple shear, pure shear and a combination of the two deformation mechanisms. They agree that the component of rigid rotation in the inclusion will be in general less or at most equal to that in the matrix, depending on a series of factors including:

- (i) the competence contrast between inclusion and matrix,
- (ii) the axial ratio of the inclusion,
- (iii) the orientation of the inclusion in relation to the flow direction, and
- (iv) the type of strain path followed by the particle (which can also dictate the sense of rotation - real or apparent).

In situations where simple shear is dominant there seem to be no problems with the indication of the sense of rotation and the elongate bodies will rotate with their largest axes towards the simple shear plane (Simpson and Schmid 1983). According to Schoneveld (1979) the rate of rotation of an elongate body is not constant, decreasing with the angle between its longest axis and the shear direction. Elongate particles will spend an inordinate amount of time with their major axes in the proximity of the shear direction, and only at very high strains will they be able to rotate through the shear plane. In this way a preferred orientation in a multiparticle system is produced.

Although most of the studied mylonites show elongate porphyroclasts aligned sub-parallel to the banding, the presence of particles with different orientations is not rare. They seem to be more frequent in the ultramylonites, apparently confirming the high deformation (and simple shear) suffered by these rocks. The sense of rotation, however, could not be determined in most cases due either to the lack of pressure shadows and internal foliation in most porphyroclasts or the presence of connection between the internal and external foliations in (garnet) porphyroclasts with inclusion

trails (see Sect.4.3).

Asymmetric microfolds ('b') affecting the mylonitic banding develop in the vicinities of large porphyroclasts in ultramylonites. As shown by Ramsay et al. (1983) and Bell and Hammond (1984), at low shear strains the asymmetry of folds is dependent on the initial orientation of the affected layer. At high shear strains (> 10) there are many difficulties with this sort of evidence, since they can indicate (1) the **opposite** sense of movement for the bulk shear strain (2) a different shear direction - in the case of undetected rotation of the fold hinges into parallelism with the movement direction (see Chaps 7 & 8). The observed folds, however, seem to show a sense of shear consistent with that determined from other sources of evidence, such as antithetic shear fractures and asymmetrical augen structures. This suggests that although these folds have possibly been formed by the effects of the large porphyroclasts acting on the flow of the surrounding matrix, they can in this case be used as an additional evidence for the bulk shear sense (Pls. 5-50,53). Since these structures are affecting an already mylonitic banding developed during highly ductile conditions, it is possible that they formed due to 'vorticity repartitioning' during shear flow. This model was proposed by Lister and Williams (1983): they compare the flow of deforming rocks with the flow of a continuous medium, the presence of competence contrasts, discontinuities or any planar or linear rheological anisotropy causing different partitioning of flow from place to place. In the L. Maree mylonites, the coupling between garnet porphyroclasts and the surrounding flowing matrix has apparently enabled the bulk shear induced vorticity to be locally transformed into spin. As pointed out by Lister and Williams (1983), if the spin has the same sense as the bulk shear induced vorticity, a perturbation of this multilayer showing competence contrast will be amplified. The disturbance in the flow field will then propagate, and the produced instability changing the flow pattern over a much larger volume leads to the development of the folds. Accordingly, the observations that these folds always show the same vergence, that they die out along the foliation, and that they have disrupted long and thickened short limbs, seems to agree with the features presented by structures formed by this kind of

mechanism (cf. Lister and Williams 1983, Berthe et al. 1980).

'Asymmetric augen structures' and 'mica fish' ('c') are observed in mylonitized gneisses (Pls. 5-51,59,64) and muscovite-bearing mylonites. The augen structures are developed by grain size reduction in rotated porphyroclasts, the asymmetry and elongation of the fine-grained 'tails' giving the sense of movement. In the case of the Loch Maree rocks the feldspar 'tails' are not as asymmetrical or as well-developed as the ones presented by Simpson and Schmid (1983, Fig.4), being probably a function of matrix-porphyroclast competence contrast and the low axial ratio of the 'clasts'. At microscopic scale most of these kinds of features were developed in garnet and amphibole crystalloclasts. In one of the samples carbonate crystals displaying these features in a quartzite could only be identified due to the simultaneous presence of amphiboles showing long tails, since the geometry of the carbonate more closely resembled microscopic 'tension gashes' (Pl.5-59). It should be noted that (1) the misidentification of these two features could lead to interpretation of an opposite sense of shear for the specimen and (2) the carbonate in this case was more competent than quartz (Sect. 5.3.2.4). Sigmoidal 'muscovite fish' (Lister and Snoke 1984) are not uncommon features in these rocks. The feature is developed in quartz-rich metasediments where large **white** mica flakes are boudinaged by a combination of brittle and crystal-plastic processes (Lister and Snoke 1984, p620). Most of the observed phyllosilicate crystals, however, show microboudinage and particularly grain size reduction. Large muscovites with (001) cleavage aligned parallel to the shear banding were cut across by narrow shear bands producing several small lenticular grains. These, in turn, appear to have suffered grain boundary sliding due to the not uncommon presence of fine-grained quartz and feldspar in between the 'new grains'. The fact that none of the other situations described by Lister and Snoke (1984, Fig.5) were observed (i.e. produced by oblique orientation of (001) cleavage in relation to the shear direction) seems to suggest that most of the large muscovite porphyroblasts were marking an older fabric (S1) parallel to which the mylonitic banding was developed.

Broken and displaced grains ('d') of garnet, feldspar and amphibole were also used as kinematic indicators. The kinematic

interpretation of these features (also called 'book-shelf' fractures) is at variance with the interpretation of extensional crenulation cleavages although in both cases we are dealing with extensional structures (cf. Pls. 5-12 and 5-51). The observation that these structures affect only those crystals not propagating into the mylonitic matrix, suggests their contemporaneity with the mylonitic banding. Due to the relatively low strain indicated by their geometry these structures are thought to have been produced during the last incremental strains affecting the rocks.

Oblique foliations ('e') marked by the optical orientation of deformation bands and elongate quartz crystals were not^{ex} as much use as kinematic indicators in these rocks due to their constant reorientation, mainly as a result of late overprinting. Although in some samples the deformation bands show an orientation approximately parallel to the XY plane of associated folds, several others did not show this kind of relationship (Fig.5.2).

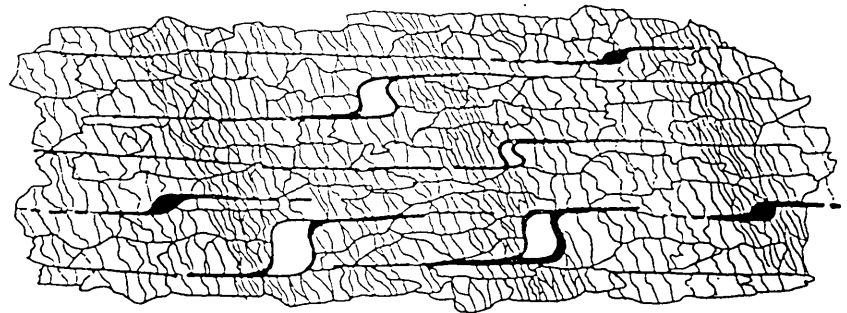


Figure 5.2 Asymmetric augen structures indicating a right lateral movement, while the oblique deformation bands in quartz crystals suggest a 'NE-SW' orientation for the maximum principal compressive stress. This indicates that the features are of different age, the deformation bands probably being younger. White sigmoidal structures are carbonate crystalloclasts while the black are amphiboles. Scale bar ~1mm. Sketch from carbonate-quartz myl. (see also Pls 5-59,59A and discussion below).

According to Simpson and Schmid (1983) these bands register the last increment of deformation. In a simple shear regime they will show crystallographic orientation and elongation oblique to the mylonitic foliation, since their XY planes will tend to be aligned perpendicularly to the direction of maximum compression. Further reorientation of these quartz aggregates, associated with D2, D3 and

D4 deformational episodes was already described in Chapter 4. In the high strain ultramylonites this kind of 'foliation' was not as evident, probably due to the dominant deformation mechanism (grain boundary sliding) active in these rocks (Sect. 5.3.2.2).

While the work of Lister and co-authors (Lister *et al.* 1978, Lister and Paterson 1979, Lister and Hobbs 1980) has shown that the crystallographic fabric asymmetry patterns in quartz and calcite are controlled by three main factors:

- (i) the particular glide system active during deformation,
- (ii) the finite strain, and
- (iii) the strain path or kinematic framework.

Miller and Christie (1981) have identified a more complex picture of the situation. They showed that other factors can also affect the pattern associated with the mylonitization (misleading the kinematic interpretation):

- (iv) the presence and importance of diffusive deformation mechanisms,
- (v) nucleation and growth of grains during recrystallization,
- (vi) abundance of other mineral phases, and
- (vii) original orientation of the grains.

Price (1981) reported situations where fabrics can be traced around refolded folds showing that in the studied case later deformation has only caused a passive rotation of the earlier fabric. He also pointed out that the type of deformation can only be determined by preferred orientation studies if the strain path can be shown to be simple. This does not seem to be the case for the Loch Maree mylonites, where microstructural study has shown the widespread recrystallization of quartz during repeated deformation (see Chapter 4). In addition to the important role of factors (iii) to (vi) above, the effects of both localized heterogeneities (*e.g.* porphyroclasts) together with grain boundary sliding are considered to be significant in the development of well-developed mylonites (Sect. 5.3.2.2). These are additional features responsible for discouraging the application of quartz 'c'-axis technique in the Loch Maree rocks.

Several sets of **oblique cleavages ('f')** were observed in these mylonites. Although in some samples they were identified as S2 or

younger foliations, in several others it was difficult to determine their nature. The fact that some of them seemed to be restricted to mylonitic rocks suggests the presence of 'S' and 'C' surfaces (Berthé *et al.* 1979, Jegouzo 1980, Ponce de Leon and Choukroune 1980), '**extensional crenulation cleavages**' (Platt 1979,1984; Platt and Vissers 1980) or **shear bands** (White *et al.* 1980). The 'C' ('cisaillement') surfaces (Fig.5.3) are zones of high shear strains, which initiate and remain parallel to the shear zone margins, being the result of variations in the amount of shear strain. They are shown in several scales appearing under the microscope as recrystallized polycrystalline aggregates with reduced grain size.

The 'S' surfaces define the plane of preferred mineral orientation, with the (001) cleavages of phyllosilicates orientated parallel to them. Initially oriented at 45° to the shear zone margins, these surfaces are related to the accumulation of finite strain. It is a schistosity produced parallel to the XY plane of the finite strain ellipsoid during the initial stages of deformation. With the progression of the deformation, the angle between 'S' and 'C' surfaces is gradually reduced by rotation of the \underline{S} fabric towards parallelism with the shear zone margins (conforming to the model of Ramsay and Graham 1970). Both 'S' and 'C' surfaces are believed to be contemporaneous (Berthé *et al.* 1979), not overprinting each other, and the acute angle between them has been used to determine the overall sense of shear (Fig.5.3).

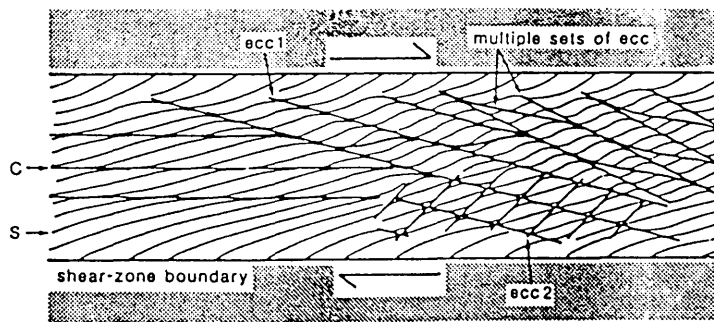


Figure 5.3 Diagram illustrating the orientation and mutual relationships of foliations in shear zones. S:shape fabrics; C:shear bands; ecc1 & ecc2, conjugate sets of extensional crenulation cleavages (reproduced from Platt 1984, fig.1). In some high strain zones where more homogeneously foliated mylonites occur, a late (but still believed to be part of the same

mylonite-forming episode) set of shear bands or extensional crenulation cleavage is observed. These structures can be formed in single, conjugate (Pl.5-12) or multiple sets. Single sets show the same sense of movement of the bulk shear deformation and were compared to the formation of Riedel 1 shear fractures (Platt and Vissers 1980). Conjugate sets show both senses of shear and were thought to be indicative of coaxial shortening (Platt and Vissers 1980, Law et al. 1984). However, experimental work by Harris and Cobbold (1984) shows the possibility of forming these features during bulk simple shear if sliding along a pre-existing foliation (layering, cleavage or schistosity) takes place. The orientation of secondary shear bands is controlled by the attitude of the foliation instead of the principal directions of total strain or orientation of the bulk shear direction. Although these structures are more frequently identified in rocks undergoing ductile deformation, probably due to the associated recrystallization of the mineral components (Sibson 1977), they were also reported in association with brittle thrusts (Platt and Leggett 1986, p.198), where they were compared to Riedel shears (Tchalenko 1970), being the variations of geometry explained in terms of confining pressure control (cf. Murrell 1979). Accordingly, in the Loch Maree mylonites the presence of shear bands showing opposite sense of shear as well as single sets indicating movement compatible with other kinematic indicators could suggest the presence of this sort of structure.

A major problem involved with the use of these structures (including **S** and **C** surfaces) in the kinematic analysis is the determination of their timing of development. As already mentioned, the S2 cleavage (particularly well developed in the mylonitized rocks), and the late sets of cleavages (Chap.3) can easily be misinterpreted as shear bands. In addition to the similar geometry of the produced crenulation, the fact that most of these later sets show a N-NE strike with variable dip direction (see Chap.3) can cause problems, since a section orientated to best show the trace of these foliations (perpendicular to the mylonitic foliation and containing the stretching lineation) will also be the orientation in which the extensional crenulation and **S** surfaces are best seen. Although Berthé et al. (1979) proposed that both foliations were formed at the same time it seems reasonable to suppose that, depending on the

strain path, the **S** surfaces might have been formed before localized yield and subsequent plastic deformation gave rise to the **C** surfaces (Lister and Snoke 1984, p.619), or even at much later stages of the (non-coaxial) deformation having no direct relationships with the other kinematic indicators; it all depends on the nature of the **S** foliation (see below). The above authors reported that unequivocal timing criteria sometimes can be found viz., the change of metamorphic conditions between the development of **S** and **C** surfaces. However this very same evidence can also be interpreted in terms of two distinct episodes of deformation and syntectonic metamorphism, which leads us towards facing all the problems involved with the determination of timing between deformation and metamorphism.

Vernon *et al.* (1983) have identified two sets of foliations in the analysis of the deformation of a granite batholith. Although recognizing features considered typical of **S** and **C** surfaces, they used the S1-S2 terminology and favored a model of progressive deformation to account for the development of those foliations, since unequivocal evidence for simultaneous or sequential development of these structures could not be found. Recognizing some of the problems presented above, Lister and Snoke (1984, p.635) proposed the use of the S1-S2 terminology where an older metamorphic complex is involved in a later shear zone. Older **S** surfaces would then be transected by **C** surfaces and if the pre-existing anisotropy is in the extensional field of the later flow, extensional crenulation cleavages will be formed. While the presence of older fabrics in the Loch Maree rocks was identified in the microstructural studies (S1-S2), it is not clear whether they could be interpreted in terms of '**S**' and '**C**' surfaces even if the widespread development of mylonitic features (Chap.4) and a progressive deformation model is adopted (see Chaps 6 & 8).

In this way, although the '**S**', '**C**' and 'extensional crenulation cleavage' terminology is useful in drawing attention to the presence of zones of **non-coaxial laminar flow**, it should have its use restricted to foliations associated with well developed mylonitic rocks in **first time deformed** 'homogeneous' (igneous and sedimentary) rocks. The S1-S2 terminology, although having a sequential connotation, is less interpretative than '**S**' and '**C**' etc. surfaces and should be used in metamorphic rocks since it leaves

open the possibility of identifying some of the foliations as corresponding to cleavages that also affect the regional (non-mylonitized) rocks. As overprinting is a common situation in areas of polyphase deformation where high strains are easily attained in the early stages (like in the present case), complete structural mapping of the surrounding (non-mylonitic) rocks should also be carried out, providing a framework in which the significance of the mylonites and associated features can be interpreted. It is possible that some of the debate about the significance and use of these structures in the modern literature is caused by the restriction of some of these studies to the mylonitic rocks only.

Concluding remarks

It should be now clear that no single criterion is sufficient to interpret the kinematics in mylonite zones. In addition to the problems involved in the application of the kinematic indicators, the movement pattern can **vary** from place to place in a complex way (Lister and Snoke 1984, p.635). It is still not clear whether this 'movement pattern variation' is caused by geologically significant factors (such as reversal of movement directions during deformation, or later reactivation of these high strain zones with a different sense of movement), or whether it is produced by the difficulties concerning the correct application of the kinematic indicators. Examples of this situation were frequently faced during sampling of folded mylonites where the mylonitic foliation had a NW-SE strike and a subvertical attitude in the field (produced by 'later' folding). If the fold was identified it was possible to unfold the steeply-dipping foliation and work out the sense of shear along the foliation. If the fold was a reclined or overturned structure whose geometry remained undetected during mapping, by simple rotation of the subvertical foliation to its presumably pre-folding sub-horizontal position, the chances of obtaining the opposite sense of movement with the use of the kinematic indicators are high (50%). The obvious solution for this problem is similar to the case for 'S-C' relationships discussed above; a careful analysis of the geometry of the mapped area or to restrict the use of kinematic to simple situations of relatively late shear zones affecting homogeneous

rocks. Nevertheless, even in this case much caution is needed and several theoretical possibilities of obtaining conflicting senses of movements can be envisaged. One example is a situation of a relatively better preserved 'pod' of rocks surrounded by high strain zones showing the same overall sense of movement (Fig 5.4). The shear sense in both sides of the 'pod' would indicate opposite senses of movement for the pod/mylonite interface. This opposite sense of movement is, in fact, produced by the partitioning of deformation and the local nature of the kinematic analysis.

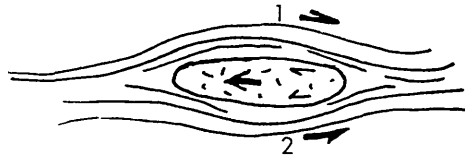


Fig 5.4 Pod of less deformed rock surrounded by high strain zones. Analysis of shear sense in positions 1 and 2 would indicate opposite sense of movement along the shear zone.

The interpretation of features (such as oblique cleavages) expressed by, for example, deformation bands in quartz crystals, should also take into account the particular deformation properties of each mineral phase and the conditions under which they are formed or modified. In the case of quartz, due to the susceptibility of this mineral to deformation, the orientation of features like deformation bands reflect only the last increment of strain. They could **only** be related to e.g. asymmetric augen structures or the mylonitic banding itself, as part of the same (progressive) deformation, **if** the increments of strain responsible for the production of all these features were added **coaxially** throughout the evolution of the rocks. As described in section 5.2, all the kinematic indicators are visible in sections parallel to the lineation and at high angles to the banding, so that structures such as asymmetrical folds observed in these sections are indicating only a short period of the kinematic history of these rock. This is due to the possibility that they have been rotated into parallelism with the linear fabric at higher shear strains. In this way, although Simpson and Schmid (1983) have concluded that **asymmetric augen structures** are the most reliable indicator of the sense of movement (probably on the basis of its 'stability' and direct association with the grain-size reduction event) they have as much potential as e.g. rotated boudins (cf. Sugden 1987, Figs 7,8,9), with the latter feature

having the advantage of providing a quantitative estimate of the shear strain. Accordingly, in the case of the Loch Maree rocks, asymmetric augen structures and pressure shadows indicate a **top to the NW sense of movement during mylonitization** (assuming a pre-F2 sub-horizontal position for the main thrust horizon) while in some cases, asymmetrical folds, antithetic shear fractures and extensional crenulation cleavages and in several cases, S-surfaces indicate a **top to the SE sense of movement**. The application of a single or association of several of the above discussed criteria can be misleading due to the large number of possible situations bound to be faced in naturally deformed rocks, so that unless some understanding of the **macroscopic structure** is achieved (Sect. 5.3.2.5) **all** the existing criteria should be applied with caution.

In terms of predominant mechanism of deformation, it can be concluded from the evidence given by the Loch Maree mylonites that simple shear was probably a far more important deformation mechanism than pure shear. However, if other sources of evidence are considered (see strain analysis- Sect.6.3), large volumes of rocks have suffered essentially pure shear, something possibly related to the partitioning of the deformation. This is in agreement with the observations of Ramberg (1975) who had already noted the inadequacy of strain geometry models based solely on simple shear or pure shear to explain the deformation of rocks. On the other hand, Bell (1981, p.288) pointed out the scale-dependency of factors such as coaxial and non-coaxial strain paths. As a function of deformation partitioning one mechanism can be predominant at a determined scale but unimportant at another, so that localized zones of e.g. pure shear can be produced in an overall simple shear regime and *vice-versa*. Although the situation is not so clear when dealing with the internal deformation of the established domains (see Sect.6.3), the preferential localization of mylonitic rocks along the boundaries between these domains together with the unequivocal association between D1 mylonitization and the emplacement of the basement rocks that indicate the relative translation of these units could only have happened if large simple shear strains were developed. The envisaged strain geometry produced is similar to the one presented by figure 4.1c which was used to illustrate the geometry of microscopic scale features.

5.3.2.2 Strain Softening Mechanisms

In mechanical terms softening of a material means that it deforms with increasing strain rate at constant stress or at constant strain rate with decreasing stress (White et al. 1980). This sort of mechanism is very evident in shear zones affecting homogeneous rocks, producing contrasting textures and mineralogy in rocks believed to have been subjected to similar conditions of pressure and temperature (Ramsay and Graham 1970). These mechanisms seem to be the reason why it is easier to further deform an already deformed zone than it is to initiate deformation elsewhere (Poirier 1980). Strain softening can be produced by several processes (White et al. 1980, Poirier 1980, Schmid 1982) viz.:

- (a) Change in deformation mechanism,
- (b) Geometrical or fabric softening,
- (c) Continual recrystallization,
- (d) Reaction softening,
- (e) Chemical softening,
- (f) Pore fluids effects,
- (g) Shear heating.

Change in deformation mechanism ('a') seems to have been an important process during the development of the Loch Maree mylonites. This mechanism is 'activated' by changes in grain size which occur during dynamic recrystallization of a rock. This is, in turn, likely to promote changes in the dominant deformation mechanism since once small grains have been produced grain boundary sliding is favoured. This leads to superplastic behaviour of the material (White 1976, Schmid et al. 1977). The occurrence of grain boundary sliding in the L.Maree rocks can be inferred from

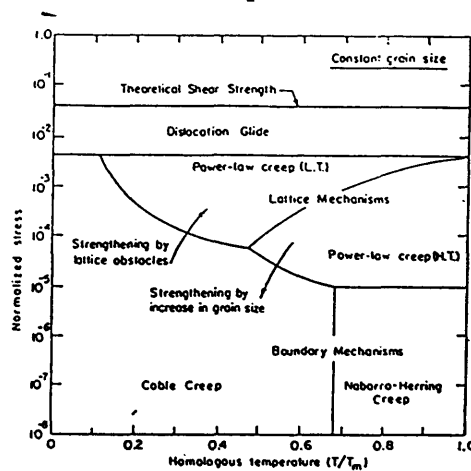
- (i) Absence of orientation of the matrix: The overwhelming majority of the mylonites or ultramylonites do not present crystallographic or grain-shape orientation, being in general equiaxial
- (ii) Extreme grain size reduction. In several ultramylonites the average grain size of the matrix is around 10 microns being incomparably smaller than the subgrains in the porphyroclasts.

According to White et al. (1980) the presence of small grain size means that high initiating stresses, low homologous temperatures (T/T_m , see below) and the presence of a dispersed second phase (which inhibits grain growth) has favoured this softening process. Although white mica (in quartzofeldspathic mylonites) and very fine biotite (in mafic mylonites) could have easily played the grain inhibition role, Poirier (1985, p.207) has noted that this mechanism is not necessary, since the stability of the grain size could be attributed to the confinement of (deformation) activity to the 'mantle', leaving the 'core' of the grains undeformed and thus inhibiting recrystallization. Nevertheless, the presence of typical 'core and mantle' structure in the studied rocks was mainly confined to the relatively coarser grained mylonites in contrast to the ultramylonites where the grain size was more homogeneous and for which superplastic behaviour is proposed.

Conditions for the appearance of superplasticity proposed by Boullier and Gueguen (1975) include:

- (i) High temperature ($T^{\circ}/T_m^{\circ} > 0.5$, T_m being the melting temperature),
- (ii) Not too high stress and strain rates,
- (iii) Moderate dislocation density, and
- (iv) High strain rate sensitivity.

These conditions were based on experimental work and, as noted by Langdon (1985), they **favour** the dominance of 'boundary mechanisms' (intercrystalline) in relation to 'lattice mechanisms' (intracrystalline) as shown in Figure 5.5 (a) & (b).



a

Figure 5.5 (a) Schematic illustration of a typical deformation mechanism map of normalized stress versus homologous temperature at a constant grain size. LT, HT: low and high temperature respectively (reproduced from Langdon 1985, fig.5).

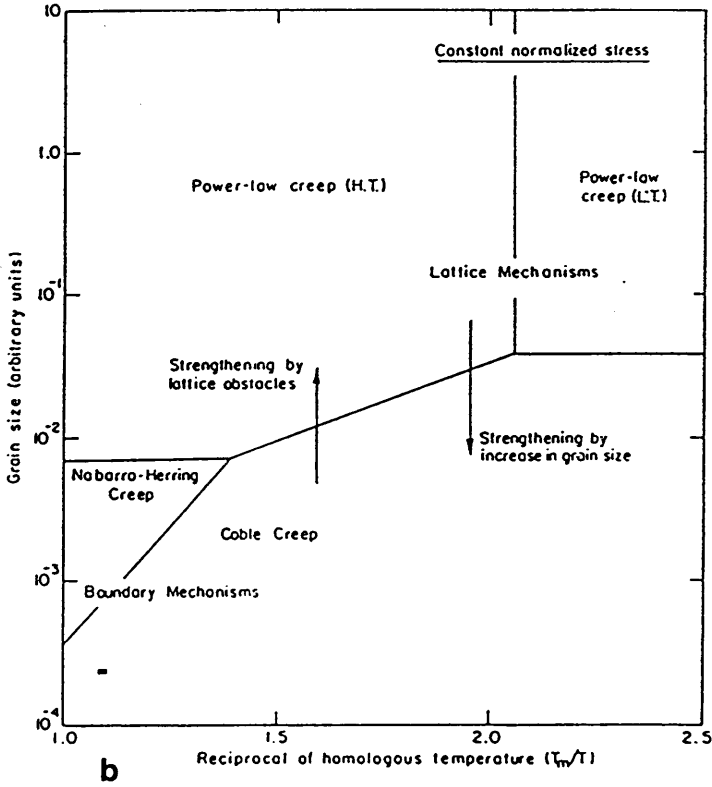


Figure 5.5 (b) Schematic illustration of a typical deformation mechanism map of grain size versus the reciprocal of homologous temperature at a constant normalized stress (reproduced from Langdon 1985, fig.6).

Although the evidence from the Loch Maree rocks suggests that conditions (i), and (iv) of Boullier and Gueguen (1975) are also likely to have been fulfilled, the most significant feature indicating superplastic behaviour seems to be the small equiaxial grains of these rocks. This suggestion seems to be reinforced by the recent work of Boullier (1980) where a bulk superplastic behaviour is proposed for very fine grained rocks despite the low

temperature (greenschist facies) and cataclastic deformation of feldspars.

The conditions for superplastic behaviour were also revised by Schmid et al. (1977) who proposed that more useful criteria than fine grain size ($<10 \mu\text{m}$), absence of preferred orientation and very low dislocation densities would be (1) the equiaxed shape of grains and (2) the grain size sensitive character of the strain. Schmid later recognized the problem that in naturally deformed rocks it is difficult to find evidence for grain boundary sliding, since a stable microstructure could also be explained in terms of dynamic recrystallization (Schmid 1982, p.101), and suggested that the only indicator for the action of grain boundary sliding is the absence of preferred crystallographic orientation (but see Sect. 5.3.2.1.f). As pointed out by Schmid et al. (1977) superplasticity is expected under a wide range of conditions, particularly at small grain size these are so general that they can apparently be fulfilled by pseudotachylites as proposed by Passchier (1982, p.77). Nevertheless, although superplastic behaviour appears to be a mechanism capable of explaining most features observed in mylonites, including the presently studied ones, it seems that due to the still remaining uncertainties about the conditions under which it can be active, much caution is necessary when extrapolating these experimental results (in metals) to naturally deformed rocks.

Geometrical or fabric softening (b) occurs when, during deformation active slip planes rotate into an easier position for slip to occur (Poirier 1980) i.e. into parallelism with the edges of the shear zone as the slip direction rotates into parallelism with the stretching lineation (White et al. 1980, p.183). Since no quartz C-axis fabric studies were carried out in the mylonites at L. Maree, the only observed situation during which this mechanism could have contributed to strain softening in these rocks, is by the rotation of elongate crystalloclasts (like phyllosilicates and amphibole) into parallelism with the shear plane, in the sort of fashion discussed in Section 5.3.2.1(a) (see also Sect. 5.3.2.3 c).

Continual recrystallization (c) and reaction softening (d) are thought to have acted simultaneously during the mylonite formation.

These mechanisms are based on the production of small strain-free ('soft') grains. Metamorphic reactions (particularly if retrogressive) can promote the formation of small recrystallized grains which can in turn behave superplastically and transform resistant phases like feldspars into soft phases like quartz and white mica (White and Knipe 1978, Etheridge *et al.* 1984). Accordingly, although uncommon, strain-free quartz aggregates were described in the rocks at Loch Maree. In addition, transformation of feldspars into quartz plus white mica was virtually ubiquitous in the ultramylonites. The main problem faced in this case, was the determination of the timing between mineral transformations and deformation. Despite the possibility that the white mica - quartz matrix was formed during a late (retrogressive) event, as a function of the the more reactive nature of the fine-grained matrix, the presence of quartz segregation bands affected by D1 deformation (stretching lineation, sheath folds etc.) indicates contemporaneity between the mylonitization processes (grain size destruction of the feldspars) and the transformation of feldspar into quartz plus muscovite (these reactions driven by abundant fluid phases - see Chap. 7).

Chemical softening (e) and pore fluid effects (f) are considered together since the introduction of fluids (mainly H₂O and CO₂), particularly along the mylonite zones, may have promoted weakening of minerals like quartz, as well as giving rise to pore fluids which might have initially increased the rock ductility (White *et al.* 1980). As pointed out by Kinley (1984) there are several difficulties involved in the study of the weakening of rocks compared to single minerals in the ductile regime. Pointing out that additional processes which are difficult to identify are likely to have operated (*e.g.* the role played by grain boundaries and subsidiary phases), this author defends the idea that it is not realistic to apply a rheological law based on a given process (*e.g.* the behaviour of 'wet' quartz) without considering the effects of competing processes. Experiments at high temperature can be even more problematic due to the production of substantial amounts of an intergranular partial melting phase which can significantly modify the rheological behaviour of the material (Mainprice and Paterson 1984). Although no specific study to evaluate the role of

hydrolytic weakening in the L. Maree rocks was undertaken, evidence for the action of permeating fluids during their development is given by, for example, their hydrous mineralogy and the presence of quartz segregation bands (see Chap.7), suggesting that hydrolytic weakening of quartz and other minerals was a likely occurrence. For this very same reason, the presence of **pore fluid effects (f)** in these rocks is a realistic assumption. According to White *et al.* (1980) pore fluids can lower the effective stress leading to cataclasis (see Sect. 5.3.2.4), or by increasing the diffusivity of grain boundaries to promote strain softening (Etheridge and Wilkie 1979).

Examining the role of mobile fluids during deformation, Etheridge *et al.* (1984) noted that under conditions of metamorphic fluid pressures greater or equal to the minimum principal compressive stress, the generation and healing of microfractures play an important part in the deformation mechanisms. The mechanism promotes the interconnection of grain boundary tubules and bubbles, which are principally responsible for rock porosity, in this way increasing the permeability of the rocks. This kind of process is more effective along large scale heterogeneities such as shear zones, where they promote strain softening.

The effects of **shear heating (g)**, leading to softening, were reviewed by Brun and Cobbold (1980) and Fleitout and Froidevaux (1980). Shear heating is produced by the transformation of mechanical energy into heat during deformation. Despite the fact that significant heat can be generated in major shear zones or at high differential stresses, it is doubted that the necessary conditions can occur in natural shear zones, since amongst other problems there is the difficulty of maintaining stresses after softening has occurred (Brun and Cobbold 1980, p.156). Although shear heating is not considered to be important enough to promote partial melting in most situations (but see Fleitout and Froidevaux 1980, p.163 and Paterson 1984, p.4268 and Sect. 5.3.2.4. below) it may well be enough to promote changes in the mechanism of deformation (or to increase the strain rate) leading to work softening.

Concluding remarks

The importance of softening processes in the localization of shear zones is well summarized by the remarks of White *et al.* (1980, p.184) reproduced here;

"the extent of the softening with respect to the adjacent country rock and consequently the width of the shear zone or shear zone system required to accommodate a given imposed strain rate at a given temperature will be dependent upon the operative processes. These in turn will reflect the mineralogy and petrology in which the shearing has occurred."

Geometric softening, considered to be more important in coarse grained protomylonites, is considered to have less importance at high temperatures. The relative importance of the softening processes is strongly temperature-dependent, and an analogy can be made by observation of the effects of temperature on the predominant deformation mechanism (*cf.* Fig. 5.4 above). But since the temperature path for these rocks is not simple (see Chap.7), and because of the complexities of the interplay between deformation and metamorphism, the application of higher resolution techniques providing a more detailed picture of the temperature variation seems to be essential for the correct evaluation of the relative importance of the deformation mechanisms.

Nevertheless all the above discussed processes or their combination are believed to have been active during the deformation of the Loch Maree mylonitic rocks. Change in deformation mechanism and pore fluid effects seem to have been equally important in these rocks. The former was probably the main factor controlling the unusually fine grain size of the ultramylonites, while the latter has both (i) promoted strain softening by increasing the diffusivity along the grain boundaries and also (ii) promoted (transient) brittle deformation (*cf.* Sect.5.3.3.4). In the case of the transformation of feldspars into fine grained quartz-mica aggregates, reaction softening, continual recrystallization, chemical softening and pore fluid effects were all intimately associated and simultaneously active so that their relative importance cannot be assessed.

5.3.2.3 Mineral Deformation Mechanisms

The facts that (1) carbonate-rich rocks mark the main thrust zone, together with (2) a constant localization of high strain zones along the contact between amphibolite bodies and their host rock and along most of the lithological boundaries (see Chap.2), seem to indicate a mineralogical and petrological control in the localization of these deformation zones (see also Chap. 8). In this way, a discussion of the most likely deformation mechanisms affecting the principal rock-forming minerals seems to be relevant for the understanding of the deformation pattern of these rocks. It can also help to explain several scales of features, from the low deformation (by lattice mechanisms) presented by quartz crystals where surrounded by micas, to the highly strained long grains present amongst feldspars (quartz had to accommodate all the strain which was not taken up by feldspar), to the rheological variations indicated by some of the mesoscopic structures in the same rock types (see Chap.6).

From the descriptive part (Sect.5.2) an order of minerals with increasing resistance to grain size reduction processes was suggested: *viz.* calcite-quartz-biotite-muscovite-feldspar-garnet-amphibole-epidote. The establishment of this sequence involves several assumptions being made, such as the homogeneity of deformation conditions at the thin section scale, and estimations of strain intensity without quantitative results (see Sect. 5.1). The determined sequence seems, however, to be consistent with experimental studies based on empirical laboratory calibrations and also observations of naturally deformed rocks elsewhere. Difficulties faced when describing the sequence of deformation of these minerals included the absence or rarity of the association of some minerals such as muscovite with amphibole, and perhaps the role played by variables such as the relative abundance and competence of mineral phases. The general 'rules' of competence contrast seem to have been obeyed (but see Sect.6.2.2.5) and the deformation sequence is compatible with the 'competence contrast lists' presented by Ramsay (1982, pp.117-118). The rarity of general references in the literature to the influence of factors other than mineralogical composition (particularly mineral proportion) and temperature controlling the relative flow of rocks during deformation, justifies a detailed examination of the crystalline deformation properties of the main rock-forming minerals at Loch Maree. The

results of this discussion will support the interpretation of the relative rheology indicators at mesoscopic scale (see Chap.6).

There is no doubt that mineral composition is a major factor controlling rock competence and an elucidative example is the common observation that relatively thin quartz bands in a mica schist (under extension) show boudinage. This suggests that quartz was more competent than mica under the considered deformation conditions. On the other hand, mylonites are frequently reported as occurring along quartzite bands in low-grade metamorphic terranes (abundant mica schists), suggesting that flow in the quartzite units was preferred to flow in mica-rich lithologies. Unless the latter observation reflects a generalized lack of identification of mylonitic features in the micaceous units (something certainly not as easy as the optical identification of deformation features in quartz), this kind of situation would suggest that factors other than mineralogical composition are more important in controlling the localization of the deformation and competence.

Some of these factors include (i) the variations of metamorphic conditions (Chap. 7), and possibly (ii) the mechanisms of deformation. Laboratory results reported by Shelton and Kronenberg (1978) show that feldspars are weaker than quartzite at 600 C and 2000 MPa but the reverse is true at 900 C and 2200 MPa, while plagioclase is stronger than clinopyroxene below 800 C and softer above this temperature (Kronenberg and Shelton 1980). A similar situation, but involving quartzofeldspathic gneisses and amphibolites, was observed in the mapped rocks (Sect. 6.2.2.5) so that the scale of relative resistance to deformation proposed here should be regarded as a broad generalization, subject to as many exceptions as the number of factors which control the rheological behaviour of deforming rocks.

(a) Carbonates

According to the literature these are relatively weak minerals that deform plastically by slip on various systems (similar to metals), and by mechanical twinning. Deformation by twinning was not very common in the L. Maree calc-mylonites, the few examples being restricted to large crystalloclasts (e.g. Pl.5-66). Accordingly,

experimental studies (Groshong 1974, Turner *et al.* 1956 in Wenk 1985) have shown that the maximum strain that can be achieved by twinning is 41% elongation and 29% shortening being even smaller (~15) in polycrystalline aggregates (Wenk 1985, p.369). Also, the importance of twinning is likely to diminish with decreasing grain size and strain rate and increasing temperature, when dislocation glide and climb are the dominant deformation processes (Langdon 1985, p.255 and Wenk 1985, pp.364,367). These (experimental) results seem to agree with the evidence for the Loch Maree calc-mylonites, where in addition to the rarity of twinning, no grain elongation, orientation or any visible stretching lineation of D1 age were observed. It is also in accordance with the high strain nature of these rocks and their probable superplastic behaviour during mylonitization (*cf.* Schmid *et al.* 1977, Pfiffner 1982).

Calcite is a weak mineral, deforming at very low shearing stresses (Barber and Wenk 1979). Tectonic movements, involving large strains, frequently occur along calcite beds marking the sole of thrusts in several fold and thrust belts. Dolomite in contrast to calcite is very strong, deforming plastically at fairly high temperatures (Wenk 1985). It was observed to be more competent than granites and gneisses in some situations (Ramsay 1982). However, the geological interpretation based on deformation features of these minerals can be quite complex, frequently demanding a detailed knowledge of the geological history of the area (Dietrich and Song 1984, Dietrich 1986). Special caution is needed due to the possibility of producing preferred orientation and twinning and the reduction of 'primary' deformation textures by recrystallization during later episodes of deformation (Wenk 1985, p.382). Recovery during these late stages under low grade metamorphic conditions or by static recrystallization are also possible (Barber and Wenk 1979), and can produce large grains surrounded by a fine matrix as described for some of the samples. The distinction between all these processes is difficult to resolve (see Vernon 1981).

(b) Quartz

The features produced by deformation of quartz are amongst the most studied phenomena under natural and experimental conditions (see Nicholas and Poirier 1976 for an overview). Theoretical

considerations have predicted that slip in quartz is very difficult due to the strong Si-O bonds. Although experimental work has confirmed these ideas, the work of Griggs showed that the presence of trace amounts of 'water' in the mineral structure could reduce by 10 to 20 times the stresses necessary to produce plastic deformation in quartz crystals at temperatures above 380°C (Griggs and Blacic 1965 *in* Nicholas and Poinier 1976, p.206). Despite the many uncertainties about the nature of the water-related species and the validity of extrapolations from deformation of single crystals to aggregates (*cf.* Mainprice and Paterson 1984), the empirical relations seem to hold true, indicating that hydrolytic weakening is an effective mechanism.

From petrological studies it appears that fluids are commonly present during metamorphism (see Fyfe *et al.* 1978 for a general account). In the Loch Maree rocks, amphibolite facies parageneses indicating the highest metamorphic conditions achieved, with a hydrous mineral assemblage like amphiboles and micas, indicate that a source for 'water' was not a problem.

The question of deformation rates and other equilibrium conditions with the geological environment, of so much concern in laboratory experiments, does not pose difficulties in naturally deformed rocks since the lower natural strain rates, pressure-enhanced solubility of water (Kronenberg and Tullis 1985) and time, will work in favour of the ductile behaviour of quartz.

A grain-size comparison between quartz-rich, feldspathic and carbonate-bearing ultramylonites shows that quartz crystals tend to present slightly larger grains than the other minerals (*cf.* Mitra 1978, p.1077, Twiss 1977 *in* Watts and Williams 1983). It is in agreement with the predictions of Twiss (*op.cit.*) that calcite, quartz, olivine and anorthite will have approximately the same grain sizes (within a factor of two) during steady-state recrystallization, for a given stress. This, together with recent results from experimental deformation of polycrystalline quartz at 700°C, showing that the strain measured from grain shape matched the total strain (Kronenberg and Tullis, 1984), could suggest that grain boundary mechanisms when compared to intracrystalline deformation processes in quartz, can be considered negligible. This finding

could provide an explanation for the boudinage of the quartz bands in mica schists (of the above described situation) since the flow in the quartzose material would be less effective than in the surrounding mica schist producing boudinage of the quartz. However, this suggestion could only be confirmed if the quartz bands preserve their 'original' texture (produced during the boudinage flow) and the influence of factors such as late recrystallization, decrease in differential stresses (Twiss 1977, ^{to be} in Simpson 1985) and grain growth inhibition can be demonstrated ineffective, something very unlikely considering the deformation history of these rocks.

However, the grain-size sensitivity and heterogeneous character of the deformation and metamorphism of these rocks, together with the rarity of equilibrium texture in most aggregates could indicate that intracrystalline deformation did take place and was probably an important deformation mechanism in quartz.

Still regarding comparative deformation of quartz and micas, Morris (1981) has suggested that rock composition is an important controlling factor, reporting predominance of pressure solution mechanisms in mica-bearing rocks synchronously with intracrystalline mechanisms in 'pure' quartzite lithologies where a 'C'-axis fabric is developed.

It seems that under considered conditions of temperature and stress one mechanism is dominant but an overlap of different processes in different minerals is a likely situation (White et al. 1976, Evans et al. 1980, Langdon 1985). This kind of situation gives rise to characteristic features in shear zones. Once fine grain bands are produced, the deformation will tend to concentrate along them. The shear zone will tend to narrow down leaving an inactive bordering zone which shows evidence for the previous deformation mechanism. The phenomenon was shown to take place in the deformation of quartz-rich clasts in conglomerates where a strong inverse relationship between finite strain ratio and grain size was demonstrated (Etheridge and Vernon 1981). The idea is that once superplasticity is achieved in the fine grain matrix, relatively larger quartz grains would progressively be deactivated, the more efficient grain-size reduction of the larger volume of feldspathic material enhanced

by reaction and chemical softening. This sort of mechanism was also proposed by Mitra (1978, p.1077) to explain the observation that quartz does not undergo as noticeable a grain size reduction and would suggest that the larger grain size of quartz is an 'original' feature (not due to later growth).

However, if strain compatibility is to be maintained and the deformation is at approximately constant volume, it would imply not only that both intra- and inter-crystalline deformation mechanisms were active, but also that there was considerable grain boundary sliding between quartz crystals specially at their contacts with the other minerals. This is well illustrated by Paterson's (1978) comments on compatibility of strain and combination of deformation mechanisms: '...in many cases other permanent deformation mechanisms will be required for complete ductility even when crystallographic slip is predominant...' (p.178).

(c) Micas

Although there are several possible slip directions in biotite and muscovite the layered structure of these minerals suggests that slip occurring on (001) is the most likely during deformation (Nicholas and Poirier 1976). Experimental deformation of these minerals shows that slip along the basal plane is subordinate, since the crystals deform mostly by bending and kinking, this being probably a function of stress orientation (see Nicholas and Poirier 1976, p.195 and references therein). According to Barber (1985), kink band development occurs when (i) geometrical considerations prohibits extensive slip, (ii) elastic bending moments exist, or (iii) only one slip system is available to relieve stress; this would explain the common occurrence of this feature in protomylonites or associated with the late deformational phases.

Etheridge and Hobbs (1974 in Bell 1979) considered that the slip geometry of mica is unfavourable for the formation of subgrains. However, the use of transmission electron microscopy has shown that in intensely deformed micas the subgrain formation is similar to that described for quartz (Bell 1979). In this way, although evidence for slip along the main cleavage was observed in some of the samples it was considered to represent an 'intermediate state' of the deformation, facilitating recrystallization which is thought

to be responsible for most of the grain size reduction of this mineral.

The localization of recrystallization along zones of intense deformation, with the newly-formed fine grains forming 'tails' marking the foliation planes or developed around crystalloclasts is extensively reported in the literature (Bell 1979, Lister and Snoke 1984). The observation that mica 'fish' are usually composed of muscovite because biotite, at this intensity of deformation, is already extremely fine-grained, is in agreement with the findings of Wilson and Bell (1979) and Kelley and Powell (1985). The former authors have shown evidences of the differential mechanical and chemical behaviour of these two micas. The round shapes of folds with fractures along the axial plane in muscovites that they describe are also observed in the Loch Maree mylonites, and are in contrast with the extreme grain size reduction of biotite. In addition, features indicating dissolution seem to be more evident in biotite crystals. Investigating the causes of such differing behaviour Bell and Wilson (1981) noted that biotite crystals show a greater variety of crystal defects, including higher dislocation density. They also found abundant unit dislocation and evidence for the action of 'segmentation', a grain-size reduction mechanism in biotite, features not seen in muscovite.

(d) Feldspars

This section will be concerned with the discussion of the mechanism of deformation in feldspars and its possible relationship with the local strain. The problems of brittle or ductile characteristics of the deformation and of their interpretation as indicators of the conditions of deformation will be discussed in the next section, where other sources of evidence will be brought together.

Feldspars are the most abundant minerals in crustal rocks but their deformation behaviour is still poorly understood. According to Carter *et al.* (1981) experiments are mainly restricted to the brittle field, and deformation at elevated temperatures and pressures, despite its importance, has received little attention. Several of the deformation features shown by feldspars are informally called 'brittle'. This designation, however, should be

restricted to the description of features with a fracture-like morphology at the grain-size scale and do not imply that the rock was deformed in a brittle fashion (or that fracturing was the only deformation mechanism of these minerals) since several other features (ascribed to 'ductile' deformation processes in the literature) were also observed.

Mitra (1978) suggests two mechanisms to account for the growing of cracks in feldspars; both depend on the percentages of matrix present. The first mechanism acts when the concentration of 'brittle' grains is high and the rock is behaving under ductile deformation conditions as a whole. The cracks initiate at contacts between grains where large concentrations of stress occur. Where there is a large percentage of matrix, plastic flow in the latter initiates fractures in the feldspar grains (Fig.5.6).

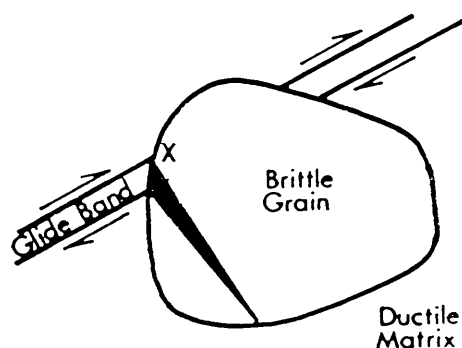


Figure 5.6. A brittle grain floating in a ductile matrix. Large amounts of glide take place in the matrix. At X such glide is stopped at the grain boundary of a brittle grain, and large stress concentration initiate a fracture in the brittle grain (reproduced from Mitra 1978, fig.5B).

In his model the orientation of the fractures depends on the orientation of the grains, i.e. on the orientation of the potential glide planes in relation to the stress system. The discontinuities develop along regions of intersection of slip or twin planes with other similar planes or grain boundaries in quartz, K-feldspar and plagioclase. They nucleate parallel and at approximately 45° to the cleavage planes in K-feldspar, and were also observed to form at high angles to the glide planes rather than at high angles to the direction of extension (Mitra 1978, p.1064).

White *et al.* (1980) present two explanations for the development of fractures in 'brittle' grains deforming in a ductile matrix. The first is the **fibre loading mechanism** whereby the tangential stress exerted by the flowing matrix on the particle surface is balanced by the tension in the initially non-deforming crystalloclast. The maximum stress is at the centre of the particle, causing a rupture perpendicular to the extension direction. Long particles are broken into halves until an equilibrium length (l) to width (w) ratio is achieved. This ratio is related to the flow stress (σ) in the ductile matrix and the fracture strength of the brittle matrix (σ_f) by the equation:

$$\frac{l}{w} = \frac{\sigma_f}{\sigma}$$

The second theory is based on the **dislocation pile up** whereby these are accumulated along the particle-matrix interface until the stress associated with the pile up causes a rupture by exceeding the fracture strength of the mineral, producing extensional fractures.

Although no systematic study of the cracks in feldspars and other 'brittle' minerals of the Loch Maree mylonites was undertaken, the observation of most of these discontinuities at several scales suggests that they have a geometry compatible with the local strain system. Their extensional nature is suggested by (i) their geometry of open cracks commonly containing biotite, muscovite and opaque mineral infills and (ii) their orientation at right angles to the banded ductile matrix and in relation to the position of pinch-and-swell structures in other minerals (Pl.5-13). These observations are in agreement with experimental results indicating the low strength of most materials under (secondary) tensile stress (Paterson 1978) and with the findings of Etheridge (1983) and Andrews (1984) from naturally deformed rocks, where fracture orientation is demonstrated to be related to the rock fabric. According to Etheridge (1983) tensile fractures are common in variable metamorphic conditions, specially greenschist facies. Their orientation to both finite and incremental strain markers indicates the tensile nature of several of these fractures since most of them are oriented at high angles to the foliation and stretching lineation; this is a familiar situation in the Loch Maree

mylonites.

This and the present interpretation are supported by the work of Tapponier and Brace (1976 *in* Carter *et al.* 1981, p63) who observed that '...nearly all stress-induced cracks are extensile in nature' due to the fact that '...brittle materials are very strong in shear and comparatively weak in tension or extension...' Although departures from the predicted orientation can be attributed to the influence of existing anisotropies as proposed by Mitra (1978) who finds support in the experimental work of Friedman and Bur (1974 *in* Carter *et al.* 1981), this is difficult to confirm due to the difficulties in isolating the different variables involved. In addition, the above referred experimental work was performed under conditions of $\sigma_2 = \sigma_3$ which does not tend to be the most typical in nature (Etheridge 1983).

Wakefield (1976) has proposed that the round or ribbon shape of crystalloclasts are inherited features (equidimensional and prismatic phenocrysts) but the observation that the relative abundance of round crystalloclasts increases with the progression of the mylonitization and that several ribbon-like crystals split along narrow bands at high angle to their elongation and close to their centres suggests that progressive grain size reduction of the 'clasts' follows ^{the} the principles of fibre loading mechanism discussed by White *et al.* (1980) and briefly outlined above.

Other kinds of fractures, presenting a geometry compatible with **Riedel shears** were also observed. While some of them seem to transect the grains and could be interpreted as extensional crenulation cleavages, others appear to be restricted to the crystal boundaries ('book-shelf' fractures). The latter feature is commonly utilized in the literature as an indicator of contemporaneity between the fracture and the mylonite foliation, representing displacement accommodation along the boundaries of the fine grains.

Features similar to those described by White and Mawer (1986), Hammer (1982), Jensen and Starkey (1985) and Gandais and Willaime (1984), and interpreted as indicators of the ductile behaviour of feldspars, were also observed in the L.Maree mylonites. As already

described in section 5.2, these features include straight and bent mechanical twinning (albite-pericline), strong undulose extinction and kink bands in low deformation conditions, to subgrains and recrystallized aggregates along preferential zones across elongate grains, forming 'tails' or crystalloclasts giving rise to core and mantle structures at higher strain. Recrystallization seems to occur from rims to centres of grains, following preferential zones of stress concentration of 'discontinuities', being perhaps accelerated as a function of 'strain enhanced diffusion' (Allison *et al.* 1979, White 1975). The round albite crystals described in ultramylonites derived from quartzofeldspathic gneisses are interpreted as the end result of the deformational and metamorphic processes active in the mylonite zones. They show in general strong undulose extinction and twinning and are surrounded by a large number of extremely small crystals forming high strain rims that make up most of the matrix in which the large crystalloclasts are immersed (Sect. 5.2). According to Burg and Laurent (1978), the nucleation of these small grains, which appears to be the predominant grain size reduction process under high strain conditions, indicates ductile deformation.

As in several of the above referred studies, features indicating brittle and ductile behaviour have been identified in the Loch Maree mylonites. 'Brittle' deformation seems to be predominant at relatively low strain while 'ductile' features are more common at high strain, suggesting that once the grains attain a critical size and shape they probably 'stabilize' or suffer very little grain size reduction; the deformation is then believed to be accommodated by grain boundary mechanisms mainly in the fine grain matrix. Superplastic behaviour is a likely situation at this stage of deformation.

(e) Amphibole, epidote and garnet

The deformation of these minerals will be discussed altogether. This is because of both the difficulties in the distinction of their relative competence as well as the general lack of data about deformation of these minerals. They have all been deformed by a combination of fracturing and ductile mechanisms, but boudinage, pinch-and-swell and other 'ductile' structures were more frequently seen in amphiboles and epidotes than in garnets. It was noted,

however, that the fracturing was a more effective process of grain-size reduction since, except for the very large garnet porphyroclasts, crystalloclasts of amphibole are in general larger than garnet crystalloclasts.

Dalziel and Bailey (1968) described the flattening of **garnets** in mylonites of the Grenville front. Some, with orthorhombic symmetry, show extension cracks normal to their longest axis which is parallel to the regional stretching lineation. Describing bend axes in garnets, they attribute the failure defining a glide direction and the orientation of the axes to tectonic rather than crystallographic control. Scanning electron microscope observations of 'old' garnets in the Loch Maree mylonites reveals that extensive fracturing is present at all scales. The geometry and concentration of these fractures as well as their irregular distribution along the tails of the deformed phenoclasts suggests that 'flattening' is the principal mechanism responsible for garnet deformation.

Despite the observation that elongated garnet invariably showed extension fractures, studies of stress distribution around rigid inclusions (Stromgard 1973) have demonstrated that circular inclusions may also develop tension fractures if $P_x/P_y < 1/3$, P_x and P_y being stresses parallel and perpendicular to the layers, respectively. An additional evidence for the tectonic origin of these fracture patterns is the presence of small idioblastic fracture-free garnets which overgrow the mylonitic foliation sometimes from an older garnet core with inclusion trails (Pls. 5-65B, 5-65C). Describing strikingly similar sets of garnets from the Arunta Block (central Australia) Obee and White (1985) attributed the grain size reduction of their older garnets to 'brittle failure' (p.708). Based on this and other microscopic scale evidence they proposed a model of successively shallowing of crustal deformation with the faults displaying a change from ductile to brittle deformation (but see discussion in Sect. 5.3.2.4).

Prior (1987) also described similar deformation structures in garnets from pelitic mylonites of the Alpine fault zone (New Zealand). However, in the present study, no evidence could be found to support the origin attributed to his two morphological types of fractures (i.e. 'corrosion cracking' and 'cataclysmic failure').

Like the deformation in feldspars, the grain size reduction of **amphiboles** took place by fracturing and recrystallization along high strain zones. Experimental data suggest this mineral is one of the strongest silicates (Nicholas and Poirier 1976, p.193). This is supported by geological observations that amphibolites are generally more competent than coarse-grained granite (Ramsay 1982, p.119, but see Chap. 6). Their ductile deformation produces boudinage and long 'tails' of fine-grained material whose asymmetry indicates the sense of shear in the matrix (Sect.5.3.2.1). When observed under the microscope this mineral has elongate shapes and well-rounded rims (Pl.5-65A) but S.E.M. images show steps parallel to cleavage (Pl.5-65B) along which grain size reduction takes place. Apart from fractures at high angles to the foliation no features like the ones described by Allison and LaTour (1977) or the variation of deformation features from mylonites to ultramylonites, as reported by Obee and White (1985) were observed in the L. Maree rocks.

The variable geometry of features shown by **epidote** seems to be controlled by viscosity contrast. So, where surrounded by feldspars and quartz, this mineral shows pinch-and-swell structure (Pl.5-13), but where surrounded by micas, it is almost idioblastic (Pl.5-37). In high strain rocks like the ultramylonites epidote crystals show round shapes and a marked grain size difference in relation to the matrix. In comparison with feldspars and amphiboles very few crystalloclasts of epidote with fine grain 'tails' were observed, usually having a more restricted range of grain sizes than the former two minerals. The paucity of data about deformation mechanisms which affect this mineral is probably a function of its occurrence as an accessory mineral in most rocks.

5.3.2.4 Brittle vs. Ductile Deformation

The determination of the brittle or ductile nature of deformation of the Loch Maree rocks during the late D1 mylonitization event represents the interpretation of an important segment of the deformational history of these rocks. It pertains directly to the understanding of the interaction between basement and cover, and

consequently places some constraints on the models invoked to explain the interplay between deformation and metamorphism. Several features interpreted in the literature as rheological behaviour indicators, as well as some basic concepts of rock mechanics which are relevant for the present discussion, will be considered.

The brittle-ductile transition is recognized in experiments by an abrupt drop in the applied stress required to induce a given amount of strain, caused by the development of a mesoscopic fracture. The term ductility is used to describe the capacity for substantial change of shape **without** visible fracturing. This does not take into account deformation mechanisms which may involve the establishment of **microscopic** fractures (cataclastic flow), which is also accompanied by a 'stress drop' (Paterson 1978, p.161). Since it is not possible to observe the stress drop in naturally deformed rocks, the recognition of microscopic rheological behaviour indicators by the geologist has been considered as useful in determining behaviour of deformed rocks during the time of their formation (Mitra 1984). Mitra (1984), however, also pointed out that the different physical properties of each mineral means that they may show diverse behaviour under similar physical conditions. From the observations of the behaviour of certain minerals (quartz and feldspars in particular) in experiments and in deformation zones of (presumably) known metamorphic conditions, several authors (Simpson 1985, Hammer 1982, Mitra 1978, 1982 and Sibson 1977) describe features which could be used as indicators of the physical conditions during mylonitization elsewhere. Although these could be valid in most cases, several other variables that are less easily defined seem to be of fundamental importance in the determination of the rheological behaviour of these minerals. These include (1) temperature, (2) lithostatic pressure, (3) fluid pressure, (4) strain rate, (5) total strain and its nature (compression or extension), (6) variable proportion of the different minerals, (7) grain size, and (8) change in the deformation mechanism (see Sect. 6.2.2.5 for a broad discussion).

Additional factors such as (9) the timing of temperature in relation to deformation and its control of the microscopic deformation mechanism (cf. Pfiffner 1982), and activation of the slip systems of the different mineral phases, (10) high pressure and temperature

'embrittlement' and (11) the pressure sensitivity resistance to flow (Paterson 1978) amongst others, seem to have been largely forgotten. Experimental studies, although fundamental for the understanding of the deformation processes, have limitations, such as the reproduction of natural strain rates. Higher temperatures are usually utilized to compensate for the effects of higher strain rates, but as pointed out by Gandais and Willaime (1984), this procedure may cause activation of different mechanisms of plastic deformation. Therefore correspondence between experimental and natural deformation is only possible when the **same** mechanism can be demonstrated to be involved.

The evidence from the presently studied mylonites seems to indicate the alternation of 'brittle' and 'ductile' behaviour of rock and minerals along the Loch Maree thrust zone. Each feature will be discussed taking into account, wherever possible, these factors.

Fractures

The concepts of **fracturing** and **plasticity** are of importance for the present discussion and will be briefly reviewed here. According to Gandais and Willaime (1984) **fracturing** in its metallurgical meaning describes any mechanism involving loss of cohesion of the crystal even when uniform flow is produced by the rolling of crushed grains produced by repeated fractures. In most silicates the initiation of cracks requires higher shear stresses, but since there are pre-existing cracks in brittle crystals the fracture strength is usually exceeded with lower stresses, due to the extension and glide (where favourably oriented in relation to the stresses). The fracture strength is highly pressure dependent and nearly temperature independent. **Plasticity** includes several mechanisms which lead to permanent strain without involving extensive inter-atomic decohesion. They are generally dependent on temperature and much less so on pressure (Gandais and Willaime 1984, p.209).

Mitra (1984, p.53) has proposed the unstable character of fractures (propagating spontaneously across grains and grain boundaries) against the stable fracturing (fractures dying out within individual

grains) to differentiate between dominantly brittle and ductile deformation respectively, the stable being typical of lower greenschist facies. Simpson (1985, p.508) describes a change from cataclastic to low temperature plasticity (kink bands) deformation in plagioclases of lower greenschist to upper greenschist facies, respectively. These are good examples of how the presence and geometry of fractures were used as indicators of the rheological conditions of deforming rocks and minerals. In addition to transitional character of the brittle-ductile 'boundary', it should be borne in mind that factors such as the pre-fracture plastic strain (a term used in experimental work to indicate features attributed to ductile behaviour which appear before the macroscopic fracture stress is reached), are bound to produce dubious features. As already pointed out by Schmid (1982, p.97) the presence of an intergranular network of micro-cracks can occur in a deforming rock without the typical stress drop diagnostic of brittle behaviour. When this happens, the bulk behaviour of the rock is still ductile, since it is taking up considerable amounts of permanent deformation which is accommodated by the dispersed system of cracks ('cataclastic flow'). In this way, the individual minerals are suffering cataclasis, a mode of deformation where a fracture is formed causing a loss of cohesion at the considered scale, but the whole rock cannot be considered to show a brittle behaviour. Schmid (1982, p.97) calls attention to the fact that the brittle-ductile transition does not necessarily coincide with the transition from cataclastic to non-cataclastic processes, something already observed by Orován (1960 in Sibson 1977). Any proposed microstructural criteria should also take into account the possibility of the presence of features formed before the considered deformation took place. They include optically visible micro-cracks with lengths roughly equal to the grain sizes commonly present in granites and quartzites (see Paterson 1978, p.150-153, Gandais and Willaime 1984, p.209), and should be of considerable importance in thrusting involving basement. Concluding the discussion about these features Paterson (1978, p.153) stated that most microcracks in several rock types are not of late brittle origin but have largely persisted from the early history of the rock.

As discussed above, features produced by deformation of feldspars

(in particular), seem to have received a lot of attention because of their possible potential as rheological indicators (Mitra op.cit., Simpson op.cit.). Examining the 'brittle-ductile' transition in feldspars Gandais and Willaime (1984) proposed that feldspars deformed in nature ($P = 200-1000 \text{ MPa}$, $\dot{\epsilon} = 10^{-10}$ to 10^{-14} s^{-1}) behave plastically above $T = 500^\circ\text{C}$. According to these authors the mechanical behaviour of feldspars seems to be controlled by the properties of the alumino-silicate framework, and thus feldspars of all compositions behave in a similar way. Realising that the lack of knowledge about processes that are essential for the determination of the kind of behaviour of these minerals under deformation, Gandais and Willaime (1984) state that with the present state of knowledge it would be **unwise** to use their deformation microstructure as a geological indicator (thermometry, barometry). This is due to the complexity of the materials, involving a large number of factors which are difficult to resolve and quantify, and that can interact and may vary with time.

Concluding remarks

From the above discussion it seems clear that no single criterion, such as the fracture pattern of minerals as proposed by Mitra (1984), can be used in isolation as indicators of deformation behaviour. This will be further illustrated, by the occurrence of features which were interpreted in terms of a transient brittle behaviour along these thrusts, indicating that the complexities involved with the development of these rocks at all scales defies the application of simplistic criteria.

Breccia and pseudotachylite

The presence of 'mylonitized breccias' (mixed mylonites) and localized fine veins possibly representing deformed pseudotachylites can also provide an insight into the deformation behaviour along the thrust zone. The conditions of formation of these rock types, usually indicators of brittle behaviour, was discussed by Sibson (1977, 1980), Passchier (1982, 1984) and microscopic scale features described in detail by Maddock (1983). These conditions include high strain rates (in discrete bands), typical of seismic faulting (Sibson 1977, 1980). Although difficult to observe with the use of

a conventional optical microscope the features presented by this rock are quite similar to the pseudotachylites described by Sibson (1980, pp.168-169), particularly in their occurrence in the proximity of strongly mylonitized basic bodies (see Chap. 2). This association, however, can be explained by the experiments of Spray (1987) who produced pseudotachylites in metadolerites. The preferential assimilation of amphibole into the pseudotachylite was explained in terms of the catalytic effects of the water contained in this mineral, causing a lowering of temperature and viscosity.

As in the pseudotachylites, the mylonitized breccias occur along the main thrust zone which could suggest some sort of genetic association between these two rock types. The observation that both of these rocks were transformed into mylonites suggests that they were formed at an early stage of the D1 event. Although pseudotachylites have been reported elsewhere as recurrent features (Stel 1981), the **absence** of mylonitized clasts in the breccia (it is a mylonitized breccia not a brecciated mylonite) seem to confirm the minimum relative age for these rocks as **early D1**. This rules out any possibility of later brittle reactivation of these zones, something which was not observed. Although being similar to the 'crush melange' described by Sibson (1977, p.195) in the Outer Hebrides thrust zone, by Platt *et al.* (1984) in the Betic Cordilleras, and by Schmid (1975) in the Helvetic Alps, these rocks were initially interpreted as the basal 'sedimentary breccia' marking the basement-cover unconformity due to the following characteristics:

- (i) spatial association with the calc-mylonites, considered to the first Laxfordian (sedimentary) unit covering the basement,
- (ii) unusual composition showing mostly fragments of 'local rocks' but some clasts are of amphibole schist and amphibolites not found amongst the mapped units,
- (iii) ductile deformation of the matrix (mylonitized breccia), and
- (iv) apparent incompatibility of deformation conditions (P,T,X,etc) for a D1 mylonite.

These features, together with the lack of petrographic studies and of the failure to understand the important role played by the fluids at that time, were the principal factors which led to the

interpretation of an original sedimentary origin for these rocks. Although this interpretation cannot be completely dismissed on the grounds of available evidence, the indications for presence of abundant fluids, the associated rock types and other sources of evidence (e.g. metamorphic history) suggests that they could be better interpreted as a tectonic feature. They could have been produced by the action of high fluid pressures, which caused local fluctuations of the 'brittle - ductile' boundary during D1 mylonitization. These neutralized the effects of increasing confining pressure at depth, decreasing intergranular frictional resistance and promoted transient brittle behaviour (cf. Sibson 1977, p.205). These rocks could alternatively be interpreted as a tectonic breccia produced by brittle behaviour at higher structural levels along the fault zone, being gradually taken to lower structural levels with the progression of the thrusting, when they would be deformed under ductile conditions, or as a combination of both processes. Despite the available evidence for decreasing P-T conditions during mylonitization (Chap. 7), an interpretation based on crustal level control for the production of these 'cataclastic' rocks, is very simplistic. It would also require quite large displacements along the fault zone to account for the estimated depth of brittle failure at 10-15km (Sibson 1977), and would not be compatible with the necessary variation of metamorphic conditions given the chosen assumptions (see Chaps. 7 and 8). In this way the fluid-controlled interpretation to explain the formation of these cataclastic features seems to be the most likely one. This interpretation, in addition to explaining the evidence (see 'mechanical effects of fluids' - Sect.7.3), could also provide an explanation for the decrease in the high differential stresses necessary for the shear failure in a thrust regime, thought to be ~4 times higher than for normal faults (cf. Sibson 1977, p.210, Murrell 1977, p.179 and Paterson 1978). The difficulties of promoting pseudotachylite formation under 'wet' conditions can be explained in terms of its formation at the time the thrust zone first developed affecting the rather impermeable rocks. Alternatively, they could have been controlled by factors such as the stress concentration around inhomogeneities and the presence of hydrous mineral phases (in the amphibolite bodies- see Sect 5.2 and Spray *op. cit.*) which would promote localized faulting (Sibson 1975, 1980). As pointed

out by Sibson (1975) '...it is to be hoped that advanced textural studies, both by optical means and transmission electron microscope, will eventually enable the recognition of those cataclastic rock-types which are necessarily the product of seismic faulting in other than dry conditions...' (p.792).

Concluding remarks

It seems evident that no single criterion for the determination of the brittle or ductile nature of the rock deformation is reliable if taken in isolation. This probably reflects the large number, and complex interplay of the ductility-controlling variables demanding not only control of the variation and distribution of P,T,X conditions but also constraints on deformation rate, differential stress, as well as several other factors (see Chaps. 6 & 7).

5.4 SUMMARY - MYLONITIC FEATURES IN THE LOCH MAREE ROCKS

The following are important points concerning the evolution of the mylonites at Loch Maree.

1. Mylonite formation developed under conditions of simple shear, with a NW-SE direction of tectonic translation, during which a slab of basement rock probably coming from the southeast was tectonically emplaced on to the cover rocks. The observed kinematic indicators include asymmetrical pressure shadows, microfolds and augen structures, displaced grains, oblique foliations and cleavages.
2. The principal zone of movement (along the marbles and calc-silicate rocks which mark the contact between the basement gneisses and the amphibole schists), is indicated by its almost total mylonitic nature and tectono-stratigraphic position.
3. The principal strain softening mechanisms active during deformation include change in deformation mechanism, geometrical softening, continual recrystallization, reaction and chemical softening, and pore fluid effects. Temporary retrogressive

metamorphic conditions promoted the development of fine-grained ultramylonites which have probably concentrated further deformation.

4. The empirically determined order of minerals showing increasing resistance to grain size reduction processes is : calcite-biotite-muscovite-feldspar-garnet-amphibole-epidote. Cataclastic deformation of the 'strong' minerals was coeval with deformation of the 'softer' grains by plastic deformation processes.

5. Mylonitized breccias and pseudotachylites observed along the main mylonitic horizons were produced by the build up of the fluid pressure, during which localized and transient deformation was promoted along marked discontinuities such as lithological contacts.

6. The assessment of the observed features in isolation, without careful investigation of the overall deformation history and associated metamorphic conditions, might lead to simplistic interpretations of the complex history of these rocks, with important consequences for the understanding of the tectonic evolution and processes active in this segment of the crust during the early Proterozoic.

- Plate 5-1 Quartzofeldspathic augen gneiss, feldspar showing porphyroclasts wrapped around by thin quartz bands; lens cap 5cm; subhorizontal surface [NG 965 715].
- Plate 5-2 Ovoidal feldspars in mylonitized quartzofeldspathic gneiss affected by F2 fold; note the absence of idioblastic feldspar megacrysts; outcrop faces NW [NG 972 716].
- Plate 5-3 Sheath fold affected by F2 parasitic fold in mylonitized quartzofeldspathic gneiss; note the large lithoclasts of the protolith ('lith') and the dark bands representing mylonitized mafic layers; coin ~2cm; subhorizontal surface [NG 972 716].
- Plate 5-4 Lithoclast ('lith') of the feldspar-bearing rock in mylonitized siliceous mica schist; note the sedimentary-or volcanoclastic-looking features of the rock; coin 2cm; outcrop faces SW [NG 971 696].
- Plate 5-4A Mylonitized siliceous mica schist showing 'graded bedding'-looking features produced by variable intensity of grain-size reduction; coin 2cm; outcrop faces SW [NG 976 691].
- Plate 5-5 'Mixed mylonite' with lithoclasts of amphibolite (amph) and large garnet crystalloclasts in fine micaceous and chlorite-rich matrix; scale 2cm; photograph of specimen [NG 954 732].
- Plate 5-6 Lineated (L1) quartz band with lithoclasts of the protolith (white dots - see Pl.5-58) folded by flattened sheath fold (half of it) in mylonitic siliceous mica schist; photograph of hand specimen; size 20cm [NG 956 708].
- Plate 5-7 Carbonate-bearing mylonite showing lithoclasts of banded amphibolite (top centre), amphibole schist (bottom centre) and quartzofeldspathic gneisses (white dots); pen parallel to composite foliation (mainly S1); subhorizontal surface [NG 951 727].
- Plate 5-8 Lithoclasts of gneiss (gn), amphibole schist and banded amphibolite (with black bands) showing no grain-size selection or disposition in carbonate-bearing mylonite; scale bar ~ 20cm [NG 951 726].

- Plate 5-9 Feldspar aggregate in quartzofeldspathic gneiss showing the initial stages of mylonitization with development of mechanical twinning and fractures in feldspars which showed (M1) granoblastic polygonal texture; XN, X10 [NG 960 715].
- Plate 5-10 Variation of intercrystalline contacts in quartzofeldspathic gneiss lithoclast (A) from well-preserved crystal boundaries in the interior of the lithoclast (B) to grain-boundary destruction along the rim (C); sketch from thin section; scale bar (for A) ~ 1.5mm [NG 972 716].
- Plate 5-11 Grain size comminution of large muscovite porphyroblast in quartzofeldspathic gneiss; note the orientation of S1 mylonitic foliation parallel to the former orientation of the cleavage in mica; XN, X10 [NG 972 716].
- Plate 5-12 Deformation bands of quartz crystals wrapping around elongate feldspar (Kf) phenocrysts in mylonitized quartzofeldspathic gneiss; note the orientation of the two sets of extension crenulation cleavages (ecc); section at low angle to lineation; XN, X10 [NG 966 721].
- Plate 5-13 Boudinaged allanite (outlined) and feldspar crystalloclasts wrapped around by elongate quartz deformation bands in quartzofeldspathic gneiss; note the orientation of the extensional fractures (E.F.) where biotite has crystallized; section at low angle to L1 lineation; XN, X10 [NG 966 721].
- Plate 5-14 Large K-feldspar crystalloclast surrounded by much finer-grained quartzofeldspathic aggregate in gneiss ('core and mantle structure'); note the early stages of development of mechanical twinning in the feldspar; section at high angle to L1 lineation; XN, X10 [NG 964 717].

Plate 5-15 Initial stages of intracrystalline deformation (fracturing) of K-feldspar (arrow) of a lithoclast of quartzofeldspathic gneiss with granoblastic polygonal texture; note the irregular nature of the grain boundaries and the fine grain size of the matrix; section at high angle to L1 lineation; XN, X10 [NG 973 704].

Plate 5-16 Generalized grain size reduction along crystal boundaries of quartzofeldspathic aggregate in gneiss lithoclast; note the intracrystalline fracture development and the associated twinning pattern (arrow); section at high angle to L1 lineation; XN, X10 [NG 973 704].

- Plate 5-17 Initial development of thin intracrystalline fracture (light 'lines' in large crystal) in well-round feldspar crystalloclast in a quartzofeldspathic ultramylonite; note the $\sim 70^\circ$ angle between both sets of fractures and the absence of orientation of the fine (external) matrix; section at high angle to L1 lineation; XN, X25 [NG 972 716].
- Plate 5-18 Wedge-shaped intracrystalline fracture in K-feldspar along which fine grain~~ed~~matrix is produced; note the well-developed twinning along the most deformed part of the crystalloclast; XN, X25 [NG 973 704].
- Plate 5-19,20 Deformation features of elongate feldspar crystalloclasts with formation of deformation bands delineated by fine perthites (dark bands in Pl. 5-19), with recrystallization along displacement zones (with no loss of cohesion) and 'necking' (Pl.5-20); the oblique foliation (S), if interpreted as a S-surface, would indicate a dextral sense of shear along the matrix in agreement with the 'book-shelf' fracture in the feldspar; sketch from thin sections of quartzofeldspathic mylonites at low angles to lineation; scale bar $\sim 0.3\text{mm}$ [NG 978 717].
- Plate 5-21 Grain size reduction along fracture in elongate crystalloclast of quartzofeldspathic ultramylonite; note the round shapes of the remaining crystalloclasts along the rims of which fine-grained matrix is produced; section at high angle to lineation; XN, X25 [NG 971 716].
- Plate 5-22 Fracture dividing feldspar crystalloclast into two halves (with slight rotation and variable extinction angles) in quartzofeldspathic mylonite; note the displacement of smaller parts of the crystalloclasts along oblique (NE) probably younger fractures that also affect the matrix; section at low angle to L1; XN, X10 [NG 971 716].

- Plate 5-23 'Book-shelf' displacement along oblique extensional fractures affecting two feldspar crystalloclasts in quartzofeldspathic mylonite; note the slightly variable angle of fractures and its absence on the matrix; section at low angle to lineation; XN, X10 [NG 971716].
- Plate 5-24 'Tuffaceous' aspect and sheath fold in quartzofeldspathic mylonite; section at high angle to L1 lineation (see also Pl. 5-325, Pl. 5-28); negative print of thin section; arrow 1.5 cm [NG 973 704].
- Plate 5-25 Detail of part of Plate 5-24 showing the structureless aspect of the matrix and irregularities of the 'crystalloclast rims; XN, X10 [NG 973 704].

Plate 5-26 Quartzofeldspathic ultramylonite stage showing the extremely fine structureless matrix observed in section cut at high angle to the linear fabric; note the very round feldspar crystalloclasts; XN, X10 [NG 971 716].

Plate 5-27 Detail of the quartzofeldspathic ultramylonites showing a foliation (S1), development of anomalous twinning in (large) feldspar crystalloclasts with irregular rims (bottom left); note the epidote crystalloclasts in the mica-rich band of section (top right); XN, X10 [NG 973 704].

Plate 5-28 Mylonitized contact between felsic (quartz and feldspar) and mafic biotite-rich bands (SW and NE of the marks, respectively) in mylonitic gneiss; note the abundant crystalloclasts in the felsic (SW) band as opposed to the mafic one (NE) where all the biotite was ^{ground down}; section at high angle to linear fabric (cf. Pl. 5-31); X10 [NG 972 716].

Plate 5-29 Aspect of mylonitized interbanded gneiss (felsic band at the bottom of photograph); note the oblique attitude of the mylonitic foliation (S1) in relation to the banding (almost E-W) whose contacts are already folded (black layers are quartz bands); negative print of thin section; X2 [NG 972 716]

Plate 5-30 Relationship between siliceous layers and S1 and S2 foliations in mafic ultramylonite; note the deformation bands parallel to S2 which could be interpreted as an 'oblique foliation'; section at low angle to linear fabric; XN, X10 [NG 971 716].

Plate 5-31 Quartzofeldspathic (NW) and micaceous (SE) bands at the ultramylonite stage; note the banded aspect of the rock in sections at low angle to linear fabric (cf. Pl. 5-28); XN, X10 [NG 971 716].

Plate 5-32 Quartzofeldspathic and mafic bands cross-cut by S1 mylonitic fabric along (F1) fold hinge; note the very round feldspar (white) and the elongate epidote crystalloclasts (grey); section at high angle to linear fabric; XN, X10 [NG 972 716].

Plate 5-33 Ultramylonite in felsic (grey) and mafic (black) bands of gneiss; note the extremely small grain-size of mafic bands and the very round shape of feldspar crystalloclasts wrapped by quartz bands some of which show quite transposed folds (bottom right); section at low angle to linear fabric; XN, X10 [NG 972 716].

- Plate 5-34 Convolute folds in mylonitized gneiss; black thin layers are mylonitic quartz bands; negative print of thin section; X2 [NG 972 716].
- Plate 5-35 Mylonitic (S1) foliation oblique to compositional bands (Sb) in quartzofeldspathic gneiss; PPL; X10 [NG 971 716].
- Plate 5-36 Progressive grain size reduction in mafic band of quartzofeldspathic gneiss; note the granoblastic texture with large biotite flakes (bottom) passing rapidly to a mylonite with sub-microscopic matrix and very round epidote (grey) and feldspar (white) crystalloclasts (top); XN, X25 [NG 978 717].
- Plate 5-37 Mylonite developed in finely interbanded gneiss; note the sub-idioblastic shape of epidote crystalloclast (bottom left) causing indentation of the banding and the contrasting grain size between mafic (black) and felsic bands; XN, X10 [NG 978 717].
- Plate 5-38 Fracture with carbonate infill cutting across calcite crystal showing conjugate kinks of twinning (bottom of grain); XN, X10 [NG 971 716].
- Plate 5-39 Thinning of quartz band against competent epidote crystalloclast in mylonitized mafic band of gneiss; section at low angle to linear fabric; XN, X10 [NG 971 716].

- Plate 5-40 Internal deformation (along grain boundaries) of well-rounded gneiss lithoclast in mafic ultramylonite; note the submicroscopic size of the matrix; XN, X10 [NG 971 716].
- Plate 5-41 Disruption of amphibole lithoclast along intergranular contacts where quartz with deformation bands (inset) has segregated; sketch from thin section; scale bar ~ 0.5mm [NG 960 724].
- Plate 5-42 Sharp transition between ultramylonite and amphibolite protolith with remnants of granoblastic texture (bottom right); note matrix grain size; XN, X10 [NG 960 724].
- Plate 5-43 Schematic representation of anastomosing pattern of mylonitic banding (black).
- Plate 5-44 Fracture affecting large amphibole crystalloclast (white) in basic mylonite; section at high angle to lineation; PPL, X10 [NG 960 724].
- Plate 5-45 Discordant mass of pseudotachylite (black) in basic mylonite; PPL, X10 [NG 960 724].
- Plate 5-46 Angular and broken feldspar crystalloclasts in submicroscopic opaque-rich matrix of (suspected) mylonitized pseudotachylite; PPL, X10 [NG 960 724].
- Plate 5-47 Mylonitic amphibole schist representing intermediate stages of grain-size reduction; PPL, X10 [NG 964 707]

Plates 5-48, 48A, 48B

Deformation patterns in 'mixed' mylonite showing garnet porphyroclast with narrow fractures in the internal zones (Pl. 5-48A) and progressive separation and grain size reduction along the 'tails' (Pl. 5-48B); note the regular fracture pattern (conjugate shear couple?) of sub-idioblastic garnet (top left of Pl. 5-48); negative print of thin section (5-48) and S.E.M. images (48A, 48B); scale \sim X4, 40 μ , 40 μ respectively [NG 954 732].

Plate 5-49 Carbonate (white) reaction product of fluid interaction with garnet crystalloclast in 'mixed' mylonite; detail of Pl. 5-55; XN, X25 [NG 967 721].

Plate 5-50 Asymmetrical folds in quartz bands and 'book-shelf' fractures in garnet ('f') and hornblende crystalloclasts (hb) in 'mixed' mylonites (cf. Plate 5-48); note that both types of kinematic markers indicate a left-lateral (on this plane) sense of shear; PPL, X10 [NG 954 732].

Plate 5-51 Boudinage of hornblende (Hb) and 'book-shelf' fracture in garnet ('f') of mixed mylonite; note the asymmetrical tails of small amphibole crystalloclasts indicating the same (left-lateral) sense of shear; PPL, X10 [NG 954 732].

Plate 5-52 Disharmonic fold with 'detachment' zone in quartz band along the margins of the large garnet porphyroclast; note the idioblastic garnet crystal overgrowing the mylonitic banding; PPL, X10 [NG 954 732].

- Plate 5-53 Asymmetrical fold affecting mylonitic banding in 'mixed' mylonite indicating left lateral sense of shear; PPL, X10 [NG 954 732].
- Plate 5-54, 54A Large garnet crystalloclast preserving biotite-amphibole rock with granoblastic texture (Pl.5-54A) from effects of mylonitization; negative print of thin section (5-54), X3; XN, X25 (5-54A); [NG 967 721].
- Plate 5-55 Garnet crystalloclast with asymmetrical carbonate pressure shadow indicating right-lateral sense of shear in 'mixed' mylonite; XN, X10 [NG 971 720].
- Plate 5-56 Ultramylonite from amphibolite; note the submicroscopic grain size of matrix and round amphibole crystalloclasts (Amph); PPL, X25 [NG 967 721].
- Plate 5-57 Structureless aspect of mylonitic quartz-mica schist in a section at high angle to the linear fabric; XN, X10 [NG 971 696].
- Plate 5-58 Large feldspar (Kf) porphyroclast with quartz and plagioclase inclusions surrounded by fine-grained quartzose mylonitic banding in siliceous mica schist; note the effects of the F2 small fold on to the quartz deformation bands; XN, X25 [NG 971 696].

Plate 5-59, 59A Asymmetrical 'augen structures' indicating right-lateral sense of movement in carbonate (ca)-bearing quartz mylonite (cf. Fig.5.2) ; PPL, X25 [NG 967 722].

Plate 5-60 Largely preserved garnet porphyroclast with inclusion trails surrounded by mylonitized mica-rich matrix of muscovite schist; XN, X10 [NG 970 696].

Plate 5-61 Idioblastic garnet (gt) surrounded by fine-grained mica-bearing matrix (black seams) in mylonitized muscovite schist; XN, X10 [NG 960 707].

Plate 5-62 Well-developed banding with pinch-and-swell structures in quartz-rich bands of mylonite 'squeezed' against feldspar and garnet crystalloclasts; note the contrasting deformation styles of feldspars, biotite (dark bands) and garnets; XN, X10 [NG 962 711].

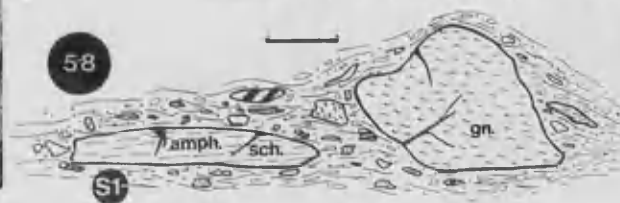
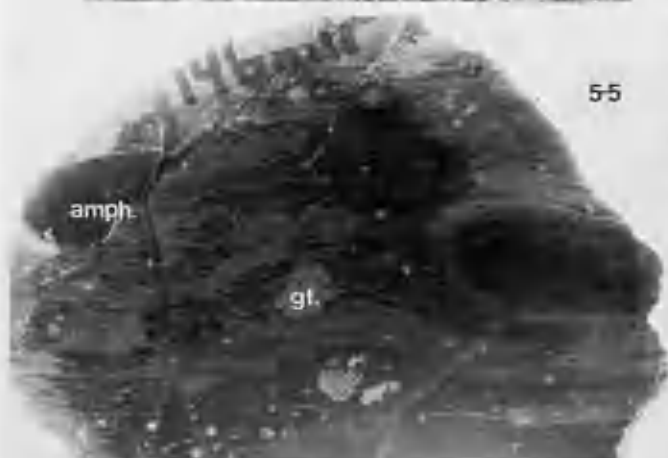
Plate 5-63 Indentation of quartz band (qz) against more competent feldspar crystalloclasts (grey colour due to incipient alteration) in quartzofeldspathic mylonite; PPL, X10 [NG 970 696].

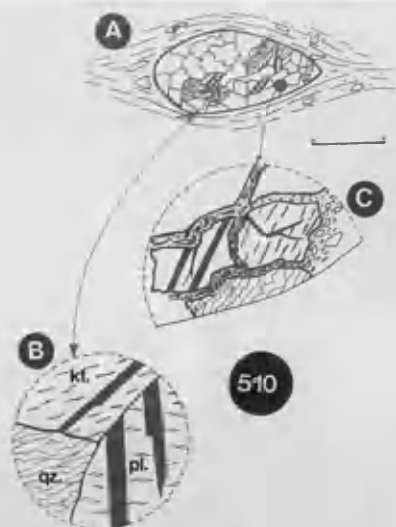
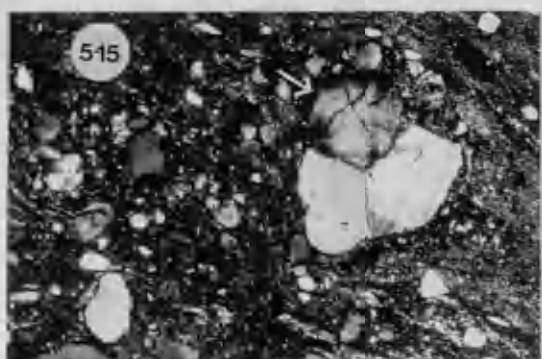
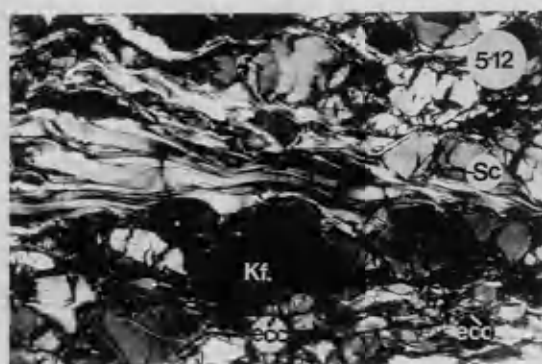
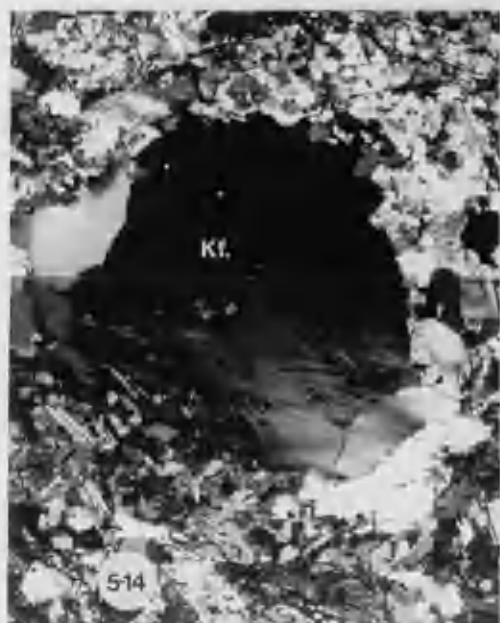
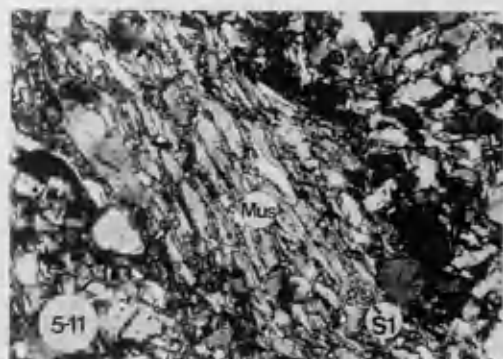
Plate 5-64 Mylonitic features along S1 foliation oblique to the banding; note the extreme deformation of the quartz-rich bands and amphibole crystalloclasts, the latter showing long 'tails' of fine-grained material; PPL, X10 [NG 971 696].

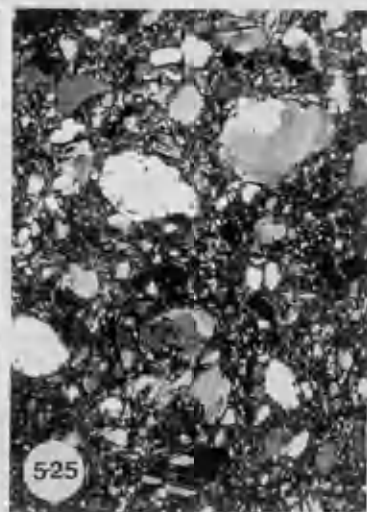
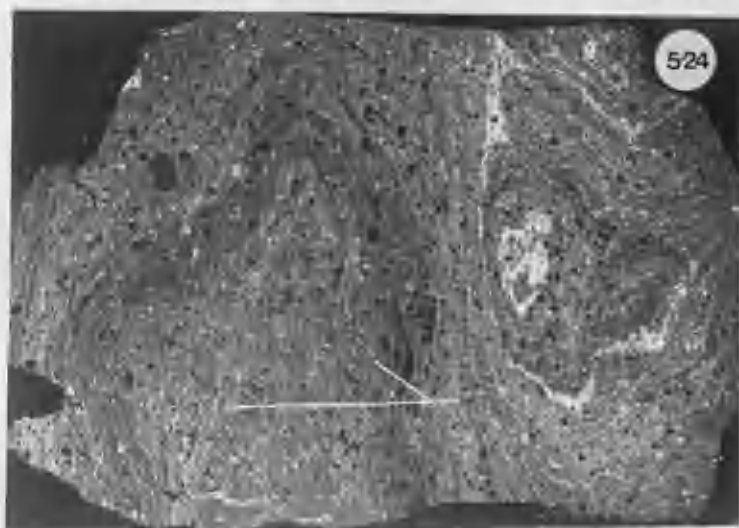
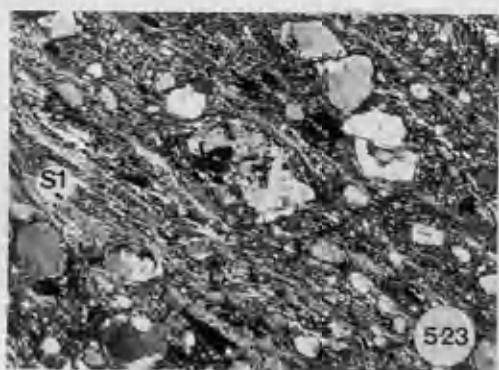
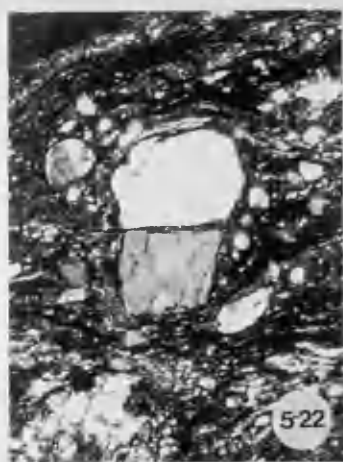
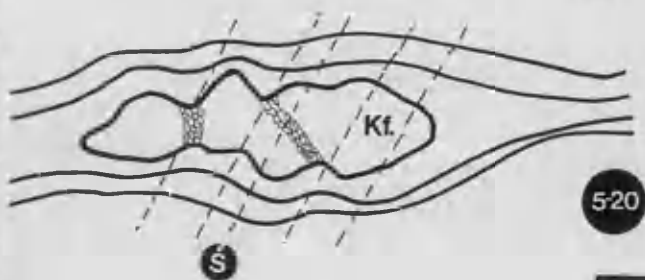
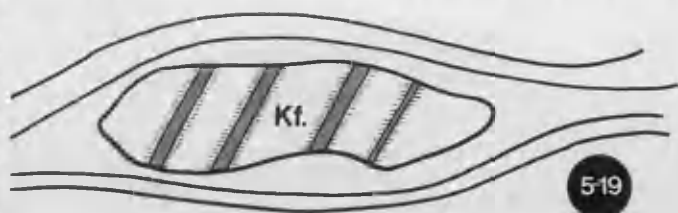
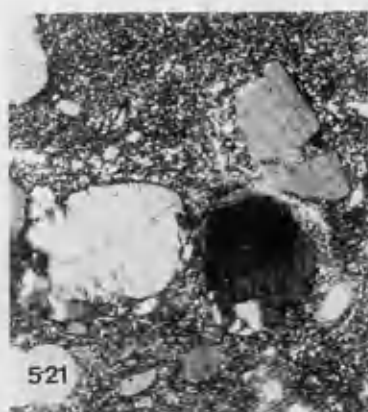
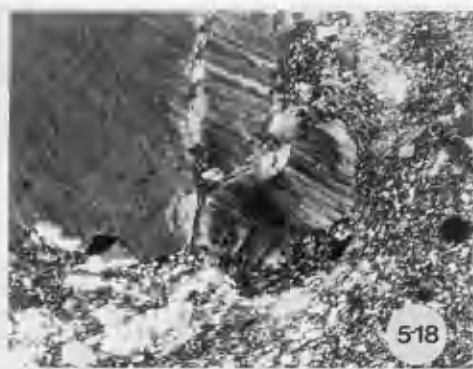
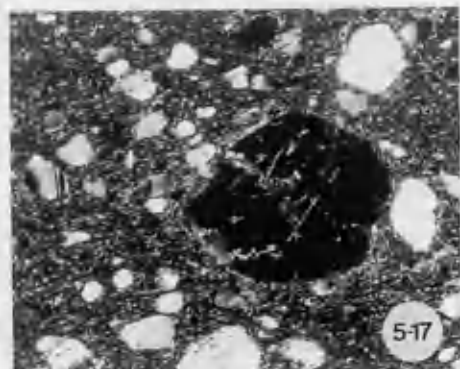
Plate 5-65 Sheath fold in ultramylonite from graphite-bearing metasediment; note the transposed folds in quartz-rich bands (left and right) of label); plates A,B,C from light bands at the top; negative print of thin section, X2 [NG 976 691]

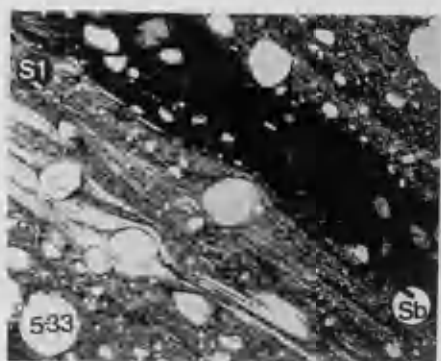
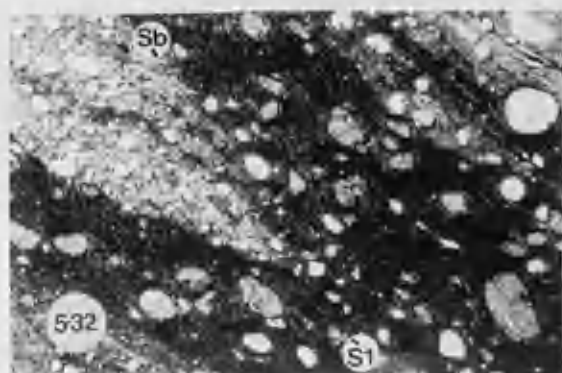
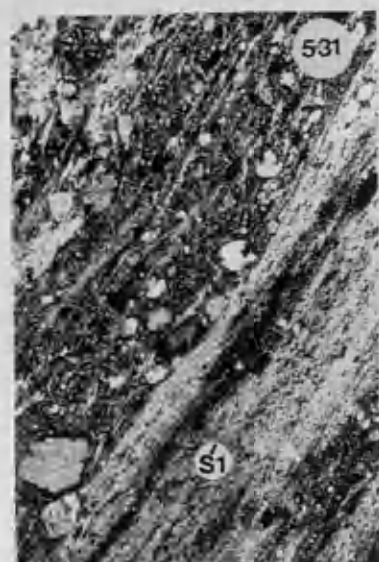
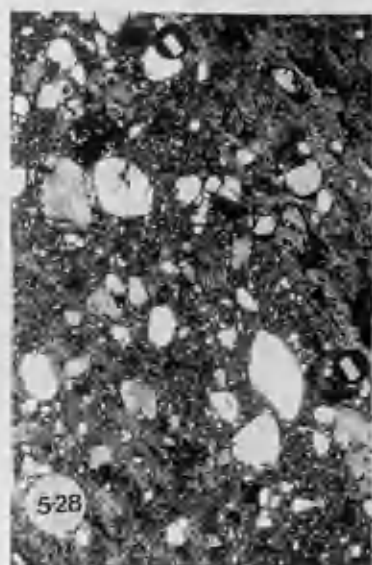
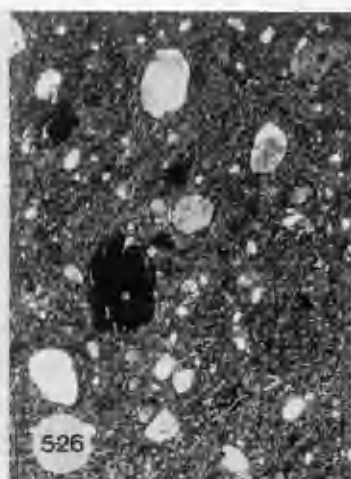
Plate 5-65A,B,C Variation of shapes of amphibole and garnets at different scales; well-round amphibole of Plate 65A shows irregular rims with indentations parallel to cleavage at higher power (Pl.65B); note idioblastic amphibole (top right of Pl. 65A) and garnets with spiral inclusion trails and irregular to perfectly straight rims overgrowing mylonitic matrix (Pls 65B,C); PPI; X2, 40 μ , 40 μ respectively [NG 976 691].

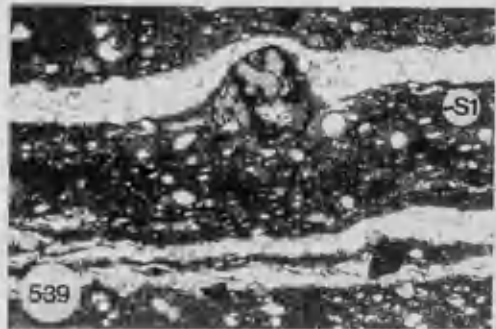
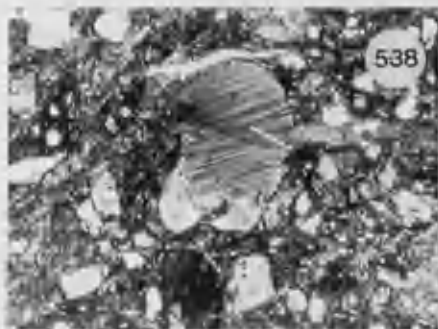
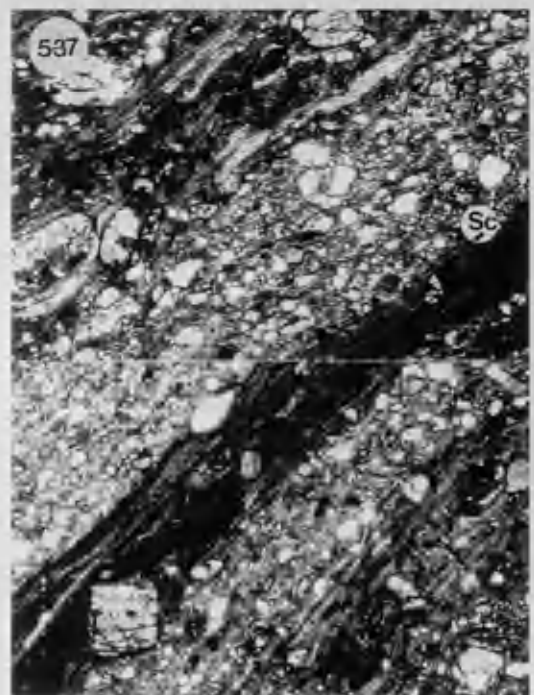
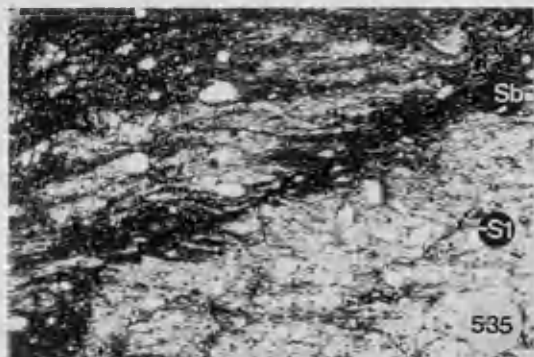
- Plate 5-66 Shear and pressure solution along S2 cleavage affecting twins of calcite porphyroclast in carbonate-bearing mylonite; XN, X25 [NG 956 708].
- Plate 5-67 Contrasting textures between calc-silicate gneiss (granoblastic) and fine carbonate-rich matrix with well-rounded amphibole crystalloclasts; XN, X10 [NG 973 704].
- Plate 5-68 Lithoclast of fine-grained structureless feldspathic rock (large dark fragment) together with amphibole and feldspar crystalloclasts in carbonate-rich matrix of calc-mylonite ; XN, X10 [NG 973 704].
- Plate 5-69 Mylonitized carbonate-bearing with elongate deformation bands of quartz and fine tails of grain-sized reduced carbonate parallel to a fold axial plane; PPL, X10 [NG 971 696].
- Plate 5-70 Ultramylonitic band affecting calc-silicate gneiss with large epidote and amphibole crystals; note the relative sizes of epidote and feldspar crystalloclasts in the matrix; XN, X10 [NG 973 704].

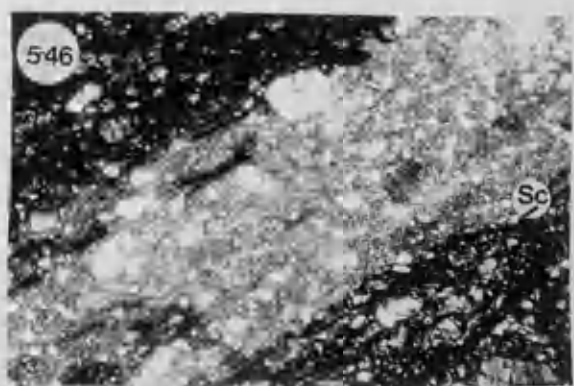
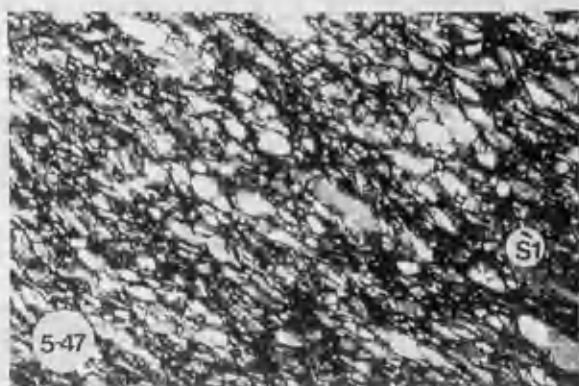
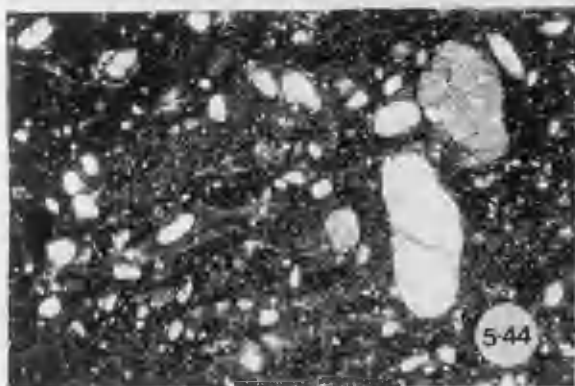
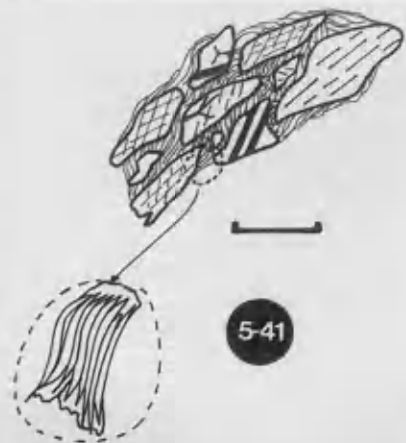
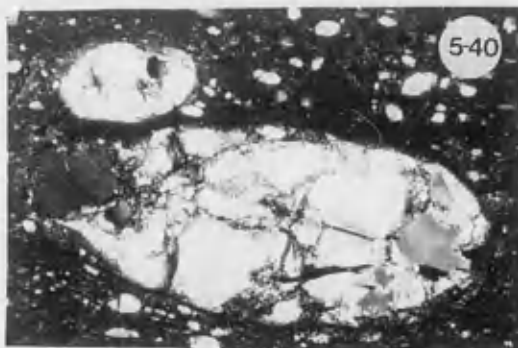


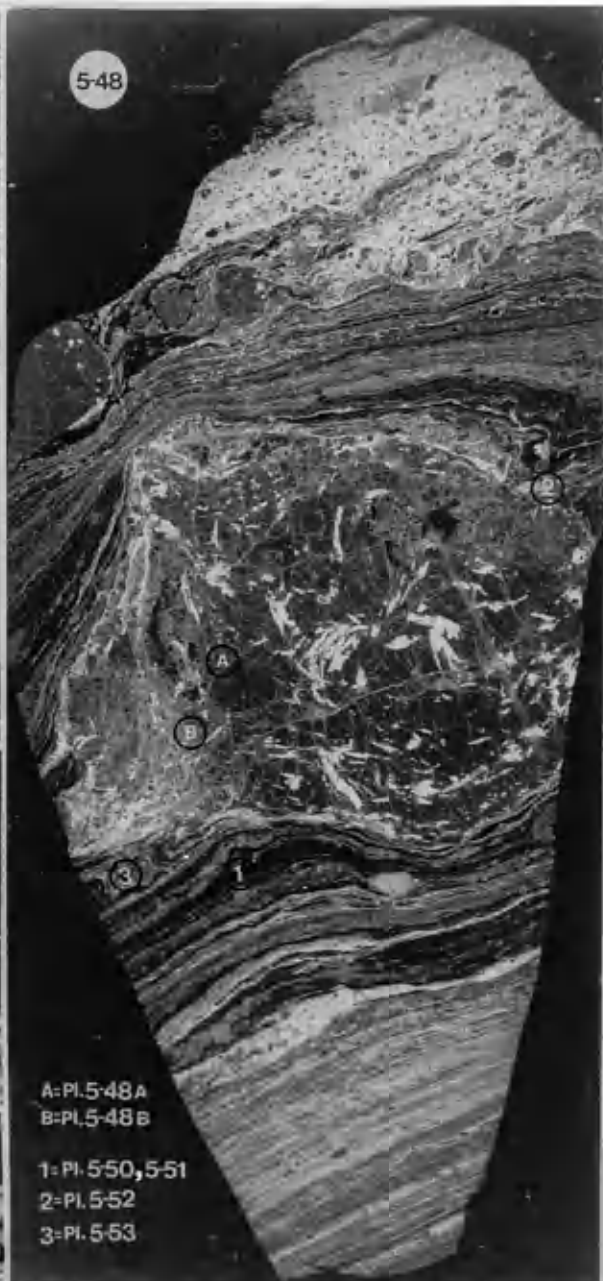
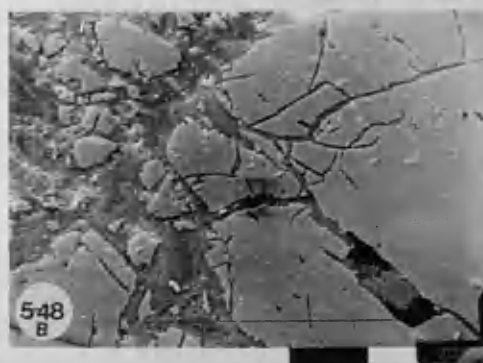




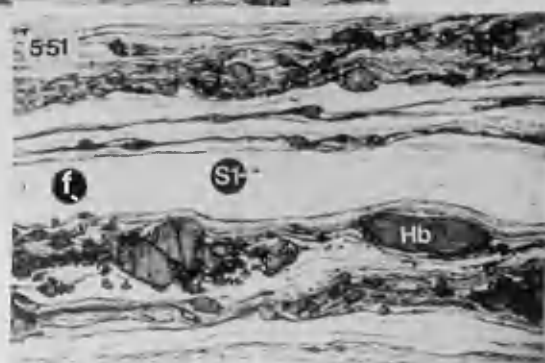
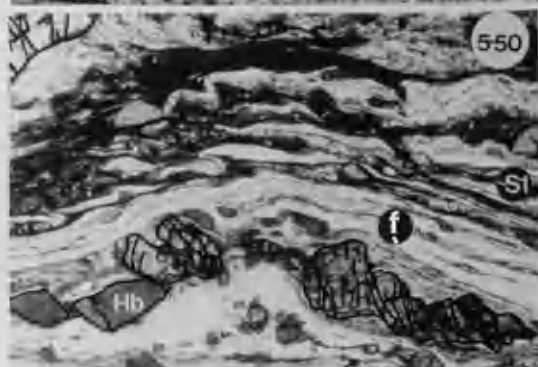
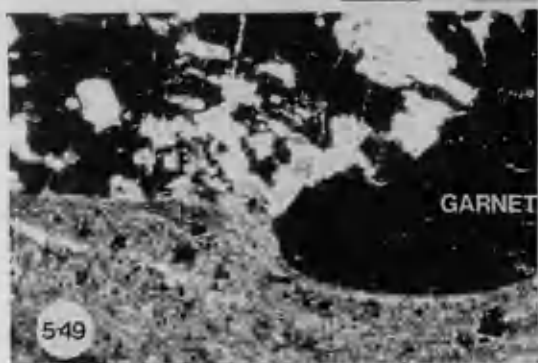


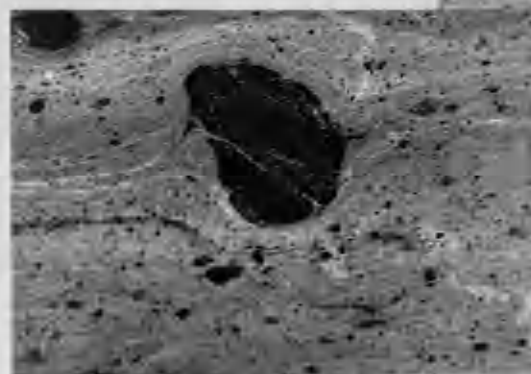
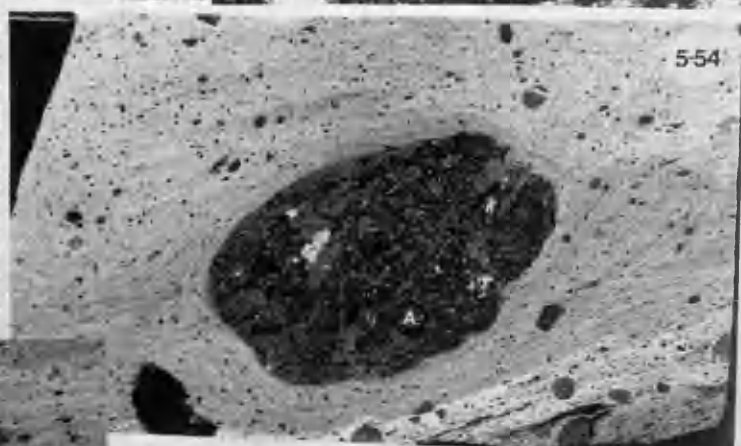
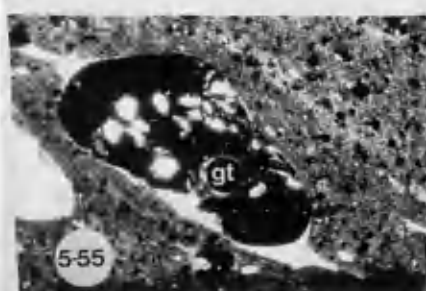
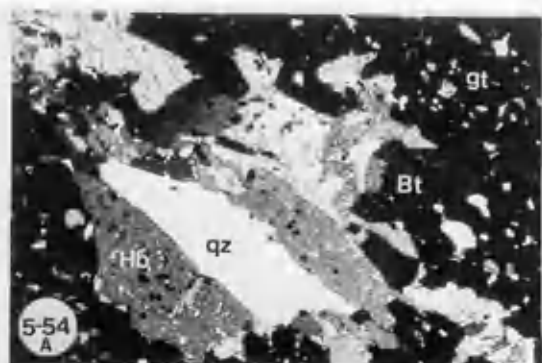


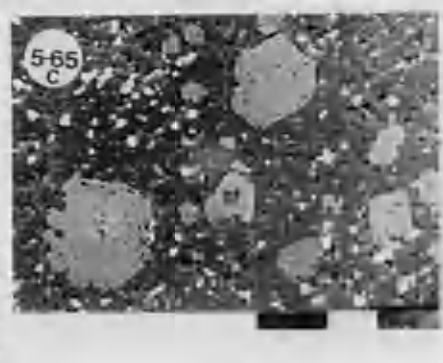
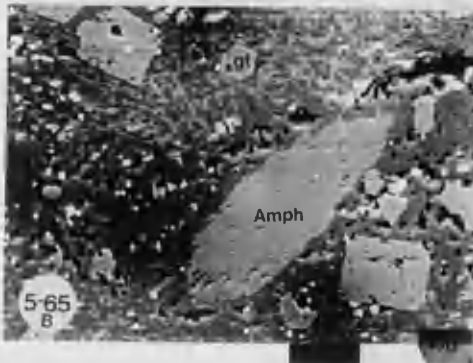
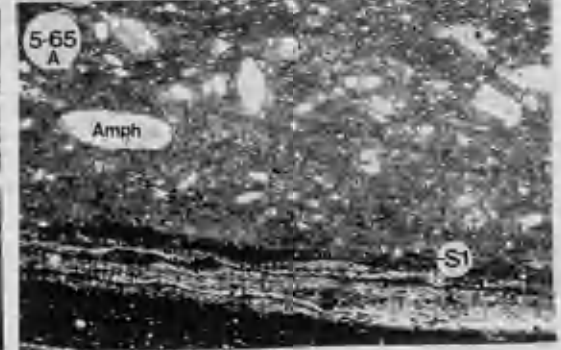
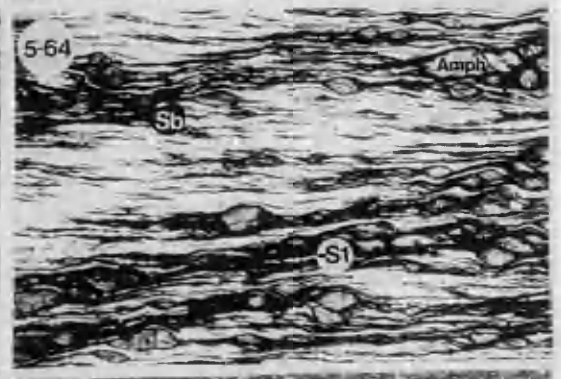
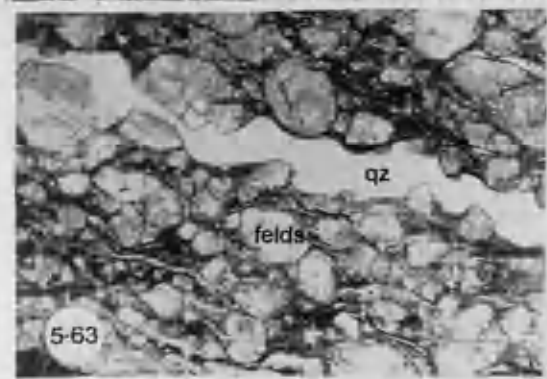
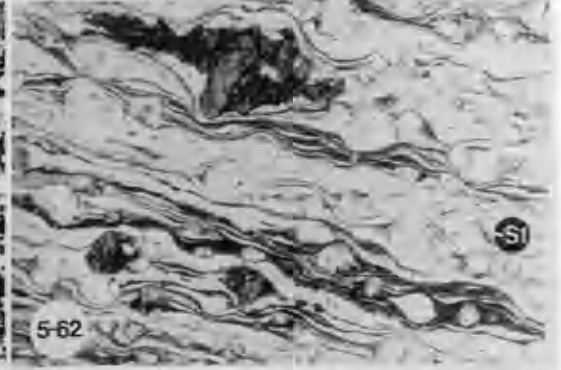
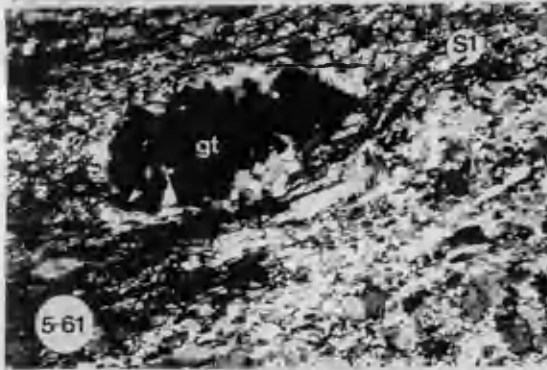
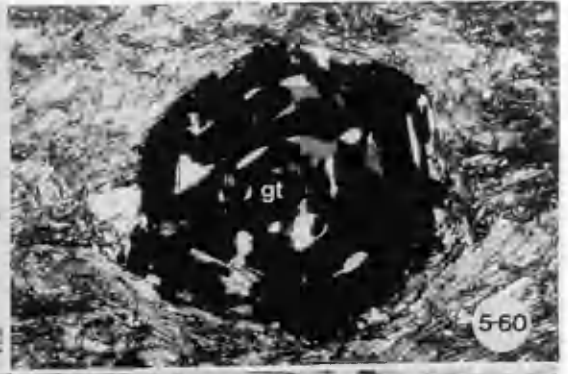


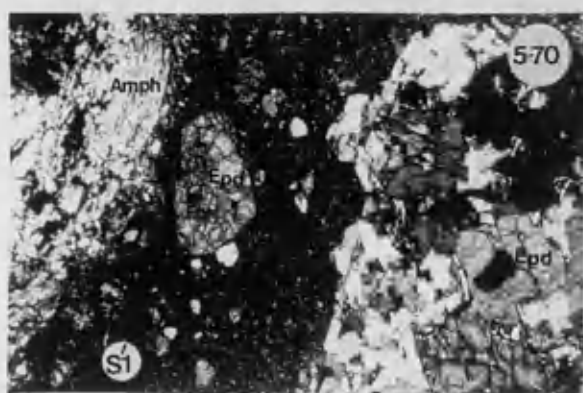
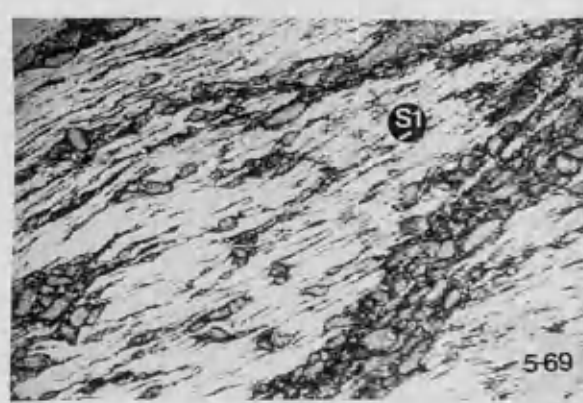
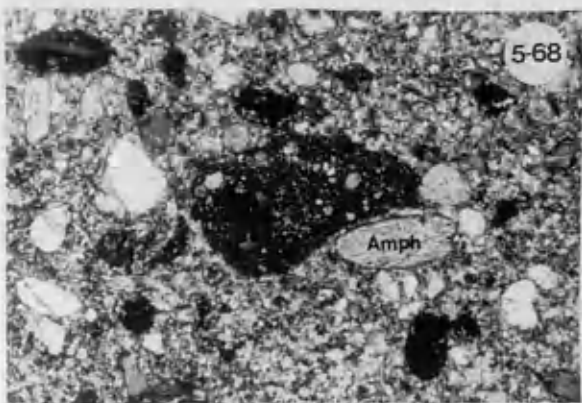
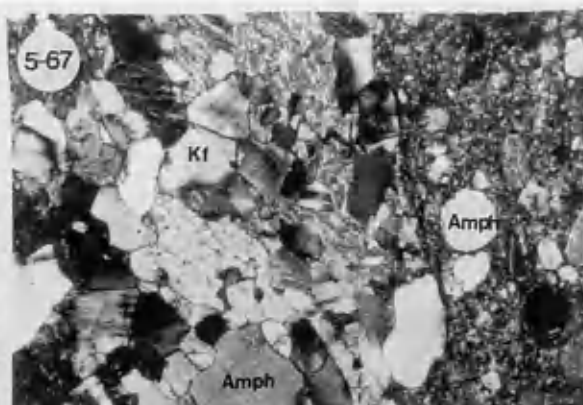
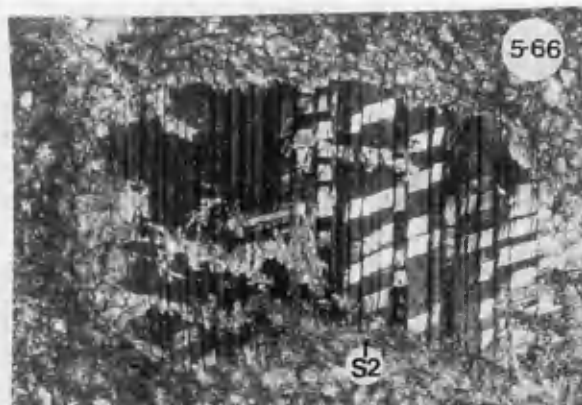


A: Pl. 5-48 A
 B: Pl. 5-48 B
 1: Pl. 5-50, 5-51
 2: Pl. 5-52
 3: Pl. 5-53









CHAPTER 6 - INTERPRETATION OF THE STRUCTURES

6.1 Introduction

6.2 Geometrical Analysis

6.2.1 Analysis of the Orientation Data

6.2.1.1 Analysis of L1-L2 deformation patterns in relation to mechanism of folding

6.2.2 Fold Geometry

6.2.2.1 Introduction

6.2.2.2 Late Folds

6.2.2.3 F4 Folds

6.2.2.4 F3 Folds

6.2.2.5 F2 Folds

6.2.2.6 F1 Folds

6.2.2.7 Discussion of the Kinematic Models

6.3 Strain Analysis

6.3.1 Introduction

6.3.2 Discussion of the Methodology

6.3.3 Interpretation of the Results

6.1 INTRODUCTION

The aim of this chapter is to assess the evidence from which the final geometries of the successively formed fold structures can be related to their stage by stage development, and to deduce their overall kinematic history. In the first section the geometry of the Letterewe synform as determined from field studies, and the interpretation that it exercises control over the development of the F3 and F4 fold sets, is assessed by an analysis of the orientation data. The second section comprises an evaluation of the deformational mechanisms likely to be responsible for the geometries of the F4, F3, F2 and F1 folds, as well as a discussion of the existing kinematic models for fold belts with the constraints provided by this study. The third section includes a (mainly) qualitative estimation of the finite strain which can be used to constrain the kinematic interpretation and the model proposed for the evolution of these rocks (Chap.8).

6.2 GEOMETRICAL ANALYSIS

6.2.1 Analysis of the Orientation Data.

The approach here does not follow the systematic fabric analysis as presented by Turner and Weiss (1963). It is rather an attempt to use the density 'pole' diagrams to cross-check and illustrate the geometry of large structures mapped in the field, according to the principles discussed in Chapter 3. As many authors have pointed out (e.g. Hopgood 1980), the use of these diagrams to work out the geometry of polydeformed rocks (such as the present case) can be very misleading where four phases of approximately coaxial folding are demonstrated from field relationships.

The uncertainties about the relative age of several features in each domain (in particular L1xL2xL3 in domain III, folds in domain IV, L1xL2 in domain II and F2xF3xF4 in domain I) precluded the use of tens to hundreds of measurements from each domain. Due to the variation of attitude and distribution of the various structural features, mainly as a result of (a) refolding and interference between structures, (b) characteristics and complexity of

deformation mechanisms and (c) rheological properties of the rocks, the mesoscopic analysis of the fabrics was restricted to domains I and II, where the geometry of the large fold can be observed in the field. In this way the different variable factors are constrained to the greatest possible extent. The measurement of the structures corresponding to each recognized deformational phase (e.g. 'S1'-total designates all the measurements of S1 in a given domain) were divided in two parts corresponding to the outcrop position along the southwestern or northeastern limbs of the large fold (cf. Maps in Annex). This procedure caused a bias in the pole density diagrams (e.g. the 'predicted sample mean attitude' values of each diagram) due to the asymmetry of the large fold (NE 'vergence') and its intersection by the topographic surface (see Sects 2.2 and 8.3), implying that far more readings from the NE limb were recorded. In addition, the variable intensity of the different fold sets (F3 and F4 respectively) on the different limbs means that any reconstruction of the geometry and attitude of the structures should not be based on averages or on positions of maxima of pole density diagrams, but instead, on qualitative data collected in areas of weak overprinting (e.g. the hinge zone of the large fold).

Domain I - Quartzofeldspathic gneisses and amphibolites

The diagram of L1 along the NE limb of the synform shows predominantly the effects of F4 folds. Since L1 and L2 are coaxial (cf. diags 5, and 12) the F2 folds should not affect the L1 distribution pattern. The effects of F3 can also be neglected since F3 folds were not identified along this (NE) limb, suggesting that the geometry and position of the (F2) synform was similar to that observed nowadays. Even if they were present, as long as they keep attitudes and geometries similar to the F3 structures observed along the SW limb (open folds with NW-SE-trending axes and shallow plunges - diag.15) of the synform, they are not expected to cause any significant influence on the L1 pattern. In this way the strongest influence on the L1 distribution pattern is caused by the F4 folds which have more SE-S-trending axes. Since these folds were preferentially developed along the NE limb of the synform the L1 scattering along this limb is expected to be high (cf. diags 6 and 7) confirming the field observation that refolding of L1 by F4

folds is the principal factor controlling the NE plunges of L1 (see Pl.3.33). Diagram 6 shows the repetition of L1 poles in the NW quadrant as well as asymmetrical girdles along small circles around the locus of the mean F4 fold axis (Diag. 17). The weaker NW secondary pole could be interpreted as indicating the predominant SE plunges of L1 since the F4 are in general relatively open symmetrical folds and the angle between the average L1 and L4 trends is relatively low ($\sim 32^\circ$). The relatively open geometry of these folds is also probably responsible for the rarity of steeply-plunging L1 lineations (Diag. 5). This pattern supports the features indicating the dominant role played by flexural mechanisms during F4 development (see Sect. 6.2.1.1 and 6.3.3 for discussion). The S-composite diagrams (S banding + S1), on the other hand, show the effects of all deformational phases younger than D1 (Diag. 1). This involves the assumption that the composite banding was an approximately planar feature at the final stages of the D1 episode, something which is not unlikely considering the high strains attained. Diagram 2 shows the scattering of S1 in domain 1. D2 and D4 folds are principally responsible for this pattern since the other sets are only locally developed. The behaviour of S1 was examined by plotting the F1 axial planes corresponding to the NE and SW limbs of the large fold as well as the entire domain (Diags 3, 4, 2, respectively). The plotting of 'total' S1 (Diag. 2) shows a well-developed girdle along a great circle, a pattern very similar to the 'total' banding indicating the isoclinal character of the F1 folds and a common post-D1 history for these structures. The pole of this girdle shows a low plunge towards the SE (05:121) and, following the classical approach, would be interpreted as marking the position of the fold axis affecting the S1 foliation. However, this pole is a composite feature representing the locus of L2 (see mean attitude sample of diagram 13) and F4 axes (eastern most pole of diagram 17). Plotting of S1 into diagrams corresponding to the reworked NE and relatively preserved SW limbs (Diags. 3 and 4, respectively) shows that the NW-extending girdle (of diagram 2) is absent in the SW limb of the synform (Diag. 4) suggesting that it was produced by F4 folding of a more SE-E - striking (S1) foliation. This seems to be confirmed by a similar asymmetry of the girdle of F2 axial planes (Diag. 29) along the limb of the large F2 fold.

The scattering shown by total L2 (Diag. 12) is very similar to total L1 (Diag. 5) with two of the density poles (the more easterly ones) showing good superposition. The locus of the predicted mean sample attitude trends approximately 10° southwards from L1 (L2 = 16:125, L1 = 07:116). Similarly to that observed for L1, the L2 locus shows two slightly different concentration poles when measurements corresponding to NE and SW limbs of the large fold are plotted, with least affected L2 lineations trending SE-E (Diags. 12 and 13). The plunge and trend variations along the SE quadrant of diagram 6 is mainly a F4 effect since there is a progressive decrease of plunges of the concentration poles as they are shifted towards the southeast and south. The diagram corresponding to the NE limb (No. 13) shows that the concentration pole is elongate towards the south where the lineations become progressively shallower and NW-plunging. This transitional pattern suggests that both variations (of trend and plunge) have a common cause, viz. the effects of the F4 folds.

The distribution of the F2 axial planes (Diag. 9) is similar to S1 demonstrating again the importance of the D4 episode. The somewhat high strike dispersion of this diagram can be interpreted in terms of an originally more E-W steeply-dipping foliation being rotated.

Diagram 11 shows the F2 axial planes along the SW limb where its low angle of strike, steeply-dipping attitude and non-pervasive nature would favour rotation rather than refolding during D4 deformation. This seems to be confirmed by field observation where the few examples of F2 refolded by F4 were identified (cf. Map 3.3). In contrast the S2 foliation is ideally positioned to be affected by the late phases (particularly F000° and F040°) which, due to their large wavelengths and intersection angles with S2 (Diags 29 and 30), would mainly cause a swing of the strike of S2 (Diag.9). Assuming that both limbs of the large synform could be affected by the late phases, the difference of S2 dispersion between these two limbs (cf. diagrams 19 and 11) would be mainly a function of F4 refolding on the NE limb. Such an interpretation seems to be reasonable even if the effects of the F3 folds are considered.

This is because these D3 effects, as well as only being developed along the SW limb of the F2 synform are expected to cause only variations of the dip of S2 since these two phases are generally co-axial (cf. diagram 15). Accordingly, the absence of a well-marked girdle extending towards the centre of this diagram (No. 15) can be attributed to the generally large interlimb angle of the F3 folds in this domain (see Chap.3); this is in marked contrast to the equivalent diagram for the amphibole schist (Diag. 18).

The S3-L3 diagram (No. 15) shows the scattering of the axial planes of recumbent folds (along the SW limb of the synform). This dispersion is probably an original feature (not caused by refolding) since the F4 folds are only locally developed in this part of the domain and the late phases are usually best observed where affecting steeply dipping foliations. This is also a likely explanation for the variations in strike (mainly) shown by S4 (Diag 16).

Domain 11 - Amphibole schists

The analysis of the density pole diagrams in domain 11 (amphibole schists) is more complex due to the close attitude of L2, L3 and L4 lineations in this (SW) part of the domain (Diags 19, 21, 23), where most of the features present overlapping girdles (see angular standard deviation values). However the patterns are similar to those obtained for domain 1 with the difference that in this case the deformational phase controlling the outcrop pattern is F3 (recumbent folds), instead of the upright F4 folds. Diagram 19 shows the dispersion of L2 lineations where a girdle with a 'weak' NW-SE elongation connects the concentration pole of SE-plunging lineations with the few that plunge NW. The weak girdle is in agreement with the geometry of this part of domain 11 (most measurements came from the SW part of domain 11) where the moderately SE plunging L2 lineations are slightly affected by sub-horizontal to low (NW)-plunging F3 folds (Diag. 21). The F2 axial planes show a large dispersion with a girdle extending roughly along a NE-SW direction (Diag. 18). The dispersion is probably caused by the F3 folds and if a great circle containing the principal concentration poles is traced, its pole (07:113) coincides perfectly with the L3 SE-plunging density pole, at

exactly 180° to the predicted mean attitude sample. The F3 axial plane diagram (20) shows a considerable dispersion. The best fit of a great circle containing the highest density contours has its pole very close to the predicted mean sample attitude of the F3 axes (Diag. 21) instead of the pole for the F4 axes as would be expected in a situation involving these two phases. Although this could be a coincidence since most of the folds have NW-SE trends and the girdle is not very well defined, the pattern could have been produced by the curved axial planes frequently observed in these folds, if this feature is also reproduced in large scale. If this is the case it was not produced by refolding. Instead it is related to the mechanism of fold formation (see section 6.3.4).

The D4 structural features in this domain are shown in diagrams 22 and 23. The contrast in dispersion between fold axes (see angular standard deviation values) and axial planes are probably due to both geological and non-geological factors. The former includes the variation of fold plunges due to the previous attitude of the affected planar structure (limbs of F3 folds, in this domain) as well as the non-cylindrical nature of the folds produced during this deformation phase; this latter factor is thought to be the one responsible for the extension of the girdle towards the centre of the diagram. A contribution of the late phases is also likely but thought to be very localized because of the irregular distribution of these structures and the problems of refolding the relatively open F4 folds. The non-geological factors can be explained by the difficulties involved in the precise location of the axial planes of these folds both as a function of (a) their large interlimb angles and (b) the indistinct nature of their axial-planar spaced cleavage. The identification of this latter features has heavily relied on the orientation criterion and although this could explain the relatively small dispersion of strikes it does not explain the variations of dip, something which could be attributed to fanning of the cleavage.

Domain III - Metasediments

Diagrams 24, 25, 26 and 27 show the D2 and D3 structural features in domain III. The large dispersions (see respective angular

standard deviation values) relative to the structures of the same age in the other domains can be explained in terms of the rheological behaviour of these rocks. The abundance of pelitic material means that folds are tighter, planar structures better developed and localized transpositions more likely than in the other domains. It also means a better development of the later folds (see Map 3.4) which are probably the main cause for the present dispersion.

In addition deformation mechanisms were probably more varied and accentuated viscosity contrasts between mica-rich matrix and feldspathic competent bands (from which most measurements were taken) have favoured the development of ptygmatic and disharmonic folds. As already referred to in section 3.3 the similar characteristics and attitudes of structures of different age in this domain means that the probability of misidentification of structures is high, even though the plotted structures were carefully selected.

Despite these factors the pole of a plane containing the concentration poles of F2 axial planes plots close to the 'predicted' mean attitude sample of F3 axes (Diags.24 and 27). The F2 axes show shallower plunges than in the other domains (cf. Diags 12,19,25). The measurements plotting in the NE quadrant correspond to the outcrops with complex refolding of F2 axes (e.g. Pls. 3.18,41). As already referred to (section 3.3) the best developed lineation in this domain ('quartz rods') is in most cases likely to be an L1- L2 feature but since it is difficult to be certain of its age on the basis of its nature (but see Sect.8.3) or orientation (cf. diagrams 25 and 27) they were not included in these diagrams.

The F3 axial planes show a NE-SW-extending girdle which is interpreted here as a product of F4 folding as suggested by field observations (cf. Diag.26).

As demonstrated in diagram 28, the F4 folds in this domain show high scattering of attitude of fold hinges, possibly resulting from the mechanism of fold formation as well as difficulties of precise location of the hinges.

The attitude of late phase structures is shown by diagrams 29, 30, 31 and 32. The axial planes show well-developed concentration

poles with slight variation of dips around the vertical position, possibly the result of cleavage fanning. The number of measured axes was not enough to be contoured, because they were difficult to measure for open folds, particularly where the plunges were steep. The axial plane diagrams represent mainly the attitude of spaced cleavages with the good concentrations in the diagrams reflecting the field criterion used for their identification (orientation).

Diagrams 35,36,37,38, and 39 show the distribution and attitudes of structural elements of several ages as measured in different domains.

6.2.1.1 Analysis of L1-L2 deformation patterns in relation to mechanism of folding.

The L1-L2 lineation patterns produced by deformation around F4 and F000° folds in domain I were analysed with the objective of providing additional evidence about the mechanism of F4 folding.

Since the maintenance of angular relationships rather than density distribution is the important factor an equal angle stereonet (Wulff net) was used in this section. From all the analysed cases only 2 examples representing two basic types of pattern observed will be discussed here. Diagram 33 shows the most frequent pattern, with the lineations distributed along small circles keeping a constant angle with the F4 fold axis. The second observed pattern shows an intermediate distribution between small and great circles (Diag. 34) with the most steeply plunging lineations presenting the highest deviations towards great circles.

The interpretation of the small circles distribution as being produced by buckling is extensively discussed in the literature (cf. Ramsay 1967, Ghosh 1974, Ghosh and Chatterjee 1985). In competent layers the early linear structures are rotated around the axis of the later folds, keeping a constant angular relationship. Since these structures were only measured for competent layers (which are the ones preserved in three dimensional outcrops) the only additional strain to be accounted for in these bands would be the one produced by tangential longitudinal strain. This would

tend to increase and decrease the angles between (folded) lineations and fold axis in the external and internal parts (in relation to the neutral surface) of the fold respectively. As noted by Ghosh (1974, p.268) in very competent bands (like these quartzofeldspathic layers interbanded with biotite-rich units) the effects of both initial (layer parallel) strain and late stage strain are negligible. It seems, however, that if the layer has suffered initial homogeneous strain, as total shortening estimates suggest (section 6.2.2.3), the angular relationship between folded lineations and fold axis will tend to remain constant. On the other hand, the transitional pattern (between small and great circles) is interpreted here as being produced during (homogeneous?) deformation of the buckle folds, possibly at the late stages of folding, as seems to be indicated by the preferential reorientation of the already more steeply plunging lineations. In any case this and the above discussion (section 6.2) seem to contradict conclusions by Oddling (1984, p.59) where the variable plunges of L1 (L2 ?) lineations were attributed to changes in shear direction throughout the history of the shear zone. In addition, the SE-plunging pattern of most fold hinges and linear features throughout the deformation history is interpreted here as an indication of the originally SE-plunging and SE-dipping of the stretching lineation and shear zone at Loch Maree (cf. Chaps 6,8).

6.2.2 FOLD GEOMETRY

6.2.2.1 Introduction

Although during the last 20 years the study of deformed rocks has seen a considerable progress in terms of the quantification of the deformation through the application of mathematical methods and principles of mechanics, the study of folds and their mechanisms of formation has received relatively little attention. Recent contributions include the work of Oertel (1974), Groshong (1975), Mitra (1978), Oertel and Ernst (1978), Pfiffner (1980), Spang et al. (1980), Spang and Groshong (1981) and Hudleston and Holst (1984), most of which concentrated on the detailed analysis of

(individual) folds at high structural level rather than on fold trains which was the priority during the 1960's, when the pioneer work of Ramberg (1961) and Biot (1961) started the systematic investigation of these structures. A possible reason for the rarity of studies involving fold geometry and strain distribution in rocks seems to be the scarcity of suitable material together with the complexities of the deformation with different parts of the structure following distinct deformation paths (see Gairola 1978). However, most natural folds seem to be the result of some sort of buckling in which irregularities on the surface between layers of different viscosities become selectively amplified during compression at low angles to the layering (Ramsay 1967, p.372). The theory of buckling was best developed for the case of single embedded layers following the early work of Biot (1961) and Ramberg (1961) on elastic and viscous materials. It has largely benefitted from experimental and mathematical work during the late sixties (Biot 1964, 1965a, 1965b; Ramberg 1963a, 1963b; Chapple 1968, 1969; Sherwin and Chappel 1968; Dietrich and Carter 1969; Ramsay 1967) in particular with the work of Sherwin and Chappel (1968) where the effects of layer parallel shortening during buckling were evaluated. In this way the conclusion of Biot (1961) and Ramberg (1961) that folding is related to the thickness of the layer being deformed and the contrast between this layer and the surrounding material is expressed by equation (1).

$$\lambda_d = \frac{2\pi t (\mu_1)^{1/3}}{6\mu_2} \quad (1)$$

where λ_d = dominant fold wavelength

t = thickness of the layer

μ_1, μ_2 = viscosity of the layer and medium respectively.

(Biot 1961, p.1614; Ramberg 1961, p.418)

This equation was modified to accommodate the pre-buckling homogeneous deformation ('layer-parallel shortening') discovered to be significant in folds with less than 15° of limb dip (equation 2 which was modified by Hudleston 1973a, p.29), beyond which the fold

development is related to its amplitude. The 'correct' wavelength (W) is dependent on the ratio W/W_d and limb dip.

$$W_d = 2\pi t \left(\frac{\mu_1}{6\mu_2} \frac{1}{2} \frac{S-1}{S^2} \right)^{1/3} \quad (2)$$

where $S = (\lambda_1/\lambda_2)^{1/2}$ of the homogeneous strain
(Sherwin and Chappel 1968 rewritten by Hudleston 1973a,p.29)

Most investigations trying to determine the nature of the folding and the rheological properties of the affected rocks have been based on fold geometry (in profile section), arc length/thickness ratios and strain distribution.

Fold shape analysis was used in this study due to the rarity and scattered nature of the potential strain markers such as the phenocrysts in some amphibolite bodies. It was thought that due to their abundance and widespread occurrence these folds could be used to constrain the kinematic analysis as well as to help with the factorization of the finite strain. The fold classification follows the approach developed by Ramsay (1967,pp.359-372) which is considered to be the only quantitatively based fold classification system available that allows folds to be compared unambiguously. Basically it involves computations made on fold profiles. The layer thickness (t_α) is measured between two tangents with the same dip (α) bounding the upper and lower surfaces defining the fold. This is expressed as a ratio (t_1) of the t_α/t_0 , t_0 being the thickness measured in the hinge, along the line connecting the two maximum inflection points (Fig.6.1A). The changes of fold shape are represented by a graph of t_1 against α (Fig.6.1).

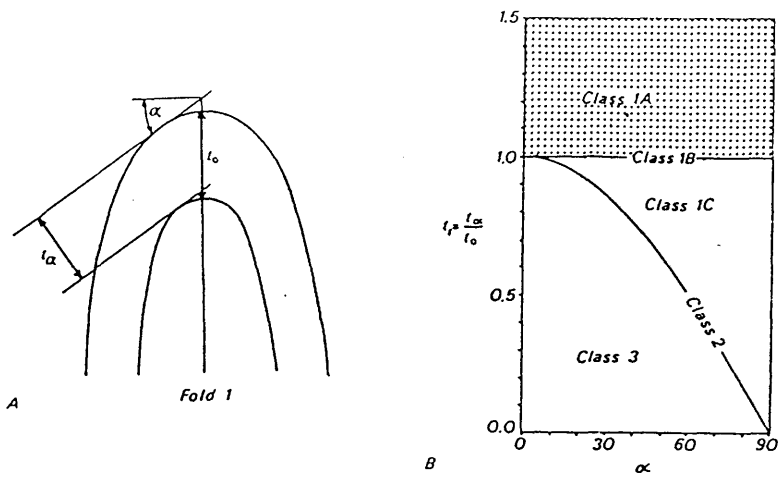


Figure 6.1. A. Fold profile showing relationship of layer thickness (t_α) to limb dip (α). B. Fold classification system based on limb dip and layer thickness (After Ramsay 1967, figs 7-18 and 7-25).

Where lines (isogons) connecting the points formed by the tangents at equal dip (α) are traced across the fold they exhibit a characteristic pattern which was used to classify the folds into three distinct classes (Fig.6.2).

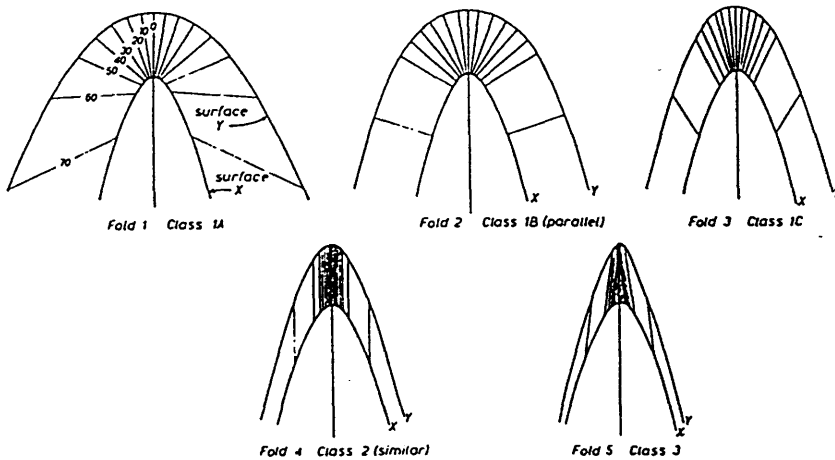


Figure 6.2. Fundamental types of fold classes. Dip isogons have been drawn at 10° intervals from the lower to the upper surfaces X and Y (Reproduced from Ramsay 1967, Fig.7-24).

Class 1 folds show a more open curvature of the outer arc compared to the inner arc. Class 2 folds have the same arc curvature and Class 3 folds show a more open curvature of the inner arc. These geometrical properties are important since they reflect the rheological properties of different layers during folding.

From more than two hundred photographs of folds, sixty-five (from two domains) were selected for treatment. Features like the

presence of reverse folding (particularly in F4 folds), asymmetrical structures with short limbs and poorly-defined markers together with the slight obliquity of some photographs, were the principal causes for their elimination. The restriction of the analysis to domains I and II folds was dictated by their known relationship with the Letterewe Synform, as well as to their more regular geometry considering the limitations of the applied method.

A bias towards high strain was certainly introduced during this analysis since well-developed folds with small interlimb angles, contrasting markers (e.g. amphibolite bands) and highly regular profiles were preferentially selected. This means that if buckling was involved in the formation of these folds the selection of well-interbanded units with a variety of lithologies would shift the results towards folds with geometry of classes 1 (1C in particular) and 3. In some cases the fold profile analysed was probably not a principal plane of the bulk finite strain ellipsoid (Hudleston 1973c, p.130) but since large deviations are not expected, this did not cause much influence on the analysis. In addition to these problems we should consider the potential handicaps involved in a graphical solution, such as the lack of precision in tracing the tangents as well as the exaggerations of irregularities produced during photographic enlargements of profiles of small folds. This was the main reason why the presentation of the fold isogons are avoided throughout this study. The preferential selection of F2 and F4 folds for analysis was not only because of their well-developed nature in the selected domains but also due to their importance for the geometry of the macroscopic fold. In addition it was hoped that the analysis of specific aspects of the deformational history given by the fold geometry and their sequential development would provide valuable elements for establishing a kinematic model for these rocks.

The analysis has followed a fashion from the youngest to the oldest structure. This approach is the simplest way of giving a qualitative view of the complexity of the deformation of these rocks as well as of making it possible to deal with the factorization of the finite strain. It is based on a reasonably detailed description of the relative sequence of events (Chap.3).

The results of the fold shape analysis (Table 6.1) indicate the predominance of folds of Class 1C geometry over all the other classes. They are the most abundant amongst F2 folds in the mylonites (85%) followed by F4 in gneisses and amphibolites of domain I (78%), and F2 in domains I and II, whereas Class 2 folds are better developed amongst F2 folds in domains II and I. Taking into account the more homogeneous composition of the amphibole schists (domain II) and the constraints discussed above it appears that the distribution of Class 2 folds is controlled by the rheological properties of the affected rocks. This is in accordance with the opinion expressed by Ramsay (1967, p.372) that many natural folds are the result of buckling, so that the variations of the mechanical properties of the affected lithologies during progressive deformation exert a strong control on the fold shape. Accordingly, although folds with Class 1C geometry were developed during all the deformational phases, they were more frequent during the relatively early stages of the (progressive) deformation when compared to the more concentric and chevron styles subsequently formed (D3 and D4). Considering that these folds affect the same material, their geometry suggests a progressive increase of viscosity (but not of viscosity contrast) through time something which has been invariably observed in many fold belts and attributed to a general decrease of the P-T conditions accompanying the progression of the deformation. Although this conclusion is generally true in terms of (absolute) viscosity the presence of features indicating buckling as early in the deformational history as D1 (section 6.2.2.5) seems to suggest that the evolution of the relative viscosity (which is the parameter that matters in terms of fold shape) was much more complex. It seems to have varied at later times during D1, as it is suggested by the rarity of viscosity contrast 'indicators' in more evolved F1 folds. The abundance of these features associated with F2 folds (more than any other phase) might indicate that the conditions (of P, T, ϵ , finite strain and strain rate etc.) prevailing during D2 were the most favourable to promote viscosity contrast. On the other hand the rather lower ductility conditions of the D3, D4 and D-late phases did not favour the development of these features.

It seems reasonable to predict that if D2 deformation had

progressed further (under increasing P, T, strain conditions) these relatively low strain features indicating buckling would give place to some others (of high strain) indicating shearing. In this way the similarities of fold styles of the successive deformation phases in fold belts of diverse ages and regions in the world (e.g. Hopgood 1973) should not constitute any surprise since these structures would tend to represent only the 'last increments' of deformation (corresponding to what was called here D1 to D-late deformational phases).

6.2.2.2 Late Folds

These structures will not be discussed in detail as they are of restricted distribution in the area mapped. This means that their low associated strains would not exert much influence on the present analysis. It is perhaps relevant to mention that these folds show features indicating development under brittle-ductile conditions with geometries and attitudes which are difficult to relate to D1-D4 structures. The presence of structures showing considerable shortening of the inner arc, sinusoidal shapes and apparently holding thickness/wavelength ratios, in addition to the associated axial-planar cleavage, seems to indicate that they were produced by a considerable shortening at high angles to the NW-SE composite foliation. Despite the uncertainties about the mechanism of formation of spaced cleavages (see review by Engelder and Marshak 1986) the observation that spacing of cleavage domains is clearly a function of strain and this is in turn a function of structural position (Engelder and Marshak op.cit, p.337) supports the relationship between this structure and the open folds.

6.2.2.3 F4 Folds

The variable style of these folds, with chevron to sinusoidal geometry in the same outcrop confirms the expected high viscosity contrast between the two predominant rock types (quartzofeldspathic gneiss and the relatively thin biotite-rich bands) in the outcrops where these folds are best developed. This sort of situation was

reproduced experimentally by Ghosh (1968) who showed that in the deformation of multilayered materials of high viscosity contrast, 'kinking' and buckling are observed. Where multilayers are affected, the tendency is to form chevron folds while during buckling of an isolated competent band, sinusoidal shapes are favoured (see Ramsay 1974). Wavelengths of several scales (Pl.3.30, Fig.6.3) are shown by quartzofeldspathic layers interbanded with biotite-rich bands.

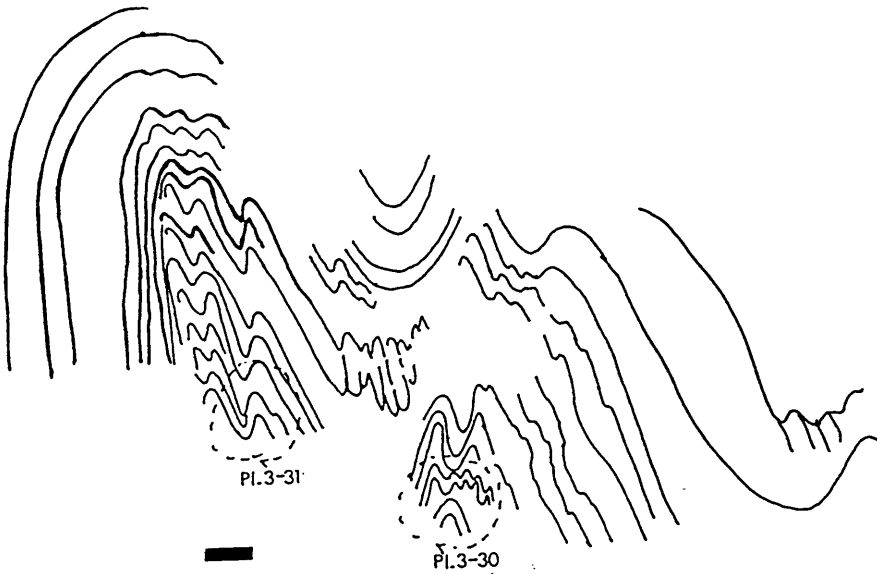


Fig.6.3 Variable wavelength of F4 folds as a function of layer thickness. Scale ~1.5m.

A rough estimate of total shortening for the first, second and third largest wavelength folds of this outcrop (Fig.6.3) shows values of 42, 65 and 68% respectively. Since there are no significant differences of composition in either rock type the finite strain differences must be a direct function of the layer thickness variation. This draws the attention to the fact that 'low strain-looking' relatively open folds in thick bands (see scale of Fig.6.3) can be indicating as little as 40-50% of its total strain. Accordingly underestimation of the strain attained during this phase is a potential source of error and should be considered when factorizing the finite strain. This is also in agreement with the experimental work of Hudleston and Stephansson (1973) who showed that fold shape was dependent on L/h (Length/height) ratios. This indicates that homogeneous strain

dominates the deformation of thick layers whereas buckling is very active in the deformation of the thin bands. However this does not mean that thin bands were not also homogeneously deformed since layer-parallel shortening before significant folding was observed in all experiments except for viscosity contrasts around one thousand (Hudleston and Stephansson 1973). As demonstrated by those authors very thin bands of granitic pegmatite (thinner and showing more viscosity contrast than the examples discussed above as the result of large grain size of minerals) within biotite schist show variation of thickness with limb dip presenting the geometry of a flattened parallel fold.

An attempt was made to determine the viscosity contrast between the above mentioned folded bands. It assumed (a) periodicity of the folds and no interference from the surrounding layers, (b) Newtonian behaviour of layer and medium, (c) plane strain and (d) body forces are negligible. The results were highly variable ($\mu_1/\mu_2 = 1.1$ to >20) as were those obtained by Hudleston (1973c). They suggest that although assumption (d) could be realistic all the others are probably not, causing variable effects (reducing and increasing) on the different parameters. Other possible causes for these inconclusive results include the small number of analysed folds which would strongly influence factors like the 'dominant wavelength'. These and other problems involved with the estimation of viscosity contrasts from fold geometry are discussed in detail by Shimamoto and Hara (1976, pp.18-21).

In addition to the fold shape analysis several other features indicate the occurrence of buckling during the evolution of these folds (see Chap.3). Although according to Biot (1961) this would suggest a minimum viscosity contrast of 1/100 (μ_1/μ_2) between layer and enclosing medium, Hudleston (1973b) has experimentally shown that buckling can occur at much lower viscosity contrast; ratios of 10/1 were obtained for folded granitic pegmatites in pelitic material (Hudleston 1973c, p.130). Even without a reliable viscosity contrast value, evidence for their relative competence during D4 was given by the analysis of fold shapes (cf. Ramsay 1967, Coward 1973, Francis 1973, Toogood 1976) as well as other structural features as discussed below.

Fold shape analysis of fifty-six F4 folds by the 'dip isogon method' (Ramsay 1967) suggest that quartzofeldspathic gneisses were the most competent rocks in domain 1, followed by amphibolites and biotite-rich bands of gneisses (Table 6.1). The acidic gneisses gave rise to Class 1 folds (predominantly 1C) while in the amphibolites and biotite 'schist' Class 3 geometry folds were developed (Fig. 6.4). The overall effect in some fold trains is of a Class 2 fold geometry produced by the alternation of Class 1C and Class 3 folds. This would allow the folds to propagate indefinitely as showed by Ramsay (1967, pp.430-436). Despite this overall geometry the isogon patterns show that these folds have not been formed regardless of the lithology. Although (slight) variations in composition along each layer can be expected due to the origin of these bands (possibly by metamorphic segregation), and a perfectly planar attitude before folding is not very likely, these assumptions are considered not to have caused major interferences in the geometry of the folds discussed here.

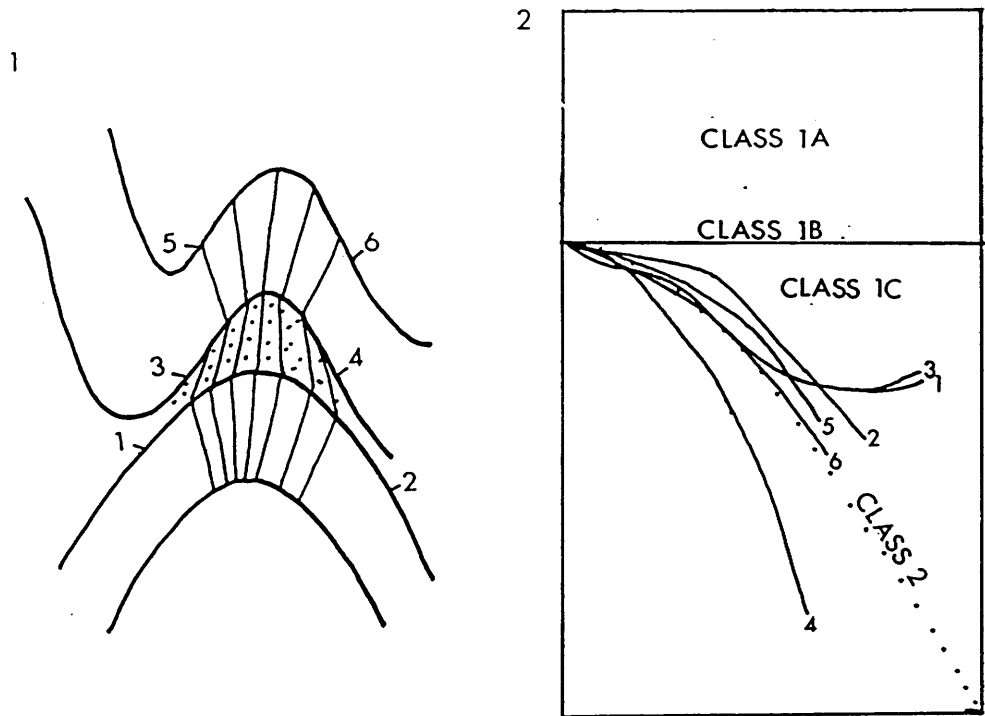


Figure 6.4 Interbanded gneiss and biotite schist (stippled). (1) shows isogon pattern and (2) the plotting of limb shapes in Ramsay's classification diagram

(see fig.6.1b).

The results of a 'visual harmonic analysis' (Hudleston 1973a) of 50 W/4 folds (Table 6.2) seem to confirm the isogon pattern method, with 2D and 3D as the most common shapes and $2D \rightarrow 2E \rightarrow 2D$ (Fig.6.5) corresponding to gneiss-amphibolite-gneiss interbanding.

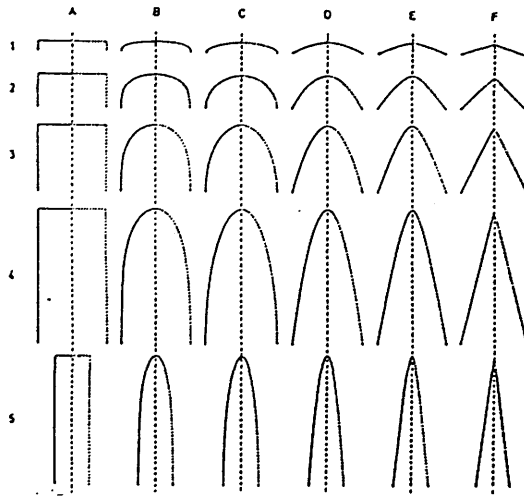


Figure 6.5 Visual harmonic analysis. 30 ideal fold forms, defined between inflexion and hinge points. 6 categories of 'shape' A-F; 5 categories of 'amplitude' 1-5 (Reproduced from Hudleston 1973a, fig.12).

In the only example where an alternation of amphibolite and biotite 'schist' was observed the basic rock shows a Class 1C geometry while the micaceous one shows a Class 3 geometry. In some of these folds (Pl.3.31) the more ductile micaceous material was not present in sufficient volume to infill the dilation spaces; they were filled in with more soluble material which was probably washed away during weathering. It appears that the volume of these spaces is controlled by the variation in thickness of the folded layers, being particularly well-developed where a multilayered sequence of bands with variable thickness has suffered the same shortening (see Ramsay 1974, Figs 6 & 7). Departure from a typical chevron geometry shown by some of these folds can be explained in terms of variable thickness of the bands and relative proportion of competent and soft interbanded layers. In some of the folds the thin incompetent bands of the biotite-rich material shows extreme deformation. It has a rough foliation with the appearance of a 'melange', *i.e.* most of the material seems to have been dragged out along the fold limb by the action of the overriding competent layer

and then tightly compressed in the core of the fold (Fig.6.6). This 'foliation' is one type of the rare examples of a new (S4) fabric in these rocks. Its geometry and composition is, however, more similar to the S4 fabrics in the amphibole schist (domain II) than in the gneisses (at least at microscopic scale - see section 4.2.4) which do not show any mesoscopic scale foliation (see Pl.3.32). This is easily explained in terms of the diverse deformation history of these two layers (see Treagus 1983).

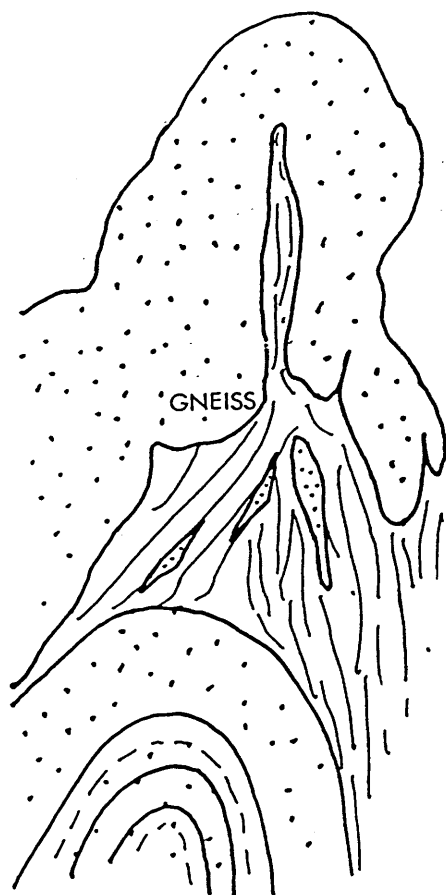


Figure 6.6 'Melange' of biotite schist in core of F4 antiform.

The approximately constant layer thickness around the hinge of some of these folds (Pl.3.31) would suggest, according to Ramsay (1974), that internal deformation of the competent layers is probably accommodated mostly by layer-parallel boundary shear, at least during the early stages of the deformation producing these folds.

The more ductile bands show slickenside^{lineations} at high angles to the fold hinges which are here interpreted as indicating displacement (by simple shear, mainly) towards the hinge regions with the less competent layer also acting as a 'lubricant' between the thick quartzofeldspathic bands. On the other hand the observation that some of these folds exhibit an inner arc sharper than the outer arc seems to indicate that tangential longitudinal strain was also active. This conclusion takes into account the fact that most of these shapes were probably formed during late stage 'homogeneous' deformation which caused the tightening of the folds. Figure 6.7 a,b, and c illustrates the sequence of events envisaged in the development of these folds.

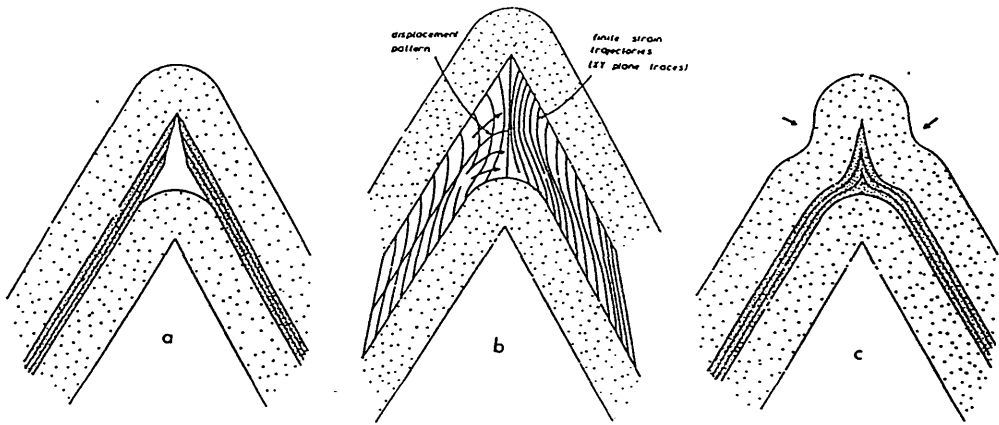
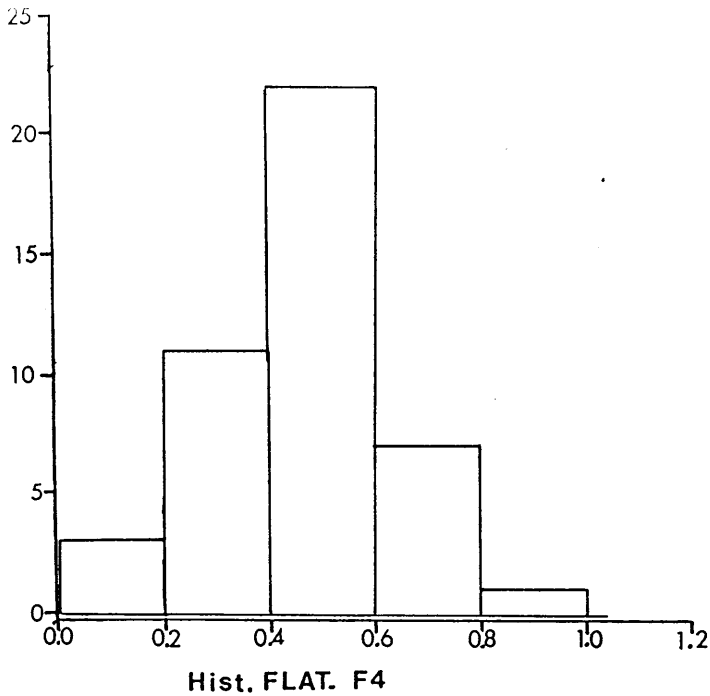


Figure 6.7. Potential dilation spaces giving rise to hinge collapse (reproduced from Ramsay 1974 Figs 13 and 14).

This determined sequence of 'events' is in agreement with observations of Ramsay (1967,p.397) that flexural slip and tangential longitudinal strain are commonly associated in nature. In the present case the late stage strain has probably overprinted the low tangential longitudinal strain, leading to the formation of Class 1C geometry folds. This implies that the deformation was not restricted to either fold limbs or hinges as predicted by fold development models (Ramsay 1967,1974), suggesting instead a combination of mechanisms, each one predominating during a certain stage of fold development as the most likely situation in nature (see also Gairola 1978). Accordingly Histogram 1 shows the results of the analysis of 44 F4 folds of domain I.



Histogram 1. Flattening of (44) F4 mesoscopic folds. Mean \approx 0.43; SD=0.16.

Most limbs present $(\lambda_1/\lambda_2)^{1/2}$ between 0.4 and 0.6 (see Table 6.1) which is a considerable high value for these (late) folds (corresponding to X:Z strain ellipses of 1:2.5 and 1:1.6 respectively). It should be kept in mind, however, that (a) these results were used as a relative parameter (in comparison with F2 folds) and (b) that significant homogeneous shortening has taken place in addition to the initial layer parallel shortening as above discussed. As noted by Ramsay (1967, p.415) the possibility of fold shape modification before flattening (tangential longitudinal strain) means that these results should be carefully interpreted because a bias towards low strains is introduced. However this does not seem to be the case here and the present results seem to be compatible with the ones obtained by Coward (1973) and Toogood (1976) for similar structures and rocks. Also, the analysis of strain based on fold shapes assumes coaxiality of the superimposed strain (Ramsay 1967, p.415) something which is very unlikely for these rocks and was an additional reason why no systematic quantitative strain analysis of these folds was carried out.

6.2.2.4 F3 Folds

The best developed F3 folds are observed in domains II and III. Chevron styles are ubiquitous in domain II possibly as a function of the finely multilayered nature of the lithology and their properties (viscosity contrast). Folds of this age in domain III

show round hinges. All the aspects of layer thickness - limb length control on the geometry and tightness discussed above for the few (F4) chevron folds were also observed in these folds (Pls 3.45 to 3.52). The structures indicative of the strain distribution in more concentric F3 folds are very similar to those observed in some of the F4 folds. They are also consistent with the strain patterns reported by Stephansson (1976), Spang and Groshong (1981) and many others, suggesting that they were formed under similar conditions (folding mechanisms) to the structures investigated by those authors. Distinguishing features include the more frequent occurrence of straight limbs in folds with constant limb length and layer thickness (Pl.3.52). The folding of few slightly thicker bands gives rise to hinge dilation which in this fold set is filled by quartz and carbonate, the latter being usually later dissolved out (Pl.3.50). The presence of the 'sinks' and abundant mineral transformations (chloritization and opaque minerals) suggests (1) the action of pressure solution mechanisms with transportation of material to distances considerably larger than the grain scale, as well as (2) a higher fluid activity than during D4 (see Chap.7).

Other factors which can be used to distinguish these folds from their F4 counterparts in terms of strain distribution are the smaller viscosity contrast between the layers with different composition and the action of more ductile deformation mechanisms at the grain scale (Sect.4.2.3). These have apparently controlled the formation of features such as (1) the variation of interlimb angle, frequently observed to be unrelated to layer thickness (Pls 3.44/45), (2) the formation of an axial planar spaced cleavage (Pl.3.45), (3) limb thrusts (Pl.3.49) and (4) curvature of the axial plane (Pl.3.47). The strong and more pervasive nature of the (folded by F2) composite banding when compared to the less developed S2 foliation might have inhibited the slip between these bands. As experimentally shown by Ghosh (1968) the friction between layers is an essential factor in flexural slip folding, with low friction favouring concentric or congruent folds while kinking is more likely at higher friction conditions. This seems to be supported by comparison of D3 microstructural features in domains I and II (Sect.4.2.3). In the former domain the

reactivation of the banding by slip was assisted by the presence of thin biotite-rich units while in the latter the 'stick up' effect has promoted the development of limb thrusts or 'flexural-slip thrusts' (Kuenen and de Sitter 1938 in Ramsay 1967). According to experiments performed by these authors a system of shear planes can be developed as a result of flexural slip folding, particularly in more homogeneous layers. This was confirmed by Ramberg (1961), who suggested that such shear planes are likely to develop in folds with $t/w < 1$ to 3. Although these rocks show a well-developed banding (suggesting that much of the slip could have happened between the layers during the early stages of deformation) the presence of the principal shear planes oriented at approximately 60° to the axial plane and conjugate to the small 'limb thrusts' (Fig.6.8) indicates that these structures are formed under 'semi-brittle' conditions. This is also so for the amphibole schists, regardless of the interbanded-looking nature of the lithology indicating that the viscosity contrasts between the amphibole and plagioclase-rich bands are practically ineffective at this stage probably as a function of the low ductility of the material (almost brittle behaviour). In this case the rock behaved as the homogeneous material of Kuenen and de Sitter (1938 in Ramsay 1967).

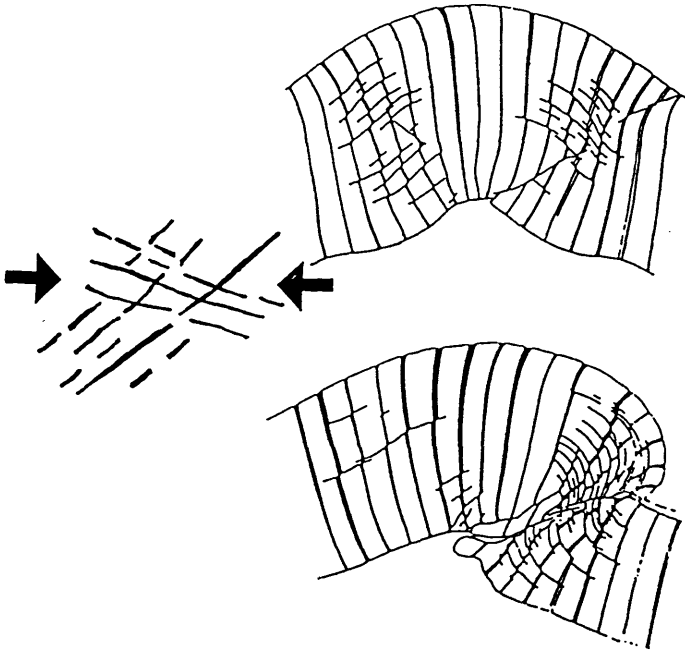
The observation that in the mica-schists these limb thrusts bear no relationship to (1) the fold hinges or to (2) the small inner arc inverse faults (Pl.3.59) or (3) structures like slickensides (all these indicative of 'tangential longitudinal strain') suggests that they were formed due to the impossibility of accommodating the overall shortening by folding only.

In terms of viscosity contrast during D3 it seems that the feldspar and amphibole-rich bands have a lower contrast than quartz and mica schists (of domain III); this is suggested by the geometry of the more evolved folds and thrusts in the metasediments (Pl.3.58). It appears that during D3 the lithological control on the geometry of the structures was not strong enough to overcome the deformation mechanism; thus it was probably a function of the relatively high structural levels (i.e. P,T,X, strain rate etc.) under which these structures formed.

Pure shear strain with the axis of maximum compressive stress

parallel to the orientation of the layering produces symmetrical upright folds with axial planes perpendicular to the axis of maximum shortening. However, if a shear couple is established during progressive deformation the resultant folds are asymmetrical with axial planes inclined opposite to the sense of layer-parallel shear where friction between the layers is low (Reches and Johnson 1976). On the other hand under high friction conditions the development of one set of kink bands inclined into the layer parallel shear direction is the observed feature. Other more complex models for producing asymmetrical folds involving both pure and simple shear have been proposed in the literature (cf. Ghosh 1966, Smith 1977, Hoepfner *et al.* 1983). Although none of these appears to explain all the features associated with these folds, it is suggested here that pure shear and interbanding slip had an important role during the development of these folds. As the presence of SW and NE 'transport direction' indicates, there was no unique sense or direction of movement for these thrusts (although most of them show a direction of transport towards the SW) so that the development of thrust planes could have occurred along any of the principal shear planes (Fig.6.8) or even propagate along the banding in a more advanced stage of development. In addition the absence of large displacements along these 'limb thrusts' (the one in Pl.3.58 was the largest observed) suggest that the thrusting was due to relatively local accommodation of the strain and would not imply large overall simple shear as the deformation controlling process (see Chap.8). In this way it is also likely that both fold and thrusts were formed under the same overall strain regime during progressively decreasing ductility conditions.

Figure 6.8 Development of flexural-slip thrusts in deformed, initially homogeneous slabs of clay (modified after Kuenen and de Sitter, 1938 in Ramsay 1967, fig.7-80).



6.2.2.5 F2 Folds

Class 1C followed by Classes 2 and 3 is the order of abundance of F2 fold geometry in domains I and II. Class 2 geometry is relatively more frequent in the amphibole schists where it is observed particularly in the mafic bands. In most cases the presence of features like 'parasitic' minor folds holding wavelength/layer thickness ratios and in some (rare) cases saddle reefs (Pl.3.34) demonstrate the active character of these competent bands during fold development. However, some of these structures affecting feldspathic bands show a Class 2 geometry (isoclinal folds) considered as being typically formed as 'passive' folds. De Sitter (1964) and Ramsay (1967,p.411) have proposed that homogeneous strain on a Class 1 fold can produce a fold with geometry very similar to a Class 2 fold, so that 'similar folds can be envisaged in mathematical terms as parallel folds which have been subjected to an infinite compressive strain' (Ramsay 1967,p.413). This is not an unlikely possibility particularly if we consider the lack of precision of the fold classification system that makes it very difficult to distinguish between strongly 'flattened' flexural folds and 'true' similar folds at high limb dips (Fig.6.9). However, in addition, there is the problem that the viscosity contrast needed to produce the fold has to disappear during the late flattening stages, so that it can flatten in a homogeneous way. This lead Hudleston (1973a) to propose that the folds initiated in an active low viscosity contrast layer and that the deformation proceeded by a combination of buckling and flattening. Following a simulation of this process Hudleston (op.cit.pp.41-43) concluded that the geometries of the resulting folds vary between parallel (almost only buckling) and similar (involving large components of flattening). In a plot of $\tan \alpha'$ against α for natural and experimentally produced folds, the difference between the two sets of curves (flattened buckle folds and simultaneous flattening and buckling) is minimal, being slightly more evident in folds of high limb dips (Fig.6.9).

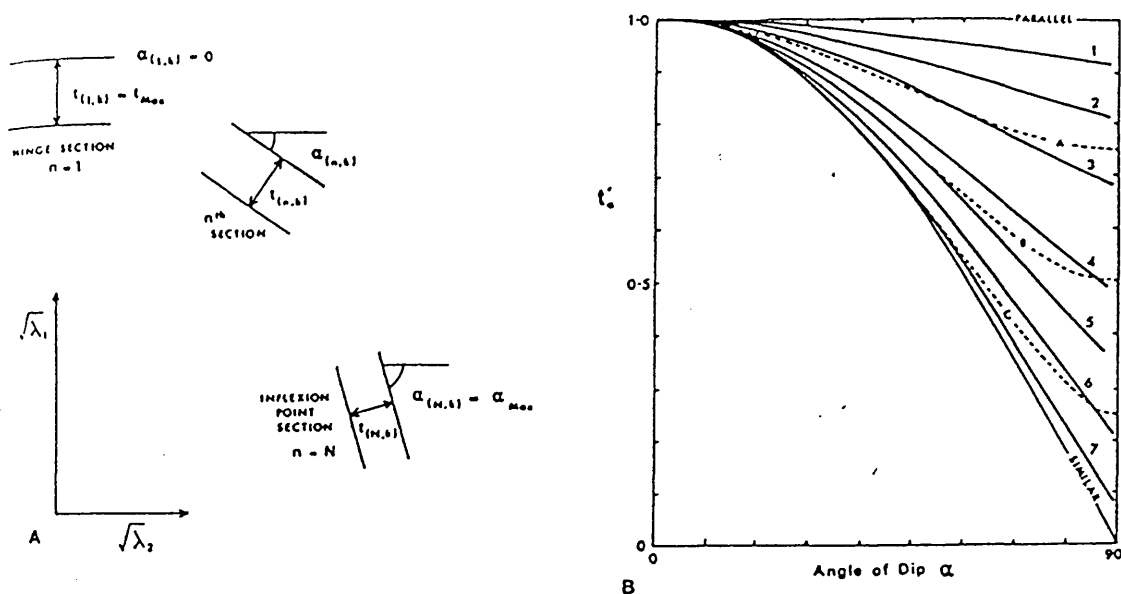


Figure 6.9. Simultaneous buckling and flattening of folds. A. Three of the N discrete sections of the fold model, after k increments of buckling and flattening. The quadratic elongation directions are those of both incremental and finite strains in the hinge section, and of incremental strains only in the other sections. B. Curves A , B and C : thickness variations with dip in parallel folds flattened by strains of $(\lambda_2/\lambda_1)^{1/2} = 0.75, 0.5$ and 0.25 respectively. Curves 1-7: thickness variations with dip in folds formed by simultaneous buckling and flattening (Reproduced from Hudleston 1973a, fig.23).

According to Hudleston (1973a) the reason why many folded competent bands seem to show geometry close to ideal flattened parallel folds may be related to (1) decreasing rheological contrast between the layers during deformation; (2) increasing resistance to continued buckling in the layer exerted by the enclosing medium as the fold closes and the less competent material is extruded from the inner arc zones (the competent layer might be forced to take up deformation by flattening) and (3) a process of simultaneous buckling and flattening affecting a parallel fold (Hudleston 1973a, pp.42-43). Although Hudleston regards reason (1) as 'the most unlikely to hold as a general rule', the presence of several features seen to indicate significant variations of viscosity contrast during deformation of the rocks at Loch Maree and these are the subject of the following discussion.

In the present work evaluation of competence contrast has relied heavily upon fold shapes, 'lobate & cusped' structures (Ramsay 1967, p.383) and boudinage. Cleavage refraction was not observed in these rocks (see sect.6.2.2.6) and the absence of suitable strain markers in adjacent bands of different composition means that these two features could not be used as viscosity indicators. It is perhaps relevant to mention that even in highly deformed (D1)

feldspar phenocrysts in porphyritic amphibolites no boudinage was observed, suggesting a low (or non-existent) viscosity contrast between them and the matrix (Sect.6.3).

The interbanded quartzofeldspathic gneisses and amphibolites show evidence for viscosity 'swapping' from D1 to D4. Where affected by late D1 boudinage the mafic bands in amphibolites were more competent than the quartzofeldspathic gneisses (Pls 3.8/9). However, the presence of cusped and lobate structures at the cores of some F1 folds indicates an early stage of D1 involving buckling when the gneiss was more competent than the amphibolite (Fig.6.10). This latter relationship seems to be maintained during most of D2 deformation, when features indicating a viscous gneiss (particularly fold shapes) are widespread. Considering that in several cases the same bands at a specific structural level are being dealt with the lateral variations of composition and different positions on a large fold (i.e. hinge or limbs) are unlikely to be responsible for this behaviour. The influence of other potentially controlling factors is discussed below.

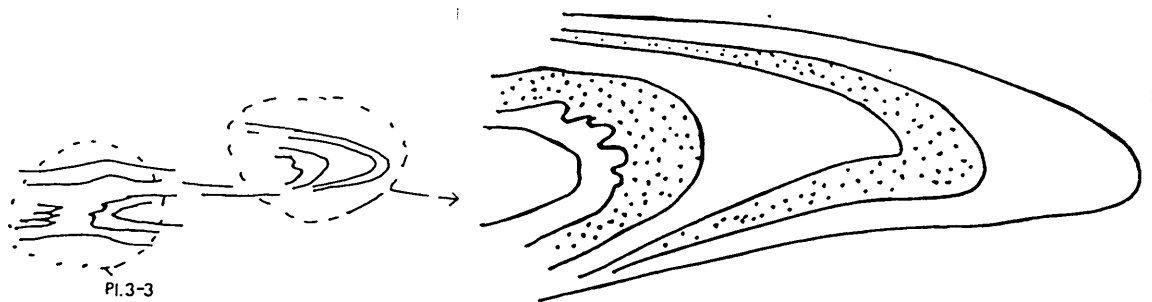
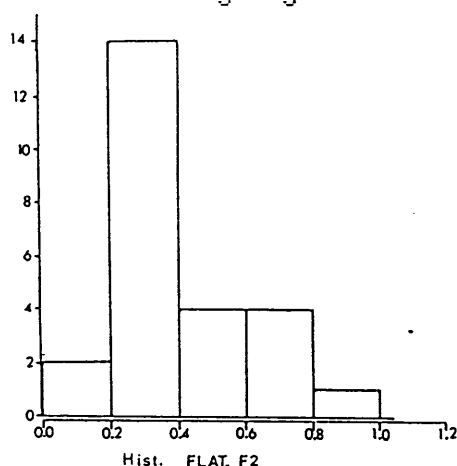


Figure 6.10 Cusped and lobate structures associated with F1 folds in mafic and felsic (stippled) bands of 'banded amphibolite'. Variation of viscosity contrast reported in the literature has been frequently attributed to metamorphic changes during progressive deformation. Granulite facies basic rocks were thought to have been retrogressed to biotite amphibolites (Coward 1973, Francis 1973, Ramsay 1982) or had their competence contrast reduced by syn-migmatitic biotitization (Sengupta 1983). However this explanation is certainly not the best one for the Loch Maree rocks. There is no evidence for a granulite facies metamorphism. If the mineralogical transformations from a 'soft' biotite-amphibolite to a 'harder' (than the gneisses) pyroxene granulite during late D1

was the cause of boudinage, this (hypothetical) metamorphism should have taken place relatively rapidly (between the early F1 buckling and the F2 shortening) and what is more unlikely, should have disappeared leaving no traces (see Chap.7).

The F2 fold shape analysis in interbanded amphibolites and gneisses produced the same results obtained for F4 folds i.e. Class 1C geometry folds for the quartzofeldspathic gneisses and Class 3 geometry for the amphibolites. Results of the visual harmonic analysis from few samples confirm the above pattern with (1) shapes $2D \rightarrow 2E \rightarrow 2D$ for amphibolite sandwiched between gneisses and (2) flattening of Class 1C folds showing higher values than for F4 folds (Histogram 2).



Histogram 2. Flattening of (25) F2 folds. Mean \sim 0.37;SD=0.2

Cusped and lobate features are quite commonly associated with both F2 and F4 fold phases; they are also occasionally observed in F1 folds. These features have cylindrical shapes (the 'fold mullions' of Wilson 1982). They are formed where a competent layer is shortened parallel to the layering and are the result of a mechanical instability. These structures have been shown in experimental and mathematical models to be controlled by viscosity contrast and layer thickness (the same factors which control the geometry of buckle folds) and can be observed to be folded at larger wavelengths (Smith 1975,1977,1979, Cosgrove 1980, Fletcher 1982, Sokoutis 1987). While evidence for competence contrast and buckling during D1 are rare the presence of late D1 boudins and F2 parasitic minor folds is quite common. This is, however, a function of the strain intensity since the F1 folds represent a

much higher strain state than the D1 boudins or F2 folds so that it does not diminish the importance of the former features indicating buckling during the early stages of the development of these (F1) folds (see Sect. 6.2.2.6).

Although Ramsay (1982) suggested that mullions or cusped-lobate structures indicate $\mu_1/\mu_2 < 10$, Sokoutis (1987) reports a much wider range of viscosity contrast (1/10 to 1/1000). He also demonstrates that the shape of the features produced is very much a function of the bulk shortening, so that at low viscosity contrasts, a much higher strain is necessary to produce cusps and lobes (Sokoutis 1987, p.241). Considering the geometry of the structures and the generally high strain shown by these folds (although the observed structure was in the core of a relatively low strain F1 fold) it is possible that the viscosity contrast was not very high and, as will be discussed below, inverted during progression of the deformation.

Ramsay (1982) called attention to the danger of estimating values of viscosity ratios on the basis of assuming that the materials involved have a linear behaviour. As already mentioned (Chap.5) there are several factors other than P-T conditions which can control the linear or non-linear behaviour of the material under deformation. The analysis of the geometry of boudinage and other features provided gives an opportunity of evaluating the behaviour of rocks (as opposed to monomineralic aggregates - see Chap.5) under particular conditions. This is because even if the exact flow laws controlling the deformation are not known (e.g. being assessed from microstructural evidence during D1 mylonitization, cf. Chap.5), it can be observed that some 'materials' have flowed more readily than others. In this way, it is not just the deformation conditions of each mineral that are important but also the influence of the combination of the several mineral species and how it affects the flow of the rock.

As briefly discussed in chapter 5 the problems of evaluating the flow laws are extremely complex since even monomineralic aggregates show different stress/strain curves from single crystals (of the same species, Fig.6.11), a feature attributed to 'orientation softening' (White et al. 1980) in the single crystals (Gandais and Willaime 1984, p.200). Examples of the complex interplay of

factors were observed in several lithologies at Loch Maree, and include the more competent behaviour of white quartz bands in mica-schists and gneisses, despite the observation that quartz seemed to be softer than muscovite (during D1 mylonitization) and quartzites generally more ductile than gneisses in high grade rocks (Ramsay 1982, p.118).

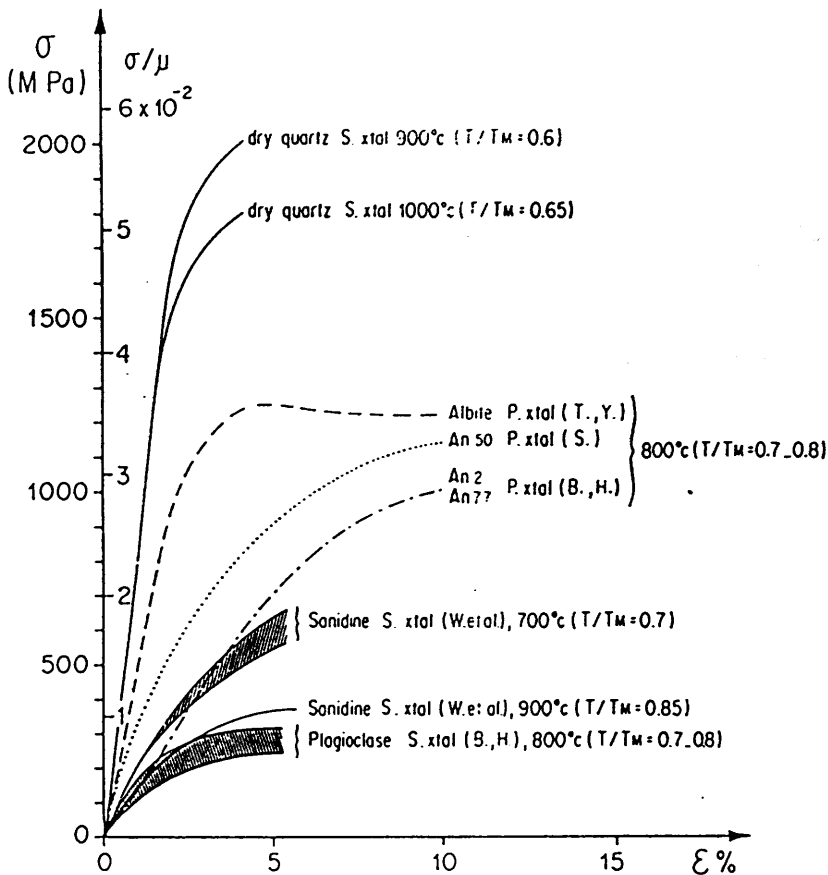


Figure 6.11 σ/ϵ (stress/strain) curves for feldspars. S.Xtal: single crystals; values from Borg and Heard, 1970 (B.H.) and Willaime et al., 1979 (W. et al.);

hatched areas represent the variations of σ as a function of the crystal orientation; the softest orientations are considered. P.Xtal: polycrystal; values from Borg and Heard, 1970 (B.,H.), Seifert, 1980 (S) and Tullis and Yund, (1980) (T.,Y.). The values for dry crystals of quartz oriented for basal glide are from Blacic, 1971 (see also Griggs 1967). (Reproduced from Gandais and Willaime 1984, fig.3)

Where thin pure ultramafic amphibole bands showing (D1) pinch-and-swell structures, immersed in more mafic bands sandwiched between felsic layers were affected by D2 shortening they formed 'parasitic' minor folds. This indicates that the ultramafic bands were more competent than the enclosing medium during D1 extension and shortening (Pl.3.20). Considering that the mafic bands of amphibolites are more competent than the felsic ones (Pls 3.8/9), this ultramafic layer can be considered also more competent than the felsic bands (of these rocks) during the late D1 extension event. A very similar relationship was observed with quartz bands in muscovite schist. They show pinch-and-swell structures attributed to D1 and cusped-lobate features associated with D2 shortening (Pl. 4.26). A possible reason for this behaviour is the nature of the predominant deformation mechanism in each of these rock types: while quartz deforms by (e.g.) dislocation glide the micas deform by a more efficient mechanism such as grain boundary sliding. As discussed in Section 5.3 the predominant deformation mechanism of these minerals and aggregates will not necessarily be the same during all stages of the deformation (e.g. grain boundary sliding needs a minimum grain size to take place) and so will not be the flowing properties of the rock.

As noted by Gandais and Willaime (1984, pp.220-221) the softening effects of water seem to be one of the most important controlling factors on the deformation of different mineral species. Experimental work shows that dry quartz is harder than feldspar (Fig.6.11) while the reverse is true in naturally deformed rocks. This indicates that the softening effects of water are more important in quartz than in feldspar. According to Tullis and Yund (1980) this weakening process is complex, depending on the equilibrium concentration of water which is in turn controlled by P, T and fluid composition. Experiments on polycrystalline aggregates comparing feldspars and other minerals have demonstrated that feldspars are weaker than quartzite at 600°C and ~ 2000MPa whereas the reverse is true at 900°C and 300 to 2000MPa (Shelton and Kronenberg 1978). Kronenberg and Shelton (1980) also showed that plagioclase is stronger than clinopyroxene below 800°C but

softer above this temperature.

The above discussion indicates that a reversal of the relative viscosity between the particular rock types could have been caused by any of the factors set out, or a combination of them. In addition it could have taken place without necessarily involving significant mineral transformations, something which was not observed in these rocks. As will be demonstrated in chapter 7 variations of P-T-X conditions between early M1, late M1, and M2 did occur and they might have played an important role in the progression of the deformation within the mylonite zones. However, these variations did not promote mineralogical changes away from these zones of severe grain size reduction (cf. Sect. 7.3) and are probably not responsible for the competence variation as it has been suggested, somewhat simplistically in the literature (cf. Coward 1973, Francis 1973, Ramsay 1982).

Modelling by Parrish et al. (1976) has produced similar folds (using the finite element method) in a quartzite layer in marble matrix, with both layer and matrix deforming according to experimentally determined non-linear flow laws. They recorded a reversing of viscosity contrast for these rock types at around 500°C due to the strong temperature-dependence of the viscosity of wet quartzite (Fig. 6.12).

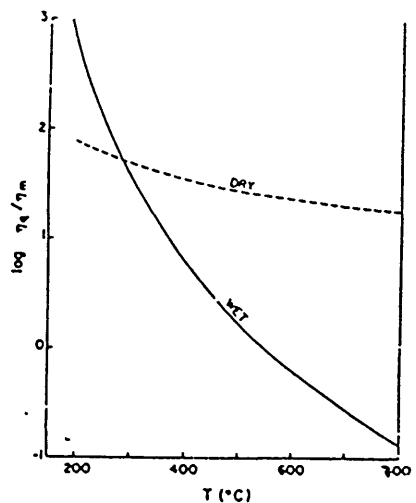


Figure 6.12 A plot of log quartzite/marble viscosity contrast at

$\dot{\epsilon} = 10^{-14}/\text{sec}$ as a function of temperature. The high temperature-dependence of the wet quartzite:marble contrast is a direct consequence of the strong temperature-dependence of viscosity of the wet quartzite (Reproduced from

Farrish et al. fig.6b).

The fold formation model then proposed, involves initial amplification of the fold at temperatures lower than 500°C (when the quartzite buckles), followed by flattening at slightly higher temperatures (550°-600°C). The 50-100°C temperature difference required is attained during progressive metamorphism, and would reduce the viscosity contrast, making then possible the formation of similar folds (Farrish et al. 1976, pp.204-205).

The investigations of boudinage and the formation of mullion structures in Newtonian and non-Newtonian materials by Smith (1975,1977) led to the conclusion that, in nature, the more competent material is often the more strongly non-Newtonian, and at fixed values of P,T and strain rate, it is the one with larger grain size. However, no significant grain size variation was observed between boudins and 'matrix' in the Loch Maree rocks. Accordingly, with the possible role of P-T conditions already assessed the influence of strain rate needs to be evaluated. In addition, the observation that amphibolites and mafic bands showed high relative viscosity during extension as opposed to low viscosity during compression (early D1 and D2) suggests that the differences of flow properties between both these types of deformation could also have played a significant role.

Finite strain values and mechanisms of deformation (pure x simple shear) are one of the most obvious differences suggested by these structures. Despite the low viscosity contrast geometry of the boudins (implying that much higher strains than the suggested by the geometry of the structures could have been achieved) the boudinage was interpreted as indicating lower strains than the folding on the basis that rocks are generally weaker under extension than under compression (Paterson 1976, Jaeger and Cook 1979) particularly under ductile deformation conditions (Etheridge et al.1984). The boudins also suggest a predominance of pure shear, while simple shear (or a simple shear component) is more likely to have been important in the development of the folds where

a non-coaxial strain path is the rule rather than the exception (Stephansson 1976, Dietrich and Carter 1969). In addition since boudinage implies compression at high angles to the layering while low angles are suggested by the buckle folds, another important difference is perhaps the role played by the existing anisotropies in relation to the local stress system. The influence of some of these factors has been discussed by Parrish et al. (1976, p.205) who suggested that an additional mechanism for viscosity contrast reduction would operate where an anisotropic lithology (in their case a mica schist in the Loch Maree rocks the amphibolites) interlayered with a less anisotropic band (quartzite against felsic bands at Loch Maree) are compressed at high and low angles to the foliation. During the boudinage stage (the better foliated) amphibolite would be more viscous (at constant T°) than during buckling because of the ease by which micas could deform by translation gliding parallel to the basal plane (but see discussion in Section 5.3.2.3). Although this mechanism could explain the situation of quartz bands within mica schist suffering initial buckling and later flattening due to the viscosity contrast reduction, as a function of fold limb rotation (increasing angle between anisotropy and maximum principal compression direction), it fails to explain the much more common situation of boudinaged quartz bands in mica schist observed in low grade metamorphic rocks.

Pfiffner and Ramsay (1982) registered the markedly non-linear accumulation of finite strain with time and showed how a comparatively small variation in strain rate leads to great differences in the finite strain during a given period of time. They also called attention to the fact that sequences developed during subphases could reflect the non-continuous character of deformation with time periods of high deformation being relatively short (cf. Dahlstrom 1970, Pfiffner 1978). On this basis it is unlikely that strain rates were constant during D1 and D2, something which is to be expected from knowledge of the driving forces for deformation (Oxburgh and Turcote 1974, Johnston et al. 1977, Turcote 1982).

As pointed out by several authors (e.g. Elliott 1973, Gandais and Willaime 1984) the deformation mechanisms are unlikely to be maintained under variable strain rates because of their different efficiency in dissipating the deformation (see Section 5.3). In addition diffusion mechanisms leading to Newtonian flow laws of the Nabarro-Herring type are slower and more likely to be replaced by non-Newtonian mechanisms (Elliott 1973, p.2659) so that the possibility of viscosity contrast inversion is favoured.

These considerations have been used to infer that flow laws vary as a function of stress and strain rate on the scale of a single fold (Parrish 1973). In addition with increasing stress or strain rate, the flow mechanisms change in such a way, that the stress dependence of strain rate changes from linear to power to exponential. In this way while a power flow law might be applicable over most of the fold (of his non-linear model), low and high strain rates were registered in the outer and inner hinge respectively.

Since most classical studies have used a linear rheological law (cf. Ramberg 1960, Biot 1961,1964, Sherwin and Chappel 1968) the implications of changes in viscosity contrast seem to be alarming in terms of modelling fold formation mechanisms. However, Chappel (1969) defends the validity of this assumption since (1) those studies were restricted to folds of low amplitude and (2) it is during this stage that the wavelengths are determined: he concludes that "the dominant wavelength analyses are probably valid for most layers of composite rheology" (p.114). More recently, Hudleston (1973c, p.121) and Stephansson (1976, p.157) have proposed that linear Newtonian viscosity is not strictly necessary for application of the theory of stress orientations during folding since flow of rocks can be considered in terms of 'effective viscosity' which is a function of strain rate.

The existence of such a 'viscosity contrast variation' makes it possible for active folding to be replaced by passive folding (e.g. Escher and Watterson 1974, Ramsay 1980) contrary to most views expressed in literature (e.g. Hudleston 1973a, Ghosh 1974, Treagus and Treagus 1981). Accordingly, folds produced by Hudleston and Stephansson (1973) in experiments where increments of buckling and

homogeneous shortening (theoretically only possible when $\mu_1 = \mu_2$) were added separately, are the best reproduction of the geometry of natural folds (Hobbs et al. 1976, p.204).

Variations of viscosity contrast might help to explain features such as the 'anomalous behaviour of hornblende-rich rocks' reported by Toogood (1976, p.143). In addition, the strong D1 transposition inferred for the amphibole-bearing rocks of domain II at Loch Maree, that are generally taken to be quite competent (cf. Ramsay 1982), may represent a more common situation than initially recognized (Fernandes 1986). It also suggests that variations of viscosity contrast can occur in a complex way so that competence contrasts relations cannot be considered as valid for long periods of time involving complex deformation (Laxfordian cycle) as proposed by Wheeler et al. 1987, p.160. The need for research in this area is summarized by Hobbs et al. (1976, p.206) as follows: "since the mathematical theory for the viscous situation has now reached a stage where the nucleation process and the variation of dominant wavelength with layer shortening in Newtonian materials is well understood...the pressing need is to develop analytical approaches for materials with non-linear relationships between stress and strain rate...."

Non-cylindrical, disharmonic and convolute F2 folds

Strongly non-cylindrical plane (F2) folds are particularly common in mylonitized rocks of domains I and II at Loch Maree. They have variable geometry (Fig.6.13) with 'B' values (Williams and Chapman 1979) rarely below 90°.

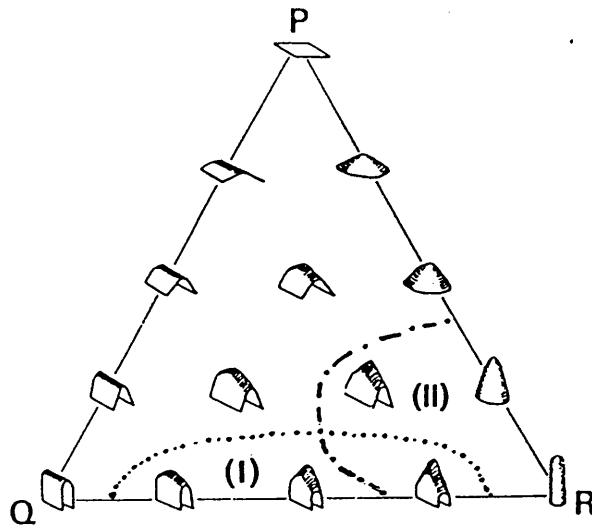


Figure 6.13 The variety of fold shapes and their positions on the PQR diagram. (a) Diagrammatic representation of fold shapes. (I) Loci of F1 folds. (II) Loci of F2 folds. (Slightly modified from Williams and Chapman 1979, fig.2a)

From their geometry most of these folds would be better denominated 'flattened non-cylindrical plane folds', plotting in field (I) of Figure 6.13. As previously described (Chap.4) the curvilinear hinge folds are intimately associated with 'supercylindrical' folds suggesting a genetic link between these fold geometries. The incipient stretching lineation and weak axial-planar foliation showed by the non-cylindrical folds would indicate that they represent a less evolved stage of the same process which produced the 'supercylindrical' folds. This possibility and other evidence of the mechanics of (F2) fold formation will be discussed below.

Detailed studies of fold geometries and strain patterns in natural and experimentally produced folds suggest that buckling is a suitable mechanism to form non-cylindrical folds (cf. Sherwin and Chappel 1968, Cobbold 1976, Gairola 1976, Johnson 1977, Dubey and Cobbold 1977). Features such as periclinal shapes and bifurcation of hinges, observed in some of the Loch Maree folds and experimentally produced by Dubey and Cobbold, were attributed by these authors to three possible factors (or their combination) viz.:

- (1) amplification of non-cylindrical deflection (cf. Sherwin and Chapel 1968);

(2) hinge lengthening slower than amplification;
(3) interference of different wavelengths. The amplification of a deflection (factor 1 above) or several initial perturbations (cf. Lewis and Williams 1978) does not account for the following commonly observed features:

(1) the development of these folds on a high strain tectonic surface as opposed to a sedimentary layering;
(2) the folds affect a considerably thick sequence of bands and seem to show a spatial periodicity (saturation model of Cobbold 1979) and;
(3) they are probably a recurrent feature being developed on successive generations of banding/foliations (Ghosh and Sengupta 1984).

Thus in a further development of this (modified buckle folds) model, it was suggested that the initial fold geometry was passively modified, as part of a progressive deformation during which simple shear played a predominant role (cf. Carreras et al. 1977, Quinquis et al. 1978, Cobbold and Quinquis 1980, Ramsay 1980). A detailed sequence of events to account for the geometry of these structures was proposed by Ghosh and Sengupta (1984, 1987), based on the evolution of three successive coaxial fold sets in India. The proposed model involves buckling with the production of non-cylindrical folds. As a function of strain or mechanical inhomogeneities inherent in anisotropic rocks the mechanical properties of the rocks would vary across and along the shear direction in different segments of the bands. Initiation of buckle folds would preferentially occur in the relatively weaker and easy-gliding segments of the deforming rock so that relatively discontinuous non-cylindrical folds would be generated. With progression of the deformation the hinges would be extended into parallelism with the strong (stretching) lineation. Accordingly, this sequence of events can perfectly account for all the features associated with the F2 folds at Loch Maree (see Chap.3) reinforcing the previous suggestion that non-cylindrical ($B = 120^\circ$) folds represent an incipient stage of evolution of these (F2) structures.

On the other hand, the *convolute and disharmonic* geometry of F2 folds in some outcrops is very similar to that of 'viscous folds', structures attributed to 'flowage of melt' by McLellan (1984). But

as recognized by the above author, "other processes in the solid state and at lower grades can give folds of similarly varied geometry and orientation" (p.341). On this basis the disharmonic folds in the Loch Maree rocks are interpreted as having been produced mainly by buckling.

Ramsay (1967, p.418) proposed that disharmonic folds are formed where the buckles are independent of one another, being a function of the large distances between the layers (greater than their initial wavelength). Although this relationship is very difficult to demonstrate in the Loch Maree rocks, the following features seem to support the action of buckling during the early stages of development of these folds:

- (1) some sort of periodicity and wavelength/thickness control on single folded layers.
- (2) Class 1C and Class 3 geometry in quartz bands and mylonitized mica schist respectively (see Table 6.1);
- (3) 'Parasitic' minor folds in (more competent) quartz bands holding relationships between wavelength and layer thickness as well as patterns indicating tangential longitudinal strain in hinges of microfolds (Sect. 4.2.2.3);
- (4) Sinusoidal shapes with (occasional) nose detachment (Pl.3-17) and frequent lobate-cusped structures along contact quartz mica schist (Pl.4.26) and frequent association with pygmatic folds ('elastics' of Ramsay and Hubber 1983, p.12).

Although there is no direct evidence for non-Newtonian behaviour of these feldspathic bands (e.g. Pls.3-15,56), Agostino (1971) has shown experimentally that for materials of non-linear flow, the orientation of axial planes of folds varies with the disposition of the competent bands, having little relationship with the orientation of the strain ellipsoid. These conclusions have been confirmed by de Capraris (1974) who proposed that a wide range of wavelengths and complex forms will be produced during deformation of non-Newtonian materials. In this way, despite factors like:

- (1) lack of distinct generations of microfabrics and;
- (2) invariable association of these structures with mylonitic rocks, most of the disharmonic and convolute folds are attributed to D2 deformational phase and its interference with D1 structures.

Factor (1) above can be explained in terms of the general lack of relationship between these structures and the strain ellipsoid (Agostino op.cit.) so that most of the D2 shortening is dissipated by buckling of these (competent) feldspathic bands within (incompetent) mica-rich mylonitic gneisses and quartzofeldspathic schists. Another clear indication of viscosity contrast between these quartzofeldspathic layers and enclosing medium is the observation that quartz bands tend to form ptigmatic folds (in profile section), while the feldspathic bands give rise to convolute and disharmonic structures. The association of these folds with mylonitic rocks (factor 2 above) can be explained in terms of the production of strongly contrasting viscosity bands during mylonitization (feldspathic and micaceous and quartzose layers, cf. Sect. 7.3) as well as the mechanism of deformation (buckling originated by mechanical instabilities within the shear zone). In addition, the action of D1 and D2 processes during the formation of these convolute structures cannot be ruled out on the basis of the lack of a coherent geometry since outcrops with this geometry of folds are of subordinate occurrence (see also Sect. 3.3 and discussion of kinematic models below).

6.2.2.6 F1 FOLDS

Kinematically important features associated with these folds include;

- (1) Lobate and cusped structures along the boundary between mafic and felsic units in amphibolites (Fig. 6-10 above) and the geometry of Class 1C \rightarrow 2 folds of the few analysed shapes;
- (2) Good development of these folds in well-interbanded units;
- (3) Parallelism of fold hinges with the shape fabric expressed by elongation of quartz aggregates and feldspar phenocrysts in the porphyritic amphibolites;
- (4) NW-SE elongation of sheath folds, that were also observed in rocks in which mylonitic features are incipient or absent.

Features (1) and (2) above indicate the action of buckling during the early stages of development of these (F1) folds. Features (3) and (4) suggest the increasing importance of simple shear with progression of D1 deformation culminating with the development of the mylonites (see also Sect. 6.3).

Despite evidence for simple shear during the development of these folds the mechanism envisaged here to have controlled their development does not follow any of the three classical models for formation of similar folds. Three of the general models which have been extensively discussed in the literature (Flinn 1962, Ramsay 1962, 1967, Hudleston 1973a) are (1) inhomogeneous simple shear parallel to the axial surface of the fold and at high angles to the layering, (2) differential flattening giving rise to differential shearing which is transmitted throughout the rock mass and (3) homogeneous strain superimposed on initially parallel folds.

Models (1) and (2) imply passive behaviour of the layers and were criticized by Flinn (1962, p.425) for their two dimensional nature as well as the lack of discrete potential shear planes (in several similar folds), along which the shear was supposed to take place. Although the first of these models (1) could account for features like the 'flame' folds (Pl.3.1) without having to face the difficulties of absence of discrete shear surfaces (Hobbs 1972) since S1 is well-developed (see also Mattauer et al. 1981) it is a two dimensional model and fails to explain the observed buckling features. It cannot account for the large extensions parallel to the fold axes, so that these ('flame') folds are better explained as a product of high deformation of cusped and lobate features (cf. Fig. 6-10), under conditions of decreasing viscosity contrast (overprinted by simple shear at later stages). Model (2) seems also to be inadequate since it fails to explain both (a) the periodicity and buckling-related features associated with many similar folds and (b) the absence of a (underlying) more competent layer from which the differential shear (due to differential deformation) is transmitted (in any case these effects would not be propagated to distances greater than about one initial wavelength- cf. Ramsay 1967, p.416). Thus if the evidence for viscosity contrast variations (Sect.6.2.2.5 above) is also considered, a modification of model (3), to include the large extensions parallel to the fold hinges recorded, can be a suitable model. Several aspects of this (envisaged) evolution model will be discussed below.

Hinge Parallel Extension

Treagus (1981) when discussing the deformation of viscous layers in progressive (and obliquely oriented) compressive strain emphasized the distinct strain styles for layers of different viscosity. The competent ones show relatively low strains and the extension lineation initially perpendicular to cleavage-bedding intersection may become closer to parallelism at high strains, when k value (Flinn 1962) becomes >1 (field of apparent constriction of Ramsay and Wood 1973) while the high strain incompetent layers show a mode of deformation similar to simple shear. Variable values of elongation parallel to the fold hinge were also reported by several authors (Ayrton and Ramsay 1974, Gairola 1977, Watkinson 1975). However, despite the fact that they reproduce features such as the remarkable cylindricity as well as the low amplitude to wavelength ratio of some of the F2 folds, they cannot account for the large bulk extension values recorded (Sect.6.3) or the evidence for simple shear mechanisms associated with several of these folds.

Hobbs *et al.* (1976) have reviewed the origin and problems of interpreting lineations that indicate hinge-parallel extension. Several types of lineations discussed by these authors were observed in the Loch Maree rocks. They include mineral lineations marked by (1) dimensional and crystallographic orientation of amphibole crystals, (2) deformed feldspar phenocrysts and (3) deformed quartz and other mineral aggregates. Although rotation has certainly occurred (particularly in high strain zones) oriented growth is a more likely explanation for the amphibole lineation. It is compatible with the metamorphic conditions and also accounts for the presence of this lineation in low strain zones of amphibolites, where feldspar phenocrysts show little or no evidence of deformation (although they are recrystallized throughout - see Chap.4). The other types of lineations include rods, mullions and boudins as well as (disrupted) hinges, and are more likely to have suffered considerable rotation at some stage of their development.

Hinge parallel extension is undoubtedly the most difficult of the observed features to be explained, so that any model capable of successfully explaining this feature (which is ubiquitous in the mapped rocks) can also account for the orientation and strain state

of rods, mullions and boudins. As discussed by Hobbs et al. (1976) the model of development of folds with hinge parallel extension (Nicolas and Boudier 1975, Watkinson 1975) is only adequate where low strain values (<15%) are recorded and because of space problems, is particularly problematic where fold hinges have low plunges. 'Apparent hinge-parallel stretching' produced by superimposition of strain ellipsoids on to already elongated objects, as suggested by Ramsay (1967, p.220), is a theoretically valid possibility but which does not apply to the present case where the strain markers show initial random distribution and orientation. Also the suitable superimposition of two or more strain ellipsoids (Grocott 1979), which seems to be a good qualitative explanation for the strain pattern (see Sect. 6.3), encounters problems in explaining (i) the continuous progressive nature of the deformation from constrictions to flattening (interpreted as associated with the NW-SE translation of the basement rocks and (ii) the magnitude of strains recorded (cf. Sect.6.3).

The association of D1 deformation with the strongest mylonitization episode has been well documented (see Sect.6.3), so that the process of formation of these folds must be compatible with the formation of the mylonites and the translation of the basement gneisses over the supracrustal sequence. In this way it is suggested here that simple shear has played an important role not only in the development but also in the reorientation of already existing (F1) folds (some of which, in domain 1 might have been formed during pre-Laxfordian times - see Chap.8). The mechanism is the same proposed for the F2 structures with the difference that much higher strains are attained during D1 (the F2 folds can be considered as a lower strain state of the same deformation see discussion below). Well-developed sheath folds are formed from amplification of original deflections or internal mechanical instabilities (at shear strains >10). Linear structures are rotated towards the (NW-SE) movement direction producing the remarkable colinear relationship shown by the D1 and D2 structures and the large values of extension recorded (Sect.6.3). Descriptive and experimental accounts of this type of mechanism are ubiquitous in the recent literature to which the reader is referred for

details (cf. Hansen 1967, Ramsay and Sturt 1973, Williams and Zwart 1977, Rhodes and Gayer 1977, Minnigh 1979, Cobbold and Quinquis 1980, Skjernaa 1980, Berthe and Brun 1980, Henderson 1981, La Tour 1981).

6.2.2.7 DISCUSSION OF THE KINEMATIC MODELS

The kinematic significance of lineation patterns has been debated for a long time in the literature (see Rhodes and Gayer 1977 for a review and Van Den Driessche 1986 for a more up to date discussion). Although several modern workers favour the here denominated 'longitudinal' model, where the transport direction is considered to be parallel to the linear fabrics (including fold axes) and to the length of the fold belt (cf. Shackleton and Ries 1984 and references therein), many others (cf. Lister and Price 1978, Mattauer *et al.* 1981, Duncan 1984, Lagarde and Michard 1986, Ridley 1986) discuss the 'transversal' model with transport direction at high angles to fold axes, parallel or transversal to a stretching lineation. This latter model advocates no major movement parallel to the length of the orogen and seems to be compatible with the kinematic interpretations of high structural levels of fold belts, particularly the Alps (cf. Schmid 1975, Siddans 1979, Beach 1981, Ramsay 1981, Pffifner 1981 and references therein). The controversy still persists (see Jacobson 1983, Van Den Driessche 1986) and it is mostly a function of the inadequacy of either model to include all the observed features. It is also a function of the failure to recognize the influence of factors such as:

- (1) the structural level under investigation. Since in a thrust pile the different units could exhibit diverse transport directions, the presentation of data relative to several structural levels of an entire 'fold belt' in a map (*e.g.* Hossack and Cooper 1986) can be very misleading;
- (2) the recognition of the true stretching character of lineations, the shear nature of the deformation zone or the presence of varied magnitude of shear zones within the 'fold belt' (cf. Lacassin and Mattauer 1985);
- (3) the effects of strain intensity upon the existing structures.
- (4) the complex interplay between thrusting and strike-slip ('transpression') which can occur at the same time in different places or at different times in the same place of the mobile belt.

Trying to clarify these problems Hansen et al. (1965) have recorded the orientation of fold axes and 'slip lines' in portions of the Norwegian Caledonides and parts of the Appalachians and Alps. The observed pattern is transverse in the outer zones and longitudinal in the inner metamorphic cores, the latter being considered as 'compatible with large scale longitudinal transport' (Hansen et al. 1965, p.410). More recent research has shown that lineations do not lie only parallel or perpendicular to the length of the 'fold belt', but present a wide range of attitudes between these two extremes (cf. Lisle 1984, Shackleton and Ries, Hossack and Cooper 1986). This was interpreted as an effect produced by rotation of fold hinges towards the movement direction, as high strain zones related to large thrusts moving towards the foreland are approached (Ramsay 1979). According to this author, hinge rotation is not a late event in the fold history but progresses during fold development, being a function of the initial orientation of the hinge, magnitude and type of strain. In the Loch Maree rocks no intermediate stages of hinge rotation (especially of F1 folds) were observed. As previously described the folds were all either extremely cylindrical or sheath like. This is, however, a natural result of the criteria adopted for the distinction between the fold phases (see Sect.3.3) so that if the F2 folds are considered as part of the same (progressive) deformation, some of these (small) folds could represent initial stages of hinge rotation (e.g. Pl.3.18). It should be emphasized however, that no 'early' major folds with hinges at high angles to the linear fabric were observed. Assuming the 'longitudinal' model with NW-SE direction of movement, the only explanation for the absence of folds showing hinges at high angles to this direction, would be that the folds were already initiated strongly non-cylindrical (Rhodes and Gayer 1977). This would also explain the presence of open (relatively low strain) F2 and later folds (e.g. Pl.3.3) with hinges parallel to the strong lineation. These structures are unlikely to have been rotated towards their present position since according to Sanderson (1973) and Cobbold and Quinquis (1980) the strain involved with a 90° rotation would make them isoclinal. Recognizing this problem and based on the geometry produced by the anastomosing character of the mylonitic foliation, Bell (1978) and Bell and Hammond (1984) propose a model by which the 'lower' strain

folds would already nucleate with axes at low angles to the stretching direction as a consequence of the triaxial ellipsoid shape of the 'pods' surrounded by anastomosing mylonitic foliation (Fig. 6.13).

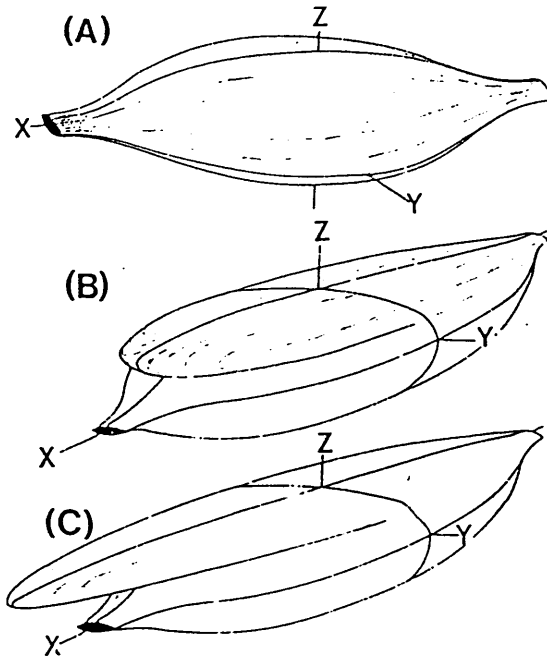


Figure 6.13. (A) Sketch of an ellipsoidal pod surrounded by anastomosing (mylonitic) foliation showing the divergence of L as well as S around the pod with respect to the bulk strain axes X, Y and Z. (B) Sketch showing a sheath fold produced by imposing a zone of inhomogeneous shear on the upper part of an ellipsoidal pod such as that shown in figure (A). Note the open style of the fold where it is oriented sub-parallel to the stretching lineation and that it has formed a sheath geometry without involving rotation of the fold axis. The X-axis of the bulk strain ellipse is approximately parallel to the long axis of the pod, and consequently much of the anastomosing (mylonitic) schistosity lies at a marked angle to the bulk XY plane. S in such localities is susceptible to folding during progressive mylonitization. (C) Attenuation and tightening of the sheath fold produced in (B) due to further inhomogeneous deformation. (Slightly modified from Bell and Hammond (1984, fig.6)

According to this model only a small volume of the rock would contain folds at high angle to the principal elongation direction. This model would also explain the rarity of features such as the

splay pattern expected during folding of the stretching lineation along the hinge zone of a developing sheath fold (Fig. 6.14) expected but not observed in naturally deformed rocks (Bell and Hammond 1984). The model, however, does not provide an adequate explanation for the asymmetry (towards NE), attitude, periodicity or the buckling related features presented by the Loch Maree folds.

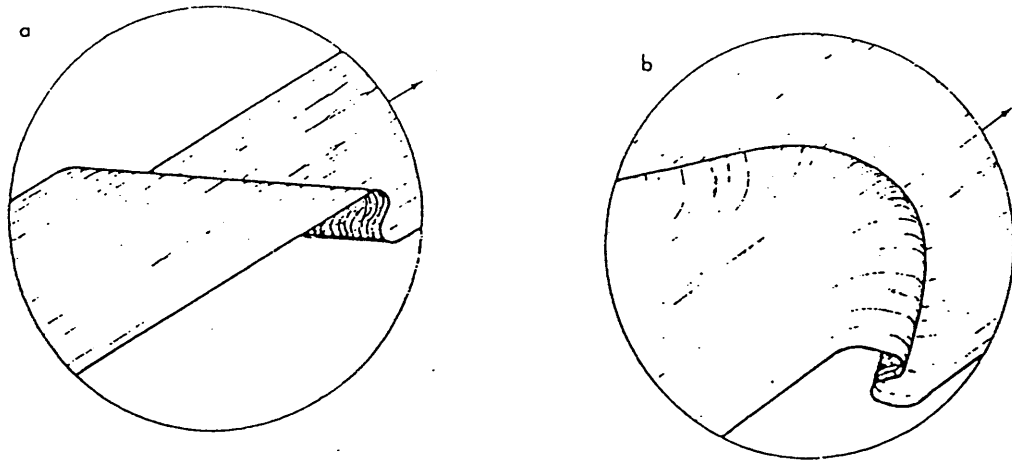


Figure 6.14. Two sketches showing the effect on an earlier formed stretching lineation of the formation and subsequent rotation of a fold initiated at a high angle to the bulk stretching direction. Figure a shows the fold geometry soon after its formation. Figure b shows the effect on the earlier lineation after subsequent rotation of the fold toward the bulk stretching direction. The older lineation could be expected to locally maintain a high angle to the fold axis. This geometry is rarely observed. (Reproduced from Bell and Hammond 1984, fig.11)

Another theoretically possible way of explaining the coaxial geometry of the F1-F2 fold sets is based on the role played by 'linear anisotropy' (Cobbold and Watkinson 1985, Watkinson and Cobbold 1981, Watkinson 1983). These authors have demonstrated that in rocks with a strong linear anisotropy folds will form with axes nearly parallel to this linear fabric for a variety of different stress fields. This model is adequate to explain some of the features of the Loch Maree rocks viz. (1) the colinear nature of the several fold sets, (2) the (restricted) thrusting towards SW

and NE associated with the F3 folds and (3) the F4 buckle folds, all of which could be produced by a NNE-SSW oriented compression. However, it is not capable of explaining the high (NW-SE) elongation strains recorded or the kinematic indicators of shear sense in the mylonites which are best observed in sections at high angles to the foliation and containing the stretching lineation (i.e. parallel to the length of the 'belt').

Lacassin and Mattauer (1985, p.741) drew attention to the problems of using geometrical analysis of folds as kinematic indicators. They hold the view that in highly deformed rocks fold geometry seems to be unrelated to the kinematic evolution. Referring to the work done in the Peninne nappes they pointed out that most studies have concentrated on the superimposed folding and little attention was given to the role played by shear and thrusting with the formation of stretching lineations. While their opinions seem to be rather extreme some of them could find support or evidence from the presently studied rocks. At Loch Maree, adding to the inconclusive evidence given by the folds in isolation, there is the regional context of these rocks. The Loch Maree rocks are part of a crustal-scale shear zones of Laxfordian age (cf. Coward 1984, Coward and Park 1987, see also Sect.8.3). This, together with (i) the lack of evidence for duplication of the stratigraphy during D1 and (ii) the abundance of small scale structures indicating simple shear, suggest the importance of the latter mechanism in the development of these 'Laxfordian belts.' While the 'longitudinal' model with a NW-SE movement direction is adopted here, finding support in the importance of simple shear mechanisms (in the early stages of deformational sequence D1-D2) and magnitude plus orientation of the strain markers, an elegant explanation to account for the geometry attitude and strain state of these folds altogether has still to be proposed. However it seems difficult and scientifically incorrect to assume that these structures bear no relation with the highly deformed rocks (as proposed by Lacassin and Mattauer op.cit.) since we can in fact recognize that they are also a product of this deformation. What seems to be a more likely explanation is that the present knowledge of the deformation processes is still not sufficient to produce a model capable of including all the features reported for these kind of rocks. In

any case a general model based on transpression seems to be able to accommodate most of the principal features displayed by these rocks (cf. Chap.8).

TABLE 6.1 RESULTS OF FOLD SHAPE ANALYSIS. I AND II REFERS TO DOMAINS.

CLASS 1C FOLDS	F2 MYLONITES (I)	F2 (II + I)	F4(I)
No of quarter wavelengths	61 (85%)	25 (66%)	44 (78%)
SHORTENING Arithmetic mean	0.293	0.370	0.431
Standard deviation	0.14	0.20	0.16
CLASS 2 FOLDS (W/H)	8 (11%)	10 (26%)	-
CLASS 3 FOLDS (W/H)	3 (4%)	3 (8%)	7 (12%)
CLASS 1A FOLDS (W/H)	-	-	5 (9%)
TOTAL-in quarter wavelengths	72 (100%)	38 (100%)	56 (100%)

TABLE 6.2 RESULTS OF 'VISUAL' HARMONIC ANALYSIS OF 25 F4 FOLDS FROM DOMAIN 1 (MOSTLY IN GNEISSES)

	A	B	C	D	E	F
1						
2			5	7	3	1
3		1	6	7	1	1
4		1	3	2	7	
5		1		1	1	2

6.3 STRAIN ANALYSIS

6.3.1 INTRODUCTION

The presence of variably deformed phenocrysts in porphyritic amphibolites (fig.6.14A below) provides a basis for assessing the geometry and intensity of strain which can then be compared with the strain patterns shown by other structures such as F1 and F2 folds. This approach is dependent upon the existence of practically undeformed phenocrysts (indicative of very low deformation) in a few limited areas: in most of the rocks the deformed phenocrysts are prolate to oblate shaped (Pls 3.11 to 3.13) resulting from low to intermediate magnitudes of D1 deformation (see Chap.3). No strain determinations were possible in the mylonites, which represent the highest strain conditions in the area (cf. Chap.5).

Due to the characteristics of the strain markers the R_f/θ method of Ramsay (1967) and Dunnet (1969) was used. In addition to being considered a very reliable technique, this method also gives information about the relations of strain to other features and permits the validity of the involved assumptions to be assessed (Hanna and Fry 1979, p.162). The following nomenclature is based on Lisle (1985) and Ramsay and Huber (1983) :

e (extension) = $(l-l_0)/l_0$, (l_0) being original length, (l) final length

X>Y>Z Principle axes of the strain ellipsoid

R_i, R_f, R_s Initial, final and strain ratio of an elliptical strain marker (long axis/short axis)

$R_{XY} = X/Y$ Axial ratio of ellipse on XY plane

$R_{YZ} = Y/Z$ Axial ratio of ellipse on YZ plane

$K = (R_{XY}-1)/(R_{YZ}-1)$

$e = \ln(1+e) = 1/2 \ln R$

$\ln R_{XY} = \ln(1+e_1) - \ln(1+e_2) = e_1 - e_2$

$$g = (RXY + RYZ - 1)$$

H = Harmonic mean of Rf values

θ' = Angle between the long axis of a marker and the established reference line

The strain data were obtained from measurements on (13) samples cut parallel to the principal sections of the strain ellipsoid (XY plane -S1 foliation) and subjected to the treatment set out by Lisle (1985). The shape of the final ellipse (Rf) is a function of the form and orientation of the initial and strain ellipse (Ramsay 1967).

Because of the time consuming calculations and uncertainties involved in the process (cf. Ramsay 1967, Owens 1984, Wheeler 1986) data collected on fracture surfaces at high angles to each other were not used.

Difficulties involved with the measurements in samples include the extreme elongation of most crystals, several of which were longer than the specimen. This meant that large markers as well as the ones representing the highest strain values of the specimen could not be measured. Sections containing X showed no variation of θ' so that the harmonic mean (H) was considered to be the best approximation to the strain. The viscosity contrast between phenocrysts and matrix was considered to be very low since foliation deflection and pinch-and-swell structures were very rare and no pressure shadows or even refraction of S1 across the amphibolite-gneiss contact were observed (cf. Gay 1968, Lisle 1985, p.24). Additional difficulties included the definition of the outlines and measurement of the short axes of small crystals, reinforcing the limitations (particularly quantitative) of the obtained values of strain.

6.3.2 Interpretation of the Results

The number and strain geometry of the analysed specimens bear no relationship with their abundance in the field. While 'L' tectonites were far more abundant than 'S' tectonites in domain I,

most of the specimens with this type of fabric could not be used because of the length of the deformed markers, frequently longer than the specimen. Specimens from the (prolate-oblate) transitional zone were difficult to obtain and rapid transition from prolate to S1 banding was the rule rather than the exception, so that almost all the analysed samples plot into distinct fields of the Flinn diagram (Fig.6.18).

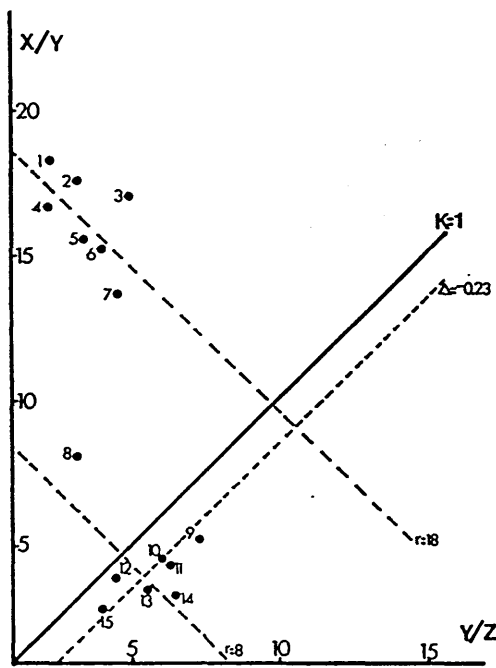


Fig.6.18 Flinn diagram of deformed phenocrysts (see text for details).

The heterogeneous nature of the deformation of these rocks (at the hand sample scale) means that the results obtained are a function of the choice of the samples and their processing. This can be illustrated by the analysis of one sample (L-198) whose results were used as guidelines for the processing of the remainder.

The strain heterogeneity is represented in Figure 6.14A (see also Fig. 6.19) sketched from a sample whose measurements are shown in

Table 6.3. The strain ellipsoid for this sample was calculated in two ways:

(1) The axial ratios of the strain ellipses were measured on the XZ and YZ planes. The axis Z was equated to the unit and the RXY was then calculated from the former relations (XZ & YZ). This axial ratio is presented as X/YCALC in Table 6.3. The resulting K-value strain ellipsoids are presented as KCALC and ELLIP.CALC.

(2) The axial ratio RXY was measured on surfaces parallel to the (S1) foliation. This axial ratio is presented as X/YMEAS, and the resulting K values and strain ellipsoid as KMEAS, and ELLIP.MEAS, respectively, in Table 6.3.

The T distribution (Fig.6.16A) is fairly symmetrical (symm.index=0.956) with few markers presenting a high fluctuation. This probably indicates an initial elliptical (r_i) shape which exceeded the strain registered for this section (R_s approx. 3.1), since a typical length/width ratio of 3 to 4 was assumed for the prismatic sections of these plagioclase crystals in dolerites. This assumption seems to have been confirmed by superposing the points distribution on to the standard curve ($R_s = 2.85$) given by Lisle (1985) reproduced here in Fig. 6.15d.

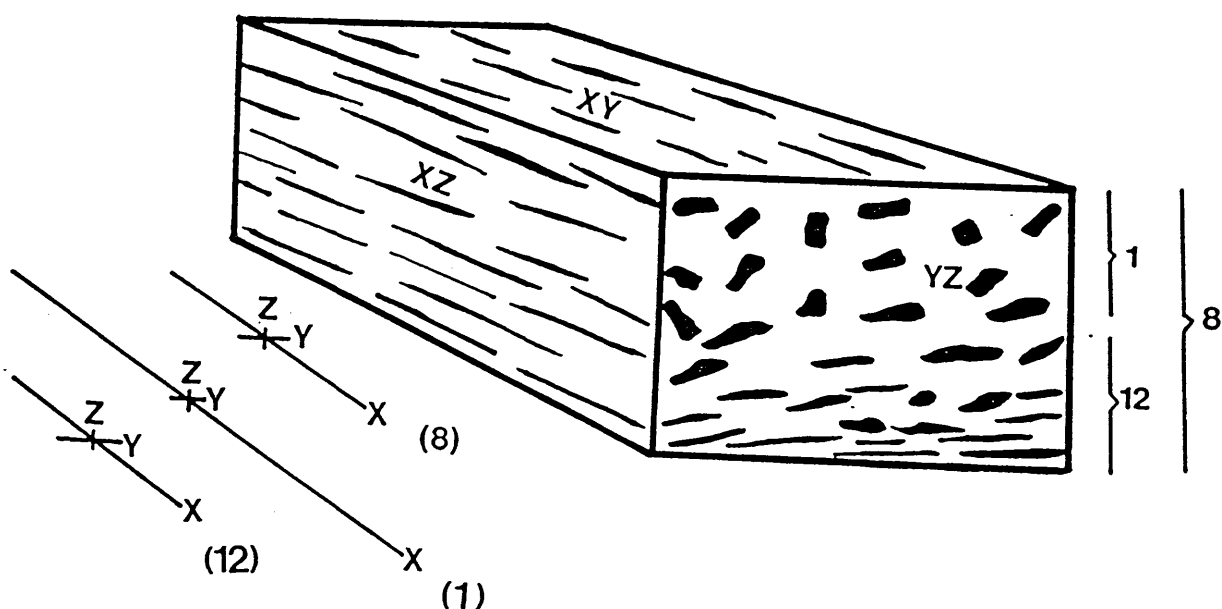


Fig. 6.14 Sketch from sample L-198 (NG 978712). Strain parameters are given in Table 6.3.

(a) Numbers 1, 8 & 12 correspond to separate analysis of top, bottom, and total sample respectively. The data are plotted on Figures 6.15 A,B,C and Flinn diagram of Fig. 6.18.

(b) Strain ellipsoids corresponding to the analysed parts of the sample. Measurements of sample no. 8 are as follows:

YZ (Rf/PHY)	XZ (H)	XY (H)
N = 69	76	89
(N = No. markers)		

Incompatibility of strain

A comparison between the results calculated by the above described different procedures show that the calculated and measured strain ellipsoid geometries would change if the specimen was treated as representing one state of strain (i.e. sample no. 8), the resulting ellipsoid shape would be different (prolate for calculated and oblate for measured). If the specimen is analysed after having been divided into two halves, the geometry of the deformation ellipsoid is maintained (samples no. 1 and 12 - Table 6.3) but the difference of K-values for the prolate strain is increased. This accentuated strain incompatibility (both methods above should ideally produce the same results) may result from the operation of a number of factors, some of which will be discussed below.

(1) Over-defined strain ellipsoid.

While an ellipse may be expressed by three parameters if the plane in which it lies is defined, an ellipsoid can be expressed by six parameters, the lengths and orientations of its three principal axes. Therefore three elliptical sections will overdefine the ellipsoid since they define a nine-parameter figure instead of a six-parameter figure. This is because any three ellipses may not necessarily come from the same ellipsoid so that they might not be compatible (Milton 1980).

(2) Heterogenous strain

Computer simulations of homogeneously deformed markers performed by Holm (1983) typically show a tight cluster at the centre of the R_f/θ diagram but naturally deformed markers are characterised by a distinct lack of this point concentration. This feature was attributed by Holm (1983, p.103-107) to the heterogeneous character of the natural strains, considered to be the only important factor differing between the compared deformed populations. He also pointed out that, although the assumption of homogeneous strain is inherent in the R_f/PHY method, its use is not invalidated at highly heterogeneous

strains. The main effect produced is to increase the scattering of the points, causing a reduction of the accuracy of the method, which in our case might have contributed to the strain incompatibility. In addition, the above referred author noted that if homogeneous strain is assumed, the scatter of points would incorrectly be attributed to effects of an initial fabric and/or shape of the strain markers (Holm 1983, p.109). However, in the case of the Loch Maree rocks, the true influence of the shape of markers can be demonstrated by comparing the results from the analysis of the sample shown in Fig.6.14A. The point distribution (Fig.6.15a) shows a positive correlation between low axial ratios (R_f) and high fluctuation in the Y_2 section producing a skewness towards negative values of θ' (Fig.6.16A). This asymmetric pattern which differs from a 'scattering' of points would be best interpreted as produced by the initial shape and orientation of the markers (flow banding?).

(3) Effects of the adopted technique

The calculation of the harmonic mean for each section containing X_i , and the assumption that it represents a reasonable approximation to the strains may have contributed to the strain incompatibility. According to Lisle (1977a) the harmonic mean is an efficient method under conditions of (a) homogeneous strain, (b) absence of a pre-deformation preferred orientation and (c) reasonably high strain ratios. While the possible effects of factors (a) and (b) was discussed above, the influence of factor (c) was considered to be minimal, even in sections perpendicular to the linear fabric (which are the ones showing the lowest values of the prolate strain - see Table 6.4).

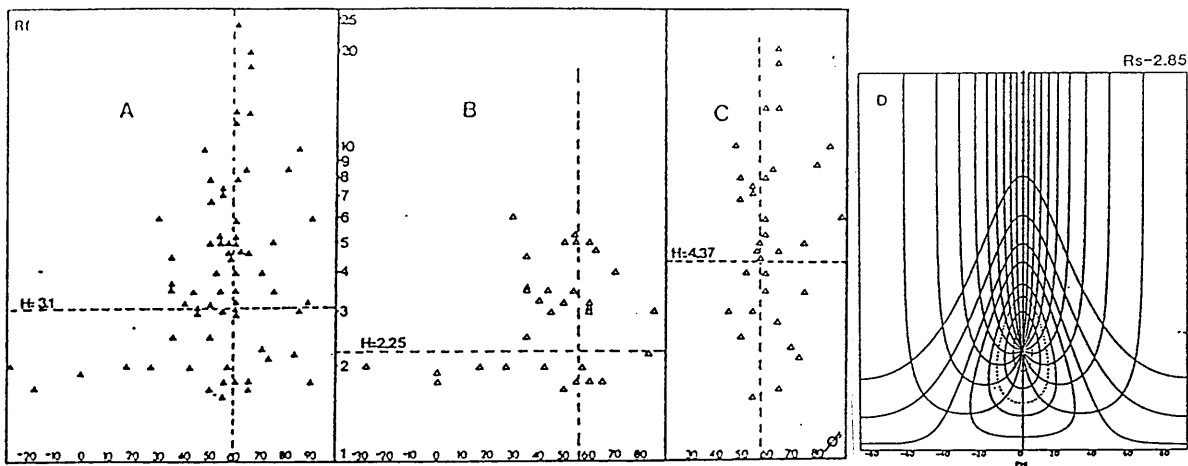


Fig. 6.15. Rf/PHI distribution of specimens shown in Fig.6.14. A- total (sample 8), B-top half (sample 1), C-bottom half (sample 12). D -Rf/PHI curve corresponding to point distribution of Fig.6.15A (after Lisle 1985).

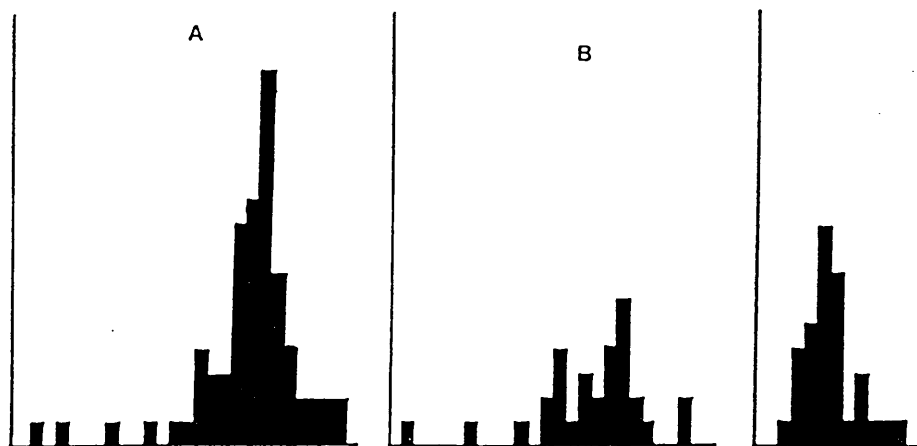


Fig. 6.16. Histograms of the plots shown in Fig.6.15. A,B,C correspond to A,B,C of Fig.6.15.

Figure 6.17 shows the variation of the harmonic mean (H) as a function of initial ratio (R_i) and strain ratio (R_s). Although this graph cannot be directly used for YZ sections (where R_s was obtained by comparison with standard curves) it gives an idea of the R_s differences to be expected and helps in the selection of the best fit standard curves.

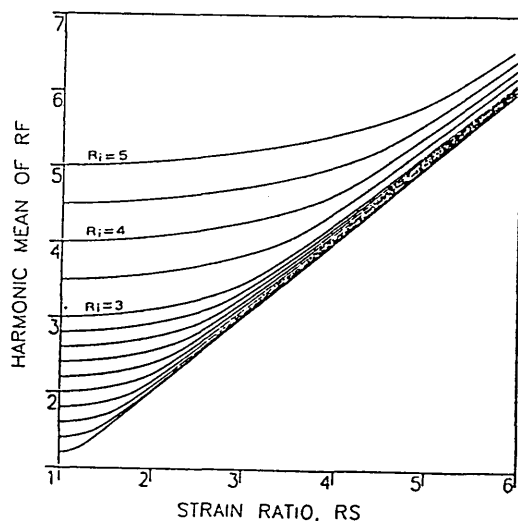


Fig. 6.17. A graph for estimating R_s from the harmonic mean of the axial ratios of deformed passive elliptical markers.

Accordingly, the value of $H = 3.1$ was obtained for sample 8, but the best fit curve was the one corresponding to $R_s = 2.85$ (Fig.6.15D). For high strain values, like those determined for all the other sections, the difference between R_s and H is insignificant (considering $R_i = 3$ to 4).

The strain incompatibility in sample 8 becomes even larger if a value of $R_s(YZ) = 2.85$ instead of 3.09 is used, indicating that factors, other than those presently discussed, are more important on its control.

- (4) The error involved with the measurements of specimens cut along the XY section should also affect the strain computations, in particular the oblate strain markers where a slight deviation from parallelism (with XY plane) would produce large variations in the measurements of the Y axis. However, a comparison between the measurements obtained for sample 1 (prolate) and sample 12 (oblate) shows that the

differences of RXY measured and calculated (Table 6.3) for oblate strain are much smaller (RXY calc./RXY meas. = 1.3) than those obtained for the prolate part of the sample (RXY calc./RXY meas. = 5.8), suggesting that the underestimation of X values would exert a stronger control on the RXY calc. values than mistakes on measurements of Y (compare RXY and RYZ meas. on both samples). Accordingly, if the calculated results are assumed to be the true ones, the values of RXY MEAS. of samples 1 and 12 (Table 6.3) would indicate an underestimation of X. This would be a more critical factor for the prolate strain as it is apparently confirmed by the largest discrepancy of both RXY (measured and calculated) corresponding to sample 1. However if sample 12 is treated as two distinct specimens there is no change of the resulting ellipsoid geometry, *i.e.* samples 1 and 12 are prolate irrespective of the method used ('MEAS.' or 'CALC.'). This conclusion had important implications for the treatment of the samples.

It seems that while factors (1) and (2) have promoted strain incompatibility, factors (3) and (4) might have even worked against it. Although factors other than the above discussed might be contributing to the incompatibility of strain (see discussion about volume variation below) the role played by strain heterogeneity seems to be of fundamental importance and the influence of this factor was kept in mind during all phases of this work, from the selection of additional samples to interpretation of the results.

6.3.3 GEOLOGICAL IMPLICATIONS OF STRAIN ANALYSIS

Despite the small number of specimens and all the above difficulties, the obtained pattern corresponds to that determined for deformed pebbles and associated thrusting in the Caledonides and Alps (Flinn 1956, Hossack 1968, Lisle 1984 and Rotschbacher & Oertel 1987). The prolate represent higher strains than the deformed oblate markers, with the ellipsoids almost invariably showing the same orientation of axes. This is at variance with the

conclusions reached during field work when oblate-shaped strain markers were considered to be representing much higher magnitudes of deformation than the prolate ones (cf. also Myers 1978), and emphasizes the necessity of strain measurements whenever markers are available.

The strain pattern and magnitude variations in the Loch Maree rocks are generally similar to those set out in the literature by Hossack 1968, Grocott 1979, 1984, Lisle 1984, Toriumi 1985, Toriumi and Noda 1986 and Ratschbacher and Dertel 1987, most of which were interpreted in terms of superimposition of two or more strain regimes. In several of these cases the longest axes of the finite strain ellipsoid represent an 'apparent stretching' direction which might not correspond to the translation direction (cf. Grocott 1979, p.475) being frequently parallel to fold axes (e.g. Ramsay 1967, p.220, Roy and Faereth 1981, p.57). In addition, if only the finite strain is recorded (i.e. the geometry of the ellipsoids corresponding to the superimposed episodes of deformation is unknown), it is not possible to be certain whether the constriction is true or apparent or the geometry due to flattening or plane strain. A superimposition model is, however, inadequate to account for the pattern obtained in this study, since there is no evidence for either deformation earlier than D1 affecting the phenocrysts or a larger scale distribution pattern of the strain geometry compatible with more than one 'episode' of deformation (e.g. Grocott 1979).

Remarkable features of this deformation include (1) the decreasing strain magnitudes from prolate to oblate strain geometry and (2) the rapid transition between these two types of strain. This deformation was frequently localized into zones (Pl.3.12) many of which, although not reaching the mylonite stage have developed a good planar fabric (see Chap.4).

Where mylonite does occur its association with D1 deformation was demonstrated on geometrical and kinematic basis (see Chap.3 and section 6.2.2.6) and from the field observation of the transition from prolate to oblate strain geometry to mylonite during D1. A natural prediction would be that the strain magnitude also increases from prolate strains in the 'host' rocks to oblate in the mylonites. However, this is not the pattern registered for the

Loch Maree rocks or for similarly deformed rocks elsewhere (cf. Flinn 1956, 1961, Hossack 1968, Lisle 1984). The decreasing strain magnitude as the thrust zones are approached observed by Flinn (1956, p.502) was interpreted as an indication that the deformation (of the surrounding rocks) was not caused by the movement on the thrust plane but was, instead, the cause of such movement (but see Milton and Williams 1981).

Magnitude of strain

The strain magnitude was expressed in terms of the parameters of r Watterson (1968, p.55), D and d of Ramsay and Huber (1983, p.202)

$$\text{where } r = (RXY + RKZ - 1) \quad (6.3)$$

$$\text{and } D = [(e1 - e2)^2 + (e2 - e3)^2]^{1/2} \quad (6.4)$$

$$\text{and } d = [(RXY - 1)^2 + (RYZ - 1)^2]^{1/2} \quad (6.5)$$

Increasing values of these parameters indicate increasing magnitude of deformation (see list of symbols). The values of r are shown as oblique lines in the Flinn diagram (Fig.6.18). The other two values (D and d) are only presented numerically (Table 6.4). A rapid comparison between the values of total strain corresponding to prolate and oblate geometry, respectively, shows that the values of D & d for these two geometries differ slightly (less than 15% and 10% respectively) while the values of r are markedly different. The latter is thought to reflect the way it is calculated more than the geological conditions so that it will not be discussed any further. Bearing in mind the small differences in values of 'total' deformation between oblate and prolate geometries, the wide gap and distance between the deformation fields and the origin (1,1) corresponding to these two types of strain in the Flinn diagram (Fig.6.18) are interpreted here as produced by the type of diagram chosen to represent these geometries (the logarithmic plot would bring these fields much closer together). Considering that the deformation magnitudes are not as large as they first appeared to be, as well as the identification of a similar pattern in other fold belts (as above referred), one possible explanation is that the registered pattern is a function of the limitations of the strain

analysis methods in determining the magnitudes of natural strains in these types of rocks. In fact, both Hossack (1968) and Lisle (1984) have applied the Rf/PHY method measuring the RYZ and RXZ (Hossack 1968) so that if the above explanation has any validity, it could suggest that this method introduces a bias towards prolate strains. Once high deformation is attained it becomes very difficult to measure the strain by any method, not only due to the magnitude of the deformation but because these are also preferential zones for chemical redistribution of components with formation of metamorphic banding (cf. Myers 1978, Ramsay and Allison 1979, see also sect.7.3).

Strain geometry

The strain geometry is difficult to explain. While features like the lack of intermediate strain markers between both deformation fields of Figure 6.18 are very much a function of sampling and the criteria adopted in their processing, the deformation field of flattening could have been produced by (1) modification (flattening) of markers initially deformed by plane strain or (2) volume change under essentially plane strain conditions.

Evidence for (1) has been discussed in sections 5.3.1 and 6.2.2.5. Ramsay and Wood (1973) have demonstrated that if there is a volume change during deformation the line separating ellipsoids of (apparent) constriction and (apparent) flattening, although keeping the same slope, is displaced either upwards (volume increase) or downwards (volume decrease). Assuming initial plane strain ($K = 1$) a best fit line through these points (of the flattening field) can be traced (Fig.6.18). A volume reduction (DV) of 23% is then calculated using equation 6.6 below.

$$e_1 - e_2 = e_2 - e_3 + \ln(1+D) \quad (6.6)$$

As explained by Ramsay and Wood (1973, p.269) the 'apparent flattening' is produced by shortening along the Z direction without a corresponding elongation along X, so that ellipsoids with oblate shapes do not necessarily imply extension along the Y axis. Evidence for volume change during D1 deformation includes the

formation of a continuous S1 banding by deformation of the phenocrysts (Chap.3) and other geochemical and microstructural features (see Chaps 4 and 5) which will be discussed in more detail in Chap.7.

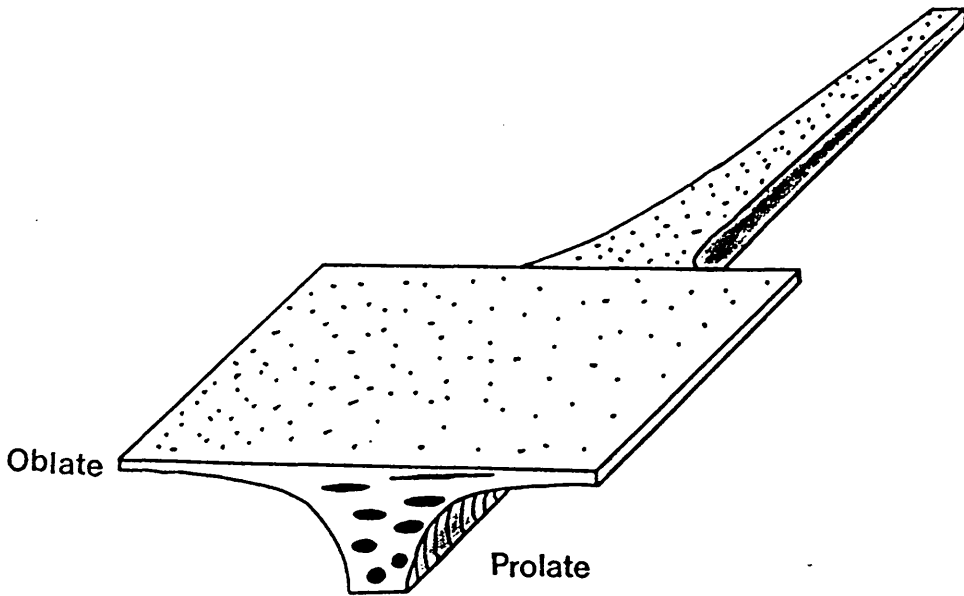


Fig.6.19. Geometry of a cube suffering prolate to oblate strain (no volume change assumed).

Prolate strains are difficult to explain geologically. Shear zone termination-related models were proposed by Ramsay and Allison (1979), Ramsay (1980), Coward and Kim (1981), Coward and Potts (1983) to account for this type of strain geometry (Fig.6.20).

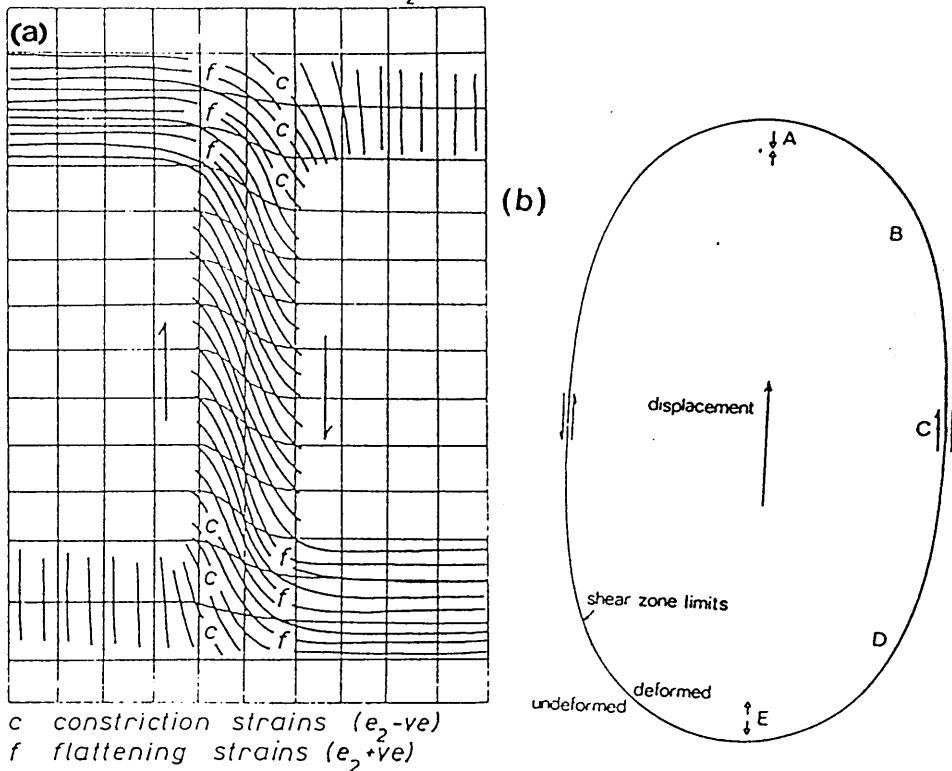


Fig.6.20. Types of strain distribution near the shear zone terminations. (a) Non-plane model. The heavy lines represent principal strain directions, points represent isotropic zones, f, and c, represent flattening ($e_2 +ve$) and constrictive ($e_2 -ve$) strains respectively (reproduced from Ramsay and Allison 1979 fig.14b). (b) Variations in k value within a shear zone, near the fault tips. At A, C and E the strains are of $k=1$. At B they tend to be more oblate. At D they tend to be more prolate. See text for details (reproduced from Coward and Potts 1983, Fig.23).

Although the scales are considerably different the same controlling mechanism of deformation (simple shear) is likely to have produced similar features (cf. Tchalenko 1970). It is suggested here that the transition between prolate and oblate strain is related to strain softening controlled localization of the deformation along narrow zones, leading to the development of mylonites (with an S-fabric) and associated thrusts. As the translation of successive units on several scales takes place structures indicating flattening and simple shear were developed in these narrow zones. The prolate strains although dominant in terms of volume would be restricted to the interior of the deforming 'pods' where the deformation was more homogeneous (Fig.6.19). The pattern of strain intensity increasing towards the underlying thrusts as noted by Chapman et al. (1979), Chapman and Williams (1981) and Law and Potts (1987) was not detected in the Loch Maree rocks. Although

the main thrust boundaries are marked by mylonites and no systematic study of strain variation on a large scale was carried out (in part as a function of the absence of suitable markers), the observation that the complete range of strain geometries and magnitudes was present in almost all scales of shear zones seems to indicate that this pattern is not simply related to the height of the markers within the thrust pile as suggested by Milton and Williams (1981). In this way, despite the apparent relationship between structural level and type of fabrics (predominantly 'S' cf. Schwerdtner et al. 1977) observed in domain III (considered to be a lower level in the thrust pile - see Chaps 2 and 7) this type of fabric is considered to have been produced by compositional rather than structural control, with the more micaceous units developing an 'S' fabric and the quartzofeldspathic an 'S>L' or 'L>S' fabric.

Bell (1981) called attention to the strain incompatibilities introduced by deformation models proposing pure and simple shear mechanisms. Law and Potts (1987) applying a pure and simple shear model to a Moine thrust sheet in Skye have recognized this problem and proposed that where two deforming juxtaposed domains are affected one by pure shear and the other by simultaneous pure and simple shear there is no strain incompatibility problem (Fig.6.21). This model is essentially that of Bell (1981) shown in Figure 4.1 considered in this study as the one which best reproduced the microscopic scale features (see Chap.4). As opposed to the discussed microstructural studies (Chaps 4 and 5), the contemporaneity of these two types of strain is more clear in the present case where no evidence for overprinting is observed. Modelling of strain patterns in terms of differing contributions of pure and simple shear in thrust sheets was presented by Coward and Kim (1981), Coward and Potts (1983), Sanderson (1982).

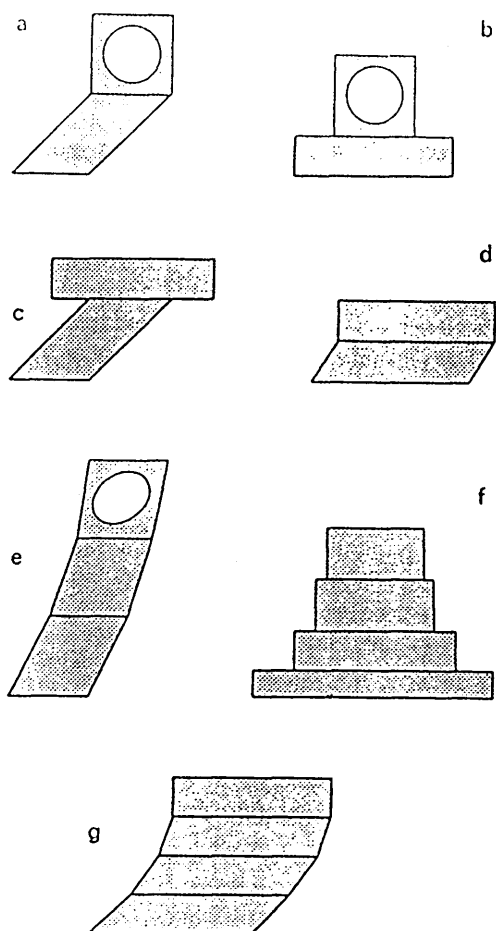


Figure 6.21. Strain compatibility considerations associated with juxtaposition of different kinematic domains. For simplicity deformation is assumed to be plane strain with X and Z in the plane of the diagram. (a) Undeformed domain underlain by zone of simple shear deformation. (b) Undeformed domain underlain by zone of pure shear deformation. (c) Zone of pure shear underlain by zone of simple shear deformation. (d) Zone of pure shear underlain by zone of combined simple and pure shear deformation. (e) Juxtaposition of three domains of simple shear deformation; angular shear strain increases downwards. (f) Juxtaposition of four domains of pure shear deformation; strain ratio increases downwards. (g) Juxtaposition of four domains with progressively changing combinations of pure and simple shear deformation; top domain is characterized by solely pure shear deformation whilst component of simple shear increases progressively downwards through the lower domains. Pure shear component is identical in all four domains. Note that strain compatibility is only maintained in situations (a), (d), (e) and (g). (Reproduced from Law and Potts 1987, fig.13).

TABLE 6.3 STRAIN FROM SAMPLE SHOWN IN FIGURE 6.14. See text for explanation and list of symbols for definition of parameters.

SAMPLE NO.	8	1	12
R(X/Z)	25.3	41.18	17.36
R(Y/Z)	3.09	2.25	4.37
R(X/Y)calc.	8.18	18.3	3.97
R(X/Y)meas.	2.91	3.11	2.99
K-calc.	2.64	8.13	0.90
K-meas.	0.94	1.38	0.68
ELLIP.calc.	PROLATE	PROLATE	OBLATE
ELLIP.meas.	OBLATE	PROLATE	OBLATE

TABLE 6.4. GEOMETRY AND AMOUNT OF DEFORMATION OF STRAIN MARKERS
(see Figure 6.18 for plotting of samples 'Sp').

Sp	R(X/Z)	R(Y/Z)	D	d	r
1	18.3	2.2	2.24	7.24	19.5
2	17.5	3.2	2.05	4.98	19.7
3	17.2	4.9	2.02	4.63	21.1
4	16.6	2.2	2.16	6.65	17.8
5	15.6	3.3	1.95	4.38	17.9
6	15.3	4.0	1.92	4.12	18.3
7	13.8	4.5	1.87	4.06	17.3
8	8.18	3.1	1.38	2.66	10.3
	TOTAL		15.59	38.39	141.9
9	5.3	7.3	2.01	6.30	11.6
10	4.7	6.0	1.80	5.00	9.7
11	4.3	6.3	1.87	5.3	9.6
12	3.97	4.3	1.47	3.37	7.3
13	3.6	5.4	1.72	4.41	8.0
14	3.3	6.4	1.96	5.42	8.7
15	2.8	3.9	1.40	2.91	5.7
	TOTAL		13.6	36.0	60.6

CAPTIONS OF DIAGRAMS (STEREONETS) 1-39

The data were processed with the use of the Statis program developed by N. Woodcock of Cambridge University. Unless otherwise stated; 1. all diagrams are equal area contoured plots; 2. planar features are represented by their poles; 3. n is the number of measurements; 4. M is the mean attitude sample; 5. S is the angular standard deviation; 6. C is the attitude of the axis of the best fit cone to data; 7. contours are in number of points per 100 per number of points % area.

DIAGRAM 1 Plot of S-composite (S_b+S_l)-total, domain 1; $n = 842$; contours <5, 5-15, 15-25, 25-35; contoured from points plot of Keppie 1967 folder 1 stereonet 4a.

DIAGRAM 2 Plot of F1 axial planes (S_1)-total, domain 1; $n = 96$; $M = 123/78$; $S = 42^\circ$; $C = 09/034$; contours <2 2-5, 5-8, 8-11.

DIAGRAM 3. Plot of F1 axial planes (S_1) NE limb, domain 1; $n = 53$; $M = 121/64$; $S = 38^\circ$; $C = 24/022$; contours <3, 3-5, 5-8, 8-11.

DIAGRAM 4. Plot of F1 axial planes (S_1)-SW limb, domain 1; $n = 43$; $M = 303/67$; $S = 42^\circ$; $C = 25/233$; contours <2, 2-4, 4-6, 6-8.

DIAGRAM 5. Plot of L1-total (mostly lineations), domain 1; $n = 765$; $M = 07/116$; $S = 23^\circ$; $C = 01/116$; contours <5, 5-15, 15-25, 25-35 and greater; attitude three concentration poles from E to S are 15/102, 16/119, 05/124.

DIAGRAM 6. Plot of L1-NE limb (mostly lineations), domain 1; $n = 564$; $M = 05/116$; $S = 24^\circ$; $C = 01/115$; contours <5, 5-16, 16-28, 28-33; attitude of E-SE concentration pole 15/100 and SE-S secondary concentration pole 13/126.

DIAGRAM 7. Plot of L1 SW limb (mostly lineations), domain I; n = 154; M = 13/119; S = 17°; C = 03/121; contours <4, 4-10, 10-29, 30-35.

DIAGRAM 8. Plot of L1 (stretched phenocrysts- mostly from SW limb), domain I; n = 47; M = 10/112; S = 15°; C = 05/107; contours <7, 7-14, 14-20, 20-26.

DIAGRAM 9. Plot of F2 axial planes (S2)-total, domain I; n = 188, M = 122/85; S = 31°; C = 10/025; contours <3, 3-7, 7-12, 12-18.

DIAGRAM 10. Plot of F2 axial planes (S2)-NE limb, domain I; n = 140; M = 126/90; S = 31°; C = 02/025; contours <4, 4-7, 7-11, 11-17.

DIAGRAM 11 Plot of F2 axial planes (S2)-SW limb, domain I; n = 48; M = 095/70; S = 25°; C = 11/012; contours <3, 3-7, 7-10, 10-13.

DIAGRAM 12 Plot of L2 (fold axes only)-total, domain I; n = 240; M = 16/125; S = 29°; C = 17/126; contours <3, 3-7, 7-12, 12-20.

DIAGRAM 13. Plot of L2 (fold axes only)-NE limb, domain I; n = 145; M = 17/128; S = 28°; C = 22/124; contours <4, 4-7, 7-10, 10-17.

DIAGRAM 14 Plot of L2 (fold axes only)-SW limb, domain I; n = 95; M = 11/108; S = 23°; C = 05/304; contours <7, 7-13, 13-19, 19-25.

DIAGRAM 15 Plot of F3 axial planes and L3 (fold axes-dots) SW limb, domain I; n = 49 (axial planes) 17 (axes); M = 82/299; S = 27; C = 87/320; contours <3, 3-5, 5-7, 7-9.

DIAGRAM 16 Plot of F4 axial planes-NE limb (mostly), domain I; n = 189; M = 328/86; S = 28°; C = 02/239; contours <3, 3-6, 6-10, 10-16.

DIAGRAM 17 Plot of L4 (axes)-NE limb mostly, domain I; n = 123; M = 29/149; S = 35°; C = 18/159; contours <3, 3-5, 5-8, 8-13.

DIAGRAM 18 Plot of F2 axial planes, domain II; n = 57; M = 301/81; S = 44°; C = 13/211; contours <3, 3-5, 5-7, 7-9.

DIAGRAM 19 Plot of L2 (mostly fold axes), domain II; n = 122; M = 30/126; S = 33°; C = 26/112; contours <2, 2-6, 6-10, 10-17.

DIAGRAM 20 Plot of F3 axial planes, domain II; n = 58; M = 255/10; S = 35°; C = 82/185; contours <2, 2-4, 4-6, 6-8.

DIAGRAM 21 Plot of L3 (mostly fold axes), domain II; n = 75; M = 05/291; S = 24°; C = 16/286; contours <3, 3-7, 7-16, 16-23.

DIAGRAM 22 Plot of F4 axial planes, domain II; n = 49; M = 148/84; S = 25°; C = 06/228; contours <3, 3-7, 7-11, 11-16.

DIAGRAM 23 Plot of L4 (mostly fold axes), domain II; n = 42; M = 06/132; S = 32°; C = 02/312; contours <4, 4-7, 7-9, 9-11.

DIAGRAM 24 Plot of F2 axial planes, domain III; n = 62; M = 312/78; S = 43°; C = 11/218; contours <3, 3-5, 5-8, 8-14.

DIAGRAM 25 Plot of L2 (mostly fold axes), domain III; n = 86; M = 00/133; S = 31°; C = 01/137; contours <2, 2-6, 6-11, 11-18.

DIAGRAM 26 Plot of F3 axial planes, domain III; n = 98; M = 137/13; S = 40°; C = 76/036; contours <2, 2-5, 5-7, 7-11.

DIAGRAM 27 Plot of F3 axes (mostly fold axes), domain III; n = 133; M = 00/128; S = 33°; C = 03/130; contours <2, 2-5, 5-8, 8-13.

DIAGRAM 28 Plot of F4 (32) axial planes (squares) and (24) axes (dots), domain III.

DIAGRAM 29 Plot of F000° axial planes (contoured) and (37) axes (dots), domain I; for the planar structures - n = 88; M = 35/88; S = 22°; C = 08/268; contours <4, 4-8, 8-16, 16-22.

DIAGRAM 30 Plot of F040° axial planes (contoured) and (21) axes (dots), domain I; for the planar structures - n = 121; M = 031/87; S = 20°; C = 02/302; contours <8, 8-16, 16-26, 26-35.

DIAGRAM 31 Plot of F060° axial planes (contoured) and (8) axes (dots), domain I; for the planar structures - n = 69; M = 232/88; S = 17°; C = 02/137; contours <8, 8-15, 15-28, 28-34.

DIAGRAM 32 Plot of F090° axial planes (contoured) and (10) axes (dots), domain I; for the planar structures - n = 47; M = 081/87; S = 22°; C = 02/168; contours <4, 4-9, 9-15, 15-21.

DIAGRAM 33 Plot of (18) L1 lineations (dots) affected by F4 fold with axis (cross) 30/160 and axial plane (line) 130/85. Note distribution of L1 along small circles of stereonet.

DIAGRAM 34 Plot of (52) L1 lineation (dots) affected by F4 fold with axis (cross) 17/340 and axial plane (line) 350/74. Note the distribution pattern of L1 not clearly along small neither great circles.

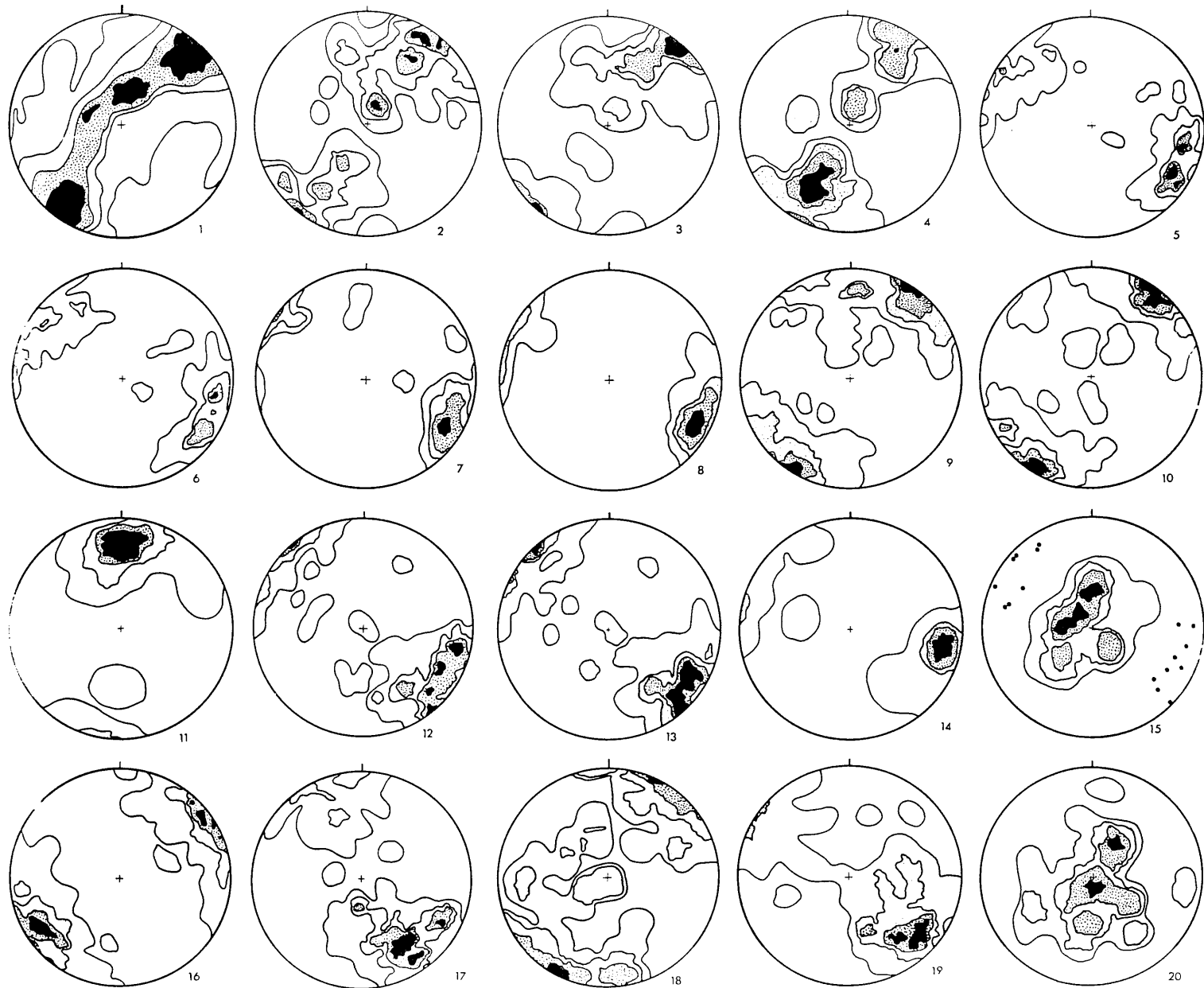
DIAGRAM 35 Plot of F-"early" structural elements in domain IV; black dots are (35) axes and open diamonds are (37) axial planes.

DIAGRAM 36 Plot of F-"mid" structural elements in domain IV; black dots are (12) axes and black triangles are (15) axial planes.

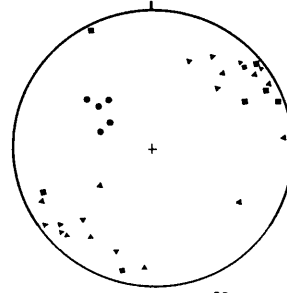
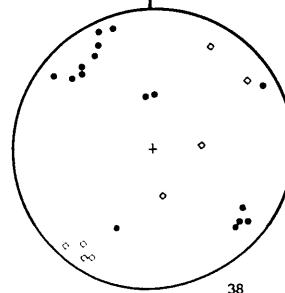
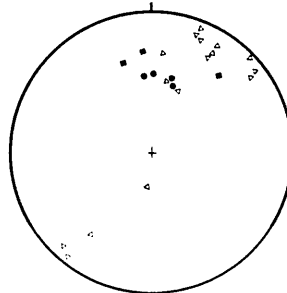
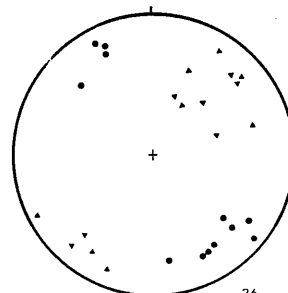
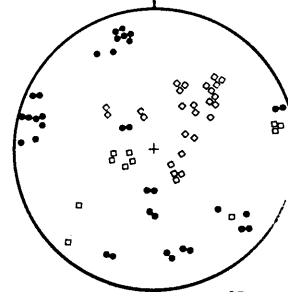
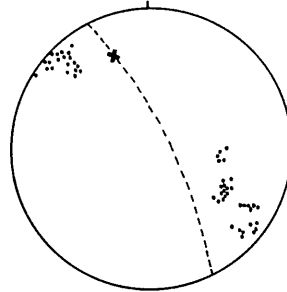
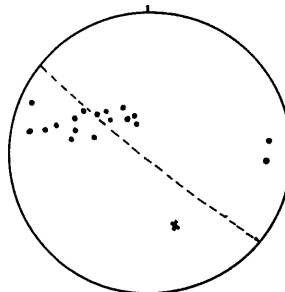
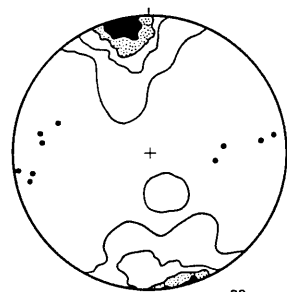
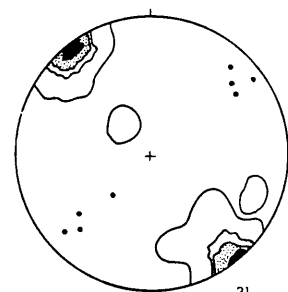
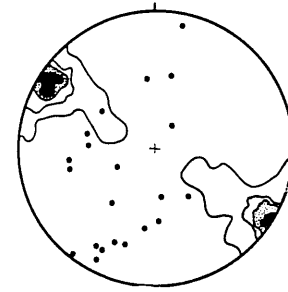
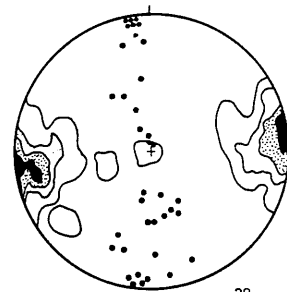
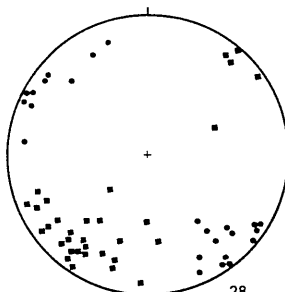
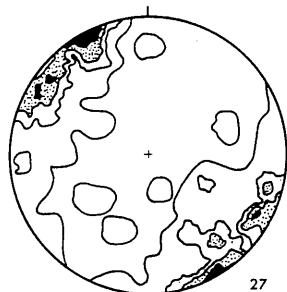
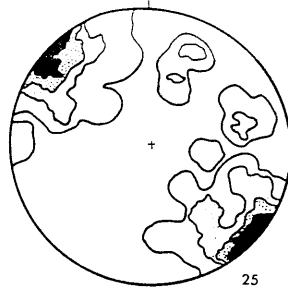
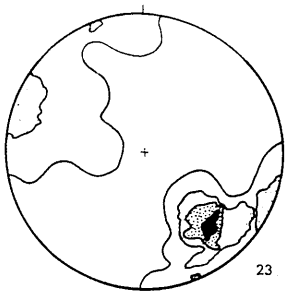
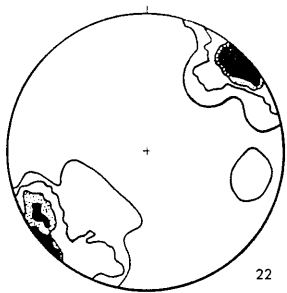
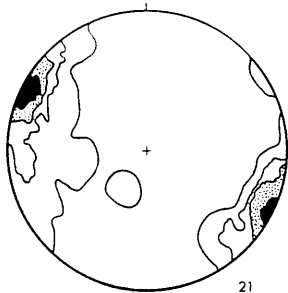
DIAGRAM 37 Plot of 'brittle' structures in domain I; (16) NW-SE faults (open triangles); (3) normal faults (black squares); and (4) brittle thrusts (black dots).

DIAGRAM 38 Plot of F1 structural elements in domain III; (16) fold axes (black dots) and (8) axial planes (open diamonds).

DIAGRAM 39 Plot of D2a shear zone elements in domain I; axial planes of folds comprise (20) sinistral (black triangles) and (8) dextral (black squares); axes of (5) sinistral folds as black dots.



DIAGRAMS 1-20



DIAGRAMS 21-39

CHAPTER 7 - METAMORPHIC CONDITIONS

7.1 INTRODUCTION

7.2 P-T CONDITIONS

7.3 CHEMICAL AND MECHANICAL EFFECTS OF FLUIDS

7.4 DISCUSSION

7.1 INTRODUCTION

The aim of this chapter is to establish the pattern of temperature variation in relation to the deformational history of the Loch Maree rocks. This pattern is then used to (i) assess a continuous evolution for D1-D2 deformation based on the determined structural sequence (Chap. 6) and (ii) constrain the proposed tectonic model for basement-cover relations in the area.

Despite the difficulties faced in applying the classical methodology of microstructural analysis in the determination of timing of deformation and mineral growth (section 4.3), a temporal framework for the development of early and late M1 and M2 mineral assemblages was obtained from the study of hundreds of thin sections. Suitable mineral pairs from these assemblages were analysed (using the electron microprobe) as a basis for calculation of temperature conditions using the garnet-hornblende and garnet-biotite geothermometers. The limited amount of data thus obtained are then compared to the metamorphic conditions as indicated by diagnostic minerals and parageneses. In addition, the role played by fluids particularly in the mobility of some elements during D1 and D2 mylonitization is discussed. These various aspects are then used as basis for assessing the metamorphic evolution of the rock assemblage and a discussion of the existing data from other Lewisian terranes.

7.2 P-T CONDITIONS

The analysed minerals including garnet-biotite and garnet-hornblende pairs were selected from rocks considered to represent the M1 and M2 metamorphic conditions as determined by the analysis of the microfabric (Chap. 4), mostly in rocks of domain II and III considered as part of the early cover sequence (*cf.* Chaps. 2 and 8). However the temperature values obtained from geothermometry should not be considered in isolation for although geologically significant, they are a function of several other factors some of which will be discussed below. The checking against petrogenetic grids and detailed microprobe investigation of compositional variation of the minerals is a recommended procedure and this was followed in part in the present study.

7.2.1 Geothermometry

Choice of geothermometers

The geothermometers used in this study (garnet-biotite - Thompson 1976, Holdaway and Lee 1977; garnet-hornblende - Graham and Powell 1984) were chosen because of (i) the available mineralogy and (ii) the intermediate range of temperatures given by these calibrations are assessed to give a reasonable approximation to the conditions that affected the Loch Maree rocks (see Sect. 7.2.1 below). Compared with other garnet-biotite geothermometers, Thompson's (1976) calibration has the advantage of being empirically determined, with the temperatures checked by field observations (Essene 1982). Despite the fact that garnets and biotites in metapelites in the temperature ranges of greenschist and amphibolite facies lie relatively close to the respective binaries (Essene 1982, p.164), this calibration, by using natural garnets and biotites, takes into account possible octahedral substitutions (Ca and Mn in garnets and Al^{+6} , Ti and Fe^{+3} in biotites), something not considered in other calibrations like those of Ferry and Spears (1978) and Indares

and Martignole (1985). On the other hand the calibration of Holdaway and Lee (1977), although based on that of Thompson (1976), has the advantage of including corrections for the considered exceptionally low values given by the low-temperature end of the latter. Figure 7.1 shows the relationships between these and some other garnet-biotite calibrations available in the literature.

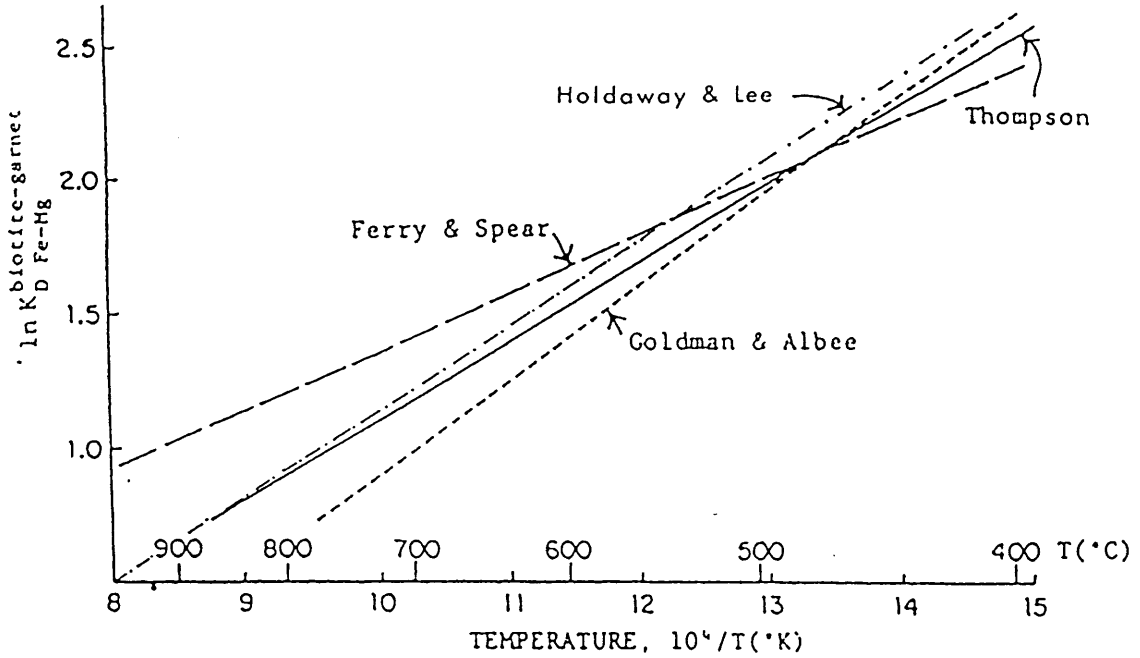


Figure 7.1 Various calibrations of the biotite-garnet KD thermometer. The Ferry and Spear (1978) version gives the highest temperatures; the Goldman and Albee (1977) calibration may be low because the isotope thermometers have been reset from the higher temperatures (Ghent *et al.* 1979); the Holdaway and Lee (1977) and Thompson (1976) calibrations differ only at the low temperature end (modified from Essene 1982, fig.3).

The garnet-hornblende thermometer was used because of both (i) the textural and structural evidence for the recrystallization

of the amphibole schists as a result of M2 and (ii) the more common occurrence of amphibole than biotite crystalloclasts in mylonites (see below). This calibration is empirical being based on the garnet-clinopyroxene geothermometer. It is applicable below 850°C to rocks with Mn-poor garnets and common hornblendes of widely varying composition.

The exchange reactions and equations used for the temperature calculations are set out in Appendix 7.1, while representative analysis of garnets, biotites and hornblendes are given in Table 7.2. For reviews of the problems involved with estimations of P-T conditions, the reader is referred to Essene (1982) and Powell (1985).

The temperatures calculated for M1 and M2 metamorphic phases at Loch Maree are presented in Table 7.1 (below).

M1 Metamorphic Conditions

The M1 temperatures were obtained from mineral pairs with granoblastic textures (cf. Pl.5.54A) preserved within large garnet crystalloclasts (garnet-biotite calibration) and also amphibole crystalloclasts (garnet-hornblende calibration). This is because of

(i) the widespread expression of the late D1 mylonitization and the susceptibility of minerals like biotite to the grain size reduction processes (cf. Chap. 6) and (ii) the higher confidence that M1 parageneses are being analysed. This procedure involved the assumptions the (i) the analysed mylonites have attained equilibrium during M1 and (ii) the composition of these mineral phases was not significantly modified during subsequent events - the late D1 mylonitization in particular. While the first assumption is not unlikely due to the generally well-established fluid loss (particularly H₂O) experienced with increasing metamorphic grade and also the absence of zoning in the analysed minerals (cf. Tracy 1982, Powell 1985), assessment of the effects of later (retrogressive) events seems to be necessary.

Effects of M1 mylonitization on to M1 temperatures

An attempt to evaluate the effects of polymetamorphism can be made by comparing the temperatures obtained from the same rock (biotite-hornblende schist) by both garnet-biotite and garnet-hornblende geothermometers, based on the temperatures obtained for M2 (not affected by the mylonitization). The recrystallized (M2) amphibole schist (sample 4, Table 7.1 above) gave the average temperatures of 444°C and 484°C using garnet-biotite and garnet-hornblende calibrations, respectively, suggesting that the latter calibration yields higher temperatures than the former (see also Graham and Powell 1984, p.21). However, the 40°C difference could be included within the error of the garnet-biotite calibration (see equations in Appendix 7.1). The average garnet-hornblende temperature of M1 for sample (1) using amphibole crystalloclasts is lower than the averages obtained from garnet-biotite within lithoclasts of the same rock, suggesting that later re-equilibration (during mylonitization) was more effective in the amphibole crystalloclasts used in the former calibration than in the relatively larger garnet-biotite gneiss lithoclasts used in the latter. Thus, if the proportion between the temperatures obtained for M2 from both geothermometers in sample (4) can be used as a correction factor on the average of garnet-biotite temperatures for M1 of sample (1) a value of 660°C is obtained for M1. This is an indication that chemical changes during mylonitization were more effective on (small) single crystalloclasts than on (larger) lithoclasts (see Section 7.3). It is also in agreement with: (i) the large variations of amphibole compositions at thin section scale observed in some samples (4 and 5 cf. standard deviations for amphibole and garnet analysis in Table 7.2) which are regarded as responsible for the wide variations of maximum and minimum temperatures obtained for these specimens (garnet-hornblende calibration), despite the fact that only Fe-pargasites (nomenclature of Leake 1978) were used for the temperature calculations and

(ii) the widespread reconstitution of the amphibole schists during M2, indicating the reactive nature of these rocks under metamorphic conditions despite their high resistance to deformation (see below).

M2 Metamorphic Conditions

The M2 metamorphic maximum was determined from amphibole schists of domain II (SW) where recrystallization of (specially) almandine and hornblende was ubiquitous. The lower M2 temperatures obtained for M2 (Table 7.1) are consistent with the structural interpretation for these rocks (Chaps. 3 and 4) where the rarity of D1 mylonitic features in this unit was suggested to be a function of the widespread metamorphic reconstitution which took place during the M2 episode. This seems to be confirmed by other indicators like the lower An content of plagioclase in places where the S2 foliation is well-developed (see Table 7.3).

The idioblastic almandine garnets overgrowing the fine mylonitic foliation in some of the pelitic mylonites (Pls 5.65A,B) are interpreted as M2 garnets. Although some of them show spiral inclusions in their cores, an indication of rotation of these crystals, the homogeneous compositions between core and rim suggests that either (i) the metamorphic conditions were maintained from a 'dynamic' to a 'static' phase of growth or (ii) that the M1 garnet was completely re-equilibrated during the M2 episode. Although garnets are known to be refractory minerals the alternative (ii), of complete recrystallization of these minerals during M2, was considered the most likely one based on the following:

- (a) the temperatures associated with D1 mylonitization are lower than those obtained for M1 and M2, and
- (b) the garnet rims are overgrowing a mylonitic foliation which has been interpreted as of late D1 age. Even though there is the possibility that this mylonitization is of D2 age (see Chaps. 3,4), the D1 age of overgrown mylonitic foliation is indicated by the lower range of temperatures obtained for

M2 with the use of these idioblastic garnets in the calculations (a result of their low pyrope and high spessartine content when compared to their M1 counterparts cf. mol% of end members of garnets L-156A1 and L-CAN, Table 7.2). This confirms the presence of pre- and post-D1 mylonitization garnet growths and eliminates alternative (i)ie. of maintenance of metamorphic conditions from the dynamic (M1) to static (M2) phases of growth of this mineral (cf. Obee and White 1985, p.708 for an interpretation of very similar evidence) which finds no support in the present study.

The homogeneous (non-zoned) nature of these garnets can be used as an indication of the temperature attained by M2. This can be derived from the inference that if these garnets have grown in a two-stage fashion (with the core and rims corresponding to M1 and M2, respectively) then they were probably zoned at the beginning of the M2 episode, and have been subsequently homogenized by diffusion. As demonstrated by Yardley (1977) in his empirical study of diffusion in garnets, elimination of zoning in this mineral requires relatively high temperatures (mean = $640^{\circ}\text{C} \pm 30^{\circ}$ and 575° to 650° for sillimanite grade zoning cf. Anderson and Buckley 1973 in Tracy 1982) when volume diffusion over significant distances in garnet may take place in geologically reasonable times (Anderson and Buckley 1963, op.cit.). However these temperatures for M2 seem too high if compared with the values determined from geothermometry (cf. Table 7.1) and petrogenetic grids, suggesting that homogenization of zoned garnets is possible under temperatures lower than those reported above since there is no evidence indicating temperatures in excess of 550°C for the M2 metamorphism.

7.2.2 Mineral Assemblages

The heterogeneous nature of the deformation of the Loch Maree rocks and the variable capacity of the different lithologies to react to the metamorphic transformations, mainly as a function of their composition (see Chaps. 4 and 5), mean that the various domains are likely to record different facets of

the metamorphic history of these rocks. Mineral assemblages from the aluminous (domain III mostly) and mafic rocks (of domains I and II) were the best indicators of the metamorphic conditions. Similarly to what is discussed in the geothermometry section, evidence for the relative age of these (M1 and M2) events comes from analysis of the microstructures and structural correlation (Chaps. 3 and 4).

The problem was to determine which of the several mineral reactions have taken place during the metamorphism of these rocks, since index minerals indicative of metamorphic zones could not be mapped as a function of several factors including the small dimensions of the mapped area. Thus, the most probable reactions were selected on the basis of the self-consistency of the indicated metamorphic conditions (i.e. reactions in different compositional systems indicating similar P-T conditions for M1 were considered as equivalent) which are at the same time, compatible with the results obtained from geothermometry (section 7.2 above).

On the other hand, the only constraints on the range of pressures under which the Loch Maree have been formed were obtained with the use of petrogenetic grids. Although mineral parageneses suitable for the use of the geobarometric calibrations of Bohlen and Liotta (1986), Powell and Evans (1983) and Ghent and Stout (1981) were available, these were not applied, either because of inadequate geological situations (cf. Lindqvist 1983) or the lack of data on mineral analysis, the latter as a function of the limited scope of this study.

7.2.2.1 Aluminous Rocks

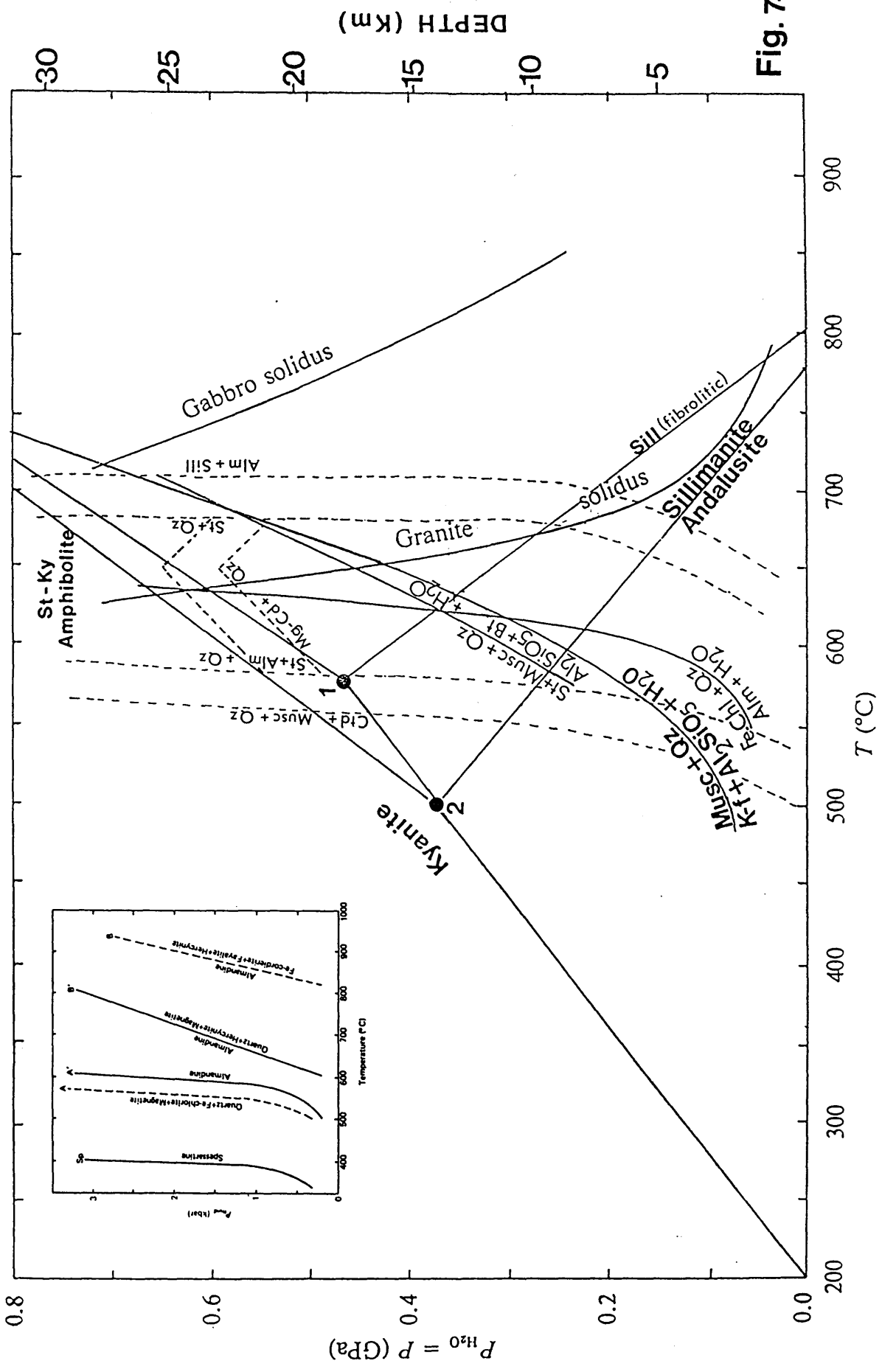
M1 Metamorphic Conditions

Pelitic rocks in domain III and thin bands of mica schist and pelitic mylonites present in the northeastern part of domain II contain staurolite (rare), almandine, feldspars, biotite, muscovite along with quartz and opaque minerals (cf. Table 2.1). Kyanite although not identified in the present study, has been reported in association with gneisses near Carnmore (approx. 3.5km N-NE from the mapped area cf. Peach et al. 1907, p.83). However, radiometric dating of these gneisses (Bakerman et al. 1975) indicate strong remobilization at c.1.9Ga which corresponds to the D1-M1 event affecting 'basement' and cover as determined in the presently studied rocks (cf. Chaps. 2,3,4). Accordingly, this same mineral (kyanite) was also described a few km NW of Letterewe where it occurs as large porphyroblasts overgrowing a foliation of possible pre-D1 age (cf. Table 8.1 and Crane 1978, p.233).

Figure 7.2 shows the principal univariant curves used for the determination of M1 metamorphic conditions in these rocks.

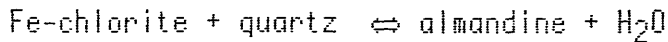
Figure 7.2 (next page) - Univariant curves used to determine P-T conditions for the aluminous rocks of the Loch Maree area. Positions 1 and 2 of the triple points are the best fit from petrographic and experimental data (Holdaway 1971), respectively (cf. Greenwood 1976, p.217). The narrow bands marked by discontinuous lines are the transition zones between metamorphic facies (modified from Greenwood 1976, Figs 1 and 2). Inset - stability relations for almandine bulk composition in the presence of an aqueous fluid. Curve sp represents the low-temperature limit of the stability field of spessartite on its own composition in the presence of an aqueous fluid. (Reproduced from Miyashiro 1973, fig. 7B-9). Abbreviations are; Alm = almandine; Bt = biotite; cd = cordierite; ctd = chloritoid; Fe-chl = ferrochlorite; K-f = K-feldspar; sill = sillimanite; st = staurolite.

Fig. 7-2

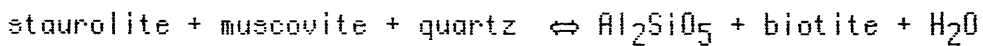


Assuming that the almandine-rich garnet was formed by the breakdown of Fe-chlorite and quartz, and that staurolite is in equilibrium with muscovite, the field of stability of these rocks is delimited by the following reactions:

(1) high temperature side of the reaction



(2) low temperature side of the reaction

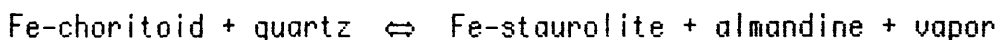


and

(3) low temperature side of the granite solidus curve.

This defines a narrow triangular field with a range of pressures between c. 3.8 and 6Kb and a range of temperatures between 620 and 640°C, conditions that are in good agreement with the average temperature of 600°C obtained for the peak of M1 by application of the correction on the results of garnet-hornblende geothermometry (cf. sample 1, Table 7.1). However, despite apparent simplicity of the situation, significant modification of these estimates is required if the following factors are considered.

1. The presence of kyanite if in equilibrium with staurolite, and in the absence of cordierite, would indicate pressures higher than c. 6Kb, placing the equilibrium above the band defined by the reaction Mg-cordierite plus quartz (Fig. 7.2), i.e. in the Staurolite-Kyanite-Amphibolite sub-facies (as opposed to the Almandine-Staurolite-Cordierite sub-facies Greenwood 1976). This would also be in agreement with the experimental results of Rao and Johannes (1979) where the equilibrium for the reaction

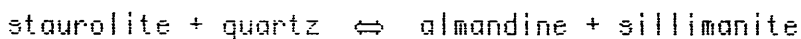


was attained at 570°C and 10Kb.

According to Greenwood (1976, p.223), of the three main P-T

facies series as defined by Turner and Verhoogen, (1960). The rarity of kyanite and absence of diopside in rocks of suitable bulk composition indicate conditions on the lower temperature side of this subfacies (Winkler 1968, p.107).

However, if the presence of the discordant banding (Sect. 3.2) is interpreted as indication of the presence of a melt phase in the quartzofeldspathic gneisses, the metamorphic conditions for the peak of M1 would be placed between the granite solidus curve and the reaction



with maximum temperatures of 680°C and pressures above 6.5Kb (cf. Rao and Johannes 1979 and Fig.7.2). This would involve the assumption that the melting phase was not formed in an earlier (pre-Laxfordian) metamorphic episode. Thus, if the structural and metamorphic sequence determined by Crane (1978) SE of Poolewe can be correlated to the present work (cf. Sect. 8.3), the gneissic banding and associated migmatitic features would be of pre-Laxfordian (Inverian) age indicating the unlikelihood of such high P-T conditions for M1.

Finally, compositions of M1 muscovites of some of the metasediments plot in the transition between the fields of almandine and staurolite-sillimanite zones (Fig.7.4). Since several of these are analyses of crystalloclasts in pelitic mylonites, their composition is expected to have been changed (cf. Sect.7.3).

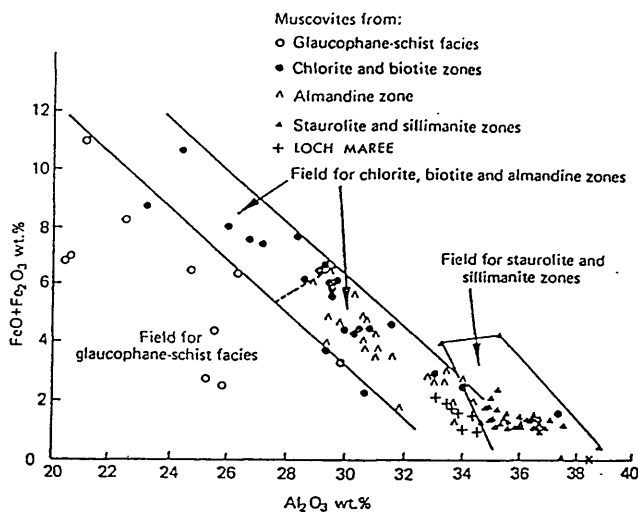
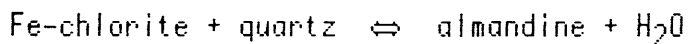


Figure 7.4 Composition of muscovites from metapelites. The cross on the abscissa at 38.4 per cent Al_2O_3 represents the idealized muscovite composition (modified from Miyashiro 1973, Fig.7B-2).

M2 Metamorphic Conditions

The limited mineral paragenesis which can be attributed with certainty to the M2 episode in these rocks (almandine-rich garnet + biotite + amphiboles) and the lack of mineral equilibrium data for the lower temperature part of the P-T field has restricted the use of petrogenetic grids in the estimation of the metamorphic conditions for this episode.

Although the temperature estimates from geothermometry may be slightly low considering some of the evidence from the mineral paragenesis (see below) it would be in agreement with the univariant curve for the reaction



if the more manganese-rich composition of the M2 garnets is taken into account. Since the M2 paragenesis in mafic rocks indicates the temperature conditions are compatible with the values obtained from the geothermometry (*i.e.* upper greenschist-lower amphibolite) there is need for estimates of the range of pressures during M2, so that an idea of the thermal regime can be obtained. For those rocks in which M2 re-equilibration has taken place, the presence of abundant garnet is the only potential indication of the prevailing pressures. Even though almandine garnet is stable over a wide range of pressures, the observation that both the distribution

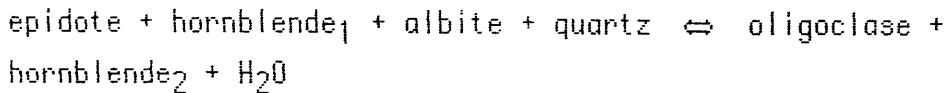
and proportion of this mineral in metapelites tend to increase with increasing pressures (Miyashiro 1973, p.221) suggests that the appearance and abundance of this mineral is favored by the higher pressure environments (Keesmann *et al.* 1971 in Deer *et al.* 1982). This would be in agreement with the exceptional abundance of idioblastic (M2) garnets in some of the metasediments along the loch shore (interbanded schists - Fig.2.1). Thus in the absence of any direct evidence the pressures for M2 will be assumed to be similar (5-8Kb) or even slightly higher than those for M1 (*cf.* Sect.7.4).

7.2.2.2 Mafic Rocks

M1 metamorphic conditions

While the aluminous rocks show evidence of amphibolite facies, the paragenesis of the mafic lithologies has been reported as indicating conditions of epidote-amphibolite facies for the Loch Maree rocks (*cf.* Keppie 1967, p.163). However, several textural features seem to indicate that the epidote has largely crystallized at late stages of M1. It shows randomly oriented prismatic shapes, overgrows plagioclase crystals with well-developed granoblastic polygonal shapes in porphyritic amphibolites and replaces garnet in a few of the garnet-bearing amphibolites. As also noted by Keppie (1967), these minerals encroach upon ferromagnesian minerals, have straight boundaries, contain inclusions of partially dissolved sphene, graphite, hornblende and biotite, "indicating that they grew during the static post-tectonic main phase metamorphism" (p.143) (main phase is equivalent to M1 in the present work). The invariable presence of epidote crystals as crystalloclasts in the mylonites (*cf.* Chap. 5) indicates their pre-D1 mylonitization ages. However, the question of whether epidote was also formed during the (M1) amphibolite facies event or represents a low temperature re-equilibration (epidote amphibolite facies) is important in that it can be used to cross-check the temperatures obtained from the geothermometry and the mineral paragenesis of aluminous rocks.

The transition from epidote-amphibolite to amphibolite facies is defined by the breakdown of epidote according to the reaction:



which was experimentally determined by Apter and Lion (1983 in Deer *et al.* 1985) to occur under conditions of 650°C at 5Kb and 675°C at 7Kb. It is a function of fluid pressure, oxygen fugacity and temperature and as it can be observed in the diagram of stability of epidote (Deer *et al.* 1985, pp.67-68), it occurs over a wider range of P-T conditions than is commonly recognized (*cf.* Miyashiro 1973).

In the case of the Loch Maree rocks, the observed paragenesis diverges from typical epidote-amphibolite assemblages in that oligoclase (An32-37) is the common plagioclase in equilibrium with epidote. Although Ramberg (1952 in Miyashiro 1973) considers that the transition between epidote amphibolite and amphibolite facies is marked by plagioclase (An30) in equilibrium with epidote, this assemblage would correspond to the staurolite zone in pelitic rocks in the Appalachians and was regarded as part of the amphibolite facies (Miyashiro 1973). This view is shared by Winkler (1968) where epidote + plagioclase + hornblende + almandine ± biotite ± quartz is considered to be a typical assemblage of the almandine amphibolite subfacies in basic rocks. (In the Loch Maree rocks the co-existing amphibole is usually a Fe-pargasite but Fe-actinolite crystalloclasts in pelitic mylonites of domain III are not uncommon - *cf.* Fig. 7.5a,b).

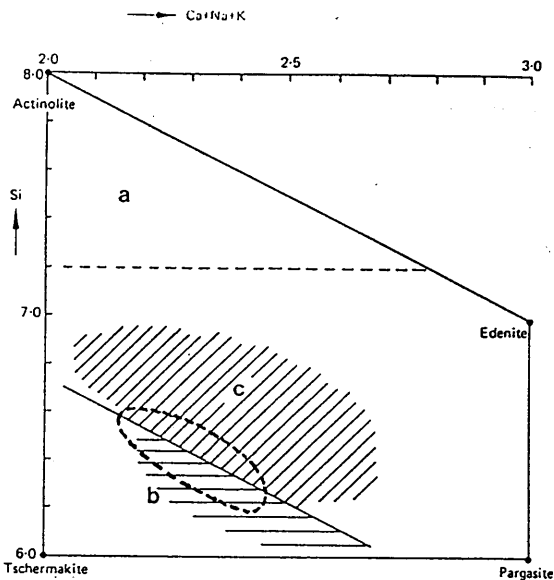


Figure 7.5a. Calcic amphiboles in metabasites of the central Abukuma Plateau (Shido and Miyashiro 1959) and Broken Hill (Binns 1965b); a = actinolite field, b = blue-green hornblende field, c = field of green and brown hornblendes in the high amphibolite and granulite facies. Hornblendes from Loch Maree plot within the elliptical area but Fe-actinolites plot out of this diagram (modified from fig. 8B-4 of Miyashiro 1973).

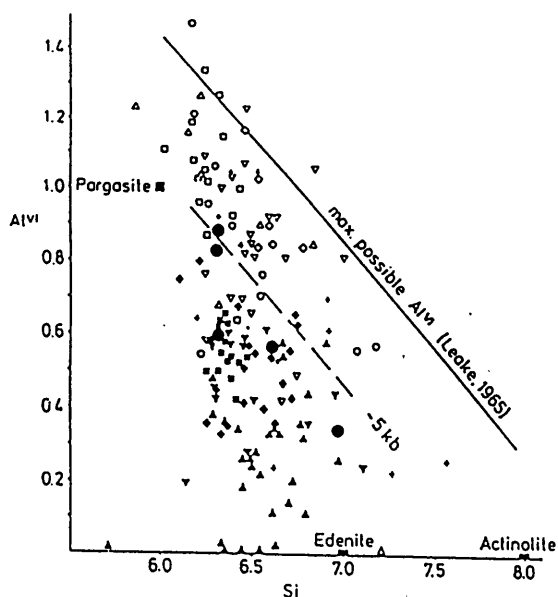


Figure 7.5b. Relation between Al^{VI} and Si of hornblendes (basis 23 O) from low-pressure regional metamorphic terrains (black symbols) and from

high-pressure metamorphic terrains (open symbols and crosses). Symbols: ▼ central Abukuma plateau, Japan (Shido and Miyashiro, 1959); ▲ Sierra de Aracena, SW Spain (Fabries, 1958; Bard, 1970); ◆ Broken Hill district, New South Wales (Binns, 1965); ■ Adirondack mountains, New York (Engel and Engel, 1962); ○ Grampian Highlands, Scotland (Wiseman, 1934; Tilley, 1938; Shido and Miyashiro, 1959; Matthews and Cheeney, 1968); □ St. Gotthard region, Swiss Alps (Steiger, 1961); ▲ Hohe Tauern, Austria (Paulitsch, 1948; Raith, 1971; Raase, 1972b); ▼ Orange area, Massachusetts (Robinson and Jaffe, 1969); ◇ Black Hills, South Dakota (Raychaudhuri, 1964); + Sanbagawa belt, Japan (Banno, 1964); ● Loch Maree. (Modified from Raase 1974, fig.1)

According to Winkler epidote continues to be stable with plagioclase of the composition An₂₅ to An₄₅ until the beginning of the Sillimanite-Almandine-Orthoclase subfacies where epidote + quartz breaks down to anorthite + garnet + hematite + H₂O at conditions of 680°C and 6Kb (Winkler 1968, p.113). Another interesting feature in the Loch Maree rocks is the predominance of epidote over clinozoizite in the quartzofeldspathic gneisses and amphibolites of domain I and the reverse in the metasediments of domain III. This was also reported by Keppie (1967) who, based on the work of Harpum (1954 in Keppie 1967), attributed the formation of epidote in the gneisses to their higher metamorphic conditions (p.164). Although part of his interpretation (i.e. that the basement and cover have been through the peak of metamorphism before the main phase of mylonitization but see Chap. 8), is in agreement with the metamorphic history of these rocks, the interpretation that the gneisses present a higher metamorphic grade (presence of epidote) because they were situated at deeper crustal levels is not convincing. This is because the P-T gradients at the interface cover-basement are not expected to be significantly different. Since the absence of epidote in the cover rocks does not obey a compositional control (quartzofeldspathic metasediments do not have epidote) a possible explanation would be differences of water content

between an older gneissose (late Scourian) basement and the more hydrated 'metasedimentary' cover rocks.

M2 Metamorphic Conditions

The evidence for the P-T conditions of M2 in these rocks is limited. The assemblage hornblende + oligoclase (An₂₆) + quartz ± almandine ± biotite ± clinozoisite in the amphibole schists of domain II indicates amphibolite facies conditions with temperatures probably lower than M1, as suggested by plagioclase and garnet compositions in an assemblage very similar to that developed during M1. Although these are the only petrological indicators of the variations of the metamorphic conditions between M1 and M2, (i.e. based on mineral assemblage), the An content of plagioclase was considered by Wenk and Keller (1969), in an exhaustive study of metabasites in the Alps, as the most sensitive indicator of the highest reached temperatures (but see Brodie 1981). The estimates are not in agreement with the results from geothermometry which showed considerable lower temperatures. However, due to the wide dispersion of values obtained for M2 with both geothermometers (cf. Table 7.1), the absolute values obtained from the latter are considered to be in error, possibly due to later heterogeneous re-equilibration of the analysed minerals. In this way M2 conditions will be considered to be of lower amphibolite facies as indicated by the mineral paragenesis discussed above.

Metamorphism of Mylonites (Mm1)

The mylonitic rocks show extensive chemical changes with retrogression to greenschist facies. However, precise determination of metamorphic conditions is difficult because of the following, and possibly other factors.

1. The extremely fine grain-size of the ultramylonites made the optical identification of the matrix-forming minerals difficult and the fine grains could have promoted late metamorphic changes with the widespread development of

sericite and chlorite.

2. It was difficult to distinguish between small relict and newly-formed minerals.

3. The rocks have a polymineralic nature. Besides early and late M1 and M2 metamorphic phases there is also evidence for low grade metamorphic transformations associated with the D3 and D4 deformation phases (?).

However, greenschist metamorphic conditions are inferred for this late D1 mylonitic event (Mm1) based on the following general evidence.

1. The An content of plagioclase crystalloclasts decreases with increasing intensity of mylonitization in both the metasediments and gneisses (cf. Table 7.3). Albite (An5) is the predominant plagioclase crystalloclast in the ultramylonites where it is regarded as the plagioclase composition with the closest possible conditions of equilibrium with the matrix.

Within lithoclasts of gneisses and/or metasediments, the An content of plagioclase increases mainly as a function of the preservation of the M1 metamorphic assemblages and the original composition of the rock (cf. Table 7.3).

2. The lack of mineral transformation despite grain-size reduction shown by protomylonites and several mafic mylonites of domain 1 (in particular) suggests a close relationship between intensity of deformation, presence of fluids, P-T conditions and mineral transformations accompanied by metasomatic mass transfer.

On these bases, the retrogressive nature of the D1 mylonitic zones is interpreted to be the product of re-equilibration (or partial re-equilibration) under conditions of abundant fluids and temperatures lower than those operative during M1 and M2. However, the evidence from this study indicates that the metamorphic conditions during M1, M2 and M 'mylonite' are well above the 'remarkably low metamorphic grade' as reported by Wheeler et al. (1985).

The bulk of the evidence discussed in Section 7.2 indicates

amphibolite facies conditions for M1, amphibolite or upper greenschist for M2 and greenschist for the mylonitization (see Fig. 7-7a).

7.2.3 Geothermal Gradients

Geothermal gradients for both M1 and M2 were between 25° and 30°C/km, thus in the range of Barrovian type metamorphism.

7.3 CHEMICAL AND MECHANICAL EFFECTS OF FLUIDS

Chemical effects of the fluids

Most of the published work about mechanisms of deformation tends to relegate the role of fluids and emphasize intragranular deformation mechanisms like dislocation creep. This is perhaps a consequence of the information that has come from experimental studies of deformation in metals (cf. McClay 1977, Poirier 1985). However, with the recognition of the importance of intergranular deformation mechanisms of the cobble creep 'type' and the intimately associated diffusion mass processes in naturally deformed rocks, there has been a resurgence of interest in the last decade in diffusion creep, particularly in connection with the geochemical changes which take place in rocks and minerals during this type of deformation (cf. Beach 1976, 1979, 1980, Gray 1977, Beach and Tarney 1978, Allison et al. 1979, Dostal et al. 1980, Kerrich et al. 1980, Jamieson and Strong 1981, Engelder et al. 1981, Floyd and Winchester 1983, Watts and Williams 1983, Anderson and Burham 1983, Etheridge et al. 1984, McCaig 1984, Berhmann 1984, Kerrich 1986).

In the Loch Maree mylonites an attempt to test the mobility of some elements suggested to be mobile in shear zones of similar metamorphic grade (cf. Winchester and Max 1984, Beach and Tarney 1978) was made through the plotting of major and trace elements of 48 samples of mafic and felsic gneisses showing several stages of mylonitization (Table 7.4_{annex}). The patterns

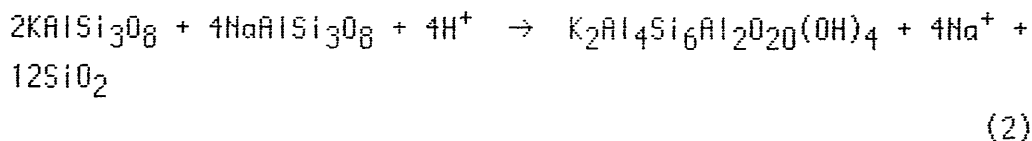
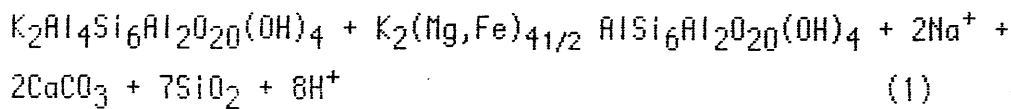
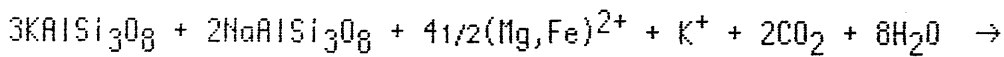
obtained were not consistent with the intensity of deformation exhibited by the rocks, suggesting that the mobility of elements in the Loch Maree mylonites differs significantly from the rocks studied by these authors. Accordingly, Mueller (1967) and Rumble (1982) have pointed out that the classification of many chemical constituents of rocks as 'mobile' or 'inert' has little basis in theory or experiment and can lead to error and confusion with respect to certain constituents. Demonstration of this can be obtained by comparing proportions present of elements considered immobile and mobile by several of these authors under similar conditions of metamorphism and deformation (but see Brady 1983).

It seems that, despite careful petrographic studies of textures and fabrics and reconstruction of the geological and recrystallization history of the rocks used by these authors, the relative mobility of elements during a particular metamorphic grade will depend on many other factors. These include original mineralogical composition, development of secondary phases, fluid/rock ratios and fluid composition. Of special importance in the identification of the geochemical transformation is the recognition that rocks have a great capacity to buffer fluid composition (Rumble 1982).

Due to the objectives of this study, the present section will concentrate on the discussion of (empirical) data from petrographic observations of mineralogical transformations suffered by the rocks, and their possible influence on deformation processes along the mylonite zones. A more detailed account of the geochemical modifications of these rocks and their implications for the characterization of the pre-metamorphic origin of these gneisses will be reported in a separate study.

The production of large quantities of muscovite, quartz, biotite and carbonate in ultramylonites represents the most conspicuous example of mineral transformations observed. These transformations involved both plagioclases and K-feldspars and can be represented by the following reactions

(Beach *et al.* 1980, p.259):



Apart from the mineralogical convergence observed in felsic and mafic mylonites (Sect.5.2) which is predicted by Korzhinskii's phase rule (as the number of mobile components in a rock increases there is a decrease of the number of phases present), the following are other features that can be demonstrated or deduced.

1. There must have been changes of pH due to the addition of hydrogen ions and base metal cations released to the fluids during reaction with the 'host' rock (*cf.* reactions 1 and 2).

2. Movement of K^+ , Na^+ , Mg^{2+} , Fe^{2+} was required for some of the reactions.

3. The abundance of carbonates varies markedly. Its presence in strain shadows around porphyroclasts, as a replacement of crystalloclasts and matrix of mylonites and also along later veins, indicates that Ca^{2+} and CO_2 were common components of the fluid phases during several stages of the deformation of these rocks. The most abundant carbonate mobilization phase during a late stage of D1 could be a result of involvement of the marbles in the mylonitization process, with CO_2 derived from devolatilization reactions (*cf.* Rice and Ferry 1982). The amount and temperature at which CO_2 is produced is a function of the composition of the marbles, with pure carbonate rocks only releasing fluids at fairly high metamorphic grades (Fyfe *et al.* 1978).

4. Conditions were favorable for silica solubility. This is indicated by the presence of (deformed and lineated) quartz

bands in (early) D1 mylonites and of quartz infill of boudin necks and other dilational features. Although not preserving their original shapes, the silica constituting the segregation bands remained in the system. This is in marked contrast with D2 activity when no sinks were formed. Accordingly, there must have been changes in the physico-chemical conditions between M1 and M2. Such a conclusion is consistent with suggestions set out previously that (i) D2 'pressure solution' has almost exclusively affected the mylonitized quartzofeldspathic gneisses (of the NE part of domain 1) and (ii) the contrast of D2 fabrics between 'healthy' and mylonitized gneisses are a function of the control exerted by D1 mylonitic textures on to the younger deformation processes affecting the rocks. It is also consistent with the suggestion (Chap. 5) that while the rate of deformation by dislocation processes is grain-size independent, in the case of diffusion processes it is inversely proportional to the cube of the grain size (cf. Beach 1980).

In addition, if the role of stress and deformation in minerals is taken into consideration (Rast 1965, Elliott 1973, Gray 1977, De Beer 1977, Gray and Durney 1979, Engelder and Marshak 1985), and simple shear in particular (Bell et al. 1986), the discussion whether D2 microscopic features (cf. Chap. 4) are produced by solution mass transfer or involved shear strain (Gray 1979b) is no longer relevant, since both types of mechanisms are likely to have been active simultaneously. The same could be said about the formation of S2 crenulation cleavage, which displays clear evidence for the contribution of (micro) folding at an early stage (cf. Gray 1979 a,b, 1981), with further localization of shear deformation along the fold limbs and axial-planar foliation (together with the corresponding solution mass transfer). As demonstrated by Ghosh (1982) and Bell (1981) this latter situation is not uncommon under natural conditions.

Mechanical effects of the fluids

The retrograde reactions are all hydration reactions and

although the volume of fluid necessary for these reactions is relatively small, calculations based on the solubility of elements like SiO_2 suggest that typical rock/fluid volume ratios are between 10^2 and 10^4 (Beach and Fyfe 1972, Kerrich et al. 1977 and Etheridge and Cooper 1981 in Etheridge et al. 1983). The origin of these fluids is largely unknown but based on isotopic studies several authors argue for a contribution of meteoric water (e.g. Etheridge et al. 1983, Engelder 1984, Kerrich and Hyndman 1985, Kerrich 1986). An indication of the origin of the fluids can be given by the volume and solubility of the material removed from the rocks. Taking into consideration the limitations of the volume of fluids which can be produced by metamorphic (dehydration) reactions, the contribution of meteoric water was proposed where large volume losses by diffusion mass transport have taken place. However, the idea that convective circulation systems are active at depth and can occasionally be fed with meteoric water provides a more likely explanation encompassing all sources of evidence (see Etheridge et al. 1983 and fig. 7.6).

In addition to the weakening effects on mineral phases (see Chap. 5) another mechanical effect of fluids on deforming rocks is to promote cataclastic deformation through hydraulic fracture. Features attributed to this mechanism were described in section 5.3 and the present section is a brief discussion of the possible role of this mechanism during D1 thrusting, as well as the causes of preferential localization of deformation along planar (and originally sub-horizontal) structures such as lithological contacts and foliations.

Price (in Fyfe et al. 1978) discussing the role of hydraulic fracture in fluid migration considers this type of fracture as 'the most important single mechanism of deformation operative in the upper crust' (p.259). The effects of this mechanism can be observed in shear zones where the geometry and orientation of quartz (or granitic melt - at higher grades) veins in relation to both the finite and incremental strain markers, indicates that these veins occupy true tensile

structures. No matter the ductility conditions these structures will only form where pore fluid pressures exceed the value of minimum principal compressive stress (cf. Ramsay and Graham 1970, Durney and Ramsay 1972, Ramsay 1980, Etheridge 1983).

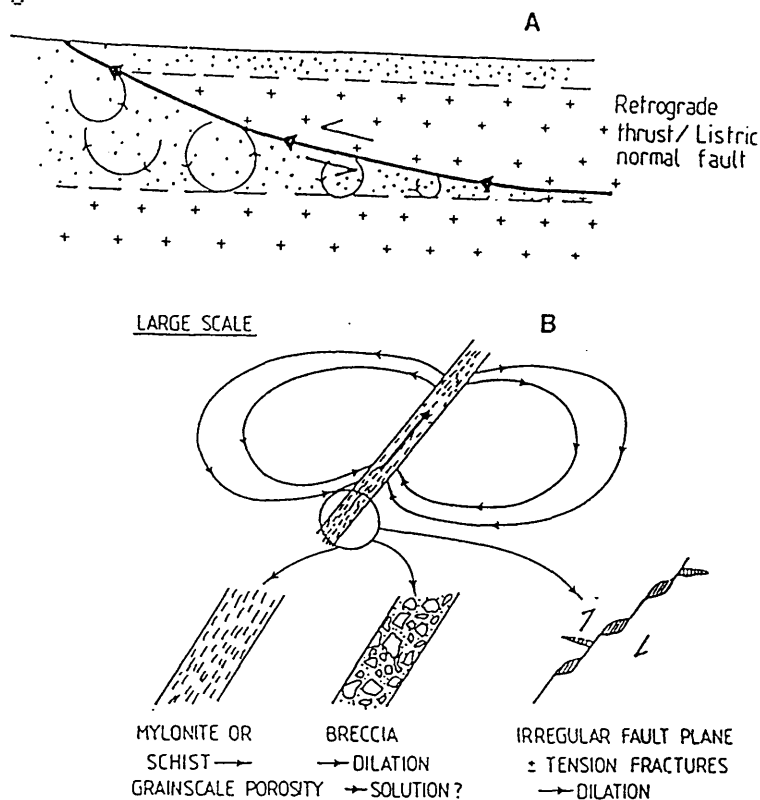


Figure 7.6. A. Convective fluid system established in the proximities of a thrust fault. The overloading and thermal relaxation are probably the forces promoting dehydration and driving the circulation of fluids; B shows part of A in detail with the possible mechanical behavior of the rocks (Modified from Etheridge *et al.* 1983, figs 7,8)

In the case of the Loch Maree rocks, although the D1 quartz segregation bands did not preserve their original shape due to effects of continuous deformation, these bands were probably segregated along zones of relative low pressure produced during mylonitization. The structural concordance between foliation and quartz band could represent an original (non-tectonic) relationship. This suggestion would find support from the following observations.

1. These rocks were foliated before the onset of the D1

thrusting event implying that the foliation surfaces could have been preferential zones for hydraulic fracturing during deformation. Values of tensile strength of rocks in a direction normal to a (penetrative) fabric are low (cf. Jaeger and Cook 1976, pp.106-108, Paterson 1978) and are thought to be even smaller during regional metamorphism (Etheridge 1984, p.233).

2.The bulk of structural and metamorphic evidence (patterns of T°C variation incompatible with an extensional regime Chap.8) points to a thrusting episode with low-angles between the planar fabrics and the principal compression direction. This would further promote the reactivation of existing planar structures (bedding, foliation) through hydraulic fracturing along which quartz would be segregated (see also Kerrich and Allison 1978, p.1657).

On a large scale, the main thrust zone along the carbonate-bearing rocks might have behaved as a more impermeable region for the migration of the fluids liberated from the dehydration of the footwall rocks. This situation was discussed by Fyfe and Kerrich (1985) who calculated that an average of approx. 4% H₂O may be lost from the underplate. These authors propose that the fluids then liberated would permeate through the thrust surface causing retrogression of the hangingwall (p.358). However there is no mention of either permeability problems or the possibility of localization of these fluids along preferential zones, a situation reported from several fold and thrust belts and inferred for the Loch Maree thrust by the concentration of features indicating brittle deformation along the marble unit. Gretener (1981), on the other hand, has shown that not only the low angle of thrusting is predicted from the mechanical behavior of a rock in the presence of discontinuities and high pore fluid, but also that abnormally high pore pressures develop in those parts of the sequence where restrictions to fluid flow prevail, being thus a basic requirement for the building up of the fluid pressure. This can provide an elegant explanation for the localization of main thrusts, quartz segregation bands and features

indicating transient brittle deformation along discontinuities like lithological boundaries. It would also suggest that the principles of mechanical behavior as applied to the 'high' structural levels of young fold belts like the Canadian Rockies and the Alps can be extended to 'deeper' parts of Proterozoic shear belts.

7.4 DISCUSSION

Shear zones are tectonic environments where deformation and metamorphism can be considered as occurring simultaneously (e.g. Beach 1980). This idea, however, is very much scale-dependent as illustrated by the early Proterozoic shear zones of the Lewisian Complex. Although these zones can be considered as 'narrow' localized zones of high deformation ('Laxfordian shear zones' of e.g. Coward 1984, Coward and Park 1987), the situation is much more complex when looked at into detail (see also Grocott 1979b). In the case of the Loch Maree rocks, several metamorphic and deformational events can be distinguished within this 'shear belt'. Although they are probably part of the same overall continuous evolution (see Chap. 8), the distinction between separate phases (with variable conditions of P-T-X etc) is important on the local scale, in terms of understanding the geometry of the structures and particularly the interplay between basement and cover of this part of the Lewisian Complex during the early Proterozoic.

The existence of co-axial folds developed under constant metamorphic conditions have been used in the modern literature as evidence for progressive deformation (e.g. Nicholas 1987, Park *et al.* 1987). In the present case, although the structural analysis points to continuous deformation (at least during D1-D2 times) the associated metamorphic conditions indicate variations of P-T-X which require discussion. Considering M1 and M2 as of approximately similar metamorphic facies, the most important feature is the P-T drop associated

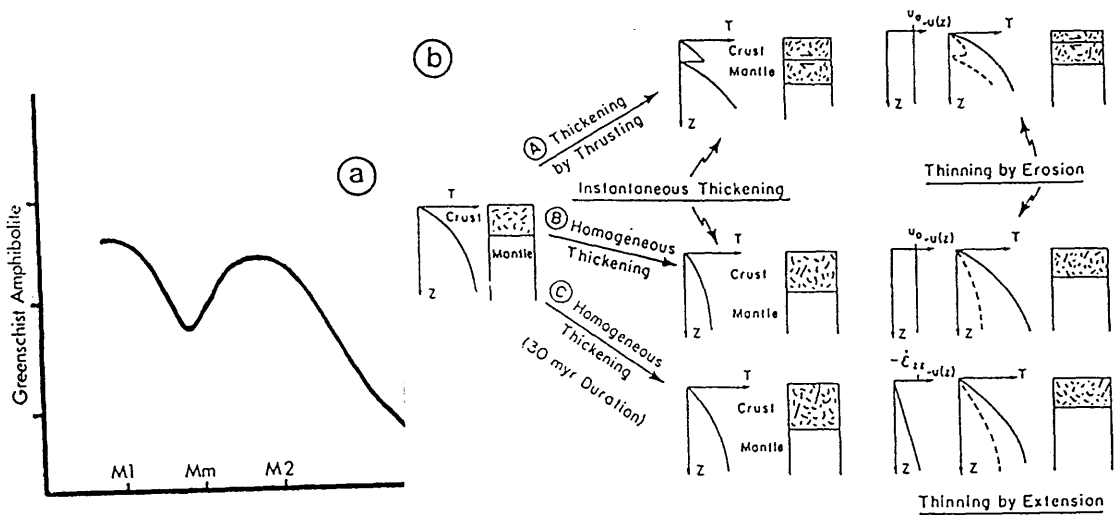


Figure 7.7. Variation of temperature conditions of the Loch Maree rocks (a) as compared to the models proposed by England and Thompson (b). (b) Sketches of the geometries of crustal thickening and thinning processes. The pre-thickening conditions in each case are the same and are shown on the left (A-C). These show the immediately post-thickening states (next two columns); the velocities, temperatures and crustal thicknesses at subsequent times are shown in the righthand three columns. (A) Thickening is accomplished instantaneously by a single thrust that emplaces 35km of continental crust over another 35km of crust and its subjacent lithosphere without perturbing their temperatures. This burden is then removed by erosion over the next 120Ma, at a constant rate u_0 . (B) As (A), except thickening is accomplished instantaneously by homogeneous strain. (C) Thickening is by homogeneous strain over a 30 Ma time interval and is followed by crustal thinning which occurs by homogeneous extensional strain at a constant rate. (Reproduced from England and Thompson 1986, fig.1).

with the late D1 mylonitization. This could be interpreted as produced during the upward movement of the basement along the main thrust horizon, reaching higher structural levels in the crust (see Chap. 8), where retrogressive metamorphic reactions would take place along zones of fluid percolation. The resultant crustal thickening would cause a perturbation of the

thermal structure of the crust.

The modelling of this kind of situation discussed by Oxburgh and Turcotte (1974), Oxburgh and England (1980) and England and Thompson (1984, 1986) involves the assumption of a rapid phase of tectonic thickening (as compared to the speed of thermal re-equilibration and uplift) which is consistent with the available estimates of deformation rates during thrusting (cf. Gretener 1981, p.33). It is also compatible with the situation in the Loch Maree district where it has as yet, not been possible to date D1 and D2 separately (M. Aftalion, pers. commun. 1987)

The principal features of the P-T-time path followed by the rocks in this sort of environment are (1) a thermal relaxation during which the temperature rises followed by (2) a period of cooling as the rocks approach the surface. As recognized by England and Thompson (1984, p.902) these models reproduce a few major controls of the evolution of the rocks. They provide a general picture to which the patterns of variation of metamorphic conditions (as determined from petrological studies) can be compared (see also Thompson and Ridley 1987). The temperature variation pattern of the Loch Maree rocks seems to be compatible with the model of thrusting as proposed by England and Thompson (1986) and which is partially reproduced here in Figure 7.7.

Comparison with P-T estimates for other Lewisian rocks.

The average of M1 metamorphic conditions for the Loch Maree rocks is plotted on the diagram of Sills and Rollison (1987) summarizing the conditions for the Lewisian Complex of the Assynt block (Fig. 7.8). They are in general agreement with

the temperatures obtained for the 'late shear zones' (c. 2.0Ga). The slightly higher temperatures of M1 obtained in this study can be explained in terms of the better development of the products of early Proterozoic deformation and metamorphism in the 'Southern Belt' than in the Assynt Block, while the M2 temperatures are slightly lower but still within the expected error ($\pm 50^{\circ}\text{C}$) for the garnet biotite geothermometer.

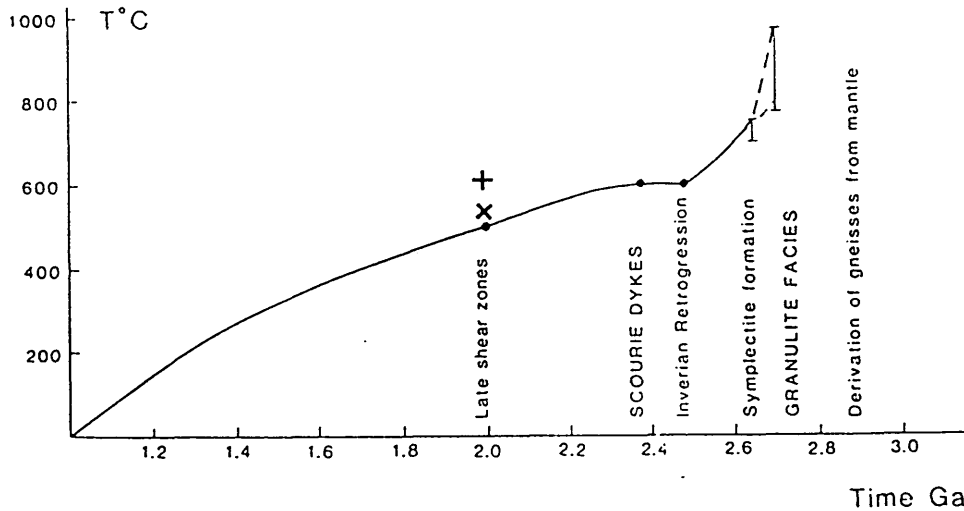


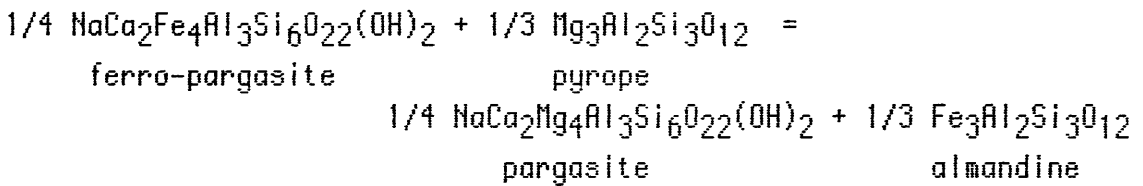
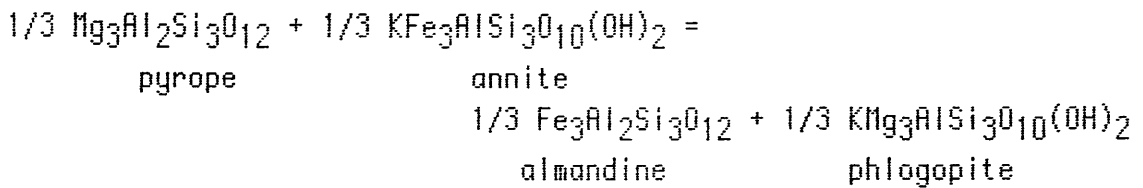
Figure 7.8 Temperature-time path for the Assynt block; + and x average of M1 and M2 respectively for the Loch Maree rocks (modified from Sillis and Rollinson 1987).

As compared to the garnet-biotite temperatures of 535° and 545°C ($\pm 50^{\circ}\text{C}$) obtained by Fettes and Mendrum (1987) for the 'initial thrust movements' in the Outer Hebrides (but see Chap. 8) the present temperature values for M1 and M2 are higher and lower, respectively.

However, it is extremely difficult to compare the present results with others reported in the literature. This is not only due to the lack of information about the relative chronology of the metamorphic and deformational episodes, but also due to the diachronous and 'cause-effect' nature of these events (see Chap. 8).

APPENDIX 7.1

The exchange reactions representing the partitioning of Fe and Mg between garnet-biotite and garnet-hornblende are:



The equations used are:

Garnet-biotite

$$T \text{ (}^\circ\text{K)} = \frac{2740 + 0.0234 P(\text{bars})}{\ln KD + 1.56} \quad \pm 50^\circ\text{C} \quad \text{Thompson (1976)}$$

$$T \text{ (}^\circ\text{K)} = \frac{6150 + 0.0246 P(\text{bars})}{R \ln KD + 3.93} \quad \pm 50^\circ\text{C} \quad \text{Holdaway and Lee (1977)}$$

$$\text{where } KD = \frac{x_{\text{Fe}}^{\text{ga}} \cdot x_{\text{Mg}}^{\text{bt}}}{x_{\text{Mg}}^{\text{ga}} \cdot x_{\text{Fe}}^{\text{bt}}}$$

Garnet-hornblende

$$T(^{\circ}\text{K}) = \frac{(2880 + 3280 X_{\text{Ca}}^{\text{ga}})}{(\ln KD + 2.426)}$$

Graham and Powell (1984)

$$KD = \left(\frac{X_{\text{Fe}}^{\text{ga}}}{X_{\text{Mg}}^{\text{ga}}} \right) \left(\frac{X_{\text{Fe}}^{\text{hb}}}{X_{\text{Mg}}^{\text{hb}}} \right)$$

Representative analysis of the garnets, biotites and amphiboles are given in Table 4.2.

SAMPLE	GARNET - BIOTITE				GARNET - HORNBLENDE				OBSERVATIONS	
	THOMPSON (1976)		HOLDRAWAY & LEE (1977)		GRAHAM & POWELL (1984)					
Temperat. °C	Min.	Mean	Max.	Min.	Mean	Max	Min	Mean	Max	
(1) L-CAN	549	616	628	538	596	607	447	565	613	M1-large lithoclast (Ga-Bt) and crystalloclast (Ga-Hb) in mixed mylonite
(2) L-CAN1	518	599	642	510	581	619	-	-	-	M1-large lithoclast (Ga-Bt) and crystalloclast (Ga-Hb) in mixed mylonite
(3) L-157X	450	482	552	450	479	541	-	-	-	M1 boudinaged garnet with biotite crystallization in extensional fractures (Fig. 4-2c)
(4) L-68	374	444	608	380	444	589	426	484	874	M2 recrystallized garnet in hornblende schist
(5) L-156A	394	407	494	398	410	489	410	527	1051	M2 recrystallized garnet & biotite+hornblende crystalloclasts in pelitic mylonite
(6) L-156A1	374	420	493	380	423	488	-	-	-	M2 recrystallized garnet & biotite+hornblende crystalloclasts in pelitic mylonite

TABLE 7.1 Temperatures for the M1 and M2 metamorphic episodes in the Loch Maree rocks as calculated in °C at 55Kb. The error involved is $\pm 50^\circ\text{C}$ for Ga-Bt calibration. The maximum and minimum temperatures were calculated using the maximum and minimum Kd values of all the analysed grains for each sample. The second values for M1 Ga-Hb thermometer (within brackets) are obtained by applying the correction described in the text. Chemical analyses of representative minerals are given in Table 7.2.

GARNETS	L-156A1 (pelitic mylonite)		L-68 (amphib. schist)		L-CAN (pelitic mylonite)		L-157X (meta-pelite)	
	No. of grains No. analysis	SD	0=8	SD	0=8	SD	0=8	SD
SiO2	14	0.56	7	0.34	5	0.23	6	0.28
TiO2	27	-	26	-	32	-	16	-
Al2O3		0.35		0.29	21.32	0.06	20.89	0.18
FeT Fe2+		29.31		30.20	33.85	0.39	29.74	0.92
Fe3+	30.79	1.41	1.966	0.55	0.156	2.53	4.42	2.53
MnO	3.00	2.53	0.099	0.23	0.153	0.10	0.023	0.023
MgO	0.97	0.22	0.204	0.116	0.229	0.08	1.34	0.22
CaO	8.01	1.40	1.92	0.44	2.58	0.08	0.305	0.305
Na2O	-	-	6.32	0.60	5.97	0.28	6.95	0.67
K2O	-	-	-	-	-	-	-	-
TOTAL	100.05	100.66	100.5	100.76	101.01	101.26	99.99	100.18
			8.000	8.000	8.000	8.000	8.000	8.000
Pyrope				END MEMBERS (MOL%)				
Almandine				7.2				5.1
Spessartine				65.3				60.5
Grossular				4.6				9.6
Antradite				16.3				13.8
				9.8				10.8

TABLE 7.2 ^A Representative analyses of minerals used for geothermometry. The first column of garnet specimens show the analyses with total iron (FeT) as given by microprobe; the second column shows the standard deviation (SD); the third and fourth columns present the results of calculation for Fe2+ and Fe3+ (with the new totals) and the number of ions on the bases of 8 oxygens respectively.

HORNBLENDES	L-68		L-CAN		L-156A1		L-68		L-CAN		L-157X		
	4	SD	10	SD	6	SD	8	SD	6	SD	3	SD	
40.92	0.58	41.46	0.80	42.01	1.39	35.48	0.91	34.63	0.86	35.03	0.72	34.90	0.36
0.55	0.11	0.48	0.08	0.12	0.1	1.58	0.35	1.74	0.25	1.99	0.22	2.08	0.26
15.26	2.00	14.89	0.69	15.19	2.19	18.21	0.32	17.28	0.71	17.86	0.32	17.80	0.21
21.13	2.63	18.23	0.59	19.13	0.88	21.61	1.05	19.72	0.88	21.92	0.71	21.45	0.25
0.15	0.09	0.05	0.08	0.03	0.05	-	-	-	-	-	-	-	-
5.85	0.98	8.07	0.35	7.28	1.29	9.35	0.60	10.70	0.43	8.89	0.37	8.49	0.11
11.37	0.22	11.15	0.28	11.24	0.18	-	-	-	-	-	-	-	-
1.46	0.15	1.72	0.21	1.40	0.27	-	-	-	-	-	-	-	-
0.70	0.05	0.30	0.12	0.29	0.16	9.34	0.56	8.61	0.35	9.15	0.41	9.02	0.34
97.39		96.37		96.69		95.57		92.68		94.84		93.74	

	M1 AMPHIBOLITES				M2 AMPHIBOLITE				AMPHIB. SCHIST		M myl: ULTRAI
	L-250A	L-198B	L-160F2	L-68	L-160F2	L-198B	L-68	L-160F2	L-68	L-202F	
Sample no.	8 11	7 10	6 11	2 2	6 11	7 10	2 2	6 11	2 2	7 8	L-202F
No. of grains	0=8	0=8	0=8	0=8	0=8	0=8	0=8	0=8	0=8	0=8	
No. analysis	0=8	0=8	0=8	0=8	0=8	0=8	0=8	0=8	0=8	0=8	
SiO2	59.27	58.80	64.79	60.47	64.79	58.80	60.47	64.79	60.47	65.99	
Al2O3	26.04	26.00	22.86	23.83	22.86	26.00	23.83	22.86	23.83	20.64	
CaO	7.60	7.53	3.54	5.41	3.54	7.53	5.41	3.54	5.41	1.09	
Na2O	7.43	7.38	9.80	8.51	9.80	7.38	8.51	9.80	8.51	10.94	
TOTAL	An = 37	An = 36	An = 17	An = 26	An = 100.99	An = 99.71	An = 98.36	An = 100.99	An = 98.36	An = 98.75	

TABLE 7.3 PLAGIOCLASE COMPOSITION

nite MYLONITE-GN	MYLONITE MAFIC GN		METASED.		LITHOCLAST METASED.	
	L-167K3	0=8	L-241	0=8	7	0=8
0=8	3 3		11 16		7 7	
8.783 3.23 0.16 2.822 An = 5	62.72 22.42 3.43 9.66 98.23	8.448 3.56 0.495 2.521 An = 16	62.82 23.26 4.26 9.24 99.58	8.285 3.620 0.605 2.356 An = 20	62.19 23.39 4.51 8.89 98.98	8.309 3.686 0.645 2.303 An = 34

7.3 (CONT.)

CHAPTER 8 - TECTONIC MODEL

8.1 INTRODUCTION

8.2 MODEL

8.3 REGIONAL CORRELATION - DISCUSSION

8.1 INTRODUCTION

The aim of this chapter is to erect a tectonic model capable of explaining the structural geometry and kinematic pattern exhibited by the Loch Maree rocks. Only the compressional structures formed during and after the D1 deformational phase are dealt with: those structures like the banding of gneisses in domain I that were formed before D1 are excluded from the model. The model relies essentially on the evidence obtained in the particular part of the Loch Maree district investigated, and it forms a basis for pointing out similarities and differences with the existing ideas about the evolution of equivalent rock assemblages in adjacent districts. It is presented to account for the relative chronology of development of the structures (D1 to D4) in the Loch Maree district, but it has implication for regional correlation of structures.

8.2 MODEL

D1-D4 deformation of the Loch Maree rocks is interpreted as having taken place in a gently-dipping ductile shear zone. The structures developed are very similar to those described from 'thin-skinned' tectonic regimes (Fig. 8.2; Chaps 5,6,7), where the marbles of domain IV correspond to the weak basal layer that is essential if the mechanical problems of thrust-faulting are to be overcome (Muller and Hsu 1980, Chapple 1978). The presence of such a layer, makes a model of thrusting driven by horizontal compressive surface forces in the early stages of evolution of the region more appropriate than one in which the thrusting was gravity-controlled, considering the available evidence (cf. Elliott 1976, Chapple 1978, Cooper 1981). Support for the existence of a compressional flow regime is provided by (i) evidence for the widespread formation of

folds associated with the shearing episode (ii) a metamorphic history consistent with crustal thickening and (iii) the asymmetry of the Letterewe synform.

The proposed model allows the Folais (domain IV) and Gleann Tulacha bands (Fig. 8.1) to be part of the same lithological assemblage that was repeated by D1 thrusting, something that fits with the suggestion of Peach et al. (1907, p.235) that differences in the appearance of marbles of these two bands could be the result of deformation.

The marbles that originally lay on the basement gneisses (as shown by the Gleann Tulacha band), are interpreted as having been moved tectonically to upper structural levels (Folais band) during the translation of the basement. The initial attitude of the ramp is difficult to determine due to subsequent tectonism, but a shallowly SE-dipping slope is suggested by the pattern of lineations (L1-L2) and the SE-plunging attitude of most folds (cf. Sect. 6.2.1)

A NW-directed movement of the hangingwall is implied by most kinematic indicators observed in the early mylonites (cf. Sect. 5.3). The magnitude of displacement is difficult to estimate. However if the average X:Z ratios of the strain (~10:1) measured in the phenocrysts is considered as homogeneously distributed (but see Sect. 6.3) over a thickness of 15-20km for the thrust slice (cf. Chap. 7), then displacements of the order of 150-200km are obtained. These estimates are, however, too high when compared to the existing figures for displacement of thrusts or even the predictions of the proposed tectonic model (see below), so that they must be in error as a function of the crude assumptions on which they are based. The estimate based on the combination of (i) temperature variation between M1 ^{and} mylonite, (ii) average geothermal gradient and (iii) plunge of L1-L2 structures indicate a more realistic (?) figure of 25 km of displacement for this thrust.

The same features observed in shear zones at microscopic scale (i.e. pods of less deformed rocks and intrafolial folds formed in a

progressive and continuous fashion; cf Tchalenko 1970, Coward 1976a and Chaps. 3,4,6) are likely to be reproduced on the crustal scale. These early (F1-F2) folds are considered to be the result of local instabilities and/or differential movement in the shear zone (cf Chap. 6) in which several localized shears would be expected to develop propagating in the direction of movement. The resultant high strain mylonitic banding (or thrust zone), on entering the compressional field for the new incremental ellipsoid in this zone of non-coaxial deformation, would be buckled resulting in the formation of folds. Such a sequence of events seems to be adequate to explain the relationship between the main thrust horizon and the (F2) Letterewe synform with the thrust and the synform representing only single structures in a much wider compressional shear zone (Fig. 8.2a).

According to this interpretation folds that initially displayed a NW vergence and had hinges at high angles to the movement direction developed an axial planar foliation (S2) as a result of shortening (Fig. 8.2b). This foliation could have been produced by the strain distribution around a frontal ramp, as material passed from a lower to an upper flat (cf. Sanderson 1982). From its position at this stage, it can be predicted that the (S2) foliation would show mylonitic features due to the localized high deformation and a sinistral sense of displacement (cf. Chap. 4) that corresponds to a shear couple where the hangingwall moved towards the NW. With the progression of the shear strain, the Letterewe synform and associated (S2) foliation would be rotated clockwise until its hinge attained parallelism with the stretching direction. The operation of such a process would account, at least in part, for the large hinge-parallel extensions recorded (cf. Chap. 6, see also Ridley 1986, fig.9) with the continuation of the deformation. It also accounts for the geometry and attitude of the (F2) Letterewe synform remaining basically the same since the end of D2 deformational phase and being subsequently affected by the F3 and F4 folds (cf. Chaps. 3,6).

On a larger scale the Loch Maree zone is envisaged as a shear zone flat of a strike-slip fault system whose corresponding small scale lateral ramps are the Laxfordian steeply-dipping shear zones of the

Lewisian Complex (cf. Coward and Park 1987).

The presence and attitude of F3 and F3 folds, with N-NW trending hinges, and considered part of the same overall regime of deformation, are essential elements of this model since they are interpreted as indicating a NE-E, SW-W orientation for the maximum compression direction (see below and Chap. 6). The hinges of these two fold phases exhibit a clockwise relationship with the L1-2 lineation and fold hinges (cf. Sect. 6.2.1, diagrams 5 and 17). This relationship is interpreted here as produced by shortening and possibly slip parallel to the shear direction but in a plane at high angles to the flat-lying shear zone. The progressive uplift of these rocks under a constantly oriented stress system produced the SW and NE directed thrusts and slides associated with the F3 folds (cf. Sect. 6.2.2.4) and the still younger and high structural level F4 open buckles (cf. Fig. 8.2c).

The crust at this stage would be deforming in a less homogeneous way so that the influence of e.g. early planar features would control the ongoing deformation when buckle and chevron folds would be formed (cf. Chap. 6). The model of evolution of these particular structures is based on simple transpression (cf. Sylvester and Smith 1976, fig.21) that has inspired Coward and Kim (1981) and Meneilly and Storey (1986) to explain the formation of late kink bands and chevron folds with plunges subparallel to the early stretching lineation. Due to the relatively low strain indicated by these late folds they would be unlikely to have been rotated towards their present position (cf. Sect. 6.2.2.3). However, their regionally consistent expression and orientation suggests that these folds do not represent conditions of local deformation.

There are significant differences between the present model and interpretations of the deformation of the Lewisian Complex (including the Loch Maree district) during the Laxfordian Cycle proposed by Coward (1984), Coward and Park (1987) and Park et al. (1987). The model has a 'top to NW' and 'up-the-slope' sense of displacement of the hangingwall, which brought the basement

gneisses from below the cover, and implies a contractional nature for this (flat) movement zone at Loch Maree. The interpretation of this shear flat as a 'local' manifestation of a much larger sinistral right-stepping strike-slip system (cf. Fig.8.3a) provides a much simpler and more elegant explanation for the emplacement of the basement gneisses than the one proposed by Park et al. (1987, fig.9). It is also consistent with the sinistral sense of displacement for Laxfordian (pre-Torrionian) shear zones as determined by Sutton and Watson (1962, p.104), Beach (1974), Beach et al. (1974) and Coward et al. (1980) in the Central Belt of the Lewisian Complex while an overall dextral sense of displacement is required in the interpretations of Coward (1984), Coward and Park (1987) and Park et al. (1987). Based on sinistral and dextral senses of displacement determined for the shear zones in the Lewisian Complex at Torrion Wheeler et al. (1987) do point out the possibility that shear senses opposed to the 'overall sense of displacement of the belt' may be of only local significance (p.159). Thus despite the fact that the size of the (F2) Letterewe synform and its relationship to the flat-lying shear zone (cf. Fig. 8.3) suggests considerable large dimensions for this shear system, these structures are still very small on the continental scale. These relations are shown by Coward and Park (1987, p.136) and reproduced here as Figure 8.3b, where the Lewisian is correlated to the Nagssugtoqidian belt of Greenland. A NW-SE convergence is proposed for this belt, giving rise to a dextral displacement along the boundary of two major crustal blocks during Laxfordian D1-D2 and Nag 2 deformation cycles.

A possible way of accommodating the evidence from the Loch Maree rocks in this much broader system would be if the presently proposed fault system belongs to an antithetic wrench system (R' of Tchalenko 1970) in relation to the major structure i.e. the mobile belt itself (Fig. 8.3). As it can be observed in Figure 8.3 the position of the principal compression direction does not significantly differ on the scale considered.

A major constraint of this model is the scale of the observed structures. Accordingly, the order of faulting proposed (R') was considered as compatible with the dimensions of the major F2

synform (Fig. 8.2b) as well as the thicknesses of crust as calculated from the metamorphic conditions (Chapter 7) considering the dimensions of the Nagssugtoqidian mobile belt.

8.3 REGIONAL CORRELATION - DISCUSSION

If a model of progressive deformation and homogeneous kinematic history like the one discussed above is considered a realistic interpretation of the deformation of the presently investigated rocks, the significance of structures indicating such an evolution (e.g. stretching lineation) can be more useful for the structural correlation than the relative age of folds. Accordingly, due to the difficulties with the use of 'geometric' correlation between the different domains, especially with the metasediments, the attitude shown by the ~~rodding~~ *rodding* lineation in this domain was utilized in the correlation (cf. Sect. 3.3). Because of this, such an approach has been used in the investigation of continental-scale structures (cf. Shackleton and Ries 1984), like the mobile belts of the African continents, for which no detailed structural data are available (cf. Coward 1976b, 1984, Coward and Daly 1984, Daly 1986).

From the discussion of the problems involved with the local correlation of structures (Sect. 3.3) and the evaluation of the role of the mechanisms controlling the development of folds (by far the most common structures in the Loch Maree area), it is clear that structural correlation of these features even across small areas of good exposure is a difficult task. In the case of the Loch Maree rocks, where the bulk of the evidence indicates that simple shear has controlled most of the deformational history (cf. Chaps 5,6), variables that are critical for structural correlation are the scale and stage of development of the folds. While it was possible to correlate small scale structures with some confidence, because of their position in relation to a large feature such as the Letterewe synform, the situation becomes considerably more complex where this control is not available. This is due to the possibility that large folds in places not far apart such as Loch

Maree and Gairloch (see Fig. 8.1), while controlled by the same deformational mechanism, can represent diverse stages of development. Correlation by fold phases in this situation can produce inconclusive results and might be an important factor in the long standing debate about correlation in fold belts (see Treagus 1987 for a re-interpretation of the correlation in the British Caledonides). Bearing this in mind and from the difficulties faced in the present study, an over-simplified flow-diagram proposing a general approach to the structural correlation in zones of complex deformation is presented below (Fig. 8.4).

Correlations in the Lewisian Southern Belt

The above discussion has implications regarding the correlation of structures in the Loch Maree district with other structures in the 'Southern Belt' of the Lewisian Complex.

1. Assuming that the Letterewe synform was formed in a shear zone of crustal dimensions, sensible criteria need to be met before any attempt is made to correlate it with other regionally expressed folds such as the Carnmore antiform to the N and the Tollie antiform on the southwest end of Loch Maree (Fig. 8.1). Although no structural analysis of the latter structures was carried out, a comparison of the characteristics of geometry, style, orientation etc. between the structures described in this study and the ones reported in the literature (Park 1970), suggest that the Tollie and Carnmore antiforms might not be equivalent to the (F2) Loch Maree synform. A rapid way of testing this suggestion would be to examine the pattern of L1-L2 stretching lineation across these folds.

2. The possibility that the age and expression of phases of thrusting can vary from place to place has implications for the interpretation of the age and geometry of the thrusts that segment the sulphide ore body in the Gairloch district. There, shear zones described by Jones et al. (1987, p.134) might correspond to D1 structures at Loch Maree, while several features reported as

related to their 'main thrust' (pp. 134-135) appear to be similar to structures associated with D3 or even younger deformational phases described in chap. 3.

Thus a more reliable correlation of structures in the above cases seems likely using structures that show the same movement pattern. In this regard, the prominent stretching lineation (as marked by the several types of mullions, stretched phenocrysts etc.) form a basis for correlation of structures in the metasediments of the Loch Maree and Gairloch districts (cf. Sect. 6.3).

Perhaps the only possible 'classical' correlation (i.e. based on geometry, style, orientation etc.) of the Loch Maree structures would be with features described by Crane (1978), who mapped the physical continuation of the Letterewe synform, NW of the area of the present study. There, it is possible that:

(a) structures ascribed by Crane (op.cit.) to a D5 event comprising folds with penetrative NW-SE foliation and associated amphibolite facies metamorphism (with local development of migmatites) are equivalent to the compositional banding in the gneisses of domain 1 at Loch Maree. This fabric for which there is no radiometric dating in either of the areas, is thought to be of Inverian age (Crane 1978, p.228). This possibility is not unlikely considering that the age of the Badcallian cycle is slightly older than c. 2.7 Ga (cf. tables 1.1 and 8.1) ^{and} the existing radiometric data for the gneisses Loch Maree indicates a late Archaean age for the quartzofeldspathic material (c. 2.6 Ga, U-Pb in zircons). A strong overprinting at c. 1.9 Ga (Rb-Sr whole rock) which has affected the already existing banding and the (few discordant) basic minor intrusions is here denominated D1 and ascribed to the Laxfordian cycle (cf. Chaps. 3,4,5,6).

(b) Crane's D6 and D7 events could perhaps be correlated with D1 and D2 at Loch Maree and his D8 to D4 and D000° of the present work. This ^{is} mainly on the basis of associated metamorphic grade and orientation of foliations and folds. Similarly to the work of Jones et al. (1987) there is no information about the variation pattern of lineations in the work of Crane (op.cit.). In addition, there is no mention of the existence of the recumbent F3 folds, but the presence of these structures around Ardlair (NW end of the

loch) was confirmed by R.G. Park (pers. commun. 1985).

Problems of Correlation

Similar kinematic histories can be misleading due to the possibility that deformational phases widely apart in time share the same kinematic characteristics. In this case radiometric dating and/or physical continuity between the areas under consideration are necessary for a successful correlation. Good examples are the similarities between the structures presently investigated and the structures developed in the Moine Thrust zone, cropping out a few miles to the east of the area mapped, or the case of the Outer Hebrides thrust zone, until recently thought to be a Caledonian structure. In the latter case striking similarities between several of the structures and textures as described by Fettes and Mendrum (1987, pp.39-41) with the ones at Loch Maree (including the post-mylonitization idioblastic garnets - cf. Sect. 5.3 and Chap. 7) would be suggestive of a possible correlation between these thrust zones. Accordingly, Smith and Fettes (1979) and Fettes and Mendrum (1987) have recently proposed a 'Laxfordian component' for the Outer Hebrides thrust. However, these authors indicate a late Laxfordian age for their 'early thrusting' (D5-D6 in their structural sequence) with maximum ages of c. 1.6 Ga, in clear contrast with the relative (D1) and absolute (c. 1.9 Ga, T.Dempster, pers commun. 1987) ages for the main thrusting episode at Loch Maree. The correlation between these structures and the late thrusts reported in this study is also unlikely. This is not only due to their different characteristics but also as a function of the SW-NE movement direction shown by the late thrusts at Loch Maree.

Concluding Remarks

Structural correlation based on fold geometry, orientation and style are considered to be hazardous where no mapping of the physical continuity between the structures is possible.

The correlation between structures within the Letterewe Synform (the present study and the work of Crane 1978) seems to be possible on the 'classical' criteria of correlation, i.e. on the basis of style, orientation etc.

Thus the most likely correlation between structure (e.g.) in the Loch Maree and Gairloch districts, is probably based on the pattern of the L1-L2 stretching lineation and consequently on the kinematic features of the deformation.

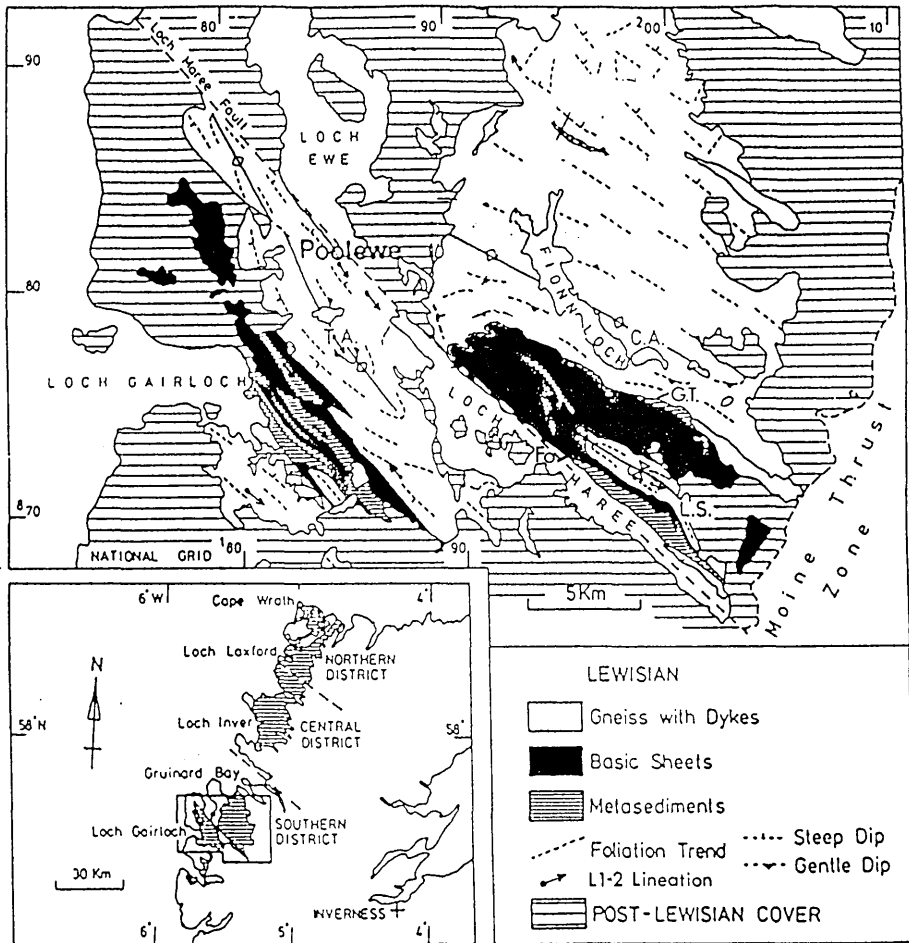


FIG. 8.1 Simplified geological map of the Lewisian Complex in the Loch Maree and Gairloch districts ; C.A.= Carnmore antiform; L.S.= Letterewe synform; T.A.= Tollie antiform; G.T.= Gleann Tulacha band; Fo= Folaís band; see structural and lithological maps for detail of the Letterewe area (modified after Crane 1978, fig.1).

CHAPTER 8 -CAPTIONS OF FIGURES

Fig. 8.2a Detail of the thrust structure shown in Fig.8.3a.This represents the Letterewe synform which is shown as a typical structure of a flat-lying shear zone, already affecting the tectonic interleaving of basement and cover

Fig. 8.2b Detail of Fig.8.2 a showing the geometry of the Letterewe synform; note the position of the S2 foliation and the incipient stage of (clockwise) rotation of the hinge towards the NW-SE extension direction.

Fig. 8.2c Transpression model to reproduce the D3-D4 continuous deformation at Loch Maree, which could be accommodated by a component of thrusting towards SW (F3 folds) together with sinistral,oblique-slip giving rise to the late F4 buckle folds.

Fig. 8.3a Large scale transpressional model proposed to account for the kinematic indicators, and rarity of thrust structures as compared to steeply-dipping shear zones.

Fig. 8.3b Relationship between the Lewisian Complex of NW-Scotland and the equivalent Nagssugtoqidian Proterozoic shear belt of Geenland (see also [Howard and Park op.cit., fig.10b](#)).

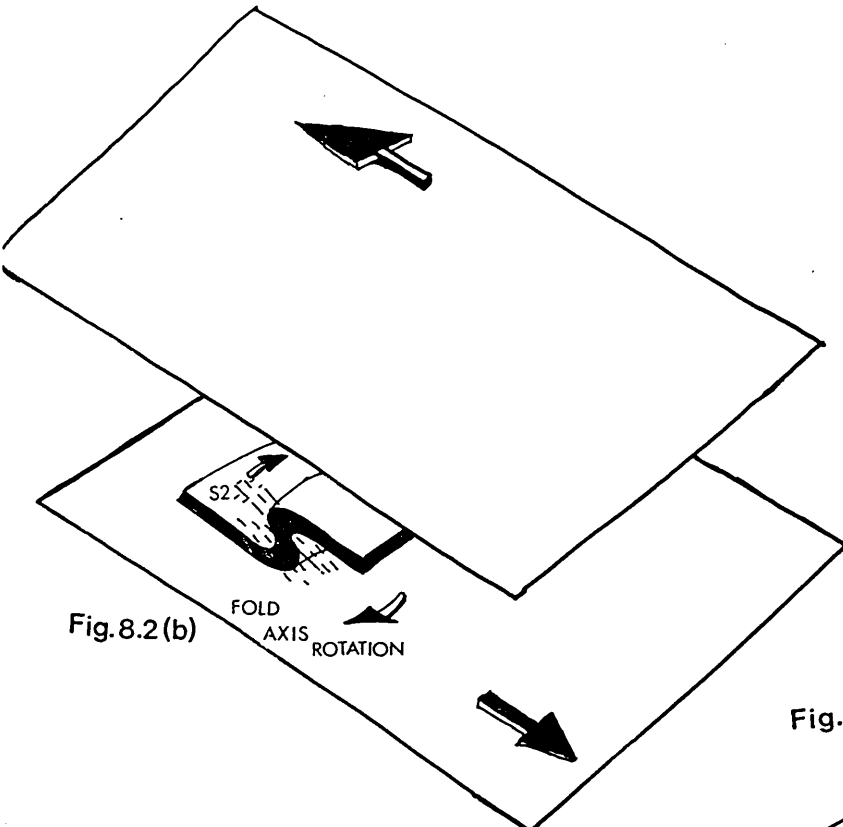


Fig. 8.2(b)

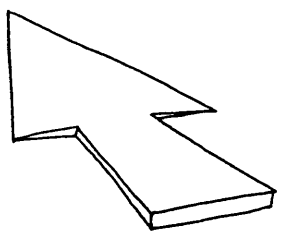


Fig. 8.2(c)

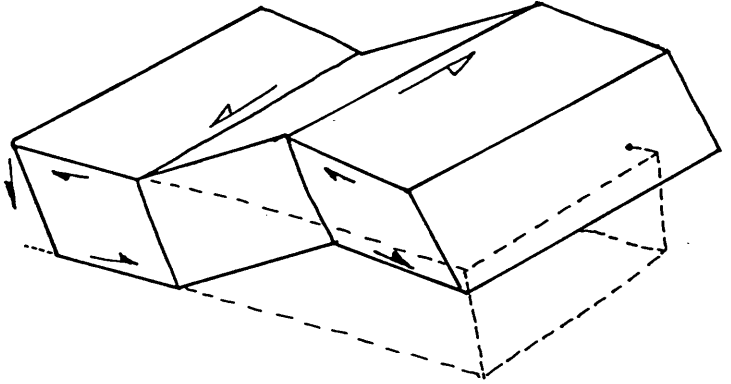
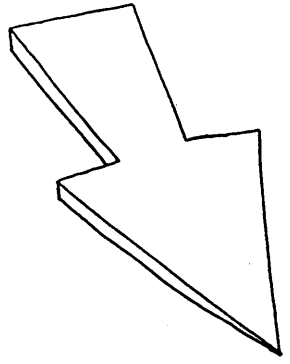
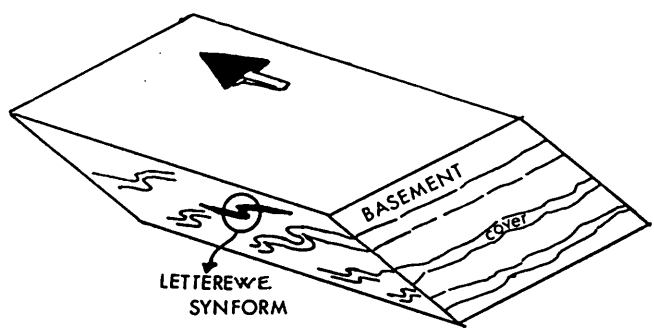


Fig. 8.2(a)



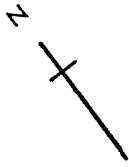
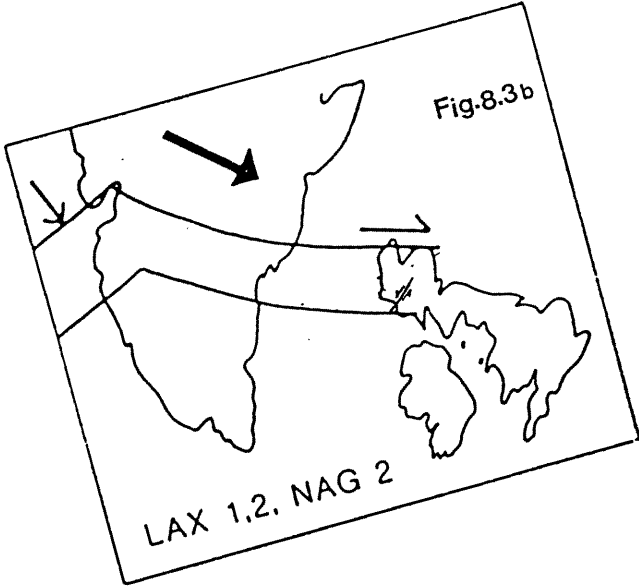
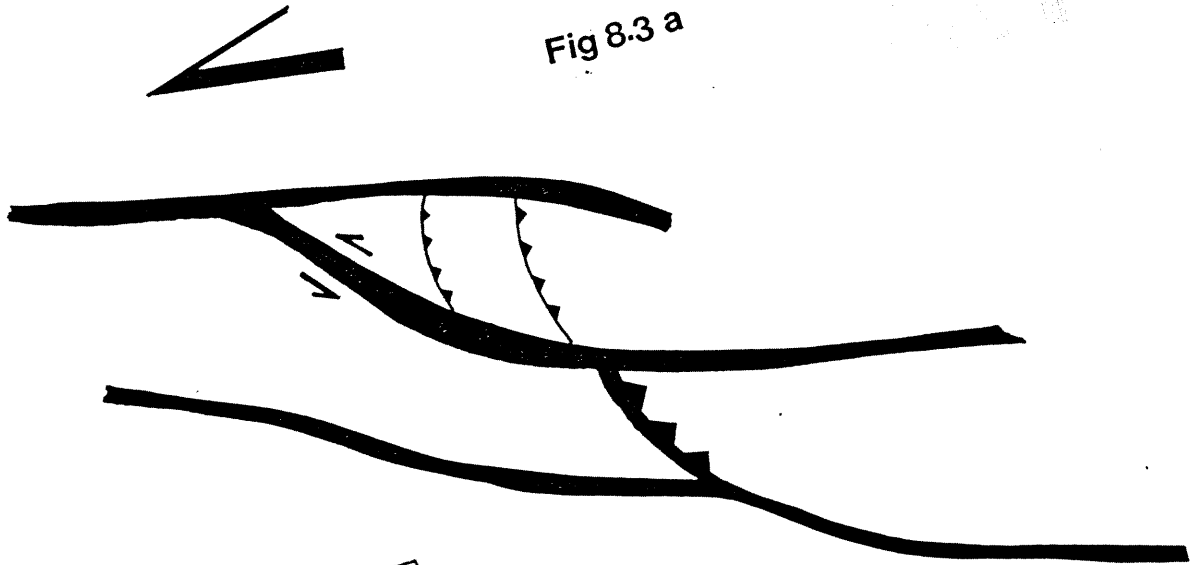
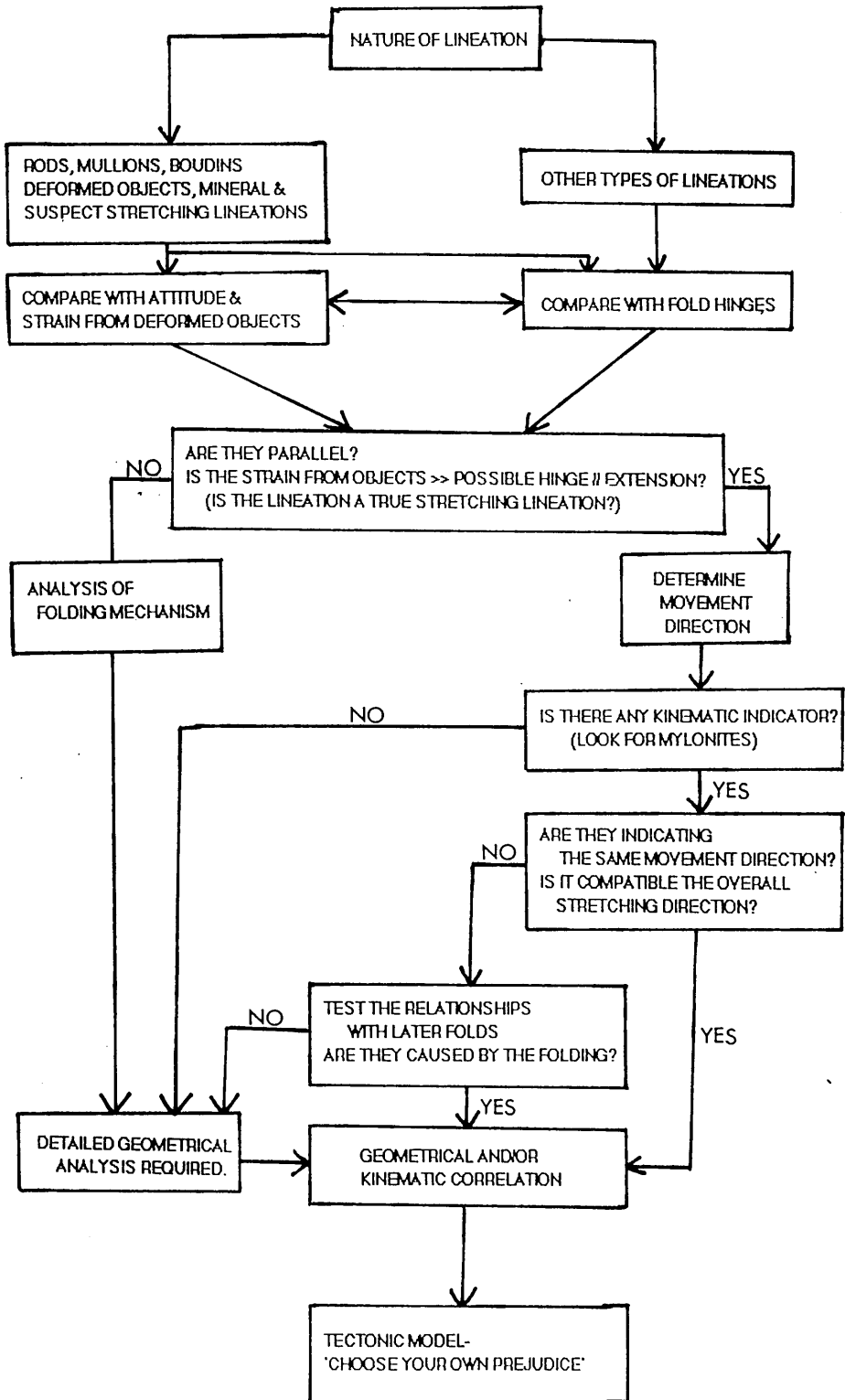


Fig 8.3 a



APPROACH TO STRUCTURAL
CORRELATION IN POORLY-KNOWN ZONE
OF COMPLEX DEFORMATION.



CHAPTER 9 - CONCLUSIONS

The following are the principal conclusions of the present study.

From the study of the rock units and their distribution (Chap.2):

1. Metasediments, amphibole schists, marbles of an early Proterozoic volcano-sedimentary sequence and late Archaean quartzofeldspathic gneisses (U-Pb zircon c. 2.6 Ga) with amphibolites are the main tectono-sedimentary units of the Lewisian Complex at Loch Maree.
2. Zones of mylonite (dated Rb-Sr whole-rock at c. 1.9 Ga) occur at major lithological boundaries within the gneiss and metasedimentary assemblages in tectonic contact.
3. Distribution of rock units is strongly controlled by a large SE-plunging synform (Letterewe synform).

From the study of the structural features, their sequential development and correlation (Chap.3).

4. The rocks are polydeformed with structures developed as a function of their (i) rheological properties (ii) orientation and geometry and (iii) strain variations. The structural domains coincide with the major lithological units whose distribution is controlled by the Letterewe synform.
5. Four phases of deformation producing NW-SE trending approximately coaxial folds and associated features were identified. In addition, there are other later sets of structures with N-S to NE-SW trends.

6. During late D1 times the gneisses and amphibolites (basement) were tectonically emplaced over the metasedimentary-volcanogenic rock assemblage (cover) with widespread development of mylonites. This deformation was particularly strong along the marble unit, corresponding to the principal movement zone of the 'Loch Maree thrust zone.'
7. The Letterewe synform is a composite structure whose geometry is a product of D2 and D4 deformational phases.
8. Correlation of structures based on style, orientation, physical continuation and combination of several sets of these features was possible on the local scale mainly due to the control provided by the geometry of the large Letterewe synform. This structure (and its associated features) was used as a local 'datum' in the correlation, with all the structures older than this fold in the cover rocks ascribed to D1 deformation.

From the fabric studies (Chap.4).

9. The expression and development of the microfabrics are a function of the composition of the affected rocks and strain (type and intensity) variation so that the classical approach of fabric analysis produced ambiguous results. No tabulation of the relationship between time, metamorphism and deformational phases was possible from the textural analysis, and assessment of the relative age of mineral growths had to be carried out independently for each case.
10. Microfabric work was found to require support from electron microprobe analysis and detailed examination of the deformation mechanisms at the microscopic scale if consistent results were to be achieved.

From the study of the mylonites (Chap.5).

11. Most of the mylonitic rocks were formed by predominantly D1 simple shear deformation during which the basement was thrust over the cover.
12. Analysis of kinematic indicators points to a NW-directed emplacement of this basement.
13. Several strain softening mechanisms are thought to be responsible for the localization of the deformation in zones of high strain. Of greater importance were heterogeneities like lithological contacts and 'soft' minerals.
14. An empirically determined sequence of minerals exhibiting increasing resistance to grain size reduction is calcite-biotite-muscovite-feldspar-garnet-amphibole-epidote.
15. High fluid pressures along lithological contacts promoted localized and transient brittle deformation during D1 mylonitization with the production of mylonitized pseudotachylites and breccias.
16. Based on the mode of deformation at microscopic scale no simple and straightforward criteria could be established from which to determine the brittle-ductile character of the deformation.
17. Fluid pressure and other variables beside P-T conditions are important for the style of deformation expressed and no single extrapolation of metamorphic conditions were found possible.

From the interpretation of the structures (Chap.6).

18. Analysis of the variation in patterns shown by D1 and D2 structures along the northeastern and southwestern limbs of the Letterewe synform confirms its composite structure (cf. conclusion 7).

19. Geometrical analysis of the (F1 to F4) folds and associated features suggests that buckling was an important mechanism during the early stages of development of these structures; layers with viscosity contrasts were shortened at low angles to the layering.

20. Viscosity contrast between quartzofeldspathic gneisses and associated amphibolites has varied in a complex way from D1 to D4 deformational phases. This was possibly a function of variations of strain rate and mechanism of deformation, existing anisotropies and their orientation in relation to the stress system, and also temperature variations; there is no evidence to suggest that mineralogical changes exercised such a control.

21. F1 and F2 folds showing variable geometries can be accommodated in a model involving (initial) buckling and superimposed simple shear, during which fold hinges rotated towards the extension direction. This model can also explain the large extensions parallel to the hinges observed in some of these folds.

22. Analysis of strain in deformed phenocrysts confirm the true nature of the hinge parallel extensions with strain values of $\underline{c.}$ 18:1 (X:Z). This indicates a NW-SE direction of extension for the D1-D2 event, consistent with the orientation obtained from the analysis of kinematic indicators observed in the mylonites.

23. Tectonites with prolate fabric are predominant and exhibit higher strains than oblate strain markers which are more common as mylonite zones are approached.

From the study of the metamorphic conditions (Chap.7).

24. Metamorphic conditions as determined from geothermometry and use of petrogenetic grids indicate amphibolite facies conditions for M1 and M2 and greenschist facies conditions for the late D1 mylonitization event.

25. Geothermal gradients of 25-30°C/Km (in the range of Barrovian-type metamorphism) were determined for M1 and M2.

26. Geochemical changes accompanying mylonitization include mobilization of Ca, K, Na, Mg, Si during conditions of abundant fluid movement (particularly H₂O and CO₂) producing mineralogical convergence in ultramylonites.

27. Decrease in temperature between M1 and M2 is consistent with a thickening of the crust by thrusting.

28. The temperatures obtained for M1 (and M2) are generally consistent with the published values for metamorphism associated with Laxfordian deformation in the Assynt region of the Lewisian Complex.

From the tectonic model (Chap.8).

29. The available evidence suggests the possibility of accommodating the deformation of the Loch Maree rocks in an overall transpressive model. D1 and D2 deformation would take place in a flat-lying crustal scale shear zone which formed in a step-over

of a much larger scale sinistral right-stepping strike-slip system produced by a NE-E SW-W orientation of shortening. D3 and D4 deformation features would be produced during generalized crustal uplift under approximately constant orientation of the maximum compression direction.

30. Reliable correlation of the structural features based on style, orientation etc. is only possible within the area occupied by the Letterewe synform. Where this control is not available correlations based on features indicating the predominant kinematic pattern are thought to be more reliable.

BIBLIOGRAPHY

- AFTALION, M., DEMPSTER, T. J., BOWES, D. R. & FERNANDES, L. A. D. (in preparation). Isotopic constraints on the timing of mylonite formation in the Loch Maree Thrust zone, Lewisian Complex, NW Scotland.
- AFTALION, M., VAN BREEMEN, O. & BOWES, D. R. 1984. Age constraints on basement of the Midland Valley of Scotland. Trans. R. Soc. Edinb. Earth Sci. 75, 53-64.
- AGOSTINO, P. N. 1971. Theoretical and experimental investigations of pygmatic structures. Bull. Geol. Soc. Am. 82, 2651-60.
- ALLISON, I. & LATOUR, T. B. 1977. Brittle deformation of hornblende in a mylonite. Can. J. Earth Sci. 14, 1953-58.
- ALLISON, M., BARNETT, R. L. & KERRICH, R. 1979. Superplastic flow and changes in crystal chemistry of feldspars. Tectonophysics 53, 141-146.
- ANDERSON, G. M. & BURNHAM, C. W. 1983. Feldspar solubility and the transport of aluminium under metamorphic conditions. Am. J. Sci. 283A, 283-297.
- ANDREWS, J. R. 1984. Fracture controlled feldspar shape fabrics in deformed quartzo-feldspathic rocks. J. Struct. Geol. 6, 183-188.
- ANGELIER, J. & HUCHON, P. 1987. Tectonic record of convergence changes in a collision area: the Boso and Miura peninsulas, Central Japan. Earth Planet. Sci. Lett. 81, 397-408.
- ASHBY, M. F. & VERALL, R. A. 1978. Flow and fracture in the upper mantle. In "Creep Engineering Materials and of the Earth". Phil. Trans. R. Soc. Lond. A288, 59-95.
- ATHERTON, M. P. 1976. Crystal growth models in metamorphic tectonites. Phil. Trans. R. Soc. Lond. A283, 255-70.
- ATKINSON, B. K. 1987. (ed.) Fracture Mechanics of Rock. Academic Press London, 534 pp.
- AYRTON, S. N. & RAMSAY, J. G. 1974. Tectonic and metamorphic events in the Alps. Schweiz. Mineral. Petrogr. Mitt. 54, 609-39.
- BAK, J., KORSTGÅRD, J. & SØRENSEN, K. 1975. A major shear zone within the Nagssugtoqidian of West Greenland. Tectonophysics 27, 191-209.
- BALLY, A. W. 1981. Thoughts on the tectonics of folded belts. In MCCLAY, K. R. and PRICE, N. J. (eds) "Thrust and Nappe Tectonics." Spec. Publ. Geol. Soc. Lond. 9, 13-32.

- BARBER, D. J. 1985. Dislocations and microstructures. *In* WENK, H. (ed.) "Preferred Orientation in Deformed Metals and Rocks: an Introduction to Modern Texture Analysis." Academic Press, New York, 145-182.
- BARBER, D. J. & WENK, H. R. 1979. On geological aspects of calcite microstructure. *Tectonophysics* 54, 45-60.
- BAYLY, H. B. 1974. Cleavage not parallel to finite-strain ellipsoid's XY-plane: discussion. *Tectonophysics* 23, 205-208.
- BAYLY, H. B. 1976. Development of chevron folds: Discussion. *Bull. Geol. Soc. Am.* 87, 1664.
- BEACH, A. 1974. The measurement and significance of displacements on Laxfordian shear zones, NW Scotland. *Proc. Geol. Assoc.* 85, 13-21.
- BEACH, A. 1975. The geometry of en echelon vein arrays. *Tectonophysics* 28, 245-263.
- BEACH, A. 1976. The interrelations of fluid transport, deformation, geochemistry and heat flow in early Proterozoic shear zones in the Lewisian Complex. *Phil. Trans. R. Soc.* A280, 569-604.
- BEACH, A. 1979. Pressure solution as a metamorphic process in deformed terrigenous sedimentary rocks. *Lithos* 12, 51-58.
- BEACH, A. 1980. Retrogressive metamorphic processes in shear zones with special reference to the Lewisian Complex. *J. Struct. Geol.* 2, 257-63.
- BEACH, A. 1981. Some observations of the development of thrust faults in the Ultradauphinois Zone, French Alps. *In* MCCLAY, K. R. and PRICE, N. J. (eds) "Thrust and Nappe Tectonics." *Spec. Publ. Geol. Soc. Lond.* 9, 329-334.
- BEACH, A., COWARD, M. P. & GRAHAM, R. H. 1974. An interpretation of the structural evolution of the Laxford front, NW Scotland. *Scott. J. Geol.* 9, 297-308.
- BEACH, A. & JACK, S. 1982. Syntectonic vein development in a thrust sheet from the External French Alps. *Tectonophysics* 81, 67-84.
- BEACH, A. & TARNEY, J. 1978. Major and trace element patterns established during retrogressive metamorphism of granulite-facies gneisses, NW Scotland. *Precamb. Res.* 7, 325-48.
- BEHRMANN, J. H. 1984. A study of white mica microstructure and

- microchemistry in a low grade mylonite. J.Struct.Geol. 6,283-292.
- BELL,A.M.1979.Factorization of finite strains in three dimensions. J.Struct.Geol. 1,163-167.
- BELL,A.M.1981a.Strain factorizations from lapilli tuff, English Lake District. J.Geol.Soc.Lond. 138,463-474.
- BELL,A.M.1981b.Vergence: an evaluation. J.Struct.Geol. 3,197-202.
- BELL,I.A. & WILSON,C.J.L.1981.Deformation of biotite and muscovite: TEM microstructure and deformation model. Tectonophysics 78,201-228.
- BELL,I.A., WILSON,C.J.L., MCLAREN,A.C. & ETHERIDGE,M.A.1986.Kinks in mica: role of dislocations and (001) cleavage. Tectonophysics 127,49-65.
- BELL,T.H.1978.Progressive deformation and reorientation of fold axes in a ductile mylonite zone: the Woodroffe Thrust. Tectonophysics 44,285-320.
- BELL,T.H.1981.Foliation development - the contribution, geometry and significance of progressive bulk, inhomogeneous shortening. Tectonophysics 75,273-296.
- BELL,T.H.1985.Deformation partitioning and porphyroblast rotation in metamorphic rocks: a radical reinterpretation. J.Met.Geol. 3,109-118.
- BELL,T.H.1986.Foliation development and refraction in metamorphic rocks: reactivation of earlier foliations and decrenulation due to shifting patterns of deformation partitioning. J.Met.Geol. 4,421-444.
- BELL,T.H. & BROTHERS,R.N.1985.Development of P-T prograde and P-retrograde, T-prograde isogradsic surfaces during blueschist to eclogite regional deformation/metamorphism in New Caledonia, as indicated by progressively developed porphyroblast microstructures. J.Met.Geol. 3,59-78.
- BELL,T.H. & DUNCAN,A.C.1978.A rationalized and unified shorthand terminology for lineations and fold axes in tectonics. Tectonophysics 47,T1-T5.
- BELL,T.H. & ETHERIDGE,M.A.1973.Microstructure of mylonites and their descriptive terminology. Lithos 6,337-48.
- BELL,T.H. & ETHERIDGE,M.A.1976.The deformation and recrystallization of quartz in a mylonite zone, Central Australia.Tectonophysics 32,235-267.
- BELL,T.H. & HAMMOND,R.L.1984.On the internal geometry of mylonite

- zones. J.Geol. 92,667-686.
- BELL, T.H. & RUBENACH, M.J. 1980. Crenulation cleavage development - evidence for progressive bulk inhomogeneous shortening from "millipede" microstructures in the Robertson River Metamorphics. Tectonophysics 68, T9-T15.
- BELL, T.H. & RUBENACH, M.J. 1983. Sequential porphyroblast growth and crenulation cleavage development during progressive deformation. Tectonophysics 92, 171-194.
- BERTHE, D. & BRAUN, J.D. 1980. Evolution of folds during progressive shear in the south Armorian shear zone, France. J.Struct.Geol. 2, 127-133.
- BERTHE, D., CHOUKROUNE, P. & JEGOUZO, P. 1979. Orthogneiss, mylonite and non coaxial deformation of granites: the example of the South Armorian shear zone. J.Struct.Geol. 1, 31-42.
- BIKERMAN, M., BOWES, D.R. & van BREEMEN, O. 1975. Rb-Sr whole rock isotopic studies of Lewisian metasediments and gneisses in the Loch Maree region, Ross-shire. J.Geol.Soc.Lond. 131, 237-254
- BIOT, M.A. 1961. Theory of folding of stratified visco-elastic media and its implication in tectonics and orogenesis. Bull.Geol.Soc.Am. 72, 1595-1620.
- BIOT, M.A. 1964. Theory of internal buckling of a confined multilayered structure. Bull.Geol.Soc.Am. 75, 563-568.
- BOHLEN, S.R. & LIOTTA, J.J. 1986. A barometer for garnet amphibolites and garnet granulites. J.Petrol. 27, 1025-1034.
- BOULLIER, A.M. 1980. A preliminary study on the behaviour of brittle minerals in a ductile matrix: example of zircons and feldspars. J.Struct.Geol. 2, 211-217.
- BOULLIER, A.M. & GUEGUEN, Y. 1975. SP-mylonites: origin of some mylonites, by superplastic flow. Contrib.Mineral.Petrol. 50, 93-104.
- BLACK, L.P., BELL, T.H., RUBENACH, M.J. & WITHNALL, I.W. 1979. Geochronology of discrete structural-metamorphic events in a multiply deformed Precambrian terrain. Tectonophysics 54, 103-137.
- BLACK, L.P., JAMES, P.R. & HARLEY, S.L. 1983. Geochronology and geological evolution of metamorphic rocks in the Field Islands area, East Antarctica. J.Met.Geol. 1, 277-304.
- BORRADAILE, G.J. 1972. Variably oriented co-planar primary folds.

- Geol.Mag. 109,89-98.
- BORRADAILE,G.J.1978.Transected folds: a study illustrated with examples from Canada and Scotland. Bull.Geol.Soc.Am 89,481-493.
- BORRADAILE,G.J.1981.Particulate flow of rock and the formation of cleavage. Tectonophysics 72,305-321.
- BORRADAILE,G.J.,BAYLY,M.B. & POWELL,C.McA.1982.(eds). Atlas of deformational and metamorphic rock fabrics. Springer-Verlag, New York, 551pp.
- BOUCHEZ,J.L. & PECHER,A.1981.The Himalayan Main Central Thrust Pile and its quartz-rich tectonites in Central Nepal. Tectonophysics 78,23-50.
- BOULTER,C.A.1976.Sedimentary fabrics and their relation to strain-analysis methods. Geology 4,141-146.
- BOWES,D.R.1969.The Lewisian of Northwest Highlands of Scotland. In KAY,M.(ed.) "North Atlantic - Geology and Continental Drift -a symposium." Am.Ass.Pet.Geol.Mem 12,575-594.Tulsa,Oklahoma.
- BOWES,D.R.1978.Shield Formation in early Precambrian times: the Lewisian complex. In BOWES,D.R. and LEAKE,B.E.(eds) "Crustal Evolution in NW Britain and Adjacent Regions". Geol.J.Spec.Pub. 10,39-80.
- BOWES,D.R. & GAAL,G.1981.Precambrian record of the eastern North Atlantic borderlands. In KERR,J.W. and FERGUSSON,A.J.(eds) "Geology of the North Atlantic Borderlands", Can.Soc.Petrol.Geol.Mem. 7,31-55.
- BOWES,D.R. & PARK,R.G.1966.Metamorphic segregation banding in the Loch Kerry basite sheet from the Lewisian of Gairloch, Ross-shire, Scotland. J.Petrol. 7,306-330.
- BOWES,D.R.,WRIGHT,A.E. & PARK,R.G.1964. Layered intrusive rocks in the Lewisian of the NW Highlands of Scotland. Quart.J. Geol.Soc.Lond. 120,153-192.
- BRADY,J.B.1983.Intergranular diffusion in metamorphic rocks. Am.J.Sci. 283A,281-200.
- BRODIE,K.H.1980.Variations in mineral chemistry across a shear zone in phlogopite peridotite. J.Struct.Geol. 2,265-272.
- BRODIE,K.H.1981.Variation in amphibole and plagioclase composition with deformation. (Abstr.) In JONES,M.E. (ed.) "The relationships between metamorphism and deformation: report of the Tectonic Studies Group discussion meeting held at the Geological Society, Burlington House, London, 12

- November 1980." J.Struct.Geol. 3,335.
- BROWN, M. 1984. Shear zone metamorphism: introduction. J.Met.Geol. 2,75.
- BRUN, J.P. & BURG, J.P. 1982. Combined thrusting and wrenching in the Ibero-Armorican arc: a corner effect during continental collision. Earth Planet.Sci.Lett. 61,319-332.
- BRUN, J.P. & COBBOLD, P.R. 1980. Strain heating in shear zones. J.Struct.Geol. 2,149-158.
- BURG, J.P. & LAURENT, Ph. 1978. Strain analysis of a shear zone in a granodiorite. Tectonophysics 47,15-42.
- BUTLER, R.W.H. 1982. The terminology of structures in thrust belts. J.Struct.Geol. 4,239-245.
- CAMPBELL, D.S. 1980. Structural and metamorphic development of migmatites in the Svecokareliides, near Tempere, Finland. Trans.R.Soc.Edinb.Earth Sci. 71,185-200.
- CARTER, N.L., ANDERSON, D.A., HANSEN, F.D. & KRANZ, R.L. 1981. Creep and creep rupture of granitic rocks. In CARTER, N.L., FRIEDMAN, M., LOGAN, J.M. and STEARNS, D.W. (eds) "Mechanical Behaviour of Crustal Rocks - The Handin Volume", Geophysical Monograph Series 24, Washington. 61-82
- CASEY, M. 1980. Mechanics of shear zones in isotropic dilatant materials. J.Struct.Geol. 2,143-147.
- CASEY, M., DIETRICH, D. & RAMSAY, J.G. 1983. Methods for determining deformation history for chocolate tablet boudinage with fibrous crystals. Tectonophysics 92,211-239.
- CHADWICK, B. 1968. Deformation and metamorphism in the Lukmanier region, central Switzerland. Bull.Geol.Soc.Am. 79,1123-1150.
- CHADWICK, P.K. 1975. A psychological analysis of observation in geology. Nature, Lond. 256,570-573.
- CHAMBERLAIN, C.P. 1986. Evidence for repeated folding of isotherms during regional metamorphism. J.Petrol. 27,63-89.
- CHAPPLE, W.M. 1969. Fold shape and rheology: the folding of an isolated viscous-plastic layer. Tectonophysics 7,97-116.
- CHAPPLE, W.M. 1978. Mechanics of thin-skinned fold-and-thrust belts. Bull.Geol.Soc.Am. 89,1189-1198.
- CHINNERY, M.A. 1966. Secondary faulting. I. Theoretical aspects. II. Geological aspects. Can.J.Earth Sci. 3,163-190.

- CHOUKROUNE, P. & GAPAIS, D. 1983. Strain pattern in the Rar Granite (central Alps): orthogneiss developed by bulk inhomogeneous flattening. J. Struct. Geol. 5, 411-418.
- CHRISTIE, J. & ORD, A. 1980. Flow stress from microstructure of mylonites: example and current assessment. J. Geophys. Res. 83, 6253-62.
- CLAESSON, S. 1986. Direct dating of thrusts in the Swedish Caledonides with the Rb-Sr thin slab technique. Geol. Foren. Stockholm Forh. 108, 277.
- CLIFF, R. A. 1985. Isotopic dating in metamorphic belts. J. Geol. Soc. Lond. 142, 97-110.
- CLOUGH, C. T. 1897. The geology of Cowal. "Mem. Geol. Surv. Scotland".
- CLOUGH, C. T., GUNN, W. & GREENLY, E. 1913. "The Lewisian gneiss". Mem. Geol. Surv. Scotland for Sheet 92, 14-38.
- COBBOLD, P. R. 1975. Unified theory on the onset of folding, boudinage and mullion structure: discussion. Bull. Geol. Soc. Am. 87, 1663.
- COBBOLD, P. R. 1976. Fold shapes as functions of progressive strain. Phil. Trans. R. Soc. Lond. A283, 129-138.
- COBBOLD, P. R. 1979. Origin of periodicity: saturation or propagation? (Abstr.) In "Description and Origin of Spatial Periodicity in Tectonic Structures: report on a Tectonic Studies Group Conference held at Nottingham University, 8 November 1978". J. Struct. Geol. 1, 96.
- COBBOLD, P. R., COSGROVE, J. W. & SUMMERS, J. M. 1971. The development of internal structures in deformed anisotropic rocks. Tectonophysics 12, 23-53.
- COBBOLD, P. R. & FERGUSON, C. C. 1979. Description and origin of spatial periodicity in tectonic structures: report on a Tectonic Studies Group conference held at Nottingham University, 8 November 1978. J. Struct. Geol. 1, 93-98.
- COBBOLD, P. R. & QUINQUIS, H. 1980. Development of sheath folds in shear regimes. J. Struct. Geol. 2, 119-126.
- COBBOLD, P. R. & WATKINSON, A. J. 1981. Bending anisotropy: a mechanical constraint on the orientation of fold axes in anisotropic medium. Tectonophysics 72, T1-T10.
- COOPER, M. A. 1981. The internal geometry of nappes: criteria for models of emplacement. In MCCLAY, K. R. and PRICE, N. J. (eds) "Thrust and Nappe Tectonics". Spec. Publ. Geol. Soc. Lond. 9 225-234.

- COSGROVE, J.W. 1980. The tectonic implications of some small scale structures in the Mona Complex of Holy Isle, North Wales. J. Struct. Geol. 2, 383-396.
- COWARD, M.P. 1973. Heterogeneous deformation in the development of the Laxfordian Complex of south west Outer Hebrides. Quart. J. Geol. Soc. Lond. 129, 139-160.
- COWARD, M.P. 1974. Flat-lying structures within the Lewisian basement complex of NW Scotland. Proc. Geol. Assoc. 85, 459-472.
- COWARD, M.P. 1976a. Strain within ductile shear zones. Tectonophysics 34, 181-197.
- COWARD, M.P. 1976b. Archean deformation patterns in southern Africa. Phil. Trans. R. Soc. Lond. A283, 313-331.
- COWARD, M.P. 1980a. The Caledonian thrust and shear zones of NW Scotland. J. Struct. Geol. 2, 11-17.
- COWARD, M.P. 1980b. Shear zones in the Precambrian crust of southern Africa. J. Struct. Geol. 2, 19-27.
- COWARD, M.P. 1984. Major shear zones in the Precambrian crust; examples from NW Scotland and Southern Africa and their significance. In "Kroner, R. and Greiling, R. (eds) "Precambrian Tectonics Illustrated". E. Schweizerbart'sche Verlagbuchhandlung, Stuttgart, 207-235.
- COWARD, M.P. & DALY, M.C. 1984. Crustal lineaments and shear zones in Africa: their relationship to plate movements. Precambrian Res. 24, 27-45.
- COWARD, M.P. & KIM, J.H. 1981. Strain within thrust sheets. In MCCLAY, K.R. and PRICE, N.J. (eds) "Thrust and Nappe Tectonics". Spec. Publ. Geol. Soc. Lond. 9, 275-292.
- COWARD, M.P., KIM, J.H. & PARKE, J. 1980. A correlation of structures and their displacement across the lower thrusts of the Moine Thrust zone, NW Scotland. Proc. Geol. Ass. 91, 327-337.
- COWARD, M.P. & PARK, R.G. 1987. The role of mid-crustal shear zones in the Early Proterozoic evolution of the Lewisian. In Park, R.G. and Tarney, J. (eds) "Evolution of the Lewisian and Comparable Precambrian High Grade Terrains". Spec. Publ. Geol. Soc. Lond. 27, 127-138.
- COX, S.F. & ETHERIDGE, M.A. 1983. Crack-seal fibre growth mechanisms and their significance in the development of oriented layer silicate microstructure. Tectonophysics 92, 147-170.

- CRANE, A. 1978. A correlation of metamorphic fabrics and the age of Lewisian near Loch Maree. Scott. J. Geol. 14, 225-246.
- CUTHBERT, S. J., HARVEY, M. A. & CARSWELL, D. A. 1983. A tectonic model for the metamorphic evolution of the Basal Gneiss Complex western S. Norway. J. Met. Petrol. 1, 63-90.
- DALY, M. C. 1986. Crustal shear zones and thrust belts: their geometry and continuity in Central Africa. Phil. Trans. R. Soc. Lond. A317, 111-128.
- DALY, M., PRIOR, D., WHEELER, J. & BUTLER, R. 1985. Brittle thrusting and low grade metamorphism at Loch Maree: a high level in the Laxfordian crust. (Abstr.) 3rd Lewisian Symposium, Leicester 1985.
- DALZIEL, I. W. D. 1981. Back-arc extension in the southern Andes: a review and critical reappraisal. Phil. Trans. R. Soc. Lond. A300, 319-335.
- DALZIEL, I. W. D. & BAILEY, S. W. 1968. Deformed garnets in a mylonitic rock from the Grenville Front and their tectonic significance. Am. J. Sci. 266, 542-562.
- DAVIS, D., SUPPE, J. & DAHLEN, F. A. 1983. Mechanics of fold and thrust belts and accretionary wedges. J. Geophys. Res. 88B, 1153-1172.
- DAVIS, G. H. 1983. Shear-zone model for the origin of metamorphic core complexes. Geology 11, 342-347.
- DAVY, Ph. & GILLET, Ph. 1986. The stacking of thrust slices in collision zones and its thermal consequences. Tectonics, 5, 913-929.
- DE BOER, R. B. 1977. On the thermodynamics of pressure solution - interaction between chemical and mechanical forces. Geochim. Cosmochim. Acta 41, 249-256.
- DE CAPRARIIS, P. 1974. Stress-induced viscosity changes and the existence of dominant wavelengths in folds. Tectonophysics 23, 139-48.
- DEER, W. A., HOWIE, R. A. & ZUSSMAN, J. 1982. "Rock-forming minerals. Vol. 1A: Orthosilicates" 2nd edition. Longman, London 919pp.
- DEER, W. A., HOWIE, R. A. & ZUSSMAN, J. 1986. "Rock-forming minerals. Vol. 1B: Disilicates" - 2nd edition. Longman, London 629pp.
- DE SITTER, L. U. 1964. Structural Geology. McGraw-Hill, New York. 551pp.
- DIETRICH, D. 1969. Origin of cleavage in folded rocks. Am. J. Sci. 267, 155-165.

- DIETRICH, D. 1986. Calcite fabrics around folds as indicators of deformation history. J. Struct. Geol. 8, 655-668.
- DIETRICH, D. & SONG, H. 1984. Calcite fabrics in a natural shear environment, the Helvetic nappes of Western Switzerland. J. Struct. Geol. 6, 19-32.
- DIETRICH, J.H. & CARTER, H.L. 1969. Stress history of folding. Am. J. Sci. 267, 129-154.
- DIETRICH, J.H. & ONAT, E.T. 1969. Slow finite deformation of viscous solids. J. Geophys. Res. 74, 2081-2088.
- DONATH, F.A. & FRUTH, L.S. 1971. Dependence of strain rate effects and deformation mechanism and rock type. J. Geol. 79, 347-371.
- DOSTAL, J., STRONG, D.F. & JAMIESON, R.A. 1980. Trace element mobility in the mylonite zone within the ophiolite aureole, St. Antony complex, Newfoundland. Earth Planet. Sci. Lett. 49, 188-192.
- DOWNING, K. & CONARD, M.P. 1981. The Okavandja lineament and its significance in Damaran tectonics of Namibia. Geol. Rolsch 70, 927-1000.
- DUBEY, A.K. 1980. Late stages in the development of folds as deduced from model experiments. Tectonophysics 65, 311-322.
- DUBEY, A.K. & COBBOLD, P.R. 1977. Non cylindrical flexural slip folds in theory and experiment. Tectonophysics 38, 223-39.
- DUNCAN, I.J. 1984. Structural evolution of the Thor-Odin gneiss dome. Tectonophysics 101, 87-130.
- DUNCAN, I.J. & SHORE, P.J. 1983. Strain variation across an imbricated thrust sequence: plane strain distortion and translation strain versus simple shear. Geol. Soc. Am. Abstr. Program 15, 374.
- DUNNET, D. 1969. A technique of finite strain analysis using elliptical particles. Tectonophysics 7, 117-36.
- DURNEY, D.W. & RAMSAY, J.G. 1973. Incremental strains measured by syntectonic crystal growths. In DE JONG, K.A. and SCHOLTEN, R. (eds) "Gravity and Tectonics". Wiley, New York. 67-96.
- ELLIOTT, D. 1972. Deformation paths in structural geology. Bull. Geol. Soc. Am. 83, 2621-38.
- ELLIOTT, D. 1973. Diffusion flow laws in metamorphic rocks. Bull. Geol. Soc. Am. 84, 2645-64.
- ELLIOTT, D. 1976. The motion of thrust sheets. J. Geophys. Res. 81, 949-63.
- ELLIOTT, D. & JOHNSON, M.R.W. 1978. Discussion on structures found in thrust belts. Jl Geol. Soc. Lond. 135, 259-260.

- ENGELDER, T. 1984. The role of pore water circulation during the deformation of foreland fold and thrust belts. J. Geophys. Res. 89, 4319-4325.
- ENGELDER, T., GEISER, P.A. & ALVAREZ, W. 1981. Penrose Conference Report: role of pressure solution and dissolution in geology. Geology 9, 44-45.
- ENGELDER, T. & MARSHAK, S. 1986. Disjunctive cleavage formed at shallow depths in sedimentary rocks. J. Struct. Geol. 7, 327-343.
- ENGLAND, P.C. & RICHARDSON, S.W. 1977. The influence of erosion upon the mineral facies of rocks from different metamorphic environments. J. Geol. Soc. Lond. 134, 201-213.
- ENGLAND, P.C. & THOMPSON, A.B. 1984. Pressure-temperature-time paths of regional metamorphism. I Heat transfer during the evolution of regions of thickened continental crust. J. Petrol. 25, 894-928.
- ENGLAND, P.C. & THOMPSON, A.B. 1986. Some thermal and tectonic models for crustal melting in continental collision zones. In COWARD, M.P. and RIES, A.C. (eds) "Collision Tectonics." Spec. Publ. Geol. Soc. Lond. 19, 83-94.
- ESCHER, A., ESCHER, J.C. & WATTERSON, J. 1975. The reorientation of the Kangamiut dyke swarm, W. Greenland. Can. J. Earth Sci. 12, 158-173.
- ESCHER, A. & WATTERSON, J. 1974. Stretching fabrics, folds and crustal shortening. Tectonophysics 22, 223-231.
- ETHERIDGE, M.A. 1983. Differential stress magnitudes during regional deformation and metamorphism: upper bound imposed by tensile fracturing. Geology 11, 231-234.
- ETHERIDGE, M.A., COX, S.F., WALL, V.F. & VERNON, R.H. 1984. High fluid pressures during regional metamorphism and deformation - implications for mass transport and deformation mechanisms. J. Geophys. Res., 89 4344-4358.
- ETHERIDGE, M.A. & VERNON, R.H. 1981. A deformed polymictic conglomerate - the influence of grain size and composition on the mechanism and rate of deformation. Tectonophysics 79, 237-254.
- ETHERIDGE, M.A., WALL, V.J., COX, S.F. & VERNON, R.H. 1984. High fluid pressures during regional metamorphism and deformation: implications for mass transport and deformation mechanisms. J. Geophys. Res. 89, 4344-4358.

- ETHERIDGE, M.A., WALL, V.J. & VERNON, R.H. 1983. The role of the fluid phase during regional metamorphism and deformation. J. Met. Geol. 1, 205-226.
- ETHERIDGE, M.A. & WILKIE, J.C. 1979. Grain size reduction, grain boundary sliding and the flow strength of mylonites. Tectonophysics 58, 159-78.
- ETHERIDGE, M.A. & WILKIE, J.C. 1981. An assessment of dynamically recrystallized grain sizes as a palaeopiezometer in quartz-bearing mylonite zones. Tectonophysics 78, 475-508.
- EVANS, B., ROWAN, M. & BRACE, W.F. 1980. Grain-size sensitive deformation of a stretched conglomerate from Plymouth, Vermont. J. Struct. Geol. 2, 411-424.
- FERGUSON, C.C. & HARTE, B. 1975. Textural patterns at porphyroblast margins and their use in determining the time relations of deformation and crystallization. Geol. Mag. 112, 467-480.
- FERNANDES, L.A.D. 1986. Structural geology of the Haukivesi area, 'Nickel Belt' of SE Finland. OUTOKUMPU OY, Preliminary Report 70pp. (unpubl.).
- FERRY, J.M. 1980. A case study of the amount and distribution of heat and fluid during metamorphism. Contrib. Mineral. Petrol. 71, 373-385.
- FERRY, J.M. 1983. On the control of temperature fluid composition and reaction progress during metamorphism. Am. J. Sci. 263A, 201-232.
- FERRY, J.M. & SPEAR, F.S. 1978. Experimental calibration of the partitioning of Fe and Mg between garnet and biotite. Contrib. Mineral. Petrol. 66, 113-117.
- FETTES, D.J. & MENDUM, J.R. 1987. The evolution of the Lewisian complex in the Outer Hebrides. In "Evolution of the Lewisian and comparable Precambrian high grade terrains". Spec. Publ. Geol. Soc. London 27, 27-44.
- FLEITOUT, L. & FROIDEVAUX, C. 1980. Thermal and mechanical evolution of shear zones. J. Struct. Geol. 2, 159-164.
- FLEMING, P.D. & WHITE, A.J.R. 1984. Relationship between deformation and partial melting in the Palmer migmatites, South Australia. Austr. J. Earth Sci. 31, 351-360.
- FLETCHER, R.C. 1974. Wavelength selection in the folding of a single layer with power-law rheology. Am. J. Sci. 274, 1029-1043.
- FLETCHER, R.C. 1982. Analysis on the flow in layered fluids at small, but finite, amplitude with application to mullion

- structures. Tectonophysics 81,51-66.
- FLETCHER, R.C. & SHERWIN, J. 1978. Arc lengths of single layer folds: a discussion of the comparison between theory and observation. Am. J. Sci. 278, 1085-1098.
- FLEUTY, M. J. 1964. The description of folds. Proc. Geol. Assoc. 75, 461-492.
- FLINN, D. 1956. On the deformation of the Funzie conglomerate, Fetlar, Shetland. J. Geol. 64, 480-505.
- FLINN, D. 1961. On deformation at thrust planes in Shetland and the Jotunheim area of Norway. Geol. Mag. 98, 245-256.
- FLINN, D. 1962. On folding during three-dimensional progressive deformation. Quart. J. Geol. Soc. Lond. 118, 385-433.
- FLINN, D. 1965. On the symmetry principle and the deformation ellipsoid. Geol. Mag. 102, 36-45.
- FLINN, D. 1978. Construction and computation of three-dimensional progressive deformation. J. Geol. Soc. Lond. 135, 291-305.
- FLOYD, P.A. & WINCHESTER, J.A. 1975. Magma type and tectonic setting discrimination using immobile elements. Earth Planet. Sci. Lett. 27, 211-218.
- FLOYD, P.A. & WINCHESTER, J.A. 1983. Element mobility associated with meta-shear zones within the Ben Hope amphibolite suite, Scotland. Chem. Geol. 39, 1-15.
- FRANCIS, P.W. 1973. Scourian-Laxfordian relationships in the Barra Isles. J. Geol. Soc. Lond. 129, 161-189.
- FURTAK, H. & RICHTER, D. 1967. Relations between fold form and tectonic shortening in flexure folds. Geol. Mitt. 7, 2.
- FYFE, W.S. & KERRICH, R. 1985. Fluids and thrusting. Chem. Geol. 49, 353-362.
- FYFE, W.S., PRICE, N.J. & THOMPSON, A.B. 1978. "Fluids in the Earth's Crust" - Developments in Geochemistry 1. Elsevier, Amsterdam 383pp.
- FYSON, W.K. 1984. Basement-controlled structural fronts forming an apparent major re-fold pattern in the Yellowknife domain, Slave Province. Can. J. Earth Sci. 21, 822-828.
- GAIROLA, U.K. 1978. Strain distribution across an experimental single-layer fold. Tectonophysics 44, 27-40.
- GANDAIS, M. & WILLAIME, C. 1984. Mechanical properties of feldspars. In BROWN, W.L. (ed.) "Feldspars and Feldspathoids". Reidel Pub., Boston. 207-246.

- GAY, N.C. 1968a. Pure shear and simple shear deformation of inhomogeneous viscous fluids. 1. Theory. Tectonophysics 5, 211-234.
- GAY, N.C. 1968b. Pure shear and simple shear deformation of inhomogeneous viscous fluids. 2. The determination of the total finite strain in a rock from objects such as deformed pebbles. Tectonophysics 5, 295-302.
- GAY, N.C. 1969. The analysis of strain in the Barbeton Mountain Land, Eastern Transvaal, using deformed pebbles. J. Geol. 77, 377-396.
- GAY, N.C. 1970. The formation of step structures on slickensided shear surfaces. J. Geol. 78, 523-532.
- GAY, N.C. & JAEGER, J.C. 1975. Cataclastic deformation of geological materials in matrices of differing composition: II. Boudinage. Tectonophysics 27, 323-331.
- GHENT, E.D., ROBBINS, D.B. & STOUT, M.Z. 1979. Geothermometry, geobarometry and fluid inclusions of metamorphosed calc-silicates and pelites, Mica Creek, British Columbia. Am. Mineral. 64, 874-885.
- GHENT, E.D. & STOUT, M.Z. 1981. Geobarometry and geothermometry of plagioclase-biotite-garnet-muscovite assemblages. Contrib. Mineral. Petrol. 76, 92-97.
- GHOSH, S.K. 1966. Experimental tests of buckling folds in relation to strain ellipsoid in simple shear deformations. Tectonophysics 3, 169-185.
- GHOSH, S.K. 1968. Experiments of buckling of multilayers which permit interlayer gliding. Tectonophysics 6, 207-250.
- GHOSH, S.K. 1970. A theoretical study of intersecting fold patterns. Tectonophysics 9, 559-569.
- GHOSH, S.K. 1974. Strain distribution in superposed buckling folds and the problem of reorientation of early lineations. Tectonophysics 21, 249-272.
- GHOSH, S.K. 1975. Distortion of planar structures around rigid spherical bodies. Tectonophysics 28, 185-208.
- GHOSH, S.K. 1982. The problem of shearing along axial plane foliations. J. Struct. Geol. 4, 63-67.
- GHOSH, S.K. & CHATTERJEE, A. 1985. Patterns of deformed early lineations over later folds formed by buckling and flattening. J. Struct. Geol. 7, 651-666.
- GHOSH, S.K. & RAMBERG, H. 1976. Reorientation of inclusions by

- combination of pure shear and simple shear. Tectonophysics 34,1-70.
- GHOSH, S.K. & SENGUPTA, S. 1973. Compression and simple shear of test models with rigid and deformable inclusions. Tectonophysics 17,133-175.
- GHOSH, S.K. & SENGUPTA, S. 1984. Successive development of plane noncylindrical folds in progressive deformation. J. Struct. Geol. 6,703-709.
- GHOSH, S.K. & SENGUPTA, S. 1987. Progressive development of structures in a ductile shear zone. J. Struct. Geol. 9,277-287.
- GOLDMAN, D.S. & ALBEE, A.L. 1977. Correlation of Mg/Fe partitioning between garnet and biotite with $^{180}/^{160}$ partitioning between quartz and magnetite. Am. J. Sci. 277,750-767.
- GOODE, A.D.T. 1978. High temperature, high strain rate deformation in the Lower Crustal Kalk Intrusion, Central Australia. Contrib. Mineral. Petrol. 66,137-148.
- GRAHAM, C.M. & ENGLAND, P.C. 1976. Thermal regimes and regional metamorphism in the vicinity of overthrust faults: an example of shear heating and inverted metamorphic zonation from Southern California. Earth Planet. Sci. Lett. 31,142-152.
- GRAHAM, C.M. & POWELL, P. 1984. A garnet-hornblende geothermometer: calibration testing and application to the Pelona schist, southern California. J. Met. Geol. 2,13.
- GRAHAM, R.H. 1978. Wrench faults, arcuate fold patterns and deformation in the Southern French Alps. Proc. Geol. Assoc. 89,125-142.
- GRAMBLING, J.A. 1981. Pressures and temperatures in Precambrian metamorphic rocks. Earth Planet. Sci. Lett. 53,63-8.
- GRATIER, J.P. & VIALON, P. 1980. Deformation pattern in a heterogeneous material: folded and cleaved sedimentary cover immediately overlying a crystalline basement (Oisans, French Alps). Tectonophysics 65,151-180.
- GRAY, D.A. 1977. Differentiation associated with discrete crenulation cleavages. Lithos 10,89-101.
- GRAY, D.A. 1979a. Geometry of crenulation-folds and their relationship to crenulation cleavage. J. Struct. Geol. 1,187-205.
- GRAY, D.A. 1979b. Microstructure of crenulation cleavage: an indicator of cleavage origin. Am. J. Sci. 279,87-128.

- GRAY, D.R. 1981. Cleavage-fold relationships and their implications for transected folds: an example from Southwest Virginia, U.S.A. J.Struct.Geol. 3, 265-277.
- GRAY, D.R. & DURNEY, D.W. 1979a. Crenulation cleavage differentiation: implications of solution-deposition processes. J.Struct.Geol. 1, 73-80.
- GRAY, D.R. & DURNEY, D.W. 1979b. Investigations on the mechanism and significance of crenulation cleavage. Tectonophysics 58, 35-79.
- GREEN, H.W. II. 1984. 'Pressure solution' creep: some causes and mechanisms. J.Geophys.Res. 89, 4313-4318.
- GREENWOOD, H.J. 1976. Metamorphism at moderate temperatures and pressures. In BAILEY, D.K. and MACDONALD, R. (eds) "The Evolution of Crystalline Rocks". Academic Press, New York, 187-259.
- GRETENER, P.E. 1981. Pore pressure, discontinuities, isostasy and overthrusts. In MCCLAY, K.R. and PRICE, N.J. (eds) "Thrust and Nappe Tectonics". Spec.Publ.Geol.Soc.Lond. 9 33-39.
- GROCOTT, J. 1977. The relationship between Precambrian shear belts and modern fault systems. J.Geol.Soc.Lond. 133, 257-262.
- GROCOTT, J. 1979a. Shape fabrics and superimposed simple shear strain in a Precambrian shear belt, W.Greenland. J.Geol.Soc.Lond. 136, 471-488.
- GROCOTT, J. 1979b. Controls of metamorphic grade in shear belts. Rapp.Gronlands Geol.Unders. 89, 47-62.
- GROCOTT, J. 1984. Geometry of superimposed colinear deformations in the Ikerasak area, Umanak district, central W.Greenland. Precamb.Res. 26, 235-263.
- GROCOTT, J. & WATTERSON, J. 1980. Strain profile of a boundary within a large ductile shear zone. J.Struct.Geol. 2, 111-117.
- GUNN, W., CLOUGH, C.T. & GREENLY, E. 1905. Sheet 58, Geological Survey of Scotland, 6" to a mile. 16S library.
- HAMILTON, P.J., EVENSEN, N.M., O'NIONS, R.K. & TARNEY, J. 1979. Sm-Nd systematics of Lewisian gneisses: implications for the origin of granulites. Nature, Lond. 277, 25-28.
- HANMER, S.K. 1982. Microstructure and geochemistry of plagioclase and microcline in naturally deformed granite. J.Struct.Geol. 4, 197-213
- HANMER, S.K. & LUCAS, S.B. 1985. Anatomy of a ductile transcurrent

- shear: the Great Slave Lake Shear Zone, District of McKenzie NWT (preliminary report). In "Current Research, Part B." Geol.Surv.Can.Pap. 85-1B,7-225.
- HANSEN,E.1965.Methods of deducing slip-line orientations from the geometry of folds. Yearbook Carnegie Institution of Washington 65,386-410.
- HANSEN,E.1971."Strain Facies". Springer-Verlag,New York. 209pp.
- HANSEN,E.,SCOTT,W.H. & STANLEY,R.S.1965.Reconnaissance of slip-line orientations in parts of three mountain chains. Yearbook Carnegie Institution of Washington 65,406-410.
- HANNA,S.S. & FRY,N.1979.A comparison of methods of strain determination in rocks from southwest Dyfed (Pembrokeshire) and adjacent areas. J.Struct.Geol. 1,155-162.
- HARRIS,L.B. & COBBOLD,P.R.1984.Development of conjugate shear bands during bulk simple shearing. J.Struct.Geol. 7,37-44.
- HARTE,B. & GRAHAM,C.M.1975.The graphical analysis of greenschist to amphibolite facies mineral assemblages in metabasites. J.Petrol. 16,347-370.
- HEARD,H.C. & RALEIGH,C.B.1972.Steady-state flow in marble at 500°C to 800°C. Bull.Geol.Soc.Am. 83,935-956.
- HOBBS,B.E.1971.The analysis of strain in folded layers. Tectonophysics 11,329-375.
- HOBBS,B.E.1981.The influence of metamorphic environment upon the deformation of minerals. Tectonophysics 78,335-383.
- HOBBS,B.E.,MEANS,W.D. & WILLIAMS,P.F.1976.An Outline of Structural Geology. Wiley and sons,New York. 571pp.
- HOBBS,B.E.,MEANS,W.D. & WILLIAMS,P.F.1982.The relationship between foliation and strain: an experimental investigation. J.Struct.Geol. 4,411-428.
- HOEPPENER,R.,BRIX,M. & VOLLBRECHT,A.1983.Some aspects on the original fold-type fabrics - theory, experiments and field applications. Geol.Rundsch 72,4211-4216.
- HOLDAWAY,M.J. & LEE,S.M.1977.Fe-Mg cordierite stability in high-grade pelitic rocks based on experimental, theoretical and natural observations. Contrib.Mineral.Petrol. 63,175-198.
- HOLLAND,J.G. & LAMBERT,R.St.J.1969.Structural regimes and metamorphic facies. Tectonophysics 7,197-217.
- HOLLAND,J.G. & LAMBERT,R.St.J.1973.Comparative major element

- geochemistry of the Lewisian of the mainland of Scotland. In PARK, R.G. and TARNEY, J. (eds) "The early Precambrian of Scotland and related rocks of Greenland". Univ. of Keele, 51-62.
- HOLLAND, J.G. & LAMBERT, R.St.J. 1975. The chemistry and origin of the Lewisian gneisses of the Scottish mainland: the Scourie and Inver assemblages and sub-crustal accretion. Precambrian Res. 2, 161-188.
- HOLM, P.E. 1983. The effect of strain heterogeneity on graphical strain analysis methods. Tectonophysics 95, 101-110.
- HOPGOOD, A.M. 1971. Correlation by tectonic sequence in Precambrian gneiss terrains. Spec. Publ. Geol. Soc. Austr. 3, 367-376.
- HOPGOOD, A.M. 1973. Significance of deformational sequence in discriminating between Precambrian Terrains. In Lister, L.A. (ed) "Symposium on granites, gneisses and related rocks". Spec. Publ. Geol. Soc. Afr., 45-51.
- HOPGOOD, A.M. 1980. Polyphase fold analysis of gneisses and migmatites. Trans. R. Soc. Edinb. Earth Sci. 71, 55-68.
- HOPGOOD, A.M. 1984. Structural evolution of Svecokarelian migmatites, southern Finland: a study of Proterozoic crustal development. Trans. R. Soc. Edinb. Earth Sci. 74, 229-264.
- HOPGOOD, A.M., BOWES, D.R., KOVVO, O. & HALLIDAY, A.N. 1983. U-Pb and Rb-Sr isotopic study of polyphase deformed migmatites in the Svecokareliides southern Finland. In ATHERTON, M.P. and GRIBBLE, C.D. (eds) "Migmatites, Melting and Metamorphism." Shiva, Nantwich, 80-92.
- HOSSACK, J.R. 1968. Pebble deformation and thrusting in the Bygdin area (southern Norway). Tectonophysics 5, 315-339.
- HSU, K.J. 1979. Thin-skinned plate tectonics during neo-Alpine orogenesis. Am. J. Sci. 279, 353-366.
- HUBER, M., RAMSAY, J.G. & SIMPSON, C. 1980. Deformation in the Maggia and Antigorio nappes, Lepontine Alps. Eclogae Geol. Helv. 73, 593-606.
- HUBERT, C., TRUDEL, P. & GELINAS, L. 1984. Archaean wrench fault tectonics and structural evolution of the Blake River Group, Abitibi Belt, Quebec. Can. J. Earth Sci. 21, 1024-1032.
- HUDLESTON, P.J. 1973a. Fold morphology and some geometrical implication of theories of fold development. Tectonophysics

16,1-46.

- HUDLESTON, P.J. 1973b. An analysis of 'single layer' folds developed experimentally in viscous media. Tectonophysics 16, 189-214.
- HUDLESTON, P.J. 1973c. The analysis and interpretation of minor folds developed in the Moine rocks of Monar of Sutherland. Tectonophysics 17, 89-132.
- HUDLESTON, P.J. 1976. Early deformational history of Archean rocks in the Vermilion district, NE Minnesota. Can. J. Earth Sci. 13, 579-592.
- HUDLESTON, P.J. & HOLST, T.B. 1984. Strain analysis and fold shape in a limestone layer and implications for layer tectology. Tectonophysics 106, 321-347.
- HUDLESTON, P.J. & STEPHANSSON, O. 1973. Layer shortening and fold-shape development in the buckling of single layers. Tectonophysics 17, 299-321.
- INDARES, A. & MARTIGNOLE, J. 1985. Biotite-garnet geothermometry in the granulite facies: the influence of Ti and Al in biotite. Am. Mineral. 70, 272-278.
- JACOBSON, C.E. 1983. Structural geology of the Pelona schist and Vincent thrust, San Gabriel mountains, California. Bull. Geol. Soc. Am. 94, 753-767.
- JAEGER, J.C. & COOK, N.G.W. 1976. Fundamentals of Rock Mechanics. 3rd Edition. Chapman and Hall, London. 593pp.
- JAMES, P.R. 1979. Strain and microfabric development in a sheared megacrystic granite gneiss from the Eyre Peninsula, South Australia. In "International Conference on Shear Zones in Rocks, Barcelona, 15-17 May". Abstract.
- JAMIESON, R.A. 1986. P-T paths from high temperature shear zones beneath ophiolites. J. Met. Geol. 4, 3-22.
- JAROUL, O., TULLIS, J. & KRONENBERG, R. 1984. The effect of varying water contents on the creep behaviour of Heavitree Quartzite. J. Geophys. Res. 89, 4298-4312.
- JOHNSON, A.M. 1977. "Styles of Folding". Developments in Geotectonics, 11. Elsevier, Amsterdam.
- JOHNSON, A.M. 1980. Folding and faulting of strain-hardening sedimentary rocks. Tectonophysics 62, 251-278.
- JOHNSON, M.R.W., KELLEY, S.P. & WINTER, D.A. 1985. Thermal effects and timing of thrusting in the Moine Thrust zone. J. Geol. Soc. Lond. 142, 863-874.
- JOHNSON, Y.A. & WINCHESTER, J.A. 1985. Geochemical and petrogenetic

- studies of Loch Maree amphibolites. (Abstr.) 3rd Lewisian Symposium, Leicester 1985.
- JOHNSTON, D.C. & WHITE, S.H. 1983. Shear heating associated with movement along the Alpine Fault, New Zealand. Tectonophysics 92, 241-252.
- JOHNSTON, M.J.S., JONES, A.C. & DAUL, W. 1977. Continuous strain measurements during and preceding episodic creep on the San Andreas fault. J. Geophys. Res. 82, 5683-91.
- JONES, E.M., RICE, C.M. & TWEEDIE, J.R. 1987. Lower Proterozoic stratiform sulphide deposits in Loch Maree Group, Gairloch, northwest Scotland. Trans. Inst. Min. Metall. (Appl. Earth sci.) 96, 128-139.
- JONES, M.E. 1981. The relationships between metamorphism and deformation: report of the Tectonic Studies Group discussion meeting held at the Geological Society, Burlington House, London, 12 November 1980. J. Struct. Geol. 3, 333-338.
- JORDAN, P. 1987. Estimation of strain rate based on microstructural observations (Abstr.). Terra Cognita 7, 123.
- KELLEY, S.P. & POWELL, D. 1985. Relationships between thrusts and shear zones in Scottish Caledonides. J. Struct. Geol. 7, 161-174.
- KEPPIE, J.D. 1967. Geology of the Lewisian Complex Around Furnace North-East of Loch Maree, Ross-Shire. Ph.D. thesis University of Glasgow, 190 pp. (unpubl.).
- KERRICH, R. 1986. Fluid transport in lineaments. Phil. Trans. R. Soc. London A317, 219-257.
- KERRICH, R. & ALLISON, I. 1978. Vein geometry and hydrostatics during Yellowknife mineralization. Can. J. Earth Sci. 15, 1653-1660.
- KERRICH, R., ALLISON, I., BARNETT, R.S., MOSS, S. & STARKEY, J. 1980. Microstructural and chemical transformations accompanying deformation of granite in a shear zone at Nieville, Switzerland; with implications for stress corrosion cracking and superplastic flow. Contrib. Miner. Petrol. 73, 221-242.
- KIRBY, S.H. 1984. Introduction and digest to the special issue on chemical effects of water on the deformation and strength of rocks. J. Geophys. Res. 89, 3991-3995.
- KIRBY, S.H. & MCCORMICK, J.W. 1984. Inelastic properties of rocks and minerals: strength and rheology. In CARMICHAEL, R.S. (ed.)

"Handbook of Physical Properties of Rocks. Vol. III",
139-280.

- KNELLER, B.C. & LESLIE, A.G. 1984. Amphibolite facies metamorphism in shear zones in the Buchan area of NE Scotland. J. Met. Geol. 2, 83-94.
- KNIPE, R.J. 1981. The interaction of deformation and metamorphism in slates. Tectonophysics 78, 249-272.
- KOISTINEN, T.J. 1981. Structural evolution of an early Proterozoic strata-bound Cu-Co-Zn deposit, Outokumpu, Finland. Trans. R. Soc. Edinb. Earth Sci. 72, 115-58.
- KRISHNA SINHA, A., HEWITT, D.A., RIMSTIET, J.D. 1986. Fluid interaction and element mobility in the development of ultramylonites. Geology 14, 883-886.
- KRONENBERG, A.K. & SHELTON, G.L. 1980. Deformation microstructure in experimentally deformed Maryland diabase. J. Struct. Geol. 2, 341-353.
- KRONENBERG, A.K. & TULIS, J. 1984. Flow strengths of quartz aggregates: grain size and pressure effects due to hydrolytic weakening. J. Geophys. Res. 89, 4281-4297.
- LACASSIN, R. & MATTAUER, M. 1985. Kilometre-scale sheath fold at Mattmark and implications for transport direction in the Alps. Nature, Lond. 315, 739-742.
- LACASSIN, R. & VAN DEN DRIESSCHE, J. 1983. Finite strain determination of gneiss: application of Fry's method to porphyroid in the southern Massif Central (France). J. Struct. Geol. 5, 245-253.
- LAGARDE, J.L. & MICHARD, A. 1986. Stretching normal to the regional thrust displacement in a thrust-wrench shear zone, Rehamna Massif, Morocco. J. Struct. Geol. 8, 483-492.
- LANGDON, T.G. 1985. Regimes of plastic deformation. In WENK, H.R. (ed.) "Preferred Orientation in Deformed Metals and Rocks: An Introduction to Modern Texture Analysis". Academic Press, New York, 219-232.
- LATHAM, J-P. 1979. Experimentally developed folds in a material with a planar mineral fabric. Tectonophysics 57, T1-T8.
- LATOUR, T.E. 1981. Significance of folds and mylonites at the Greenville Front in Ontario. Bull. Geol. Soc. Am. 92, 411-413.
- LATOUR, T.E. & BARNETT, R.L. 1987. Mineralogical changes accompanying mylonitization in the Bitterroot dome of the Idaho batholith: Implications for the timing of deformation.

- LAUBSCHER, H.P. 1975. Viscous components in Jura folding. Tectonophysics 27,239-254.
- LAW, R.D., KNIFE, R.J. & DAYAN, H. 1984. Strain path partitioning from the Moine Thrust zone. J. Struct. Geol. 6,477-497.
- LAW, R.D. & POTTS, G.J. 1987. The Tarskavaig Nappe of Skye, northwest Scotland: a re-examination of the fabrics and their kinematic significance. Geol. Mag. 124,231-248.
- LEAKE, B.E. 1978. Nomenclature of amphibolites. Canadian Mineral. 16,501-520.
- LEBEDEVA, N.B. 1979. Significance of mechanical heterogeneities of rocks for formation of flow cleavage. Tectonophysics 54,61-79.
- LEWIS, R.W. & WILLIAMS, J.R. 1978. A finite-element study of fold propagation in a viscous layer. Tectonophysics 44,263-283.
- LINDQUIST, J.E. 1983. Metamorphism and b_0 values of white mica in the Jämtland supergroup of the central Scandinavian Caledonides. Geol. Fören. Stockholm Forh. 105,71-72.
- LISLE, R.J. 1977. Estimation of the tectonic strain ratio from the mean shape of deformed elliptical markers. Geol. en Mijn. 56,140-144.
- LISLE, R.J. 1985. "Geological Strain Analysis: A Manual for the Af/θ Method". Pergamon Press, Oxford. 100pp.
- LISTER, G.S. & HOBBS, B.E. 1980. The simulation of fabric development during plastic deformation and its application to quartzite: the influence of deformation history. J. Struct. Geol. 2,355-370.
- LISTER, G.S., PATERSON, M.S. & HOBBS, B.E. 1978. The simulation of fabric development in plastic deformation and its application to quartzite: the model. Tectonophysics 45,107-158.
- LISTER, G.S. & PATERSON, M.S. 1979. The simulation of fabric development in plastic deformation and its application to quartzite: fabric transition. J. Struct. Geol. 1,99-115.
- LISTER, G.S. & PRICE, G.P. 1978. Fabric development in a quartz-feldspar mylonite. Tectonophysics 49,37-48.
- LISTER, G.S. & SNOKE, A.W. 1984. S-C mylonites. J. Struct. Geol. 6,617-638.
- LISTER, G.S. & WILLIAMS, P.F. 1979. Fabric development in shear zones: theoretical controls and observed phenomena.

J.Struct.Geol. 1,283-298.

- LISTER, G.S. & WILLIAMS, P.F. 1983. The partitioning of deformation in flowing rock masses. Tectonophysics 92,1-34.
- MADDOCK, R.H. 1983. Melt origin of fault-generated pseudotachylites demonstrated by textures. Geology 11,105-108.
- MANZ, R. & WICKHAM, J. 1978. Experimental analysis of folding in simple shear. Tectonophysics 44,79-90.
- MAINPRICE, D.H. & PATERSON, M.S. 1984. Experimental studies of the role of water in the plasticity of quartzites. J.Geophys.Res. 89,4257-4269.
- MARCOS, A. & ARBOLEYA, M.L. 1975. Evidence of progressive deformation in minor structures. Geol.Rundsch. 64,278-287.
- MASON, R. 1984. Inverted isograds at Sulitjehma, Norway: the result of shear zone deformation. J.Met.Geol. 2,77-82.
- MATTAUER, M., FAURE, M. & MALAVIEILLE, J. 1981. Transverse lineation and large-scale structures related to Alpine obduction in Corsica. J.Struct.Geol. 3,401-409.
- MATTHEWS, P.E., BOND, R.A.B. & VAN DEN BERG, J.J. 1974. Analysis and structural implications of a kinematic model of similar folding. Tectonophysics 12,129-154.
- MAWER, C.K. 1983. State of strain in a quartzite mylonite, Central Australia. J.Struct.Geol. 5,401-409.
- MAX, M.D. 1981. The interdependence of strain and metamorphic recrystallization in basic dykes in NW County Mayo, Ireland. (Abstr.) In JONES, M.E. "The relationships between metamorphism and deformation: report of the Tectonic Studies Group discussion meeting held at the Geological Society, Burlington House, London, 12 November 1980." J.Struct.Geol. 3,337.
- MAYCOCK, I.D. 1962. The Torridonian sandstone round Loch Torridon, Wester Ross. Reading University Unpubl. Ph.D. thesis, 305pp.
- McCAIG, A.M. 1984. Fluid-rock interaction in some shear zones from the Pyrenees. J.Met.Geol. 2,129-141.
- McCLAY, K.R. 1977. Pressure solution and Cobble creep in rocks and minerals: a review. J.Geol.Soc.Lond. 134,57-70.
- McCLAY, K.R. 1981. What is a thrust? What is a nappe? In McCLAY, K.R. and PRICE, N.J. (eds) "Thrust and Nappe Tectonics." Spec.Publ.Geol.Soc.Lond. 9,7-9.

- McLELLAN, E. 1984. Deformation behaviour of migmatites and problems of structural analysis in migmatite domains. Geol. Mag. 121, 339-345.
- McMECHAN, M. E. & PRICE, R. A. 1982. Transverse folding and superposed deformation, Mount Fisher area, southern Canadian Rocky Mountain thrust and fold belt. Can. J. Earth Sci. 19, 1011-1024.
- MEANS, W. D., HOBBS, B. E., LISTER, G. S. & WILLIAMS, P. F. 1980. Vorticity and non-coaxiality in progressive deformations. J. Struct. Geol. 2, 371-378.
- MENEILLY, A. W. & STOREY, B. C. 1986. Ductile thrusting within subduction complex rocks on Signy Island, South Orkney Islands. J. Struc. Geol. 8, 457-472.
- MERCIER, J. C. C. 1980. Magnitude of the continental lithospheric stresses inferred from rheomorphic petrology. J. Geophys. Res. 85, 6293-6303.
- MILLER, D. M. & CHRISTIE, J. M. 1981. Comparison of quartz microfabric with strain in recrystallized quartzite. J. Struct. Geol. 3, 129-141.
- MILTON, N. J. 1980. Determination of the strain ellipsoid from measurements on any three section. Tectonophysics 64, T19-T27.
- MILTON, N. J. & WILLIAMS, G. D. 1981. The strain profile above a major thrust fault, Finmark, N. Norway. In McCLAY, K. R. and PRICE N. J. (eds) "Thrust and Nappe Tectonics." Spec. Publ. Geol. Soc. Lond. 9 235-240.
- MITRA, G. 1978. Ductile deformation zones and mylonites: the mechanical processes involved in the deformation of crystalline basement rocks. Am. J. Sci. 278, 1057-1084.
- MITRA, G. 1979. Ductile deformation zones, Blue Ridge basement rocks and estimation of finite strain. Bull. Geol. Soc. Am. 90, 935-951.
- MITRA, G. 1984. Brittle to ductile transition due to large strains along the White Rock Thrust, Wind River mountains, Wyoming. J. Struct. Geol. 6, 51-61.
- MITRA, S. 1976. A quantitative study of deformation mechanisms and finite strain in quartzites. Contrib. Mineral. Petrol. 59, 203-226.
- MITRA, S. & TULLIS, J. 1979. A comparison of intracrystalline deformation in naturally and experimentally deformed

- quartzites. Tectonophysics 53, T21-T27.
- MOODY, J. B. & HUNDLEY-GOFF, E. M. 1980. Microscopic characteristics of orthoquartzite from sliding friction experiments. II. Gouge. Tectonophysics 62, 301-309.
- MORRIS, A. P. 1981. Competing deformation mechanisms and slaty cleavage in deformed quartzose meta-sediments. J. Geol. Soc. Lond. 138, 455-462.
- MUELLER, R. F. 1967. Mobility of the elements in metamorphism. J. Geol. 75, 565-582.
- MULLER, W. H. & HSU, K. J. 1980. Stress distribution in overthrusting slabs and mechanics of Jura deformation. In SCHEIDEGGER, A. E. (ed.) "Rock Mechanics." Springer-Verlag, Berlin, 219-232.
- MURREL, S. A. F. 1977. Natural faulting and the mechanism of brittle shear failure. J. Geol. Soc. Lond. 133, 175-190.
- MYERS, J. S. 1978. Formation of banded gneisses by deformation of igneous rocks. Precamb. Res. 6, 43-64.
- NARAHARA, D. & WILTSCHKO, D. U. 1986. Deformation in the hinge region of a chevron fold, Valley and Ridge Province, central Pennsylvania. J. Struct. Geol. 8, 157-168.
- NAYLOR, M. A., MANDL, G. & STJEPSTEIJN, C. H. K. 1986. Fault geometries in basement-induced wrench faulting under different initial stress states. J. Struct. Geol. 8, 737-752.
- NICHOLAS, A. 1987. "Principles of Rock Deformation." D. Riedel, Dordrecht, 208pp.
- NICHOLAS, A. & BOUDIER, F. 1975. Kinematic interpretation of folds in Alpine-type peridotites. Tectonophysics 25, 233-260.
- NICHOLAS, A. & POIRIER, J. P. 1976. "Crystalline plasticity and solid state flow in metamorphic rocks. (Selected topics in geological sciences)." John Wiley and Sons, New York, 444pp.
- OBEE, H. K. & WHITE, S. H. 1985. Faults and associated fault rocks of the southern Arunta block, Alice Springs, Central Australia. J. Struct. Geol. 7, 701-712.
- O'DRISCOLL, E. S. 1964. Cross fold deformation by simple shear. Econ. Geol. 59, 1061-1093.
- OERTEL, G. 1981. Strain estimation from scattered observations in an inhomogeneously deformed domain of rocks. Tectonophysics 77, 133-150.
- OERTEL, G. 1983. The relationship of strain and preferred orientation

of phyllosilicate grains in rocks - a review.

Tectonophysics 100,413-449.

- OERTEL, G. 1985. Re-orientation due to grain shape. In WENK, H.R. (ed.) "Preferred Orientation in Deformed Metals and Rocks: An Introduction to Modern Texture Analysis." Academic Press, New York, 259-265.
- OERTEL, G. & ERNST, W.G. 1978. Strain and rotation in a multilayered fold. Tectonophysics 48,77-106.
- OLESEN, N.O. 1978. Distinguishing between inter-kinematic and syn-kinematic porphyroblastesis. Geol.Rundsch. 67,278-287.
- O'NIONS, R.K., HAMILTON, P.J. & HOOKER, P.J. 1983. A Nd isotope investigation of sediments related to crustal development in the British Isles. Earth Planet.Sci.Lett. 63,229-240.
- ORD, A. & CHRISTIE, J.M. 1984. Flow stresses from microstructures in mylonitic quartzites of the Moine Thrust zone, Assynt area, Scotland. J.Struct.Geol. 6,639-654.
- OWENS, W.H. 1984. The calculation of a best-fit ellipsoid from elliptical sections on arbitrarily oriented planes. J.Struct.Geol. 6,571-578.
- OXBURGH, E.R. & ENGLAND, P.C. 1980. Heat flow and the metamorphic evolution of the eastern Alps. Eclog.Geol.Helvet. 73,379-398.
- OXBURGH, E.R. & TURCOTTE, D.L. 1974. Thermal gradients and regional metamorphism in overthrust terrains with special reference to the Eastern Alps. Schweiz.Mineral.Petrograph.Mitt. 54,641-510.
- PARK, A.F. & BOWES, D.R. 1983. Basement-cover relationships during polyphase deformation in the Svecokareliides of the Kaavi district, eastern Finland. Trans.R.Soc.Edinb.Earth Sci. 74,95-118.
- PARK, R.G. 1966. Nature and origin of Lewisian basin rocks of Gairloch, Ross-shire. Scott.J.Geol. 2,179-199.
- PARK, R.G. 1969. Structural correlations in metamorphic belts. Tectonophysics 7,323-338.
- PARK, R.G. 1970. The structural evolution of the Tollie antiform - a geometrically complex fold in the Lewisian north-east of Gairloch, Ross-shire. J.Geol.Soc.Lond. 125,319-349.
- PARK, R.G., CRANE, A. & NIAMATULLAH, M. 1987. Early Proterozoic structure and kinematic evolution of the southern mainland Lewisian. In Park, R.G. and Tarney, J. (eds) "Evolution of the Lewisian and

- comparable High Grade Terrains". Spec.Publ.Geol.Soc.Lond. 27,139-151.
- PARK, R.G. & TARNEY, J. 1987. (eds) "Evolution of the Lewisian and comparable Precambrian high grade terrains". Spec.Publ.Geol.Soc.Lond. 27,27-44.
- PARRISH, D.K. 1973. A nonlinear finite-element fold model. Am.J.Sci. 273,318-334.
- PARRISH, D.K., KRIUK, A. & CARTER, N.L. 1976. Finite element folds of similar geometry. Tectonophysics 32,183-207.
- PASSCHIER, C.W. 1982. Pseudotachylite and the development of ultramylonite bands in the Saint-Bartholemy Massif, French Pyrenees. J.Struct.Geol. 4,69-79.
- PASSCHIER, C.W. 1984. The generation of ductile and brittle shear bands in a low-angle mylonite zone. J.Struct.Geol. 6,273-281.
- PATERSON, M.S. 1976. Some current aspects of experimental rock deformation. Phil.Trans.R.Soc.Lond. A283,163-172.
- PEACH, B.N., HORNE, J., GUNN, W., CLOUGH, C.T., HINXMAN, L.W. and TEALL, J.J.H. 1907. "The geological structure of the north-west highlands of Scotland". Mem.Geol.Surv.G.B.
- PEACH, B.N. & HORNE, J. 1930. "Chapters on the Geology of Scotland". Oxford University Press, London. 232pp.
- PERCEVAULT, M.N. & COBBOLD, P.R. 1982. Mathematical removal of regional ductile strains in central Brittany: evidence of wrench tectonics. Tectonophysics 82,317-328.
- PFIFFNER, O.A. 1980. Strain analysis in folds (Infrahelvetic Complex, Central Alps). Tectonophysics 61,337-362.
- PFIFFNER, O.A. 1981. Fold-and-thrust tectonics in the Helvetic Nappes (E.Switzerland). In MCCLAY, K.R. and PRICE, N.J. (eds) "Thrust and Nappe Tectonics." Spec.Publ.Geol.Soc.Lond. 9,319-328.
- PFIFFNER, O.A. 1982. Deformation mechanisms and flow regimes in limestones from the Helvetic zone of the Swiss Alps. J.Struct.Geol. 4,429-42.
- PFIFFNER, O.A. & RAMSAY, J.G. 1982. Constraints on geological strain rates: arguments from finite strain states of naturally deformed rocks. J.Geophys.Res. 87,311-321.
- PLATT, J.P. 1983. Progressive refolding in ductile shear zones. J.Struct.Geol. 5,619-622.
- PLATT, J.P. 1979. Extensional crenulation cleavage. J.Struct.Geol.

1,95.

- PLATT, J.P. 1984. Secondary cleavages in ductile shear zones. J.Struct.Geol. 6, 439-442.
- PLATT, J.P., BEHMANN, J.H., MARTINEZ, J.M.M & VISSERS, R.L.M. 1984. A zone of mylonite and related ductile deformation beneath the Alpujamaide Nappe Complex, Betic Cordilleras South Spain. Geol.Rundsch 73, 773-785.
- PLATT, J.P. & LEGGETT, J.K. 1986. Stratal extension in thrust footwalls, Makran accretionary prism: Implications for thrust tectonics. Bull.Am.Ass.Pet.Geol. 70, 191-203.
- PLATT, J.P. & VISSERS, R.L.M. 1980. Extensional structures in anisotropic rocks. J.Struct.Geol. 2, 397-410.
- POIRIER, J.P. 1980. Shear localization and shear instability in materials in the ductile field. J.Struct.Geol. 2, 135-142.
- POIRIER, J.P. 1985. "Creep of Crystals: High Temperature Deformation Processes in Metals, Ceramics and Minerals". Cambridge Univ.Press. 260pp
- PONCE DE LEON, M.I. & CHOUKROUNE, P. 1980. Shear zones in the Iberian Arc. J.Struct.Geol. 2, 62-68.
- POPPER, K. 1959. "The Logic of Scientific Discovery" Hutchinson, London, 479pp.
- POWELL, C.McA. 1979. A morphological classification rock cleavage. Tectonophysics 58, 21-34.
- POWELL, C.McA. & VERNON, R.H. 1979. Growth and rotation history of garnet porphyroblasts with inclusion spirals in a Karakoram schist. Tectonophysics 54, 25-43.
- POWELL, D. & MACQUEEN, J.A. 1976. Relationships between garnet shape, rotational inclusion fabrics, and strain in some Moine metamorphic rocks of skye, Scotland. Tectonophysics 35, 391-402.
- POWELL, R. 1985. Geothermometry and geobarometry: a discussion. J. Geol.Soc.Lond. 142, 29-38.
- POWELL, R. & EVANS, J.A. 1983. A new geobarometer for the assemblage biotite-muscovite-chlorite-quartz. J.Met.Geol. 1, 331-336.
- POWELL, R. & POWELL, M. 1977. Plagioclase - alkali feldspar geothermometry revised. Mineral.Mag. 41, 253-256.
- POWER, G.M. & PARK, R.G. 1969. A chemical study of five amphibolite bodies from the Lewisian of Gairloch, Ross-shire.

- Scott, J. Geol. 5, 26-41.
- PRICE, G.P. 1981. Application of the photometric method to fabric mapping around folds. Tectonophysics 78, 85-100.
- PRICE, G.P. 1985. Preferred orientations in quartzite. In WENK, H.R. (ed.) "Preferred Orientation in Deformed Metals and Rocks: An Introduction to Modern Texture Analysis." Academic Press, New York, 385-406.
- PRICE, N.J. 1975. Rates of deformation. J. Geol. Soc. Lond. 131, 553-575.
- PRICE, N.J. & McCLAY, K.R. 1981. Thrust and nappe tectonics - introduction. In McCLAY, K.R. and PRICE, N.J. (eds) "Thrust and Nappe Tectonics." Spec. Publ. Geol. Soc. Lond. 9, 1-12.
- RAGAN, D.M. 1969. Structures at the base of an ice fall. J. Geol. 77, 647-667.
- RAMBERG, H. 1960. Relationships between length of arc and thickness of pygmatically folded veins. Am. J. Sci. 258, 36-46.
- RAMBERG, H. 1961. Relationship between concentric longitudinal strain and concentric shearing strain during folding of homogeneous sheets of rock. Am. J. Sci. 259, 382-390.
- RAMBERG, H. 1963. Fluid dynamics of viscous buckling applicable to folding of layered rocks. Bull. Am. Ass. Petrol. Geol. 47, 484-515.
- RAMBERG, H. 1964. Selective buckling of composite layers with contrasted rheological properties, a theory for the simultaneous formation of several orders of folds. Tectonophysics 1, 307-341.
- RAMBERG, H. 1975. Particle paths, displacement and progressive strain applicable to rocks. Tectonophysics 28, 1-37.
- RAMBERG, H. 1980. Diapirism and gravity collapse in the Scandinavian Caledonides. J. Geol. Soc. Lond. 137, 261-270.
- RAMBERG, H. & GHOSH, S.K. 1977. Rotation and strain of linear and planar structures in three-dimensional progressive deformation. Tectonophysics 40, 309-337.
- RAMSAY, D.M. 1976. An additional criterion in the aberrant fold relationship. Tectonophysics 31, T1-T4.
- RAMSAY, D.M. 1979. Analysis of rotation of folds during progressive deformation. Bull. Geol. Soc. Am. 90, 732-738.
- RAMSAY, D.M. & STURT, B. 1970a. Polyphase deformation of a polymictic Silurian conglomerate from Mageroy, Norway. J. Geol. 78, 264-280.
- RAMSAY, D.M. & STURT, B.A. 1973b. An analysis of noncylindrical and

incongruous fold pattern from the Eocene rocks of Soroy, northern Norway. I. Noncylindrical, incongruous and aberrant folding. Tectonophysics 18,81-107.

- RAMSAY, D.M. & STURT, B.A. 1973. An analysis of noncylindrical and incongruous fold pattern from the Eocene rocks of Soroy, northern Norway. II. The significance of synfold stretching lineation in the evolution of noncylindrical folds. Tectonophysics 18,109-121.
- RAMSAY, J.G. 1958. Superimposed folding at Loch Morar, Inverness-shire and Ross-shire. Quart. J. Geol. Soc. Lond. 113,271-307.
- RAMSAY, J.G. 1967. Folding and Fracturing of Rocks. McGraw Hill, New York. 568pp.
- RAMSAY, J.G. 1969. The measurement of strain and displacement in orogenic belts. In "Time and Place in Orogeny", Sp. Publ. Geol. Soc. Lond. ,43-79.
- RAMSAY, J.G. 1974. Development of chevron folds. Bull. Geol. Soc. Am. 85,1749-54.
- RAMSAY, J.G. 1976. Displacement and Strain. Phil. Trans. R. Soc. Lond. A283,3-25.
- RAMSAY, J.G. 1980a. Shear zone geometry: a review. J. Struct. Geol. 2,83-99.
- RAMSAY, J.G. 1980b. The "crack-seal" mechanism of rock deformation. Nature, Lond. 284,135-9.
- RAMSAY, J.G. 1981. Tectonics of the Helvetic Nappes. In McCLAY, K.R. and PRICE, N.J. (eds) "Thrust and Nappe Tectonics." Spec. Publ. Geol. Soc. Lond. 9 293-309.
- RAMSAY, J.G. 1982. Rock ductility and its influence on the development of tectonic structures in mountain belts. In HSU, K.J. (ed.) "Mountain Building Processes." Academic Press, London p111-127.
- RAMSAY, J.G. & ALLISON, I. 1979. Structural analysis of shear zones in an alpinised Hercynian granite, Maggia Lappen, Pennine zone, Central Alps. Schweiz. Min. Pet. Mitt. 59,251-279.
- RAMSAY, J.G. & GRAHAM, R.H. 1970. Strain variation in shear belts. Can. J. Earth Sci. 7,786-813.
- RAMSAY, J.G. & HUBER, M.I. 1983. The Techniques of Modern Structural Geology. Volume 1, Strain Analysis. Academic Press, London. 360pp.
- RAMSAY, J.G., KLIGFIELD, R. & CASEY, M. 1983. The role of shear in the

- development of the Helvetic fold-and-thrust belt, Switzerland. Geology 11,439-442.
- RAMSAY, J.G. & WOOD, D.S. 1973. The geometric effects of volume change during deformation processes. Tectonophysics 16,263-277.
- RAMSON, D.M. 1971. Host control of recrystallized quartz grains. Mineral.Mag. 38,83-88.
- RAO, B. & JOHANNES, W. 1979. Further data on the stability of staurolite and quartz and related assemblages. Neues Jb.Mineral.Mh. 437-447.
- RAST, N. 1965. Nucleation and growth of metamorphic minerals. In PITCHER, W.S. and FLINN, G.W. (eds) "Controls of Metamorphism." Oliver and Boyd, Edinburgh, 73-102.
- RAST, N. & PLATT, J.I. 1957. 'Cross-folds'. Mineral.Mag. 94,159-167.
- RATSCHBACHER, L. & OERTEL, G. 1987. Superimposed deformations in the Eastern Alps: strain analysis & microfabrics. J.Struct.Geol. 9,263-276.
- RHODES, S. & GAYER, R.A. 1977. Noncylindrical folds, linear structures in the x-direction and mylonite development during translation of the Caledonian Kalak Nappe Complex of Finnmark. Geol.Mag. 114,329-341.
- RICE, J.M. & FERRY, J.M. 1982. Buffering, infiltration and the control of intensive variables during metamorphism. In FERRY, J.M. (ed.) "Reviews in Mineralogy vol.10 - Characterisation of Metamorphism through Mineral Equilibria." Min.Soc.Am., 263-326.
- RIDLEY, J. 1982. Arcuate lineation trends in a deep level, ductile thrust belt, Syros, Greece. Tectonophysics 88,347-360.
- RIDLEY, J. 1986. Parallel stretching lineations and fold axes oblique to a shear displacement direction—a model and observations. J.Struct.Geol. 8,647-654.
- RISPOLI, R. 1981. Stress fields about strike-slip faults inferred from stylolites and tension gashes. Tectonophysics 75,T29-T36.
- ROBERTS, D. & STRONGÅRD, K.E. 1971. A comparison of natural and experimental strain patterns around fold hinge zones. Tectonophysics 14,105-120.
- ROBERTS, J.L. 1972. The mechanics of overthrust faulting: a critical review. 24th Internat.Geol.Congr.Rept.Sect.3, Ottawa, 1972, 593-598.
- ROBERTS, J.L. 1977. The structural analysis of metamorphic rocks in orogenic belts. In SAXENA, S.K. and BHATTACHARJI, S. (eds)

"Energetics of Geological Processes." Springer-Verlag, New York. 151-168.

- ROCK, N.M.S. 1987. The geochemistry of Lewisian marbles. In PARK, R.G. and TARNEY, J. (eds) "Evolution of the Lewisian and Comparable Precambrian High Grade Terrains." Spec. Publ. Geol. Soc. Lond. 27, 109-126.
- ROY, A.B. 1978. Evolution of slaty cleavage in relation to diagenesis and metamorphism: a study from the Hunsruckschiefer. Bull. Geol. Soc. Am. 89, 1775-1785.
- ROY, S.S. & FAERSETH, R.B. 1981. Strain analysis of polyphase deformed conglomerate from the Sunnhordland region, west Norway. Norsk Geologisk Tidsskrift 61, 47-58.
- RUTTER, E.H. 1986. On the nomenclature of mode of failure in rocks. Tectonophysics 122, 381-387.
- RUTTER, E.H., PEACH, C.J., WHITE, S.H. & JOHNSTON, D. 1985. Experimental 'syntectonic' hydration of basalt. J. Struct. Geol. 7, 251-266.
- SANDERSON, D.J. 1973. The development of fold axes oblique to the regional trend. Tectonophysics 16, 55-70.
- SANDERSON, D.J. 1976. The superimposition of compaction and plane strain. Tectonophysics 30, 35-54.
- SANDERSON, D.J. 1979. The transition from upright to recumbent folding in the Variscan fold belt of southwest England: a model based on the kinematics of simple shear. J. Struct. Geol. 1, 177-180.
- SANDERSON, D.J. 1982. Models of strain variation in nappes and thrust sheets: a review. Tectonophysics 88, 201-233.
- SANDERSON, D.J., ANDREWS, J.R., PHILLIPS, W.E.A. & HUTTON, D.H.W. 1980. Deformation studies in the Irish Caledonides. J. Geol. Soc. Lond. 137, 289-302.
- SCHONEVELD, Chr. 1979. The geometry and significance of inclusion patterns in syntectonic porphyroblasts. Ph.D. thesis, University of Leiden, the Netherlands. Unpub.
- SCHMID, S.M. 1975. The Glarus overthrust: field evidence and mechanical model. Eclog. Geol. Helv. 68, 247-280.
- SCHMID, S.M. 1982. Microfabric studies as indicators of deformation mechanisms and flow laws operative in mountain building. In HSU, K.J. (ed) "Mountain Building Processes." Academic Press, London. 95-110.

- SCHMID, S.M., BOLAND, J.N. & PATERSON, M.S. 1977. Superplastic flow in finegrained limestone. Tectonophysics 43, 257-291.
- SCHMID, S.M., PATERSON, M.S. & BOLAND, J.N. 1980. High temperature flow and dynamic recrystallization in Carrara marble. Tectonophysics 65, 245-280.
- SCHOLL, D.W., VON HUENE, R., VALLIER, T.L. & HOWELL, D.G. 1980. Sedimentary masses and concepts about tectonic processes at underthrust ocean margins. Geology 8, 564-568.
- SCHWERDTNER, W.M., BENNETT, P.I. & JAMES, T.W. 1977. Application of L-S fabric scheme to structural mapping and palaeostrain analysis. Can. J. Earth Sci. 14, 1021-1032.
- SCOTT, W.H. & HANSEN, E. 1968. Movement directions and the axial-plane fabrics of flexural folds. Year Book Carnegie Institution of Washington 67, 254-58.
- SEGALL, P. & POLLARD, D.D. 1983. Joint formation in granitic rocks of the Sierra Nevada. Bull. Geol. Soc. Am. 94, 563-575.
- SHACKLETON, R.M. & RIES, A.C. 1984. The relation between regionally consistent stretching lineations and plate motions. J. Struct. Geol. 6, 111-120.
- SHERWIN, J.A. & CHAPPLE, W.M. 1968. Wavelengths of single layer folds. A comparison between theory and observation. Am. J. Sci. 266, 167-179.
- SHIMAMOTO, T. & HARA, I. 1976. Geometry and strain distribution of single-layer folds. Tectonophysics 30, 1-34.
- SIBSON, R.H. 1974. Frictional constraints on thrust, wrench and normal faults. Nature, Lond. 249, 542-543.
- SIBSON, R.H. 1975. Generation of pseudotachylite by ancient seismic faulting. Geophys. J. Roy. Astr. Soc. 43, 775-94.
- SIBSON, R.H. 1977. Fault rocks and fault mechanisms. J. Geol. Soc. Lond. 133, 167-179.
- SIBSON, R.H. 1980. Transient discontinuities in ductile shear zones. J. Struct. Geol. 2, 165-171.
- SIBSON, R.H., WHITE, S.H. & ATKINSON, B.K. 1979. Fault rock distribution and structure within the Alpine fault zone: a preliminary account. In WALCOTT, R.I. and CRESSWELL, M.M. (eds) "The origin of the Southern Alps." Bull. Roy. Soc. N.Z. 18, 55-65.
- SIDDANS, A.W.B. 1972. Slaty cleavage: a review of research since 1815. Earth Sci. Rev. 8, 205-32.
- SIDDANS, A.W.B. 1977. The development of slaty cleavage in a part of the French Alps. Tectonophysics 39, 533-557.

- SIDDANS, A.W.B. 1979. Arcuate fold and thrust patterns in the Subalpine chains of southeast France. J. Struct. Geol. 1, 117-126.
- SILLS, J.D. & ROLLINSON, H.R. 1987. Metamorphic evolution of the mainland Lewisian complex. In PARK, R.G. and TARNEY, J. (eds) "Evolution of the Lewisian and comparable Precambrian high grade terrains." Spec. Publ. Geol. Soc. Lond. 27, 81-92.
- SHORE, P.J. & DUNCAN, I.J. 1984. Finite strains from non-coaxial strain paths. I. Computational techniques. Tectonophysics 110, 127-144.
- SIMPSON, C. 1980. Oblique girdle orientation patterns of quartz C-axes from a shear zone in the basement core of the Maggia Nappe, Ticino, Switzerland. J. Struct. Geol. 2, 243-246.
- SIMPSON, C. 1983a. Strain and shape-fabric variations associated with ductile shear zones. J. Struct. Geol. 5, 61-72.
- SIMPSON, C. 1983b. Displacement and strain patterns from naturally occurring shear zone terminations. J. Struct. Geol. 5, 497-506.
- SIMPSON, C. 1985. Deformation of granitic rocks across the brittle-ductile transition. J. Struct. Geol. 7, 503-511.
- SIMPSON, C. & SCHMIDT, S.M. 1983. An evaluation of criteria to deduce the sense of movement in sheared rocks. Bull. Geol. Soc. Am. 94, 1281-1288.
- SKJERNAA, L. 1980. Rotation and deformation of randomly oriented planar and linear structures in progressive simple shear. J. Struct. Geol. 2, 101-109.
- SINHA, A.K. & GLOVER, L.III. 1978. U/Pb systematics of zircons during dynamic metamorphism. Contrib. Mineral. Petrol. 66, 305-310.
- SMITH, D.I. & FETTES, D.J. 1979. The geological framework of the Outer Hebrides. Proc. R. Soc. Edinb. 77B, 75-83.
- SMITH, R.B. 1975. Unified theory of the onset of folding, boudinage, and mullion structure. Bull. Geol. Soc. Am. 86, 1601-1609.
- SMITH, R.B. 1977. Formation of folds, boudinage, and mullions in non-Newtonian materials. Bull. Geol. Soc. Am. 88, 312-320.
- SMITH, R.B. 1979. The folding of a strongly non-Newtonian layer. Am. J. Sci. 279, 272-287.
- SMYTHE, D.K. 1971. Viscous theory of angular folding by flexural flow. Tectonophysics 12, 415-430.
- SMYTHE, D.K. 1987. Deep seismic reflection profile of the Lewisian

- foreland. In PARK, R.G. and TARNEY, J. (eds) "Evolution of the Lewisian and Comparable Precambrian High Grade Terrains." Spec. Publ. Geol. Soc. Lond. 27, 193-203.
- SODRE BORGES, F. & WHITE, S.H. 1980. Microstructural and chemical studies of sheared anorthosites, Roneval, South Harris. J. Struct. Geol. 2, 273-280.
- SOPER, H.J. & BARBER, A.J. 1982. A model for the deep structure of the Moine thrust zone. J. Geol. Soc. Lond. 139, 127-138.
- SPANG, J.H. & GROSHONG, R.H. Jr. 1981. Deformation mechanisms and strain history of a minor fold from the Appalachian Valley and Ridge Province. Tectonophysics 72, 323-342.
- SPANG, J.H., SIMONY, P.S. & MITCHELL, W.J. 1980. Strain and folding mechanisms in a similar style fold from the northern Selkirks of the Canadian Cordillera. Tectonophysics 66, 253-267.
- SPRAY, J.G. 1987. Artificial generation of pseudotachylite using friction welding apparatus: simulation of melting on a fault plane. J. Struct. Geol. 9, 49-60.
- STABLER, C.L. 1968. Simplified Fourier Analysis of fold shapes. Tectonophysics 6, 343-350.
- STEARNS, D.W., COUPLES, G.D., JAMISON, W.R. & MORSE, J.D. 1981. Understanding faulting in the shallow crust: contributions of selected experimental and theoretical studies. In CARTER, N.L., FRIEDMAN, M., LOGAN, J.M. and STEARNS, D.W. (eds) "Mechanical Behaviour of Crustal Rocks - the Handin Volume." Geophysical Monograph Series No. 24. Washington D.C. 1981, 215-229.
- STEEL, R.J. & WILSON, A.C. 1975. Sedimentation and tectonism (?Permo-Triassic) on the margins of the North Minch Basin, Lewis. J. Geol. Soc. Lond. 131, 183-202.
- STEL, H. 1981. Crystal growth in cataclasites: diagnostic microstructures and implications. Tectonophysics 78, 585.
- STEPHANSSON, O. 1976. Finite element analysis of folds. Phil. Trans. R. Soc. Lond. A283, 153-161.
- STRINGER, P. & TREAGUS, J.E. 1980. Non-axial planar S1 cleavage in the Hawick rocks of the Galloway area, Southern Uplands, Scotland. J. Struct. Geol. 2, 317-331.
- STURT, B.A. & HARRIS, A.L. 1961. The metamorphic history of the Loch Tummel area, central Perthshire, Scotland.

Liverp.Manch.Geol.J. 2,689-711.

- SUGDEN, T. 1987. Kinematic indicators: structures that record the sense of movement in mountain chains. Geology Today 9, 93-99.
- SUK, M. 1985. "Petrology of Metamorphic Rocks". Developments in Petrology 9. Elsevier, Amsterdam. 160pp.
- SUTTON, J. & WATSON, J. 1951. The pre-Torridonian History of the Loch Torridon and Scourie Areas in the North-West Highlands, and its bearing on the chronological Classification of the Lewisian. Quart. J. Geol. Soc. Lond. 106, 241-308.
- SUTTON, J. & WATSON, J. 1962. Further observations on the margin of the Laxfordian complex of the Lewisian near Loch Laxford, Sutherland. Trans. R. Soc. Edinb. Earth. Sci. 65, 89-106.
- SYLVESTER, A.G. & SMITH, R.R. 1976. Tectonic transpression and basement-controlled deformation in San Andreas fault zone, Salton Trough, California. Bull. Am. Ass. Petrol. Geol. 57, 74-96.
- TCHALENKO, J.S. 1970. Similarities between shear zones of different magnitudes. Bull. Geol. Soc. Am. 81, 1625-1640.
- THOMPSON, A.B. 1976. Mineral reactions in pelitic rocks II. Calculation of some P-T-X (Fe-mg) phase relations. Am. J. Sci. 176, 425-454.
- THOMPSON, A.B. & ENGLAND, P.C. 1984. Pressure-Temperature-Time paths of regional metamorphism II. Their inference and interpretation using mineral assemblages in metamorphic rocks. J. Petrol. 25, 929-955.
- THOMPSON, A.B. & RIDLEY, J.R. 1987. Pressure-temperature-time (P-T-t) histories of orogenic belts. Phil. Trans. R. Soc. Lond. A321, 27-45.
- TOBISCH, O.T. 1967. The influence of early structures on the orientation of late-phase folds in an area of repeated deformation. J. Geol. 75, 554-64.
- TOBISCH, O. & FISKE, R.S. 1982. Repeated parallel deformation in part of the eastern Sierra Nevada California and its implications for dating structural events. J. Struct. Geol. 4, 177-195.
- TORIUMI, M. 1985. Two types of ductile deformation/regional metamorphic belt. Tectonophysics 113, 307-326.
- TORIUMI, M. & NODA, H. 1986. The origin of strain patterns resulting from contemporaneous deformation and metamorphism in the

- Sambagawa metamorphic belt. J.Met.Geol. 4,405-420.
- TRACY, R.J. 1982. Compositional zoning and inclusions in metamorphic minerals. In RIBBE, P.H. (ed.) "Feldspar Mineralogy. Review in Mineralogy." 2nd edition. Mineral. Soc. Am., 353-397.
- TREAGUS, J.E. 1987. The structural evolution of the Dalradian of the Central Highlands of Scotland. Trans. R. Soc. Edinb. Earth. Sci. 78, 1-15.
- TREAGUS, J.E. & TREAGUS, S.H. 1981. Folds and the strain ellipsoid: a general model. J. Struct. Geol. 3, 1-17.
- TREAGUS, S.H. 1973. Buckling stability of a viscous single-layers system, oblique to the principal compression. Tectonophysics 19, 271-289.
- TREAGUS, S.H. 1979. Three-dimensional strains in fold-hinge zones - discussion and reply. Tectonophysics 53, 147-150.
- TREAGUS, S.H. 1981. A theory of stress and strain variations in viscous layers, and its geological implications. Tectonophysics 72, 75-104.
- TREAGUS, S.H. 1983. A theory of finite strain variation through contrasting layers, and its bearing on cleavage refraction. J. Struct. Geol. 5, 351-368.
- TULLIS, J. 1980. The use of mechanical twinning in minerals as a measure of shear stress magnitudes. J. Geophys. Res. 85, 6263-6268.
- TULLIS, J. 1982. Deformation of feldspars. In RIBBE, P.H. (ed.) "Feldspar Mineralogy." Reviews in Mineralogy, Mineralogical Society of America. 2nd edition, 297-325.
- TULLIS, J. & YUND, R.A. 1980. Hydrolytic weakening of experimentally deformed Westerly granite and Hale albite rock. J. Struct. Geol. 2, 439-451.
- TURNER, F.J. & VERHOOGEN, J. 1960. "Igneous and Metamorphic Petrology". 2nd edition. McGraw-Hill, New York. 694pp.
- TURNER, F.J. & WEISS, L.E. 1963. "Structural Analysis of Metamorphic Tectonites". McGraw-Hill, New York. 345pp
- VAN DEN DRIESSCHE, J. 1986. Structural evolution of the Thor Odin Gneiss Dome - discussion. Tectonophysics 121, 351-354.
- VAN ROERMUND, H., LISTER, G.S. & WILLIAMS, P.F. 1979. Progressive development of quartz fabrics in an shear zone from Monte Mucrone, Sesia-Lanzo zone, Italian Alps. J. Struct. Geol. 1, 43-52.

- VAUCHEZ, A. 1987. The development of discrete shear-zones in a granite: stress, strain and changes in deformation mechanisms. Tectonophysics 133, 137-156.
- VERNON, R. H. 1974. Controls of mylonitic compositional layering during non-cataclastic ductile deformation. Geol. Mag. 111, 121-123.
- VERNON, R. H. 1977. Relationship between micro-structures and metamorphic assemblages. Tectonophysics 39, 439-452.
- VERNON, R. H. 1978. Porphyroblast-matrix microstructural relationships in deformed metamorphic rocks. Geol. Rundsch. 67, 288-305.
- VERNON, R. H. 1981. Optical microstructure of partly recrystallized calcite in some naturally deformed marbles. Tectonophysics 78, 601-612.
- VERNON, R. H. & FLOOD, R. H. 1979. Microstructural evidence of time-relationships between metamorphism and deformation in the meta-sedimentary sequence of the Northern Hill end Trough, New South Wales, Australia. Tectonophysics 58, 127-137.
- VERNON, R. H., WILLIAMS, V. A. & D'ARCY, W. F. 1983. Grain size reduction and foliation development in a deformed granite batholith. Tectonophysics 92, 123-146.
- WAKEFIELD, J. 1977. Mylonitization in the Lethakane shear zone, Eastern Botswana. J. Geol. Soc. Lond. 133, 263-275.
- WATKINSON, A. J. 1975. Multilayer folds initiated in bulk plane strain, with the axis of no change perpendicular to the layering. Tectonophysics 28, T7-T11.
- WATKINSON, A. J. 1981. Patterns of fold interference: influence of early fold shapes. J. Struct. Geol. 3, 19-23.
- WATKINSON, A. J. 1983. Patterns of folding and strain influenced by linearly anisotropic bands. J. Struct. Geol. 5, 449-454.
- WATSON, J. 1983. Lewisian. In CRAIG, G. Y. (ed.) "Geology of Scotland." Scott. Acad. Press., Edinburgh, 23-47.
- WATTERSON, J. 1975. Mechanism for the persistence of tectonic lineaments. Nature Phys. Sci. 253, 520-521.
- WATTS, M. J. & WILLIAMS, G. D. 1983. Strain geometry, microstructure and mineral chemistry in metagabbro shear zones: a study of softening mechanisms during progressive mylonitization. J. Struct. Geol. 5, 507-517.
- WEAVER, B. L. & TARNEY, J. 1980. Rare-earth geochemistry of Lewisian granulite-facies gneisses, northwest Scotland:

- implications for the petrogenesis of the Archaean lower continental crust. Earth Planet.Sci.Lett. 51,279-296.
- WEBER,K.1981.Kinematic and metamorphic aspects of cleavage formation in very low-grade metamorphic slates. Tectonophysics 78,291-306.
- WEISS,L.E. & MCINTYRE,D.B.1957.Structural geometry of Dalradian rocks at Loch Leven, Scottish Highlands. J.Geol. 65,575-602.
- WENK,H.R.1985.Carbonates. In WENK,H.R. (ed.) "Preferred Orientation in Deformed Metals and Rocks: An Introduction to Modern Texture Analysis." Academic Press,New York. 361-384.
- WENK,H.R. & KELLER,J.1969.Isograds in amphibolite series der Zentralalpen. Schweiz.Min.Petr.Mitt. 49,157-198.
- WHEELER,J.1986.Average properties of ellipsoidal fabrics: implications for two and three-dimensional methods of strain analysis. Tectonophysics 126,259-270.
- WHEELER,J.,PRIOR,D. & DALY,M.1984.Thrusting and low grade supracrustals in the Laxfordian.(Abstr.) In "Tectonic Studies Group, 15th annual meeting, Swansea." p.93.
- WHEELER,J.,WINDLEY,B.F. & DAVIES,F.B.1987.Internal evolution of the major Precambrian shear belt at Torridon, NW Scotland. In PARK,R.G. and TARNEY,J.(eds) "Evolution of the Lewisian and comparable Precambrian high grade terrains." Spec.Publ.Geol.Soc.Lond. 27,153-163.
- WHITE,J.C. & MAWER,C.K.1986.Extreme ductility of feldspars from a mylonite, Parry Sound, Canada. J.Struct.Geol. 8,133-143.
- WHITE,S.1973.Syntectonic recrystallisation and texture development in quartz. Nature,Lond. 244,276-278.
- WHITE,S.1976.The effects of strain on the microstructures, fabrics, and deformation mechanisms in quartzites. Phil.Trans.R.Soc.Lond. A283,69-86.
- WHITE,S.H.1979.Sub-grain and grain size variations across a shear zone. Contrib.Mineral.Petrol. 70,193-202.
- WHITE,S.H.,BURROWS,S.E.,CARRERAS,J.,SHAW,N.D. & HUMPHREYS,F.J. 1980.On mylonites in ductile shear zones. J.Struct.Geol. 2,175-187.
- WHITE,S.H. & KNIFE,R.J.1978.Transformation and reaction-enhanced ductility in rocks. J.Geol.Soc.Lond. 135,513-516.

- WILCOX, R. E., HARDING, T. P. & SEELY, D. R. 1973. Basic wrench tectonics. Bull. Am. Ass. Petrol. Geol. 57, 74-96.
- WILKINS, R. W. T & BARKAS, J. P. 1978. Fluid inclusions, deformation and recrystallization in granite tectonites. Contrib. Mineral. Petrol. 65, 293-298.
- WILKINSON, P., SOPER, N. J. & BELL, A. M. 1975. Skolithos pipes as strain markers in mylonites. Tectonophysics 28, 143-157.
- WILLIAMS, G. E. 1969. Petrography and origin of pebbles from Torridonian strata (Late Precambrian), northwest Scotland. In KAY, M. (ed.) "North Atlantic geology and continental drift - a symposium." Am. Ass. Pet. Geol. Mem. 12, 609-629.
- WILLIAMS, J. R. 1980. Similar and chevron folds in multilayers using finite-element and geometric models. Tectonophysics 65, 323-338.
- WILLIAMS, P. F. 1970. A criticism of the use of style in the study of deformed rocks. Bull. Geol. Soc. Am. 81, 3282-3296.
- WILLIAMS, P. F. 1972. Development of metamorphic layering and cleavage in low grade metamorphic rocks at Bermagui, Australia. Am. J. Sci. 272, 1-47.
- WILLIAMS, P. F. 1977. Foliation: a review and discussion. Tectonophysics 39, 305-328.
- WILLIAMS, P. F. 1981. Relative timing of folding and development of axial plane foliations. (Abstr.) In "Report on the Canadian Tectonics Group 1981 inaugural meeting". J. Struct. Geol. 4, 231-235.
- WILLIAMS, P. F. 1985. correlation in multiply deformed terrains. J. Struct. Geol. 7, 269-280.
- WILLIAMS, P. F. & COMPAGNONI, R. 1983. Deformation and metamorphism in the Band area of the Sesia Lanzo zone, western Alps, during subduction and uplift. J. Met. Geol. 1, 117-141.
- WILLIAMS, P. F. & SCHONEVELD, CHR. 1981. Garnet rotation and the development of axial plane crenulation cleavage. Tectonophysics 78, 307-334.
- WILLIAMS, P. F. & ZWART, H. J. 1977. A model for the development of the Seve-Koln Caledonian nappe complex. In SAXENA, S. K. and BHATTACHARJI, S. (eds) "Energetics of Geodynamic Processes." Springer, New York, 169-187.
- WILSON, C. J. L. 1973. The prograde microfabric in a deformed quartzite sequence, Mount Isa, Australia. Tectonophysics 19, 39-81.

